Switchable luminescent probes using resonance energy transfer

Thesis

UNRESTRICTED.

SWITCHABLE LUMINESCENT PROBES USING RESONANCE ENERGY TRANSFER

K Eszter Borbas

The Open University
2004

Submission date: 29 September 2004
Award date: 21 February 2005.

ProQuest LLC.
789 East Eisenhower Parkway
P.O. Box 1346
Ann Arbor, MI 48106 – 1346

Declaration

I declare that the work presented in this thesis is the result of my own investigations, and where the work of others is cited, it is fully acknowledged. The material embodied in the thesis has not been submitted, nor is currently being submitted for any other degree.

.....

Katalin Eszter Borbas

.....

Dr James I Bruce

ABSTRACT

Understanding the molecular basics of recognition events in chemistry is crucial for a wide range of disciplines. Luminescence spectroscopy is an appealing way of obtaining information on molecular-scale recognition events, as sensitive, real-time detection and subnanometer spatial resolution can be achieved.[1]

Measurements in biological media are generally difficult because of the interference from the sample and the non-zero background.

Resonance energy transfer (RET) between a luminescent donor and acceptor (**D-A**) is possible when excitation of the **D** is followed by energy transfer to **A**, that emits at increased wavelengths. Molecules that undergo RET triggered by the presence of a target molecule would allow a specific signal to be identified, as emission would occur only in the presence of the species of interest. Due to the increased emission wavelengths, interference with sample autofluorescence is avoided.

The synthesis of donor-acceptor-quencher (**D-A-Q**) triads, equipped with coumarin donors, nucleoside quenchers,[2] and organic or lanthanide acceptors, that are able to undergo triggered RET will be presented.

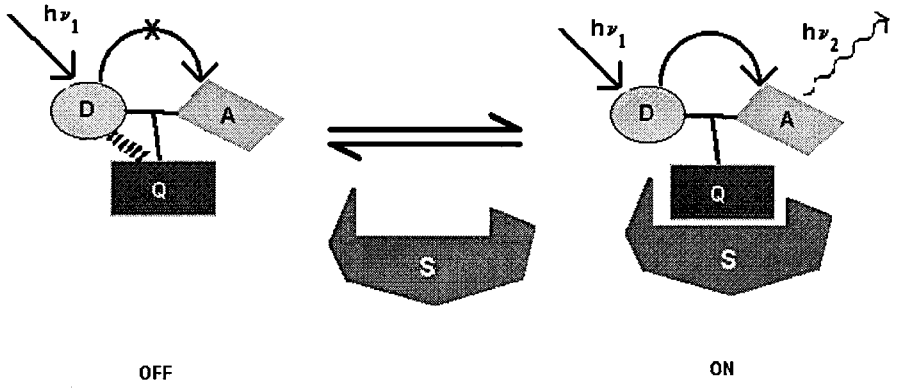

*Figure 1. **D**: donor, **A**: acceptor, **Q**: quencher, **S**: substrate*

RET from **D** to **A** is quenched by **Q** that is in the close proximity of the **D**. In the absence of the substrate (**S**) the quencher quenches the **D**, and RET is not possible. If **S** is present, the quenching is disrupted by the **Q-S** binding, and emission from **A** is observed (*Figure 1*). A cocktail of **D-A_1-Q_1**, **D-A_2-Q_2**, **D-A_3-Q_3**,... triads offers the possibility of simultaneous detection of several species.

The photophysical properties of the triads have been determined and their behaviour was studied in the presence of their substrates. The information gained enables the design of improved triads and the tuning of their photophysical properties.

References

1. *Molecular fluorescence,* B. Valeur, WILEY-VCH Verlag GmbH, Weinheim, **2002**
2. A. M. Seide, A. Schulz, M. H. M. Sauer, *J. Phys. Chem.*, **1996,** *100,* 5541-5553

ACKNOWLEDGEMENTS

I would like to thank Dr James I Bruce for his supervision, guidance and encouragement throughout the three years.

I am grateful to Dr Andrew Beeby and Dr Laurent Porres of the University of Durham for their help with the photophysical measurements.

Thanks also to the OU Chemistry Department staff, in particular to Mr Gordon Howell, Mr Graham Jeffs, Mr Colin Haynes and Mr Pravin Patel.

I would like to thank the EPSRC MS Service (University of Wales, Swansea) for the high resolution MS measurements, and Professor Alan Perkins and Ms Elaine Blackshaw for the radioimaging, and for the access to the laboratories and equipment at the Department of Academic Medical Physics at the University of Nottingham.

I would like to thank The Open University and Universities UK for funding.

Finally a big thanks to my family, and my friends, both in Hungary and the UK, Shailesh, Catia, Maci, Kukuc, Pöttömke and Fish.

Kösz mindent.

TABLE OF CONTENTS

1 LIST OF ABBREVIATIONS

A	adenine
A	acceptor
A	absorption
Ac	acetyl
AcN	acetonitrile
AU	arbitratry units
B	any nucleoside base
bipy	bipyridyl
Boc	tert-butoxycarbonyl
c120	coumarin 120 (4-methyl-7-aminocoumarin)
c2	coumarin 2 (4,6-dimethyl-7-(N-ethyl)-aminocoumarin)
c343	coumarin 343
cc.	concentrated
CE	catechol estrogens
CHEQ	chelation enhanced quenching
cps	counts per second
Cys	Cysteine
D	Donor
dA	deoxyadenosine
dC	deoxycytidine
DCC	dicyclohexylcarbodiimide
DCM	dichloromethane
DEAD	diethyl azodicarboxylate
dG	deoxyguanosine

DIAD	diisopropyl azodicarboxylate
DMAP	*N*-dimethylaminopyridine
DMF	dimethylformamide
DMSO	dimethyl sulphoxide
DNA	deoxyribonucleic acid
dsDNA	double stranded DNAs
dT	deoxythymidine
EDCI	1-(3-dimethylaminopropyl)-3-ethylcarbodiimide hydrochloride
eq	equivalent
ES	electrospray
Et	Ethyl
EtOAc	ethyl acetate
Fmoc	9-fluorenylmethyloxycarbonyl
G	Guest
GABA	γ-aminobutyric acid
Glu	glutamic acid
Gly	Glycine
H	Host
HBA	DL-4-amino-3-hydroxybutyric acid
HG	host-guest complex
HOBt	1-hydroxybenzotriazole
NHS	*N*-hydroxysuccinimide
IC	internal conversion
IR	infrared
ISC	intersystem crossing

K	equilibrium constant
Ln	lanthanide
m	mass
MB	molecular beacon
MLCT	metal to ligand charge transfer
MOPS	3-(*N*-morpholino)propanesulfonic acid
mp	melting point
MS	mass spectrometry
MW	molecular weight
NMA	*N*-methylaniline
NMR	nuclear magnetic resonance
PET	photoinduced electron transfer
PFP	pentafluorophenyl
Ph	phenyl
PyBOP	(benzotriazol-1-yloxy)tripyrrolidinophosphonium hexafluorophosphate
Q	quencher
q	number of associated water molecules
RET	resonance energy transfer
Rho	rhodamine B
SBFI	sodium-binding benzofuran isophthalate
SBFP	sodium-binding benzofuran phthalate
S_n	n^{th} singlet excited state
ssDNA	single stranded DNA
T	Temperature

t	Time
TBAF	tetrabutylammonium fluoride
TEA	Triethylamine
TFA	trifluoroacetic acid
THF	Tetrahydrofuran
TLC	thin layer chromatography
T_n	n^{th} triplet excited state
TPP	Triphenylphosphine
U	Uracil
z	Charge
Φ_F	quantum yield
ε	molar absorption coefficient
λ_{em}	emission wavelength
λ_{ex}	excitation wavelength
λ_{max}	absorption maximum
τ	lifetime
Å	Ångström

2 INTRODUCTION

Understanding the molecular basics of recognition events in chemistry, biology and materials science is crucial for a wide range of disciplines, for example medicine, pharmacology, or information technology. In order to gather information on these processes, suitably designed reporter molecules are essential. Luminescence is a particularly appealing way of obtaining information on molecular-scale processes, as highly sensitive, real-time detection, combined with subnanometer spatial resolution is achievable.

The aim of the project is to design and synthesise luminescent molecules that are capable of binding to target molecules and can signal the binding event in complex media (for example biological samples).

2.1 Recognition

In 1894 Emil Fisher introduced the 'lock and key' concept of molecular recognition.[1] He suggested, that the host molecules possess rigid complementary structures (lock) into which the guests (key) can fit perfectly. The theory was modified by Koshland[2] and Cram in the 'induced fit' model,[3] who assumed that a certain preorganisation is essential for the binding to take place, but the host (**H**) can rearrange slightly in order to better accommodate the guest (**G**) (*Figure 1*).

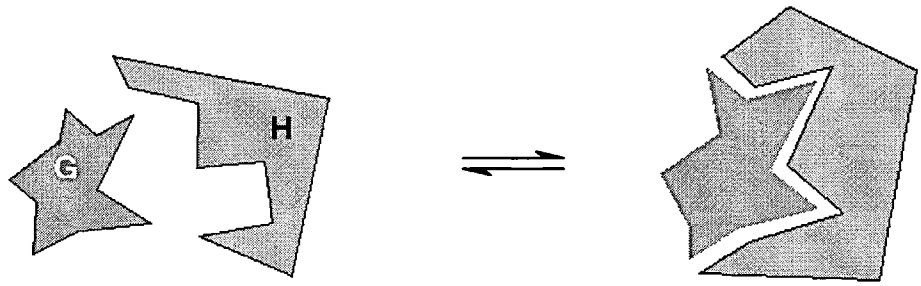

*Figure 1. Recognition between the host (**H**) and the guest (**G**) can be described by the induced fit model. A level of pre-organisation is required, but both **H** and **G** can change their shapes during the binding to make the interaction stronger.*

2.1.1 Recognition in nature

Nature provides innumerable examples for recognition events. These include for example enzyme-substrate interactions, DNA double helix formation, nucleic acid binding by DNA-binding proteins for several purposes (DNA-duplication, gene expression)[4] or antigen recognition by antibodies (which is basically proteins complexing other proteins, carbohydrates, lipids and nucleic acids).[5] The information on binding events between cells and viruses, bacteria or other cells is scarce but from data already available it seems likely, that protein-sugar and sugar-sugar interactions play important roles.[6] These processes have been monitored by various techniques such as X-ray crystallography, NMR, UV-Vis and fluorescence spectroscopy, mass spectrometry, which have provided valuable information on the nature of the recognition and binding in biological systems.

2.1.2 Recognition in chemistry

The subject of supramolecular chemistry is the formation and fate of architectures built from small, stable moieties that are held together by forces

that are weaker than covalent bonds. The formation of these architectures can usually be described as a 'host' incorporating a 'guest', although there are cases when this is not true. For the 'host-guest' interaction to be favourable (i.e. to have the host **H** + **G** $\rightleftharpoons$ **HG** equilibrium to the right) the free energy of the reaction forming the **HG** has to be negative.

Host-guest systems have been used for several different purposes. Apart from modelling biological processes, they have found application in sensors for biologically or environmentally important species such as dissolved oxygen, [7] metal ions[8] or DNA.[9] Sensors are devices that signal the presence of a molecule or ion by a specific signal. The signalling can take place for example by a change in their electrochemical, luminescence or NMR properties. Sensors usually contain a recognition unit to bind the target and a reporter unit to enable the monitoring of the event (*Figure 2*).

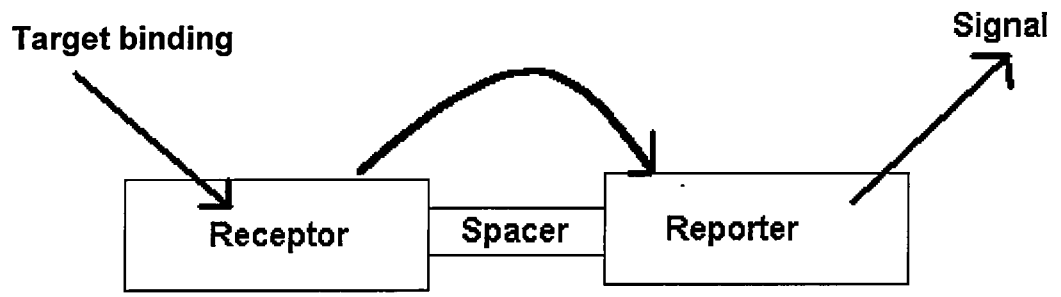

Figure 2. A general sensor, containing a recognition unit and a reporter unit. Although sometimes missing, the spacer can play an important role by isolating the two functional units. This enables quantitative estimation of crucial sensor parameters, such as binding constants in the ground and excited states.

Molecules that are capable of emitting light upon certain stimuli (for example thermal- or photoexcitation, interaction with other molecules) are convenient means of monitoring events that take place on the molecular level.

Luminescence and in particular fluorescence has increasingly been applied for the detection of recognition phenomena. Although in a number of cases it has proved superior to the more established techniques (for example radiolabelling, colorimetry, NMR), fluorescence sensing poses difficult questions. Despite the examples of single molecule detection, [9] in complex biological media sensitivity can be significantly reduced. One of the reasons is autofluorescence of the medium, caused by the presence of luminescent species, for example DNA, RNA, fluorescent proteins and porphyrin-containing molecules, like haemoglobin. Also, the luminescence intensity of the probes can be affected by quenching, caused by solutes in the medium, for example dioxygen or halides. In some cases it is possible to reduce the quenching, by removal of the oxygen by degassing, or by cooling the sample to decrease the diffusion rates of the quenchers. Many fluorophores are pH-sensitive, and protonation or de-protonation can change the fluorescent quantum yields significantly.

2.2 *Fluorescence*

Luminescence is the emission of photons from electronically excited states.[8,10] Depending on the timescale, luminescence phenomena can be divided into two major groups. (a) In a *singlet excited state* the electron in the higher-energy orbital is paired up with the second electron in the lower orbital (i.e. they have spins of opposite orientation). Returning from the excited state to the ground state is symmetry-allowed and the rates of emission are typically 10^8 s^{-1}. Such a transition is called *fluorescence*. (b) If emission between *states of different multiplicity* takes place, i.e. the electrons have the same spin, return from the triplet excited state to the ground state requires an electron to change orientation. This type of transition is called *phosphorescence*. Phosphorescence is spin-forbidden, and as a consequence phosphorescence lifetimes are on the millisecond-second timescale.

Absorption and emission of light can be illustrated using the Jablonski diagram (*Figure 3*). The ground state and the first and second excited states are S_0, S_1, and S_2, respectively. Transitions between electronic energy levels are considered instantaneous (femtosecond scale).

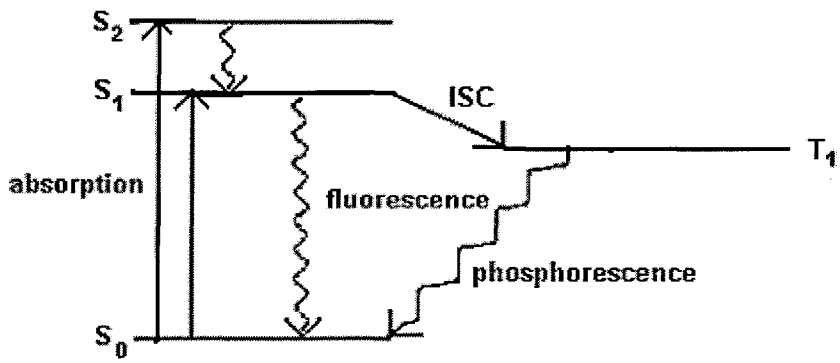

Figure 3. The Jablonski diagram.[10] *After absorption of a photon the excited fluorophore can undergo a series of events. ISC: intersystem crossing*

After absorption of a photon the fluorophore can undergo a series of processes. If the molecule is excited to one of the higher vibrational levels of the excited electronic states (v = 1, 2...), it may relax back to the lowest vibrational level (v = 0) of the first excited state (S_1). In a condensed phase this is the case almost without exception. From S_1 the fluorophore can get back to S_0 by emission of a photon (fluorescence). Intersystem crossing (ISC) between S_1 and T_1 (the singlet and triplet first excited states) is also a possibility. The $T_1 \rightarrow S_0$ transition (phosphorescence) is spin-forbidden and takes place at a considerably slower rate than fluorescence. Several other factors can influence the main processes (for example solvent effects, quenching, solvent relaxation, excited state reaction).[8]

The efficiency of the fluorescence can be described by the fluorescence quantum yield (Φ_F). The quantum yield is the ratio of the excited molecules that return to S_0 by emitting a photon by fluorescence and the number of the molecules in the excited state (*Eq 1*).

$$\Phi_F = \frac{k_r^S}{k_r^S + k_{nr}^S} = k_{kr}^S \cdot \tau_S \qquad \textit{Eq 1}$$

k_r^S is the radiative deactivation with emission of fluorescence, k_{nr}^S is the overall non-radiative constant, and τ_S is the lifetime of the S_1 excited state. k_{nr}^S consists of two terms, the rate constant for the $S_1 \rightarrow S_0$ internal conversion (k_{IC}^S), and the rate constant of intersystem crossing (k_{ISC}^S). The lifetime of the S_1 excited state, τ_S is given by *Eq 2*.

$$\tau_S = \frac{1}{k_r^S + k_{nr}^S} \qquad \textit{Eq 2}$$

Fluorescence spectra are represented as the fluorescence emission intensity plotted versus wavelength (nm) or wavenumber (cm^{-1}). Emissions are observed at longer wavelengths than the excitation wavelengths, as a loss of energy is inevitable. The energy difference between the absorption maximum and the emission maximum is called the Stokes shift. There are several factors that influence the magnitude of the Stokes shift. Some examples are relaxation from higher vibrational states to the lowest vibronic state, excited state reactions, and solvent effects.

As the same transitions are involved in both absorption and emission, fluorescence emission spectra often resemble the mirror images of the absorption spectra. Deviations are numerous, and are usually indicators of a difference in the arrangement of the nuclei in the ground and the excited states, or excited state reactions.

2.2.1 Photoinduced electron transfer

Photoinduced electron transfer (PET) is a process that is often responsible for quenching of the fluorescence. PET can take place if:

1. the excited fluorophore (**A***) can receive an electron from an electron-rich quencher (**D**). This is called a reductive electron transfer (*Figure 4a*).
2. the excited fluorophore (**D***) can donate an electron to an electron-poor quencher (**A**). This is called an oxidative electron transfer (*Figure 4b*).

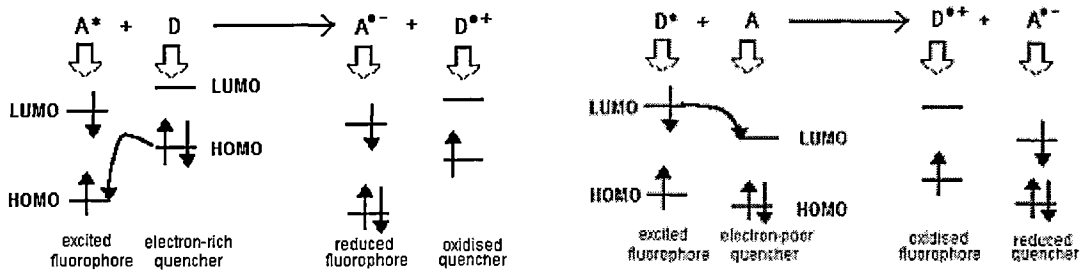

4a *4b*

Figure 4.[8] PET 4a, reductive electron transfer. 4b, oxidative electron transfer. PET is involved in many photochemical reactions. Many artificial fluorescent sensors exploit PET, the binding of the target to the receptor enabling the 'switching on' or 'switching off' of the electron transfer procedure, and thus the 'switching off' or 'switching on' of the fluorescence.

2.2.2 Resonance energy transfer

The excitation energy of a fluorophore (donor) can be transferred to a suitable acceptor if there is sufficient interaction between the two molecules. The energy transfer can occur if the absorption spectrum of the acceptor (**A**) overlaps the emission spectrum of the donor (**D**). This means that there are a number of vibronic transitions in the donor, which have almost the same energy as corresponding transitions of the acceptor. The term Resonance Energy Transfer (RET) is often used to describe the phenomenon, as such transitions are in resonance.

The interaction between the **D** and the **A** can be Coulombic, or due to intermolecular orbital overlap. The former consists of both long-range dipole-dipole interactions and short-range multipolar interactions, while the latter obviously can only be of short range. Long-range non-radiative transfers take place according to Förster's mechanism.[11-12] The transfer rate constant is dependent on the sixth power of the reciprocal of the distance between the donor and the acceptor. Short-range transfers can be described by Dexter's

mechanism.[13] The rate constant displays exponential dependence from the distance of the donor and the acceptor. [8,13]

RET has been applied for the measurement of distances between biologically important molecules. This 'spectroscopic ruler' is useful in the 10-100 Å range. Appropriately labelled pairs of biomolecules can display RET if they are close enough to each other, thus revealing the existence of association-dissociation processes, their dynamics, or enabling for example the determination of membrane thickness.[14] (*Figure 5*)

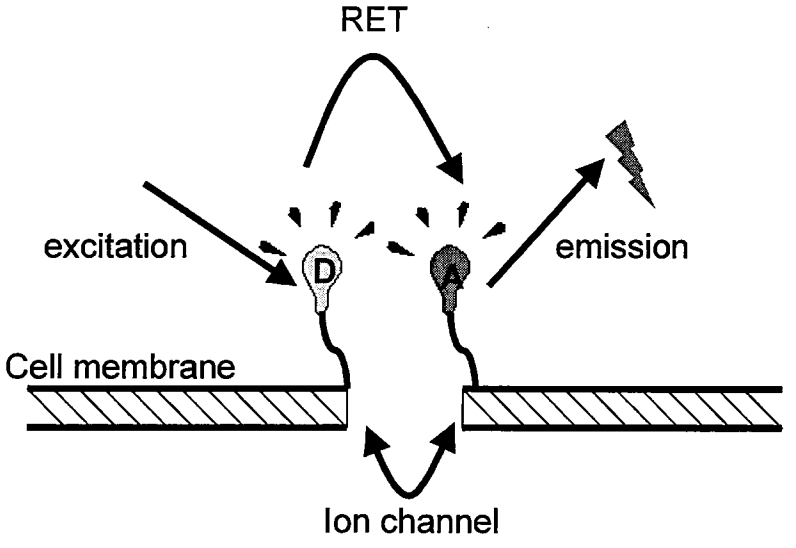

*Figure 5. Using RET for monitoring biological processes. The donor (**D**) and the acceptor (**A**) have to be close enough (approximately 80-100 Å) for RET to take place. A decrease in the **A** emission intensity reveals an increase in the **D-A** distance, in this case the opening of the ion channel.*[14]

Another useful property of RET is the 'red-shift' caused in the emission spectrum, which means that for example in fluorescent biological media the emission maximum of interest can be far away from the maximum of the background fluorescence.

The energy of the acceptor can be transferred to a non-luminescent acceptor as well as a luminescent one. This has been exploited in the detection of specific

oligonucleotide sequences by molecular beacons (MB).[15] MBs are single-stranded oligonucleotides with a **D** and a quencher (acceptor) attached to the 3' and 5' ends. In the absence of the target the beacon adopts a conformation which brings the **D** and the **A** close to each other. Initially the donor emission is quenched, and the beacon remains dark. Hybridization with the target sequence forces the ends of the beacon apart, energy transfer becomes impossible, and the beacon emits light. MBs have been used for example to detect nucleic acids in homogeneous assays, and the real-time monitoring of DNA-RNA hybridization in living cells.[16] Tyagi *et al.* have synthesised wavelength-shifting MBs.[17] The donor can transfer its energy to two acceptors, a non-luminescent and a luminescent one. If the MB is unhybridized, RET to the quencher is preferred and the beacon is non-luminescent. In the presence of the target the quencher is removed and upon donor excitation, emission from the luminescent acceptor is seen (*Figure 6*).

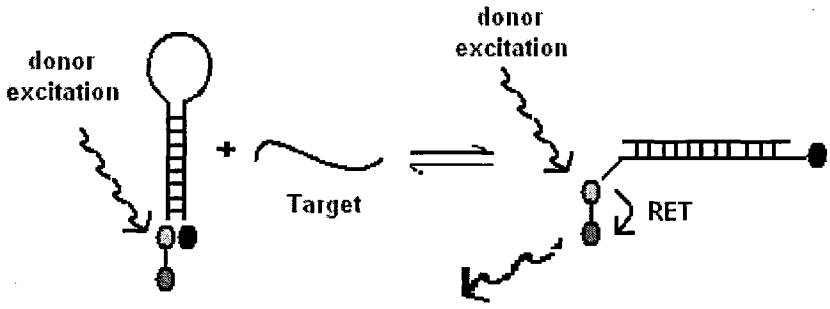

Figure 6. The principle of the wavelength-shifting molecular beacons. Hybridization removes the quencher from the donor's proximity, making RET from the donor to the luminescent acceptor possible.

2.2.3 *Fluorophores in luminescent probes*

2.2.3.1 *Organic fluorophores*

Organic compounds with delocalised double bonds are the most commonly used fluorophores, because the HOMOs and LUMOs of these molecules are divided by relatively small energy gaps, and excitation can be achieved by UV or visible light. Similarly, the emitted light is in the UV-Vis region, making the detection convenient. Some examples are quinine, porphyrins, coumarins, rhodamines and eosin (*Figure 7*).

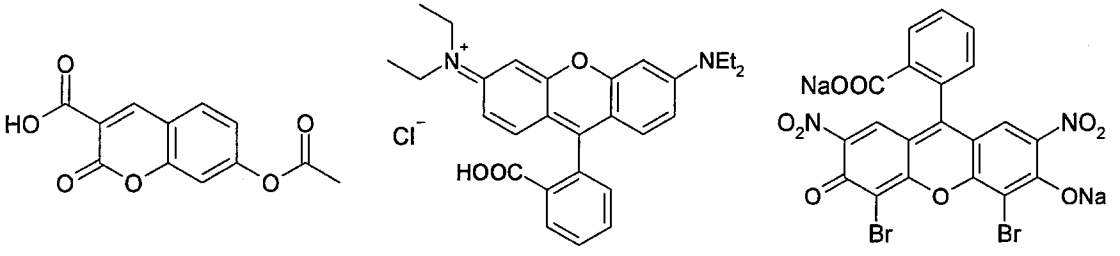

7-Acetoxycoumarin-3-carboxylic acid

rhodamine B

eosin B

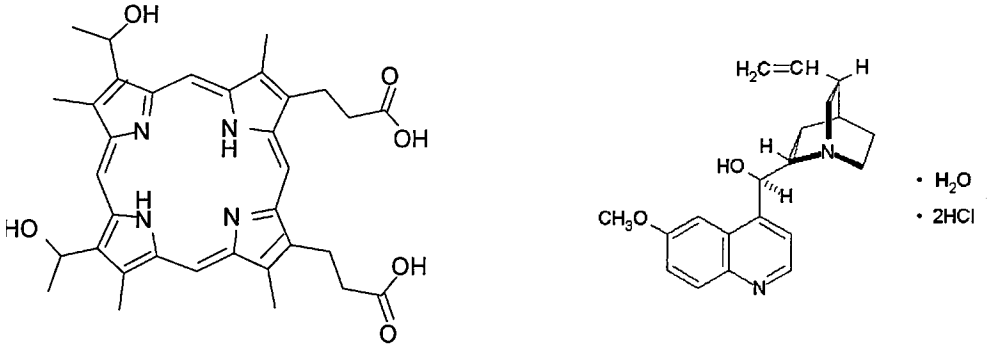

Haematoporphyrin

quinine dihydrochloride monohydrate

Figure 7. Widely used organic fluorophores.

2.2.3.2 *Luminescent transition metal complexes*

Several complexes of the metals of the d-block have luminescence, and many have been used as reporters in luminescent probes. The rhodium(II) complex $Rh(bipy)_3^{2+}$ has emission maxima around 590 nm and 645 nm, while

$Ru(bipy)_2Cl_2^+$ emits light at 710 nm. Both Pt(IV) and Ir(III) have luminescent complexes, but can easily undergo redox reactions, which reduces the stability and the quantum yield of the complexes. The Pd(IV) analogues of platinum are usually too unstable to be used as fluorophores.[18]

2.2.3.3 Luminescent lanthanide complexes

Lanthanide ions, for example europium(III) and terbium(III) have long-lived luminescence, and sharp, line-like emission spectra, which makes signal detection easy. Europium emission is > 550 nm, while terbium emits at wavelengths > 450 nm.[19]

To obtain a suitably luminescent compound, the lanthanide central ion has to be sensitised by a strongly absorbing antenna species, that can transfer its energy efficiently to the metal. Lanthanides have low absorption coefficients, as the f-f transitions corresponding to the absorption are parity forbidden. The antenna overcomes this by channelling its energy from the lowest lying triplet state. This triplet state has to be approximately 1000-2000 cm^{-1} above the emitting state of the lanthanide. It is also necessary for the antenna to be physically close to the metal, to make the sensitization efficient, as the energy transfer is distance-dependent. The antenna triplet state can also be quenched by other species present, oxygen for example, and this competing reaction is also minimised if the metal-antenna distance is short.

It is important to saturate the co-ordination sphere of the metal to stabilise the complex and to reduce quenching of the luminescence by nearby O-H, N-H or C-H oscillators. This can be done either by providing sufficient numbers of

carbonyl and tertiary amino donors, or by replacement of the hydrogens for deuterium atoms, or for fluorine.[20]

2.2.3.4 Near IR-emitting lanthanide complexes

In general, complexes with europium and terbium central ions are well established, and there are examples of their use in fluoroimmumoassays and fluorescence microscopy. Less work has been done on complexes with near-IR emitting lanthanides ytterbium and neodymium. These are of particular interest for medical imaging purposes. Luminescence detection *in vivo* is complicated in many cases by excitation wavelengths < 340 nm, at which wavelength many natural species absorb. For europium and terbium complexes aromatic antennae with absorption maxima at 320-360 nm are used. If europium and terbium are replaced with the near-IR emitting Nd or Yb, sensitising can be achieved by metal complexes or organic molecules absorbing at ~ 500 nm. As human tissue becomes more transparent on increasing of the wavelength, it is easy to see the advantages of using near-IR emitters for medical imaging.

Efficient sensitisation of neodymium and ytterbium has been possible with a number of antennae. Purely organic materials, like fluorescein, eosin or fluorexon[#] have been successfully used. They all have absorption maxima around 500 nm, and in many cases several differently functionalised derivatives are available, which facilitates the ligand synthesis.

When luminescent metal complexes are used as antenna chromophores, the sensitising metal is usually a d-block element, as it is synthetically more difficult

---

[#] fluorexon: Bis[*N*,*N*-bis(carboxymethyl)aminoethyl]fluorescein

to produce f-f bimetallic complexes. There are examples of porphyrin-palladium complexes being used as antennae, and a terpyridyl complex of platinum has been applied for the sensitisation of neodymium.

2.3 Sensors

Depending on the target, sensors can be categorised as recognising (a) cations, (b) anions, and (c) neutral species. The most abundant examples are those of cation recognition as cations are generally spherical. Therefore the host can be constructed by considering only the size of the ion (the radius of the sphere) and the charge density. Anions can possess a wide range of structures (for example spherical – F^-, trigonal – CO_3^{2-}, tetrahedral – SO_4^{2-}), and in solution can display pH-dependent speciation (for example HCO_3^- and CO_3^{2-}). When designing a probe for a given anion, both of these have to be taken into account. Also, anions usually have high free energies of hydration (for example -1315 kJ mol^{-1}, CO_3^{2-}; –335 kJ mol^{-1}, HCO_3^-; -465 kJ mol^{-1}, F^-),[21] making the construction of artificial receptors applicable in aqueous media difficult.

The development of efficient fluorescent sensors for biological applications is complicated because of the large differences in the concentration of the same species in various cell types and thus the need for a linear response for a concentration range of several orders of magnitude. Useful probes for intracellular metal ion measurements would impose strict rules upon the properties of the sensor molecules. Apart from high selectivity for the ion in question in the presence of other metal ions it would have to:

1. be water soluble
2. have dissociation constants in the concentration ranges of the metal ions to be measured
3. have a change in fluorescence upon chelation with the ion
4. have excitation wavelength > 340 nm to avoid excitation of aromatic amino acids and DNA and the usage of quartz optics

5. have emission wavelengths > 500 nm to exclude autofluorescence
6. have fast response time, preferably on the millisecond time scale
7. be able to operate under cellular conditions (pH, toxicity, stability).

2.3.1 Cation probes

There are several fluorescent probes for all of the alkaline and alkaline earth metals[28-37] except for magnesium, but only a few exist for some of the transition metals (for example zinc, [22-24] copper(II) or mercury(II) [25]). This is mainly because while ions of the first and second group are spherical, possessing one or two positive charges (but only one of them), transition metals can have several oxidation states and are able to form complexes of various geometries.

2.3.1.1 Transition metal probes

Tsien and co-workers constructed the fluorescent Zn^{2+} sensors Zinpyr-1 (**1**) and Zinpyr-2 (**2**).[22,23] The molecules absorb and emit in the UV-visible region, have high quantum yields (Φ_F = ~0.9) and low dissociation constants (> 1 nM). The sensors utilise fluorescein as a reporter and three to five-fold fluorescence enhancements were observed upon Zn^{2+}-binding. Photoinduced electron transfer from the alkyl nitrogens can quench the fluorescence of the fluorescein reporter. As the PET can be suppressed both by the complexation of zinc and protonation of the alkyl nitrogens, the probes were pH-responsive as well as zinc-responsive.

Another fluorescein-based Zn^{2+} sensor was constructed by Hirano *et al.*[24] ACF-2 (**3**) can be excited with visible light and shows ~24-fold fluorescent intensity enhancement upon addition of 5 μM Zn^{2+}. Most biologically important metal ions

induced < 20% fluorescence enhancement, the only exception being Cd^{2+}, with a six-fold fluorescence enhancement. No data were available for competition with protons (all measurements were performed at pH 7.5), but the aniline-type nitrogen is expected to have a lower pK_a value than the nitrogen next to the chromophore in Zinpyr, consequently being less available for protonation.

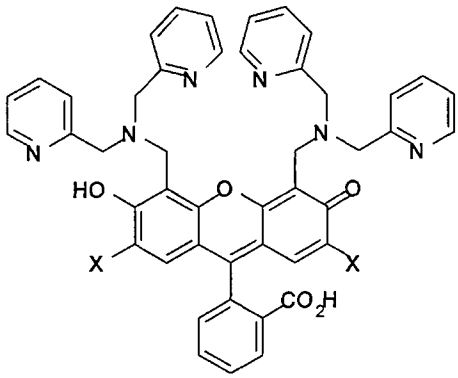

X = Cl **1**, X = H **2**

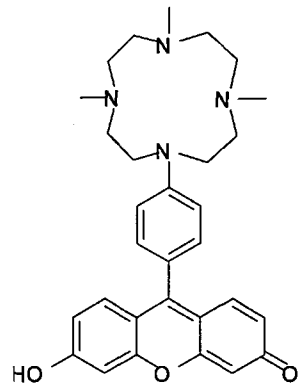

3

The fluorescent probe **4** exploits chelation enhanced quenching (CHEQ) of fluorescence caused by the incorporation of transition metal ions[25]. **4** is sensitive to two transition metal ions, Hg(II) and Cu(II). Titrations showed eighteen-fold and four-fold overall emission changes with Hg(II) and Cu(II) respectively. The authors explained the differences in the observed CHEQ by proposing different binding modes for Cu(II) and Hg(II). According to their suggestion Cu(II) binds to the four amino groups solely, as both **4** and its open-chained analogue displayed similar affinities for Cu(II). Hg(II) forms the complex with the two nitrogens adjacent to the anthracene and also interacts strongly with the aromatic rings as shown in **4a**. This idea was supported by the observations in the UV-Vis spectrum of the anthracene. The absorption peak of the anthracene at 368 nm changed upon addition of Hg(II), resulting in complete loss when ~3 equivalents of metal ion were added.

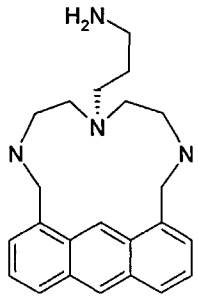

4

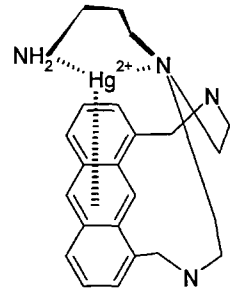

4a

Shen and Sullivan[26] have synthesised a series of polypyridine-based rhenium complexes for applications in luminescent sensing of pH, anions, and cations. Treatment of the lead-responsive complex **5** in methanolic solution with $Pb(OAc)_2$ results in 270% increase in integrated intensity and ~20 nm red shift in the emission maximum. The same complex showed only moderate red shifts and only 25% emission intensity increase upon addition of large (fifty-fold) excess of barium. The emission of the zinc analogue of **5a** in acetonitrile is red-shifted to ~600 nm, and protonation of the lone pair results in quenching of the fluorescence.

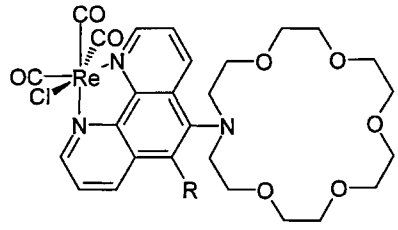

5 R = H, **5a** R = NMe_2

2.3.1.2 Alkali and alkaline earth metal ion probes

The detection of alkaline and alkaline earth metal ion in cells, blood samples and urine is of major importance, because deviations from the normal concentrations can be indicators of pathological conditions.

So far results on the development of fluorescent probes for Na^+, potassium, Li^+, Cs^+ and Ca^{2+} have been reported. Although ^{19}F-NMR detection of Mg^{2+} in cells has been possible for a long time, and it is possible to estimate the mitochondrial magnesium concentration with luminescent probes,[27] selective fluorescent magnesium probes are currently unavailable.

The lariat ether derivative **6** contains two pyrene ring reporters[28]. Upon complexation with alkaline earth metal ions the exciplex emission (λ_{max} = 480 nm) attributed to the intramolecular π–π stacking of the rings decreases, and the monomer emission (λ_{max} = 395 nm) increases dramatically. The spectral change is ascribed to the co-operative binding of the metal ion by the crown ether moiety and one of the sidearms. Alkali metal ions (Li^+, Na^+, K^+) did not induce changes in the emission spectra. Stability constants (log *K*) in acetonitrile : chloroform (99:1) for 1:1 complexes **6**:Ca^{2+}, **6**:Sr^{2+}, **6**:Ba^{2+} were determined to be 7.6, 6.8 and 6.9 respectively, the sensor showing size selectivity towards Ca^{2+} and Sr^{2+} in the presence of seven other alkali or alkaline earth metal ions.

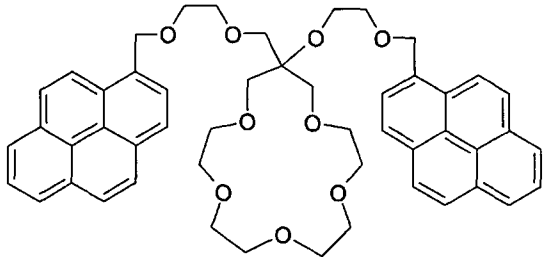

6

Tsien and co-workers have synthesised a series of calcium-responsive fluorescent probes to determine the physiological role of cytosolic free calcium.[29] The sensors **indo-1** (**7**) and **fura-2** (**8**) contain 8-coordinate tetracarboxylate binding sites and stilbene-type chromophores. The double

bond of the stilbene is rigidified by incorporation into a heterocycle. The absorption maximum for the free ligand **fura-2** is at 362 nm and this is shifted by complexation with Ca^{2+} to 355 nm. Similar results were obtained for **indo-1**. Both the free and the complexed species have bright fluorescent emissions, **fura-2** having an emission wavelength maximum at 512 nm for the free anion and 505 nm for the calcium complex. However, the wavelength shift induced by the metal binding is not significant. The quantum yields for the free and the complexed **indo-1** are 0.38 and 0.56, respectively, while for **fura-2** these values are 0.23 and 0.49. Apparent dissociation constants determined in aqueous solutions containing physiological concentrations of Na^+, K^+, and Mg^{2+} were 250 nM for **indo-1** and 224 nM for **fura-2**. Competition experiments with **fura-2** indicated that the absorption and emission spectrum of the complexed ligand changed only slightly unless in the presence of a very large excess of magnesium ions.

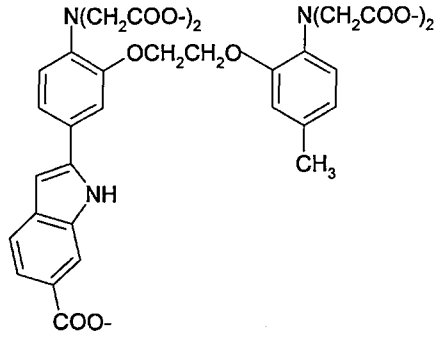

indo-1

7

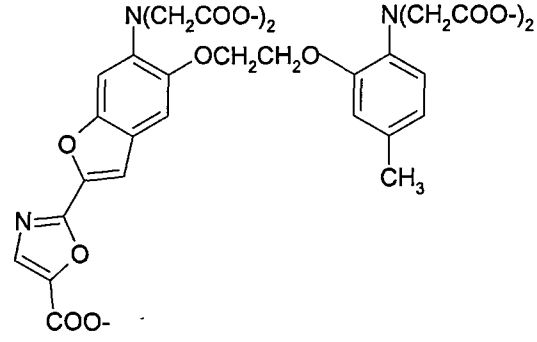

fura-2

8

Blackburn *et al.* sought a water-soluble extraction agent and lithium-responsive indicator. The monoaza-crown ether **9** responds to complexation with lithium by shifting the emission maximum to shorter wavelengths (from 485 nm to 462 nm).[30] The fluorescence quantum yield of the complex (Φ_F = 0.04) is greater

than the uncomplexed azacrown ether. The nitrogen next to the aromatic ring is less basic than alkyl-substituted nitrogen atoms in general, which minimises interference with protons. Complexation measurements were carried out in acetonitrile, and there was no indication of competition by other alkaline metal ions. The poor quantum yield is the major drawback of the probe.

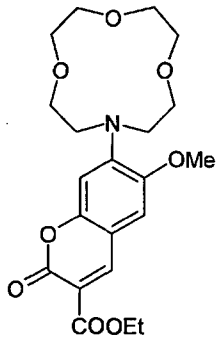

9

Smith *et al.* have described an early example of a sodium probe, **FCryp-1**.[31] The cryptand was designed to measure the concentration of intracellular free sodium using ^{19}F-NMR. The ligand contained four carboxylate groups, masked by esterification, which helped the transfer of the sensor through the cell membranes. Once inside, the esterases cleaved the ester groups, rendering the molecule sufficiently water-soluble (up to 10 mM). Incorporation of a chromophore provided the fluorescent sensor **Fcryp-2** (**10**).[32] The free molecule has emission maximum at 460 nm, which is shifted to 395 nm when sodium is added. The quantum yield of the complex in aqueous solution (pH 7.0, 37 °C, 100 mM KCl) is higher than 0.7. The emission wavelength is too short for general applications, but **Fcryp-2** proved to be a useful tool for Na^+ measurements for cells that do not autofluorescence strongly at 395-450 nm (e.g. lymphocytes and fibroblasts). The cryptand forms a 1:1 complex with sodium, and the dissociation constant is ~6 mM. The affinity of the sensor

towards potassium was too low to be determined, and the presence of biologically relevant concentrations of Ca^{2+} and Mg^{2+} did not affect the absorption or emission spectra.

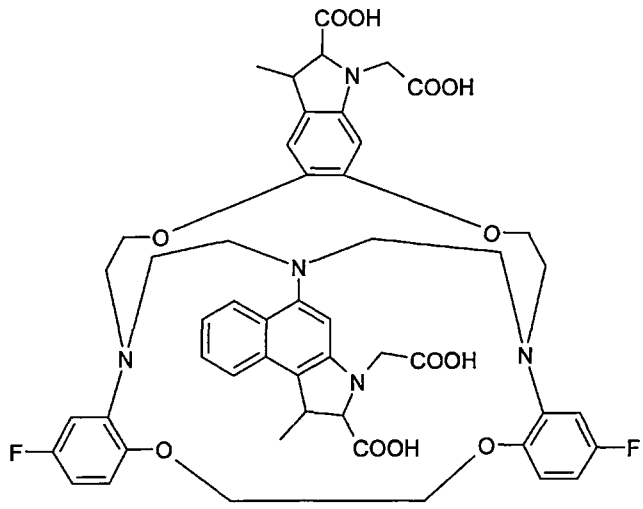

Fcrypt-2

10

Minta and Tsien[33] synthesised a series of compounds to obtain a fluorescent sodium indicator applicable to measurements of cytosolic free sodium. Several reporter and binding units were tested, until the authors finally settled with sodium-binding benzofuran isophthalate (**SBFI**) (**11**). **SBFI** contains two benzofuran fluorophores linked to isophthalate groups. The selectivity of **SBFI** for sodium over potassium was determined to be ~20. The effective dissociation constant (against the background of ~120 mM K^+) was approximately 20 nM. In order to determine the applicability of the sensors for biological conditions, a series of stability measurements was carried out. At pH 7.05, both in mixtures of Na^+ and K^+, and solutions containing $[K^+]+[Na^+]$ = 135 mM and Mg^{2+} at concentrations reasonable for vertebrate cytoplasm, K_a values were measured to be 17-19 mM. The fluorescence quantum yields are 0.08 and 0.045 with and without Na^+, respectively. Sodium binding shifts both the excitation and the

emission spectra to shorter wavelengths. Excitation can be performed at 360 nm. Emission maxima are 551 nm without Na^+ and 525 nm for the complex.

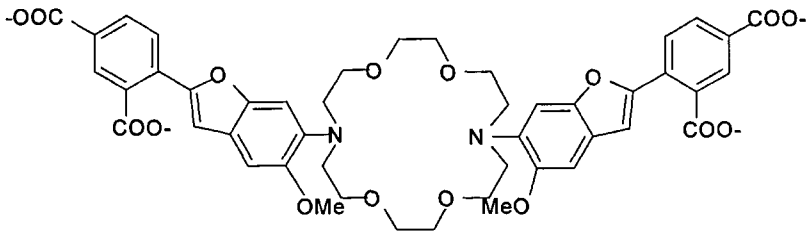

SBFI

11

SBFI (**11**) and an isomer, sodium-binding benzofuran phthalate (**SBFP**) were tested in lymphocytes and fibroblasts. Both dyes could be introduced by microinjections, but when the tetraethyl esters were synthesised and incubated with the cells, only the **SBFI** appeared in the cytoplasm, which makes it the preferred probe of these two.[34]

Potassium is a major ionic constituent of living cells. Intracellular concentrations are typically ~150 $mmol \cdot dm^{-3}$, while extracellular levels are approximately 4 $mmol \cdot dm^{-3}$. Monitoring changes in potassium ion concentration is important in order to study for example the effect of drugs, or ionic equilibrium disorders. During signal transduction, neurons change their potential by rapidly releasing potassium ions into the environment. The cells compensate for the cation loss by initial sodium uptake. The normal $[K^+]$ and $[Na^+]$ are finally restored by the sodium-potassium pump. As changes in $[K^+]$ are < 5%, responses in fluorescence are consequently low. The fluorescent probes **CD18** (**12**)[35] and **CD222** (**13**)[36] were prepared for intracellular and extracellular measurements of potassium ions. K_d(**CD18**) is 140 mM under physiological conditions, while K_d(**CD222**) is 13.5. The increased stability of the complex is due to the replacement of the azacrown-ether for the cryptand in the binding moiety. Both

CD18 and **CD222** offer good selectivity over sodium ions. The coumarin-based reporters are excitable at wavelengths close to 400 nm and have emission maxima of 486 nm and 476 nm, respectively.

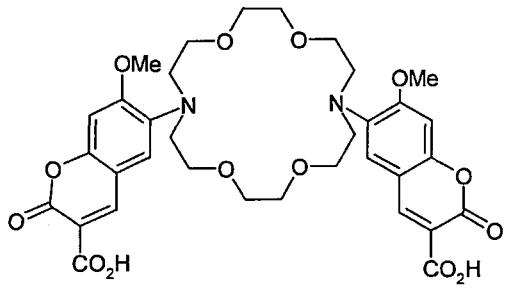

CD18

12

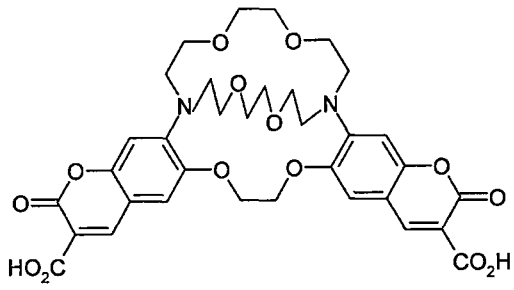

CD222

13

For the detection of caesium ions and their removal from nuclear waste calix[4]biscrown ether-type ligands were suggested.[37] Valeur and co-workers constructed the fluorescent sensors **Calix-COU1** (**14**) and **Calix-COU2** (**15**), incorporating calixarene ligands.

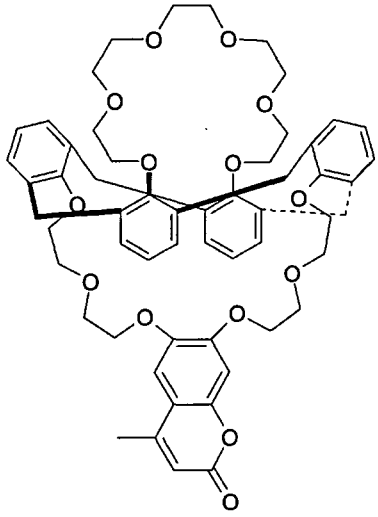

Calix-COU1

14

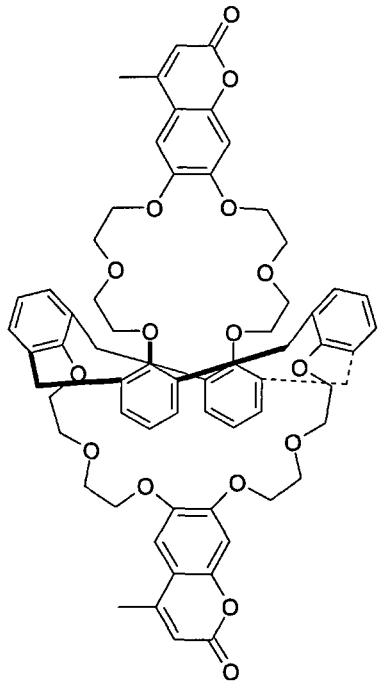

Calix-COU2

15

The 3,4-dimethoxycoumarin-derivatives signal the binding of the metal ion. The sensors are particularly sensitive to caesium ions, and also show very good selectivity towards potassium ions in the presence of sodium ions. Cation-binding measurements were conducted in non-aqueous media (acetonitrile and ethanol) to determine the K_a values for the Cs^+, K^+, and Na^+ complexes. The fluorescent sensors exhibited excellent selectivity towards caesium *vs* sodium ions and promising results were obtained for the selectivity towards potassium *vs* sodium.

For ion detection in biological samples water-soluble probes are usually sought. The authors claim that the insolubility of **Calix-COU1** and **Calix-COU2** in water is more an advantage than a drawback, as their aim is to immobilise the sensors in polymer films, in which case water solubility could enhance leaking. As leaking is determined by several factors (for example the mode of immobilisation), however, solubility is not the single most important parameter.

2.3.1.3 pH sensors

Examples for the sensing of H^+ (pH) are abundant and the vast majority exploit the Brønsted-Lowry basicity of aliphatic amines.[38] In a 'typical' pH sensor the chromophore is bound to an amine by a methylene or ethylene spacer. If not protonated, fluorescence is quenched by photoinduced electron transfer (PET). Protonation of the amine lone pair disrupts the PET, and the presence of the protons is signalled by the 'switching on' of the fluorescence. Naturally the pK_a of the amine can be tuned by attaching groups of varying electronegativity to the amine. Two examples of pH-sensitive fluorescent probes working on the basis of PET-quenching are **16** and **17**.

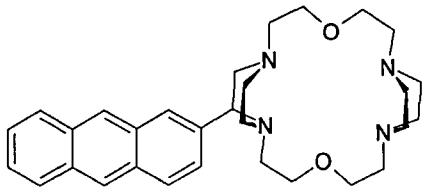

16

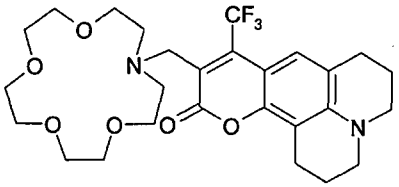

17

Some of the H^+-responsive probes, such as the Pb^{2+}-receptor-containing **16**,[39] or **17**,[40] which shows metal ion-induced fluorescence enhancement with several alkali and alkaline earth metals, were originally designed for the detection of other cations, rather than H^+. Due to the presence of the aliphatic amines, they are sensitive to changes in the pH. If it is crucial to avoid the competition between the target cation and the protons, it is common to attach the amines of the receptor to an aromatic ring, and thus raising their pK_a values.

The compounds **18, 19** and **20**[41] were designed to be proton probes and have pK_a values of 7.1, 4.7 and 9.6, respectively. **18** and **19** have the same coumarin reporter. Substitution of two hydrogens by a hydroxyl in the 2 position on the N-ethyl groups decreased the pK_a by 2.4. In **20** the same diethylamino receptor that is present in **18** is attached to a strongly electron-withdrawing group, which decreases the pK_a.

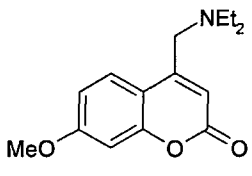

18

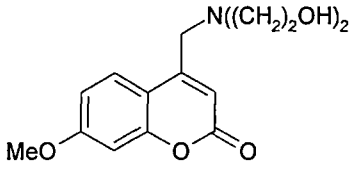

19

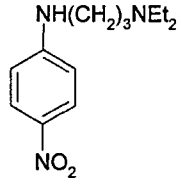

20

2.3.2 Anion receptors

Anions play important roles in a number of biological processes, for example a large number of enzymes bind anions as co-factors or substrates, and anions can act as bases, nucleophiles, redox agents or phase-transfer catalysts.[42] Anion probes have become increasingly abundant in the past decade. Several examples exist for the halides fluoride and chloride, and hydroxide, carbonate and hydrogencarbonate, phosphate, and especially the polyanion DNA.

Sessler and co-workers have synthesised the extended octaethylporphyrin analogue, sapphyrin (**21**) and found that the diprotonated form is an efficient binder of fluoride ions.[43] The sapphyrin showed over a thousand-fold selectivity for fluoride against both chloride and bromide. Upon addition of TBAF to the methanolic or DCM solution of the probe, the fluorescence emission decreased and was shifted to longer wavelengths.

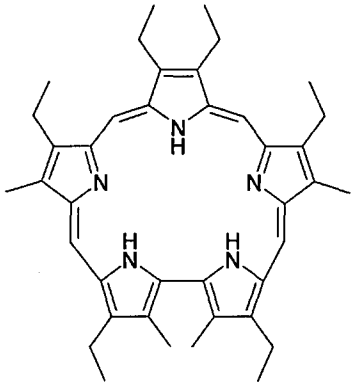

21

A recently synthesised fluorescent anthracene derivative (**22**) bears two phenylurea groups at the 1 and 8 positions.[44] Fluorescence was efficiently quenched by fluoride ions. The probe has 120-fold selectivity for fluoride in the presence of chloride and even greater than that of bromide.

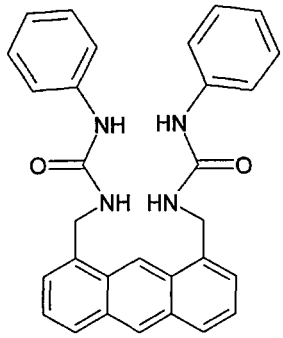

22

The zinc complex of a tris(2-aminoethyl)amine functionalised anthracene molecule was reported to be a useful probe for a series of carboxylate ions.[45] The binding event was signalled by quenching of the fluorescence of the zinc complex, presumably due to intramolecular electron transfer from the zinc-bound carboxylate subunit to the photoexcited anthracene moiety.

The same reporter without the metal centre was used by Czarnik and co-workers for chelation enhanced fluorescence detection of non-metal anions at pH 6.[46] The anthrylpolyamine molecule is nonfluorescent when the benzylic nitrogen lone pair is not protonated. Complexing phosphate or carboxylate brings an OH-group of the anion into close proximity of the benzylic nitrogen, thus protonating it, which results in the recovery of the fluorescence. A similar, although less pronounced, effect is achieved with acetate or sulphate. These latter species are fully deprotonated at pH 6, but are capable of stabilising an ammonium ion in their vicinity. If the anthracene is dialkylated with the polyamino moiety, the probe is only weakly fluorescent at pH 7.[47] Complexation with pyrophosphate doubles the fluorescence intensity. The molecule can discriminate between pyrophosphate and phosphate, having a 2200-fold higher affinity for the former, allowing for real-time pyrophosphate hydrolysis.

Pyrophosphate and other anions possessing two binding sites are recognised by yet another bis-alkylated anthracene derivative. Fluorescence from the 9,10-bis(phenylthiourea) modified anthracene reporter is quenched due to PET from the thioureas to the anthracene, when dicarboxylates or pyrophosphate are bound to the probe.[48] The fluorescence of the monoalkylated analogue of the same receptor was quenched selectively by acetate, dihydrogen phosphate and fluoride, but not with either chloride or bromide.[49]

There are several examples for the recognition of both nucleotides and DNA, of which only a few will be mentioned here. Lehn and co-workers synthesised the acridine-appended polyaza-macrocycle probe for the sensing of nucleotides and the monitoring of nucleotide hydrolysis.[50] The acridine moiety serves both as a luminescent reporter and to stabilise the complex by stacking interaction with the nucleotide base. The triphosphate polyanionic part forms multiple hydrogen bonds with the polyammonium macrocycle. Electrostatic interactions play and important role, as at pH 7 the macrocycle is protonated, and its positive charges can interact with the negative phosphates. **23** also binds strongly to DNA, but is not capable of promoting its chemical or photochemical cleavage.

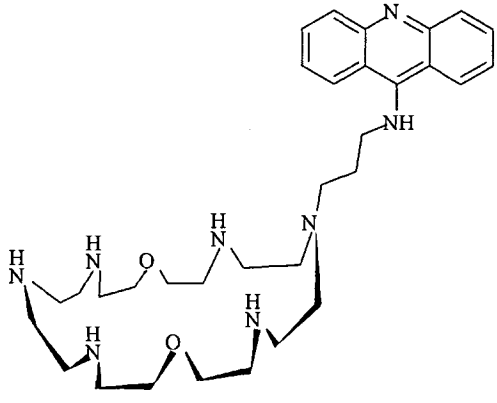

23

Lanthanide luminescence has been exploited in several cases for detecting DNA. An elegant way of probing single-stranded DNA by fluorescent sensors was developed by Sammes and co-workers.[51] The complementary DNA strand (probe) was labelled with europium(III), which under the analysis conditions is not fluorescent. Then an intercalator-sensitiser unit (**24**), capable of both chelating the lanthanide ion and stacking between the nucleobases, was added.

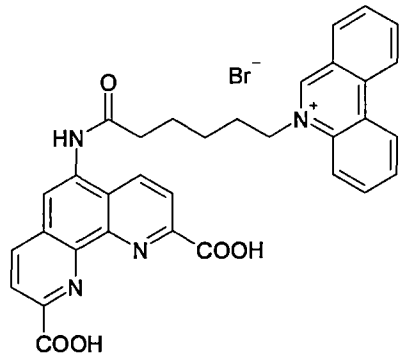

24

The presence of the sensitizer unit resulted in 'switching on' of the lanthanide luminescence. The intercalating phenanthridinium salt was linked covalently to the lanthanide chelating 1,10-phenanthroline-2,9-dicarboxylic acid. The principle of the probe is outlined in *Figure 8*.

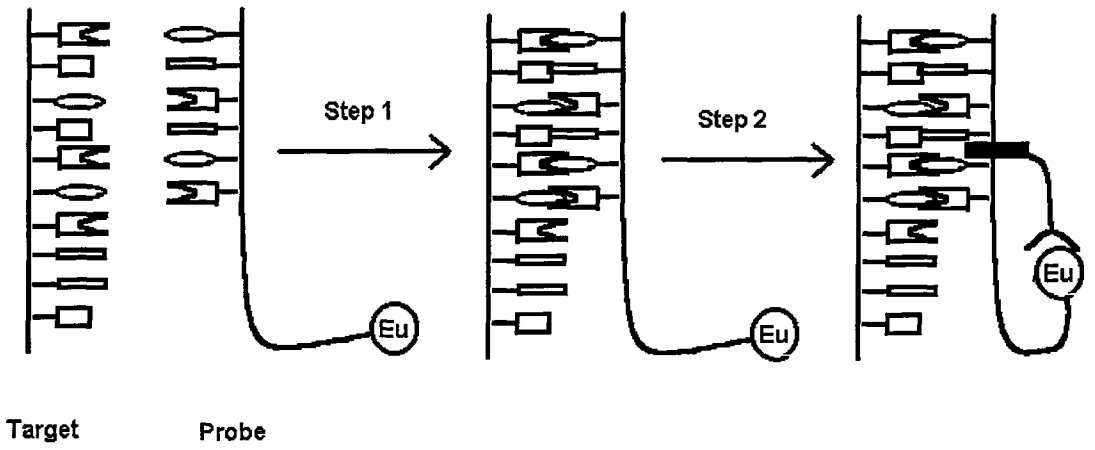

Figure 8. The principle of the intercalating DNA-probe with luminescent europium(III) reporter. Step 1: Labelled probe seeks and hybridises to target DNA strand. Step 2: The intercalator-sensitizer moves along the duplex until it reaches the metal ion. Only the co-operative complex gives rise to a signal upon irradiation.

The europium and terbium complexes of **25** were found to intercalate with poly(dAdT), poly(dGdC) and calf-thymus DNA.[52] The tetraazatriphenylene chromophore serves as the sensitizer for the lanthanide luminescence. The excited state of the heterocycle is quenched upon intercalation with DNA, and it consequently loses its ability to sensitize the lanthanide emission, thus signalling the presence of the nucleic acid. Nucleic acid binding had similar effects on the near-IR emission of Yb(III)·**26**, where a porphyrin derivative replaced the tetraazatriphenylene antenna.[53]

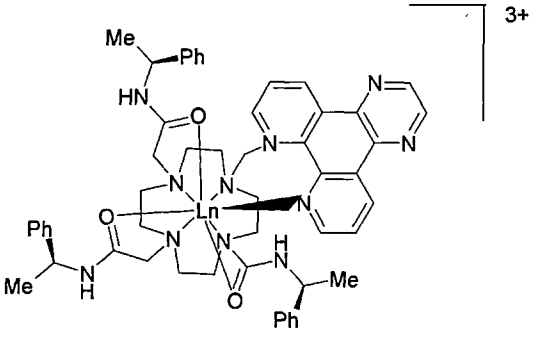

25

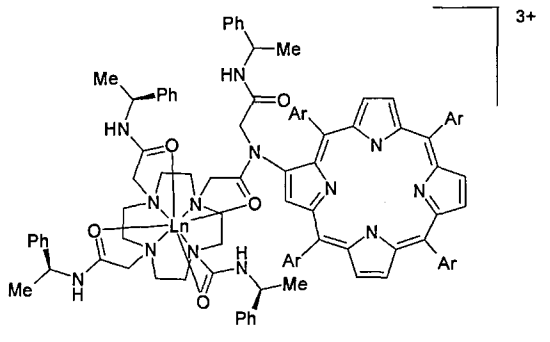

26

The fluorescence of the europium complex **27** is quenched by halide ions, presumably due to a heavy atom effect,[54] and hydroxide ions above pH 10, too.[55] The quenching by chloride was pH-independent and was not affected by a range of other biologically important ions, i.e. phosphate, citrate, lactate or carbonate. The N-demethylated analogue of the complex can function as a pH-responsive fluorescent probe, because protonation and deprotonation of the ring nitrogen affects the ability of the antenna to sensitize the terbium.

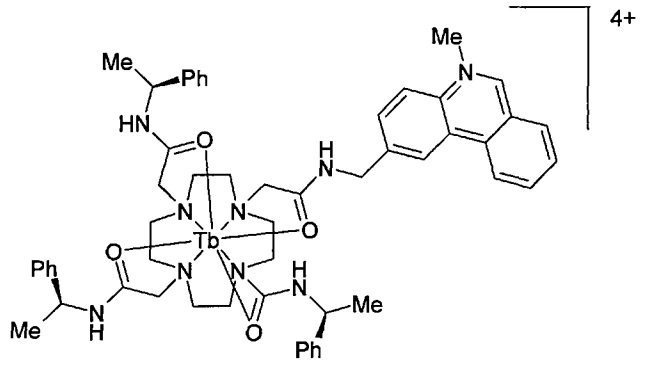

27

The affinity of the water-soluble probe **28** for phosphate, lactate, citrate, malonate, hydrogencarbonate / carbonate and acetate was determined.[56] The affinity constants were dependent on several factors, among them the charge of the anion and the mode of binding. Thus carbonate that is mainly hydrogencarbonate, and possesses one negative charge at the pH of the measurements, forms a chelate with the cation, resulting in the loss of a proton and a decrease of the charge; increasing the binding constant. The binding event induces up to threefold intensity increases in the emission spectra at 618 nm. It was possible to monitor complex formation with carbonate in aqueous solutions simulating the anionic composition of extracellular fluids.

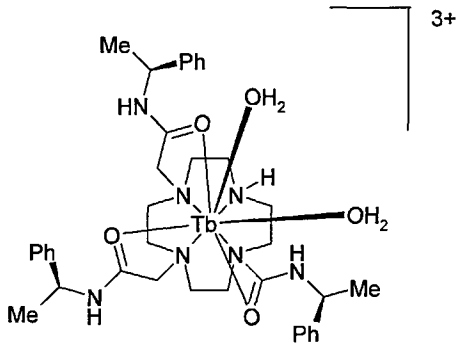

28

Beer and co-workers have synthesised a series of selective abiotic anion receptors.[57] Most of their work on dihydrogenphosphate-responsive probes uses electrochemical detection by the means of various metallocene reporters, but they have also reported a series of ruthenium-bipyridyl complexes that signal the presence of anions.[58]

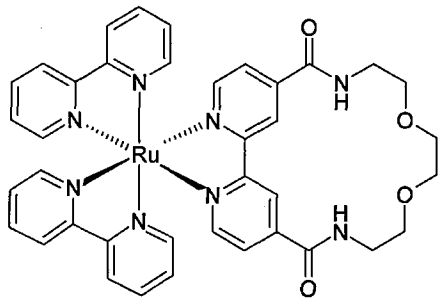

29

Upon addition of chloride or dihydrogen phosphate the MLCT fluorescence emission from the ruthenium(II) polypyridyl complex **29** was blue-shifted. Also considerable fluorescence intensity enhancements were observed. The acyclic (**30**) and calix[4]arene (**31**) analogues of **29** were also synthesised and had similar spectral and anion binding properties.

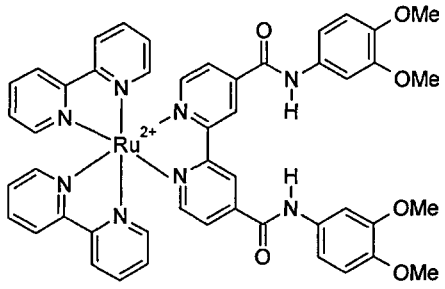

30

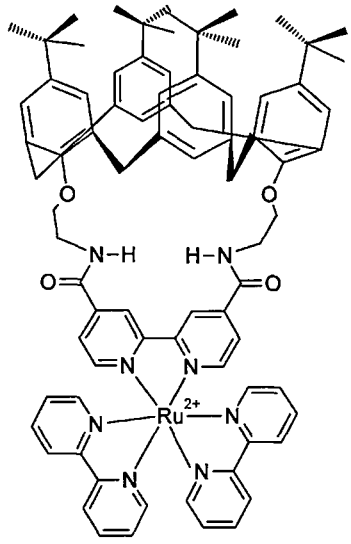

31

The calix[4]arene ligand **31** senses dihydrogen phosphate selectively (as determined electrochemically) in the presence of tenfold excess of hydrogensulphate or chloride.[59]

While the $[Ru(bipy)_3]^{2+}$ (**30**) has enhanced affinity for dihydrogen phosphate in the presence of chloride ions, **32** binds chloride selectively in the presence of phosphate, as both NMR and fluorescence measurements confirmed.[60] Excess $H_2PO_4^-$ had no effect on the emission spectrum of **32**, while addition of chloride increased the emission intensity and shifted the emission from the ruthenium by 6 nm to higher wavelengths. This makes **32** one of the first chloride-selective fluorescent probes.

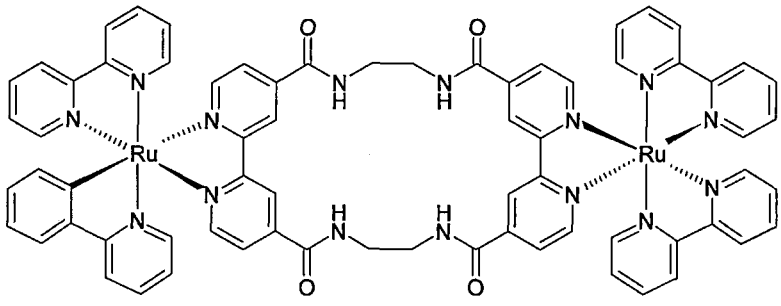

32

The metal-centred luminescence of the europium bipyridyl complex **33** is increased eleven-fold when nitrate ions were added to the solution of the ligand in acetonitrile.[61] With terbium, sevenfold increases in fluorescence intensities were detected. Other anions (chloride, fluoride and acetate) had similar effects on the luminescence of the complexes. The association constants were determined to decrease in the fluoride > acetate > chloride > nitrate order for the 1:1, 1:2 and 1:3 (ligand : anion) complexes.

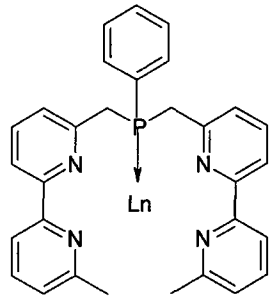

33

2.3.3 Sensing neutral species

Although fluorescent probes for neutral species exist, there are far fewer of them, than probes for cation or anion sensing. Only a few examples will be given here, more can be found in de Silva's review of molecular switches. [27]

Yoon and Czarnik reported in 1992 the quenching of fluorescence from anthrylboronic acid in the presence of sugars.[62] Another example of sugar sensing was described by Shinkai and co-workers, who combined fluorescence and circular dichroism to investigate recognition of saccharides in methanol : water 1:1.[63] The cyanine dye **34** formed intramolecular 1:1 complexes with monosaccharides, binding D-fructose most strongly (K_a = $1.3 \cdot 10^5$). Upon complexation the fluorescence intensity increased by approximately threefold, probably due to the rigidification of the structure of the dye. Those sugars that

can only form 2:1 complexes with diboronic acids induced no increase in the fluorescence intensity.

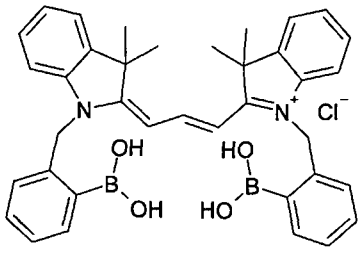

34

The compound **35** has been designed to serve as an artificial receptor for uronic and sialic acids in aqueous solutions.[64] Saccharide (diol) binding was ensured by the incorporation of the boronic acid moiety into the receptor, while the 1,10-phenanthroline-Zn(II) chelate helped the recognition of the carboxylate.

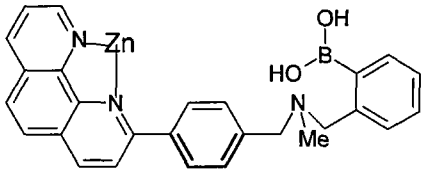

35

The log K values of several monosaccharides and uronic acids with the zinc-free receptor **35** were too low to be determined. Complexation of zinc considerably increased the stability of the receptor(Zn(II))·uronic acid complexes. Fluorescence emission spectra were recorded in water / methanol (1:2) at pH 8.0, at 375 nm. Addition of D-monosaccharides to the solution of the zinc complex induced 1.5-fold, while that of D-glucuronic acid and D-galacturonic acid 3.5-fold and twofold fluorescence enhancements.

The binaphthyl derivative was synthesised by Shinkai and co-workers and applied for chiral monosaccharide recognition. Preliminary results with **36**, the first artificial receptor for chiral sugar recognition, suggested that chiral discrimination between enantiomers could be enhanced by rigidifying the

structure of the host, as in **37**. This indeed was found to be true, as the magnitude of fluorescence enhancement was different for enantiomeric sugars, the greatest difference (1.0:8.7 = D:L) was observed for xylose. [65]

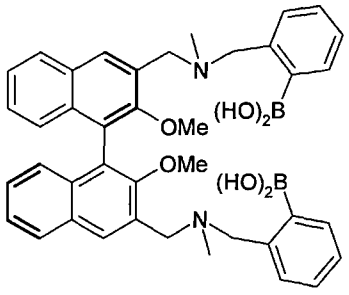

36

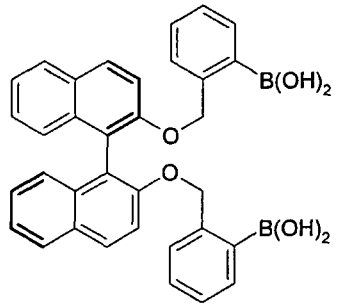

37

Cooper and James synthesised the fluorescent probe **38** for the signalling of D-glucosamine hydrochloride at pH 7.18.[66] The boronic acid moiety serves to recognise the diol 'unit' in the target molecule, while the aza-crown ether binds the ammonium function. As both the boronic acid and the nitrogen atom of the aza-crown ether can participate in PET, the fluorescence is only recovered when both receptors are occupied by the guests.

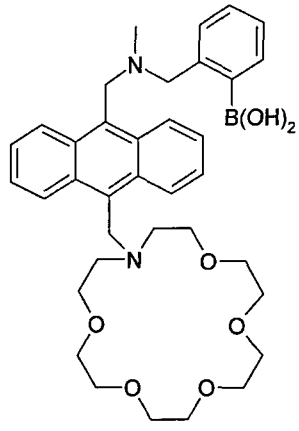

38

The fluorescent PET sensor **39** shows two to three-fold fluorescence enhancement in methanol / water (3:2) in the presence of GABA, or related amino acid zwitterions.[67] The amino function of the amino acid is recognised by the monoaza-18-crown-6 ether receptor already known from the D-glucosamine

probe (**38**) synthesised by Cooper and James, while the guanidinium unit binds the carboxylate end.

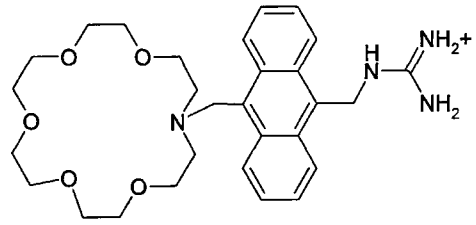

39

Motesharei and Myles have incorporated the fluorescent probe **40** into alkanethiolate-functionalised gold nanoparticles, in order to probe molecular recognition events at organic interfaces (*Figure 9*).[68] The receptor moiety of **40** is fluorescent itself, and when barbiturate ligand **41** occupies the binding pocket the fluorescence emission is shifted by 4-11 nm to longer wavelengths, the effect being most pronounced for non-polar, aprotic solvents, and can be completely reversed by rinsing with ethanol. When covalently bound to the gold particles, the recognition event shifted the emission wavelength by 12-14 nm in acetonitrile and dichloromethane, respectively.

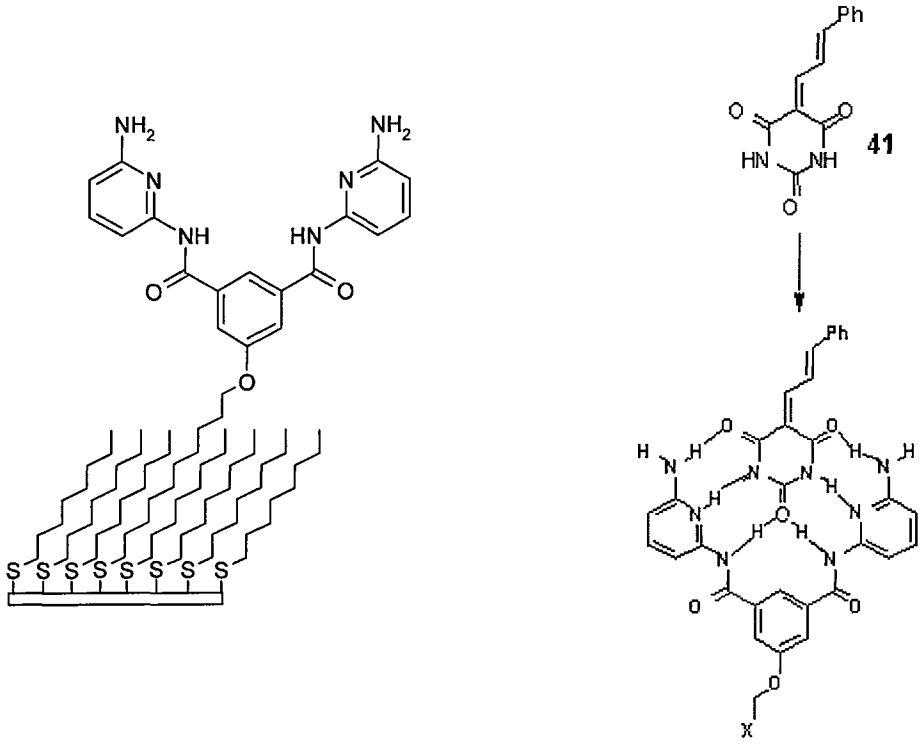

40

*Figure 9. Binding of a barbiturate ligand (**41**) by fluorescent **40** attached to gold nanoparticles.*

The electron-deficient double bond in compound **42** can undergo Michael addition with thiols, thus signalling the presence of organic molecules using irreversible interaction.[69] In the absence of thiols fluorescence is quenched because of PET from the fluorophore to the alkene. When thiols are bound to the probes, fluorescence enhancements up to threefold can be observed, the exact values depending on the thiol, the effect being biggest for 2-mercaptoethanol and smallest for L-cysteine.

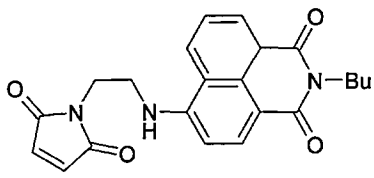

42

Squaraine-derivatives **43a** and **43b** are sensitive to biologically relevant aminothiols cysteine and cystine derivatives, among them glutathione and homocysteine.[70] In acetonitrile / water (20:80) solution both compounds reacted with cystein and their fluorescence, displayed at around 640 nm was efficiently quenched. Furthermore, the initially coloured squaraines were bleached. The likely mechanism for this reaction is attack of the nucleophilic sulphur atom on the electron-deficient carbon of the central four-membered ring *(Scheme 1)*. Other nucleophiles, such as amines, sulphides, alcohols and phenols did not produce colour changes.

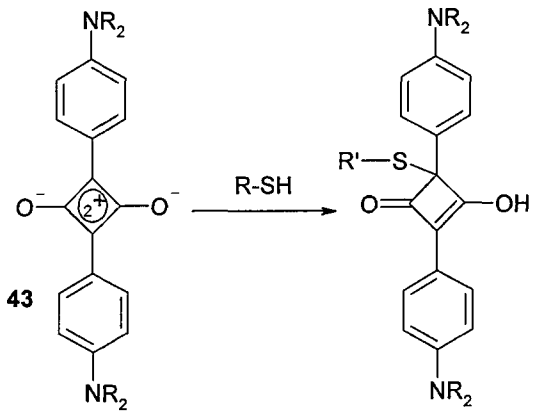

*Scheme 1. The reaction likely to be occurring between **43** and thiol derivatives.*

***43 a**: R = -$(CH_2)_2O(CH_2)_2OCH_3$, **43 b**: R = -$(CH_2)_2OC(O)NH(CH_2)_3CH_3$*

Catechols occur in a number of biologically important molecules, among them in catechol estrogens (CE), whose DNA-adducts are thought to play an important part in hormonal carcinogenesis. In these adducts catechol estrogen quinones react with adenine and guanine. It is also hoped that CE-DNA adducts will be employed as biomarkers for the early detection of estrogen-induced cancers. Stack *et al.* have developed the 2,2-dibromomalonamide derivative (**44**) bearing two anthracene fluorophores for the detection of catechols, and have tested it on a range of catechols, among them the adducts with guanine and adenine.

Detection of the target compounds occurs via cyclic ketal formation through replacement of the bromine atoms in the 2 position by the two oxygen atoms of the catechol. Reaction between the targets and the probe was possible only at elevated temperatures (50 °C) in DMF in the presence of caesium carbonate base, and the detection took an hour. The CE-DNA adducts could be detected at low femtomolar level with the excess of the probe attached to a polystyrene resin.

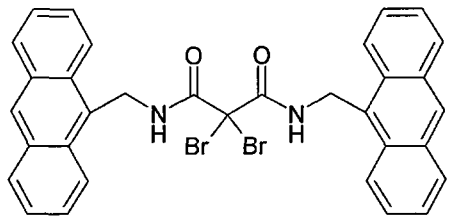

44

Nitric oxide is an important intra- and extracellular messenger,[71] but is produced in low concentrations and is unstable, which makes its detection difficult. Nagano and co-workers have equipped a boron dipyrromethane chromophore with a 3,4-diaminophenyl group to yield a non-fluorescent molecule (DAMBO) (**45a**), which reacts rapidly with nitric oxide to produce a highly fluorescent triazole (DAMBO-T) (**45b**).[72]

Above pH 7, DAMBO-T rapidly lost its fluorescence due to deprotonation of the triazole, which resulted in the increased electron-donating ability of the triazolate functional group, and acceleration of the PET to the fluorophore. The pH-independent DAMBO-P^H (**46**) has an increased electron-density on the reaction site, which increases sensitivity for NO, and two propionic acid substituents on the dipyrromethane moiety to optimise PET and increase hydrophilicity, and avoid quenching through stacking. DAMBO and its

derivatives proved highly selective for nitric oxide even in the presence of the very reactive singlet oxygen (*Figure 10*).

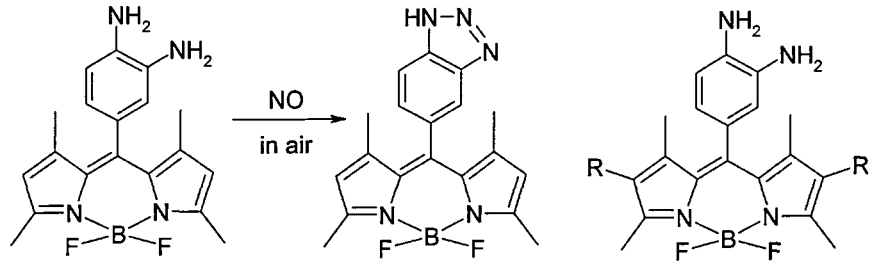

*Figure 10. Nitric oxide-sensitive DAMBO (**45a**), its triazole derivative DAMBO-T (**45b**), and pH-independent DAMBO-PH (**46**).*

The same research group have designed and synthesised the fluorescein-based singlet-oxygen probe 9-[2-(3-carboxy-9,10-dimethyl)anthryl]-6-hydroxy-3H-xanthen-3-one (DMAX) (**47a**), which is more sensitive to its target species, than any known singlet oxygen probe so far.[73] The molecule's 9,10-dimethylanthracene moiety acts as a very fast singlet oxygen trap. While DMAX is practically non-fluorescent, the endoperoxide (DMAX-EP) (**47b**) formed when the probe reacts with oxygen is highly fluorescent (*Figure 11*). The work on this probe has also provided useful information on the conditions governing the fluorescence of fluorescein derivatives. It has been found, that dividing the molecule into a fluorophore part, i. e. the xanthene moiety, and a 'fluorescence switch' part, which is the benzoic acid derivative is a reasonable approximation, and frontier orbital energies of these two parts can be calculated separately. When the HOMO of the fluorescence switch is higher than that of the fluorophore, fluorescence from the excited fluorophore can be quenched by PET from the switch. On the other hand, if the HOMO of the fluorophore lies higher then that of the switch, fluorescence is observed. This theory has been

tested by the synthesis and photophysical characterisation of a number of fluorescein derivatives.

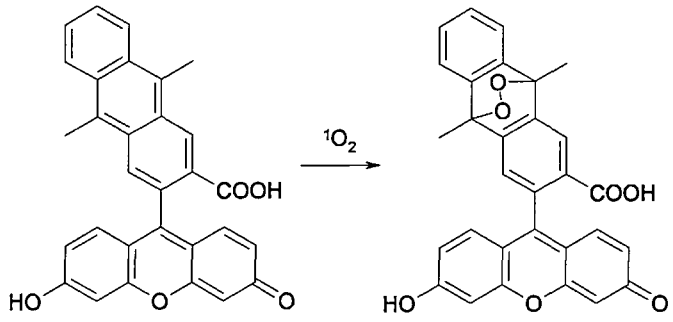

47a **47b**

*Figure 11. The singlet oxygen-probe DMAX (**47a**), and its endoperoxide DMAX-EP (**47b**).*

Parker and co-workers have incorporated the terbium complex **48** into sol-gel thin films in order to obtain an operational fluorescent probe for sensing oxygen concentration changes in aqueous solutions[74]. The quenching of the fluorescence by the dissolved oxygen was independent of the pH over a pH range of 2 to 9. The measurements were reproducible after keeping the probes for long periods of time open to air, indicating that no serious degradation processes take place. Despite slight variations in the microenvironment of the films, the data obtained with different sensors and during different measurements were comparable, making **48** a promising candidate as a widely applicable oxygen sensor.

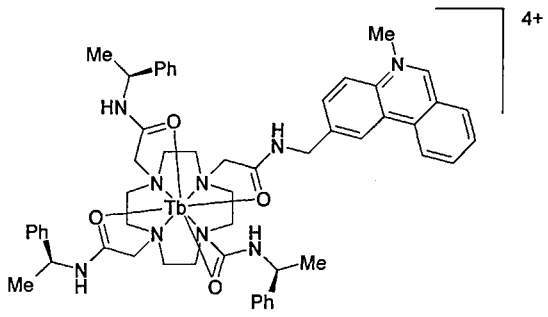

48

2.4 *Molecular logic systems*

Many of the probes mentioned previously can be looked upon as molecular-scale devices. Obviously, the fact that they perform (or could perform) tasks that resemble the functions of electronic devices that are currently in use, does not mean that in the near future computers made from molecular switches could replace silicon-based computers. One of the crucial problems is the 'wiring' together of the parts. As the majority of the switches use one or more chemical species as input combined with light (of a specific wavelength), and has light (of a different, longer wavelength) output, the connection of even two switches can be a difficult task. For example complex molecular logic gates (like INHIBIT, NAND or XNOR), which can provide in electronics any truth table by simply connecting the necessary AND and XOR gates in the right order, still have to perform the desired arithmetic functionally, rather than physically.

Nevertheless, molecular-scale analogues of several currently used electronic logic systems exist.[75] AND gates can be constructed by slightly modifying the PET-based probes mentioned before, by the addition of an extra receptor for a second species. Thus PET can quench the fluorescence of the fluorophore from either receptors, making the presence of *both* target species (both inputs are 1) necessary for the output to equal 1 (for emission to take place). [#]

[#] From the point of view of the primary process (PET) this is again a functional rather than a physical logic gate, as it exploits the equivalence A + B = NOT(NOT(A)·NOT(B)), i.e. if PET is suppressed in both receptor A and receptor B, than NOT(PET) (=emission) is observed.

An example of AND logic gate is **49**.[76] The alkyl amine receptor unit requires protonation for PET to be suppressed, while the benzocrown needs sodium ions. As the fluorescence can only be observed when both species are present, **49** fulfils the truth table of a logical AND gate (shown beside **49**).

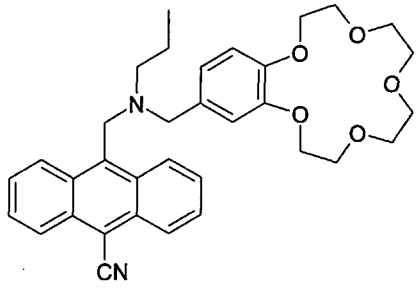

49

I_1	I_2	O
0	0	0
0	1	0
1	0	0
1	1	1

The truth table of an AND logic gate

Another example could be **38**, if the two inputs are supplied by two different species (i.e. a glucose molecule and an ammonium ion instead of glucosamine hydrochloride).

Molecular-scale models of other electronic devices (memories, switches, motors, etc) have also been constructed. These molecules perform their function upon irradiation, electrochemical activation or stimuli by chemical species. The 'outcome' of the action can be similarly varying, ranging from the emission of light to controlled motion of the molecules.[77]

3 OBJECTIVES OF THE PROJECT

Despite the wide range of fluorescent probes already available, there are still a number of difficulties to be overcome. The sensitivity of the probes is reduced by both autofluorescence from the sample, and the non-zero background. The binding of the target is usually signalled by an enhancement or decrease of the already existing fluorescence signal. As fluorescence is affected by numerous factors, it can be difficult to obtain a clear and unambiguous signal from the probe.

The sensitivity of the luminescent probes could be increased by exploiting triggered resonance energy transfer (RET). Resonance energy transfer has been applied to the study of biomolecules as the fluorescent signal obtained has an emission maximum shifted from the fluorescence of the sample. Triggered RET means that the fluorescence from the acceptor is 'switched on' when the desired event occurs, otherwise it is switched off. In the ideal case this results in the observation of a unique fluorescent signal against a non-fluorescent background.

The aim of the project is to synthesise and characterise a series of donor-acceptor-quencher (**D-A-Q**) triads that are able to undergo triggered Resonance Energy Transfer in competitive media. The RET from the donor to the acceptor is quenched by the quencher that is in the close proximity of the donor. If the quencher is bound to a target species, the quenching is disrupted and emission from the acceptor can be observed (*Figure 12*).

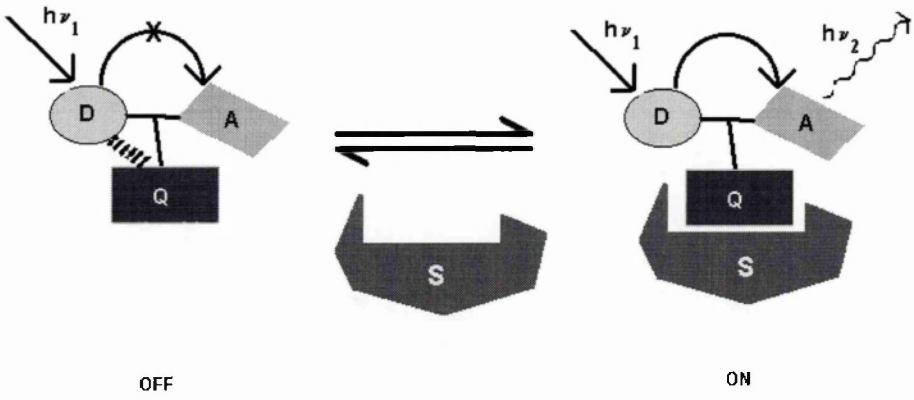

*Figure 12. Schematic representation of the designed **D-A-Q** triads. When the substrate (**S**) is present, fluorescence from the acceptor (**A**) can be observed, otherwise the quencher (**Q**) quenches RET from the donor (**D**) to the **A** and the probe is switched 'OFF'.*

3.1 The organic donor – acceptor - quencher triad

The first target molecule (**50**) consists of coumarin 2 as the donor, coumarin 343 as the acceptor and uridine as the quencher (*Figure 13*). The three moieties are held together by a suitable scaffold molecule, that was chosen to be the 4-amino-3-hydroxybutyric acid. This molecule contains three different functional groups and enables selective reaction of each group.

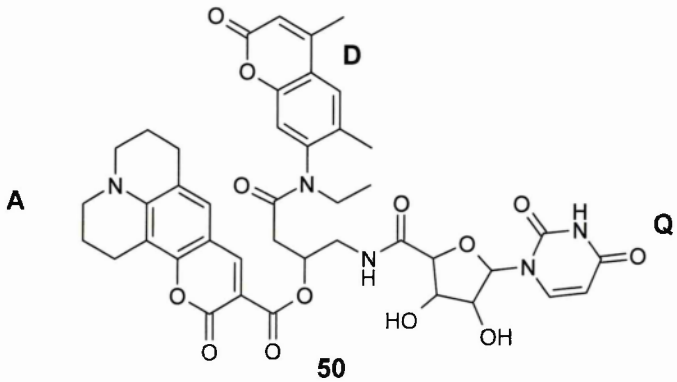

*Figure 13. The first triad (**50**), consisting of coumarin 2 (**D**), coumarin 343 (**A**) and uridine (**Q**).*

The emission spectrum of coumarin 2 overlaps the absorption spectrum of coumarin 343, making them a suitable donor-acceptor pair for RET. Uridine was

chosen as the quencher, as it is known to be able to quench coumarin excited states,[78] and combines this ability with a recognition site. The quenching process is expected to be interrupted by the binding of the uridine to the complementary base (adenosine). If the coumarin 343-uridine pair is replaced by other **A-Q** pairs, the binding events between the quenchers and their substrates are signalled by emission of lights of different wavelengths. If a 'cocktail' of the **D-A-Q** triads is used, the common excitation wavelength enables the simultaneous monitoring of a series of binding procedures.

3.2 The triads with europium and terbium lumophores

Coumarin 2 can act not only as a donor for the coumarin 343 acceptor, but also as a sensitizer for the lanthanide ions europium and terbium. Europium and terbium have emission wavelengths in the > 450 nm region, long-lived emission, and their lifetimes are typically on the millisecond timescale. This enables the removal of any short-lived background luminescence by time gating. As emission from the lanthanide ions occurs between electronic energy levels, the emission bands are sharp peaks.

D-A-Q triad (**51**) with the same coumarin 2 donor and uridine quencher, but a lanthanide ion acceptor was designed. As incorporation of the lanthanide into the triad occurs through complexation with a suitable chelator, the 4-amino-3-hydroxybutyric acid scaffold was replaced by cyclen (*Figure 14*).

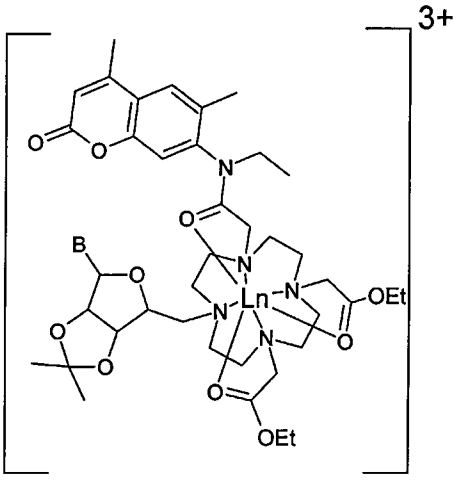

51

*Figure 14. The second **D-A-Q** triad (**51**). **D**: coumarin 2, **A**: acceptor: europium(III) or terbium(III), **Q**: quencher uridine or adenosine. Scaffold: cyclen*

Cyclen can be N-substituted to enable binding of the donor and the quencher, and the four nitrogen atoms chelate the lanthanide ion. To further increase the stability of the complex and avoid fluorescence quenching of the lanthanide by bound water molecules, ethylacetylcarboxylate arms are to be attached to the cyclen to saturate the co-ordination sphere of the metal ion.

The presence of a quencher in the ligand can have various effects on the lanthanide luminescence. The luminescence intensity of the complex would decrease compared to that of an analogous compound without the quencher. It is also possible that while the luminescence intensity remains intact, the luminescence lifetime changes. It is possible that the presence of a substrate could induce further changes in the lifetime. As europium and terbium lifetimes can be measured conveniently and precisely, it would be a fast and very specific way of detecting the substrate.

3.3 The triads with neodymium and ytterbium lumophores

Near infrared emitting lanthanide ions neodymium and ytterbium cannot be sensitised by coumarin 2, whose emission energy levels are too high above the excited state energy levels of these lanthanides. As there is no overlap between the donor emission spectrum and the acceptor excitation spectrum. Therefore other antennae with longer emission wavelengths are needed. It is known that both fluorescein and rhodamines are able to sensitise neodymium and ytterbium. Preliminary measurements suggested that luminescence from both compounds decreases in the presence of the nucleotides adenosine and uridine. As these measurements have not indicated the superiority for our purposes of either antennae, rhodamine was chosen for the antenna - near IR – quencher triads, as rhodamine is easier to functionalise and handle than fluorescein (*Figure 15*).

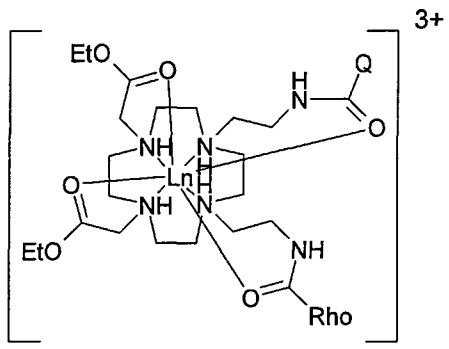

52

*Figure 15. The third **D-A-Q** triad. **D**: rhodamine B, **A**: acceptor: neodymium(III) or ytterbium(III), **Q**: quencher uridine or adenosine. Scaffold: cyclen*

3.4 Exciplex for DNA detection

A wide range of polyaromatic compounds are known to intercalate with DNA. It is possible that the flat bicyclic coumarin structure of the coumarin 2 donor

could fit into the DNA double strand. This is expected to be signalled by a decrease in the fluorescence intensity of the coumarin 2, or, if coumarin 2 is used as a donor for a further luminescent molecule, a decrease in its ability to sensitize the acceptor. If this acceptor is not coumarin 343 or the lanthanides europium or terbium, but rhodamine, a decrease in the luminescence intensity of the rhodamine is expected. As rhodamine can be used to sensitize the near infrared emitting lanthanides neodymium and ytterbium, the interaction of the coumarin 2 with the DNA would be in the end signalled by changes in the lanthanide luminescence (*Figure 16*).

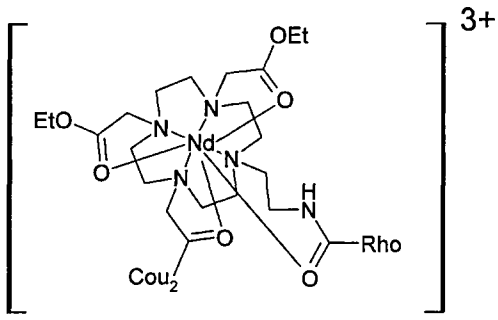

53

*Figure 16. The coumarin 2 – rhodamine B exciplex **D1**: coumarin 2, **A** or **D2**: acceptor or donor 2: rhodamine B, **Ln**: neodymium or ytterbium. Scaffold: cyclen*

Rhodamine B is not expected to intercalate with DNA, as it has four ethyl groups attached to two nitrogen atoms, which would prevent it from fitting between the DNA base pairs. Therefore the presence of the DNA would be indicated by a decrease of lanthanide luminescence intensity when the coumarin 2 is excited at approximately 330 nm, while the luminescence intensity would remain intact when direct excitation of the rhodamine antenna at around 450-550 nm is carried out. It is also possible that DNA would affect the lanthanide luminescent lifetimes.

4 EXPERIMENTAL

Cyclen, anhydrous europium(III) chloride, terbium(III) chloride, neodymium(III) chloride and ytterbium(III) chloride were obtained from Strem Chemicals, DEAD from Lancaster Synthesis. Fmoc-chloroformate and rhodamine B were supplied by Aldrich. All other chemicals were purchased from Acros and used without further purification. N-Fmoc-γ-O-^{t}Bu-glutamic acid, dry acetonitrile and dry DMF were purchased from Fluka. Sodium iodide, magnesium sulphate, potassium carbonate and all solvents, apart from DMF and acetonitrile were obtained from Fischer.

1,4-Cyclen oxalamide,[79] 5'-oxidised 2',3'-isopropylideinenucleotides, [80] and N-Boc-glycine were synthesised according to literature procedures.[78]

Sodium iodide and potassium carbonate were dried at 90 °C for 24 hours prior to use. Tetrahydrofuran was distilled from potassium and benzophenone, dioxan from lithium aluminium hydride, acetonitrile from phosphorus pentoxide, under argon atmosphere, and stored over molecular sieves. Chloroform was distilled from lithium aluminium hydride under argon and used immediately. TEA was distilled from calcium hydride under argon and stored under argon over molecular sieves. All other solvents were used as purchased.

Reactions involving N-methylaniline or coumarins were conducted in the dark. Thin Layer Chromatography was done on Merck fluorescent silica or on Fluka fluorescent alumina plates with iodine, $KMnO_4$ or UV visualisation. ^{1}H NMR and ^{13}C NMR data were obtained using a 300 MHz JEOL instrument. LC-MS was performed on a VG Quattro 2 equipment coupled to a Waters HPLC system. Accurate masses were obtained through the EPSRC Swansea Mass

Spectrometry Service (University of Wales, Swansea). Melting points were determined using an Electrothermal digital melting point apparatus, and are uncorrected. Infrared spectra were recorded on a Perkin Elmer 1710 Infrared Fourier Transform Spectrometer. Elemental analysis was performed by MEDAC Ltd, Egham, Surrey. UV spectra were measured on a Uvikon XL (Bio-Tek Instruments) spectrometer. Excitation spectra and emission spectra of the organic triads, the europium and terbium complexes, and the luminescent lifetimes of the europium and terbium complexes were measured on a Fluoromax-P (Jobin-Yvon) fluorimeter. Luminescent lifetimes of the organic triads were determined by a Jobin-Yvon Fluorolog FL-3-22 / Tau-3 Spectrofluorimeter.

Emission intensities and luminescent lifetimes of the Nd and Yb complexes were determined the following way. Samples were illuminated over an area of 1 cm^2 with the 355 nm Q-switched output of a Nd:YAG laser (Spectra Physics) operating at 10 Hz. Typical pulse energies were 3-4 mJ with a pulse FWHM of 8 ns. The IR photoluminescence was collected at right angles and focussed onto the entrance slit of a Jobin-Yvon Triax 320 monochromator with a grating blazed at 900 nm and was detected with a nitrogen-cooled germanium photodiode/amiplifier (North Coast EO-817P) operating in high sensitivity mode. The signal was captured and averaged by a digital storage oscilloscope (Tektronix TDS320) and transferred to a PC for data analysis. Decays were analysed by iterative deconvolution and non-linear least-squares analysis of the instrument response profile with single functions.

4.1 Organic triads

4.1.1 Triad synthesis with the 4-Amino-3-hydroxybutyric acid scaffold

4.1.1.1 N-Boc-4-amino-3-hydroxybutyric acid

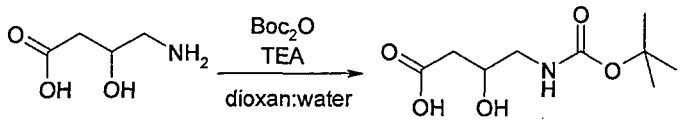

54 **55**

D,L-4-amino-3-hydroxybutyric acid (**54**) (1.19 g, 10 mmol) was dissolved in water (6 mL), triethylamine (2.1 mL, 1.6 g, 15 mmol, 1.5 eq), 1,4-dioxan (6 mL) and di-tert-butyl dicarbonate (2.42 g, 11 mmol, 1.1 eq) were added and the mixture was stirred at room temperature. The mixture became clear after 1 hour and the reaction was allowed to proceed for two more hours. Ethyl acetate (25 mL) and water (30 mL) were added and the phases were separated. The aqueous phase was acidified to pH 2 with 1:1 HCl and extracted with ethyl acetate (3·25 mL). The combined organic phases were dried over $MgSO_4$, filtered, and the ethyl acetate was removed *in vacuo*. The product (**55**) is a white solid. Yield: 96% (2.10 g); MS: 219 $[M+H]^+$; ^1H NMR (CD_3CN, δ): 1.35 (s, 9 H, Boc), 2.29 (dd, 1 H, CH_2-1, J_1 = 8.4 Hz, J_2 = 15.7 Hz), 2.43 (dd, 1 H, CH_2-2, J_1 = 4.4 Hz, J_2 = 15.7 Hz), 3.22-3.05 (m, 2 H, CH_2) 3.66 (s, 1 H, OH), 4.13-4.00 (m, 1 H, C<u>H</u>-OH), 5.41 (br s, 1 H, NH); ^{13}C NMR ($CDCl_3$) 28.18 (CH_3, Boc), 38.33 (CH_2), 45.33 (CH_2), 60.37 (CH), 171.36 (CO), 175.62 (CO); mp: 98-99 °C; IR (ν_{max} / (cm^{-1}), KBr): 3573, 3505, 3387, 2983, 2940, 2680, 2584, 1685, 1531.

4.1.1.2 N-Fmoc-4-amino-3-hydroxybutyric acid

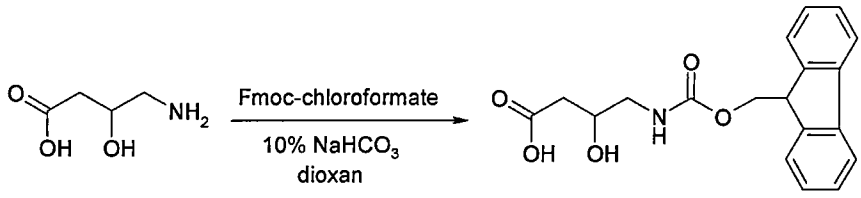

54 **56**

D,L-4-amino-3-hydroxybutyric acid (**54**) (1.19 g, 10 mmol) was dissolved in 10% $NaHCO_3$ (25 mL), 1,4-dioxan (15 mL) was added and the solution was cooled in an ice-water bath. Fmoc-chloroformate (2.60 g, 11 mmol, 1.1 eq) was introduced in small portions, and the reaction was conducted at ice-water bath temperature for 4 hours and at room temperature for a further 8 hours. The reaction mixture was poured into water (600 mL) and washed with diethyl ether (2·100 mL). The water phase was acidified to pH 2 with conc. HCl. Precipitation of the product occurred immediately. The vessel was kept in the fridge overnight and the white, voluminous solid was filtered out by suction. The product is washed with small portions of water on the filter and dried *in vacuo*. **56** Is a white, crystalline solid. Yield: 91% (3.11 g); MS: 342 $[M+H]^+$; ^1H NMR ($CDCl_3$, δ): 2.33 (dd, 1 H, C^4H_2-1, J_1 = 11.1 Hz , J_2 = 8.6 Hz), 2.47 (dd, 1 H, C^4H_2-2, J_1 = 15.4 Hz , J_2 = 3.8 Hz), 3.17 (d, 2 H, C^2H_2, J = 5.1 Hz), 3.92 (m, 1 H, C<u>H</u>-OH), 4.14 (t, 1 H, CH-Fmoc, J = 6.6 Hz), 4.32 (d, 2 H, CH_2-Fmoc, J = 6.6 Hz), 7.22-7.36 (m, 4 H, CH), 7.60 (d, 2 H, CH, J = 7.3 Hz), 7.73 (d, 2 H, CH, J = 7.3 Hz); ^{13}C NMR: 40.38 (CH_2), 47.36 (CH_2), 67.71 (CH_2), 68.52 (CH), 120.88 (CH-ar), 126.100 (CH-ar), 128.10 (CH-ar), 128.72 (CH-ar), 142.51 (CH-ar), 145.22 (CH-ar), 159.00 (CO), 175.16 (CO); mp: 87-88 °C; IR (ν_{max} / (cm^{-1}), KBr): 3321, 3067, 2956, 2361, 2341, 1697, 1654, 1636, 1617, 1542, 1508, 1449.

4.1.1.3 Coupling NMA to N-Boc-4-amino-3-hydroxybutyric acid

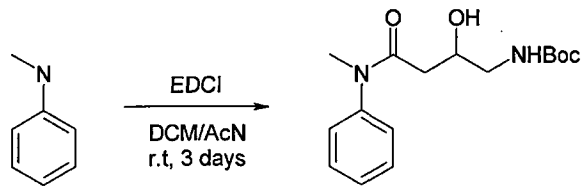

57 **58**

NMA (**57**) (112 µL, 0.11 g, 1 mmol) was dissolved in DCM (10 mL), a solution of N-Boc-4-amino-3-hydroxybutyric acid (**56**) (0.22 g, 1 mmol dissolved in 5 mL AcN) was added and the solution was stirred at room temperature while EDCI (0.19 g, 1 mmol) was added in small portions. The reaction was allowed to proceed for 3 days. DCM (25 mL) and water (30 mL) were added to the reaction mixture, the phases were separated, and the water phase was extracted with DCM (3·25 mL). The combined organic phases were washed with water (30 mL), dilute acid (25 mL 1 M HCl), dilute base (30 mL 1 M NaOH) and water (25 mL), dried over $MgSO_4$, filtered, and evaporated concentrated to ~2 mL. The solution was applied onto a silica column and chromatographed with hexane / EtOAc (6:4). Evaporation of the solvents yielded **58** as a colourless solid. Yield: 46% (0.15 g); ^{1}H NMR ($CDCl_3$, δ): 1.32 (s, 9 H, Boc), 1.75 (br s, 1 H, NHBoc), 2.12-2.15 (m, 2 H, CH_2), 2.83-2.97 (m, 1 H, CH_2-1, J_1 = 12.9 Hz, J_2 = 6.3 Hz, J_3 = 5.7 Hz), 3.10-3.27 (m, 1 H, CH_2-2), 3.20 (s, 3 H, N-CH_3), 3.94 (m, 1 H, CH-OH), 4.93 (br s, 1 H, NH), 4.55 (br s, 1 H, OH), 7.10 (d, 2 H, CH, J = 7.1 Hz), 7.26-7.38 (m, 3 H, CH); ^{13}C NMR: 28.28 (Boc-CH_3), 37.36 (CH_2), 37.10 (N-CH_3), 45.36 (CH_2), 67.99 (CH-O), 79.21 (C_q), 127.09 (CH), 127.99 (CH), 128.23 (CH), 172.43 (CO).

*4.1.1.4 Removal of the Boc protection from **58***

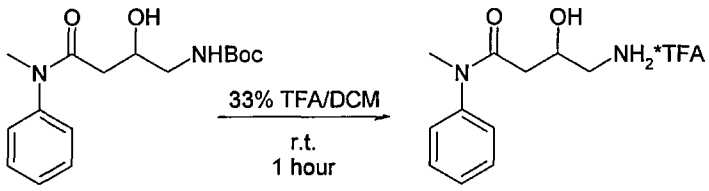

58 **59**

58 (0.15 g, 0.5 mmol) was dissolved in DCM (10 mL), TFA (5 mL) was added, and the reaction mixture was stirred at room temperature for 1 hour. The volatile components were evaporated and the sample dried *in vacuo* to obtain the TFA-salt of the product (**59**) in quantitative yield as a brown solid. MS: 209 $[M+H]^+$; ^1H NMR (CD_3OD, δ): 2.21 (dd, 1 H, CH_2-1, J_1 = 15.9 Hz, J_2 = 5.5 Hz), 2.31 (dd, 1 H, CH_2-2, J_1 = 15.9 Hz, J_2 = 7.0 Hz), 2.67 (dd, 1 H, CH_2-1, J_1 = 12.5 Hz, J_2 = 2.9 Hz), 2.97 (dd, 1 H, CH_2-2, J_1 = 12.5 Hz, J_2 = 9.3 Hz), 3.12 (s, 3 H, NCH_3), 4.08-4.15 (m, 1 H, CH-OH), 7.20-7.23 (m, 2 H, CH), 7.29 (m, 2 H, CH); ^{13}C NMR: 37.74 (NCH_3), 40.21 (CH_2), 45.43 (CH_2), 66.06 (CH-OH), 128.49 (CH), 129.42 (CH), 131.12 (CH), 144.71 (CN), 172.01 (CO).

4.1.1.5 Alkylation of N-methylaniline with chloroacetic acid

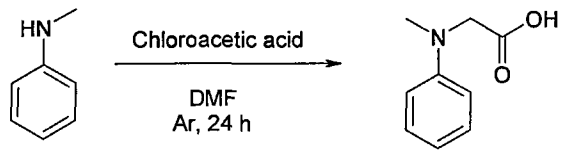

57 **60**

N-Methylaniline (**57**) (112 µL, 0.11 g, 1 mmol) was dissolved in DMF (8 mL), chloroacetic acid (0.45 g, 5 mmol, 5 eq) and potassium carbonate (2 g) were added, and the reaction mixture was stirred at 80 °C under argon atmosphere for 24 hours. The DMF was removed *in vacuo*, the residue suspended in DCM (30 mL), water (30 mL) was added and the phases were separated. The water

phase was acidified to pH 3 and extracted with DCM (3·30 mL). The combined organic phases were dried over $MgSO_4$, filtered, and evaporated to dryness to yield the product (**60**) as a yellow solid in 70% yield (0.12 g). ^1H NMR ($CDCl_3$, δ): 2.98 (s, 3 H, NCH_3), 4.10 (s, 2 H, CH_2), 6.66 (d, 2 H, $C^{2,5}H$, J = 8.6 Hz), 6.69-6.93 (m, 1 H, C^4H), 7.12-7.41 (m, 2 H, $C^{1,6}H$), 9.37 (br s, 1 H, COOH); ^{13}C NMR: 31.98 (NCH_3), 54.11 (CH_2), 112.80 (CH), 118.00 (CH), 129.24 (CH), 170.53 (CO).

4.1.1.6 Alkylation of aniline with ethyl bromoacetate

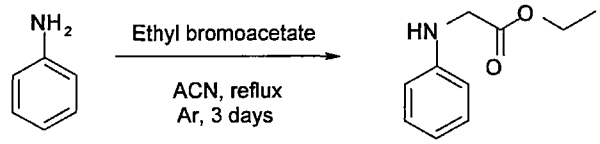

61 **62**

Aniline (**61**) (0.09 g, 1 mmol) was dissolved in acetonitrile (8 mL), ethyl bromoacetate (1.7 g, 10 mmol), sodium iodide (1.23 g, 10 mmol), and potassium carbonate (2 g) were added, and the reaction mixture was refluxed under argon atmosphere for 3 days. The acetonitrile was removed *in vacuo*, the residue suspended in DCM (30 mL), water (30 mL) was added and the phases were separated. The water phase was extracted with DCM (2·30 mL). The combined organic phases were dried over $MgSO_4$, filtered, and evaporated to dryness to give product (**62**) as a dark brown oil. ^1H NMR ($CDCl_3$, δ): 1.19 (t, 3 H, CH_3, J = 7.1), 4.06 (s, 2 H, NCH_2), 4.16 (q, 2 H, CH_2, J = 7.1), 6.60 (d, 2 H, $C^{2,5}H$, J = 7.9 Hz), 6.55-6.60 (m, 1 H, CH), 7.03-7.17 (m, 2 H, CH); ^{13}C NMR: 14.12 (CH_3), 45.84 (CH_2), 53.46 (CH_2), 113.00 (CH), 118.23 (CH), 129.24 (CH), 146.90 (C_q), 171.04 (CO);

4.1.1.7 Alkylation of N-methylaniline with ethyl bromoacetate

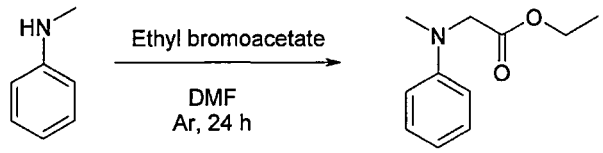

57 **63**

N-Methylaniline (**57**) (112 µL, 1 mmol, 0.11 g) was dissolved in DMF (8 mL), ethyl bromoacetate (554 µL, 0.84 g, 5 mmol, 5 eq), and potassium carbonate (2 g) were added, and the reaction mixture was stirred at 80 °C under argon atmosphere for 24 hours. The DMF was removed *in vacuo*, the residue suspended in DCM (30 mL). Water (30 mL) was added to the solution, and the phases were separated. The water phase was extracted with DCM (3·30 mL). The combined organic phases were dried over $MgSO_4$, filtered, concentrated to ~2 mL and applied onto a silica column. Elution with ethyl acetate / hexane (1:9) gave the desired product (**63**) as a yellow oil in 86% yield (0.17 g). MS: 194 [M+H$^+$]; ^{1}H NMR ($CDCl_3$, δ): 1.13 (t, 3 H, CH_3, J = 7.1 Hz), 2.97 (s, 3 H, NCH_3), 3.95 (s, 2 H, NCH_2), 4.07 (q, 2 H, CH_2, J = 7.1 Hz), 6.59-6.68 (m, 3 H, CH-ar), 7.10-7.18 (m, 2 H, CH-ar); ^{13}C NMR: 14.13 (CH_3), 39.38 (NCH_3), 54.39 (CH_2), 60.72 (CH_2), 112.19 (CH-ar), 117.19 (CH-ar), 129.07 (CH-ar), 148.80 (N-C_q), 170.91 (CO).

4.1.1.8 N-Boc-aminoethanol

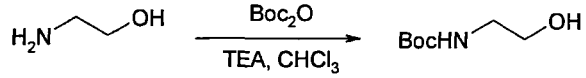

64 **65**

2-Aminoethanol (**64**) (1.22 g, 20 mmol) was dissolved in a mixture of chloroform (20 mL) and TEA (4 mL, 2.88 g, 28.5 mmol, 1.5 eq). Boc_2O (4.00 g, 18.3 mmol,

0.92 eq) was added in small portions to the solution, and the reaction mixture was stirred at room temperature for 3 hours. Water (20 mL) was added to the reaction mixture, and the stirring continued for 12 hours at room temperature. The phases were separated, the aqueous phase was extracted with chloroform (2·30 mL), the combined organic phases were washed with 0.5 M HCl (30 mL) and water (2·25 mL), dried over $MgSO_4$, filtered, and evaporated to dryness. The sample purified by silica column chromatography by elution with DCM to yield **65** as a colourless oil. Yield: 70% (2.30 g); MS: 161 $[M+H]^+$; ^1H NMR ($CDCl_3$, δ): 1.36 (s, 9 H, Boc), 3.18 (t, 2 H, CH_2, J = 5.1 Hz), 3.58 (t, 2 H, CH_2, J = 5.1 Hz), 3.99 (br s, 1 H, NH), 5.49 (br s, 1 H, OH); ^{13}C NMR: 28.10 (CH_3), 45.53 (CH_2), 61.37 (CH_2), 79.07 (C_q), 156.48 (CO); IR (ν_{max} / (cm^{-1}), film): 3348, 2977, 2934, 2882, 1685, 1526.

4.1.1.9 Alkylation of NMA with ***65*** via *the Mitsunobu reaction*

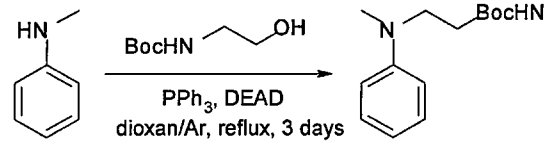

57 **66**

N-Methylaniline (**57**) (112 µL, 0.11 g, 10 mmol), TPP (0.26 g, 10 mmol) and N-Boc-aminoethanol (**65**) (0.16 g, 10 mmol) were dissolved in dry 1,4-dioxan (10 mL). The reaction mixture was stirred under argon in an ice-water bath while DEAD (156 µL, 0.17 g, 10 mmol) in dry dioxan (10 mL) was added dropwise. The solution was allowed to warm up to room temperature and then was refluxed for 3 days under argon. The solvent was removed at reduced pressure, the residue dissolved in 3 mL DCM / EtOAc (95:5), applied onto a silica column, and chromatographed with hexane / EtOAc (9:1). Yield: ~10% (0.02 g); MS: 250

$[M+H]^+$; ^1H NMR ($CDCl_3$, δ): 1.37 (s, 9 H, Boc), 2.75 (s, 3 H, CH_3), 3.23-3.26 (m, 2 H, CH_2), 3.36-3.40 (m, 2 H, CH_2), 6.92-7.66 (m, 5 H, CH); ^{13}C NMR: 28.56 (CH_3), 29.95 (NCH_3), 38.28 (CH_2), 77.60 (C_q), 112.33 (CH), 116.72 (CH), 129.43 (CH), 156.16 (CO).

4.1.1.10 Coupling N-Boc-glycine to coumarin 120

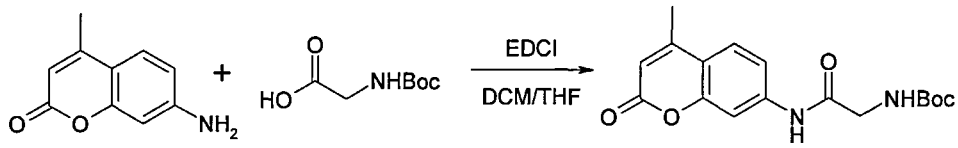

67 **68** **69**

Coumarin 120 (**67**) (0.50 g, 2.86 mmol) was dissolved in DCM (20 mL) and THF (10 mL), N-Boc-Glycine (**68**) (2.00 g, 11.43 mmol, 4 eq) and EDCI (2.02 g, 10.52 mmol, 3.7 eq) were added and the solution was stirred at room temperature for 24 hours. The solvents were evaporated, the residue dissolved in DCM (30 mL) and water (30 mL), the phases were separated and the aqueous phase was extracted with DCM (2·30 mL). The combined organic phases were washed with water (2·30 mL), dried over $MgSO_4$, filtered and evaporated to dryness. The solid was suspended in Et_2O (50 mL), filtered, washed with Et_2O (2·10 mL), and dried. The product (**69**) was obtained in 31% yield (0.30 g) as a white solid. MS: 332 $[M]^+$, 665 $[M+M+H]^+$; ^1H NMR ($CDCl_3$, δ): 1.32 (s, 9 H, Boc), 2.29 (s, 3 H, CH_3), 3.72 (s, 2 H, CH_2), 6.06 (s, 1 H, CH), 7.52 (s, 1 H, CH), 7.62 (s, 1 H, CH); ^{13}C NMR: 18.20 (CH_3), 29.83 (CH_3), 43.81 (CH_2), 106.90 (CH), 112.70 (CH), 115.68 (CH), 125.04 (CH), 141.53 (C_q), 152.98 (C_q), 152.99 (CO), 161.69 (CO).

*4.1.1.11 Removal of the Boc protection from **69***

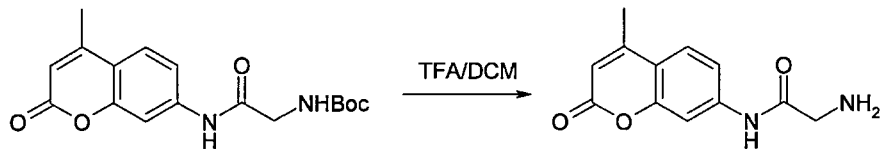

69 **70**

69 (0.29 g, 0.87 mmol) was dissolved in DCM (15 mL) and TFA (11 mL), and the solution was stirred at room temperature for 0.5 hours. The solvents were evaporated and the sample dried at reduced pressure for 24 hours to give the trifluoroacetate salt of **70** in quantitative yield. MS: 232 $[M+H]^+$, 465 $[M+M+H]^+$; ^1H NMR (CD_3OD, δ): 2.32 (s, 3 H, CH_3), 3.77 (s, 2 H, CH_2), 6.11 (s, 1 H, CH), 7.28-7.31 (m, 1 H, CH), 7.52-7.56 (m, 1 H, CH), 7.68 (s, 1 H, CH); ^{13}C NMR: 18.49 (CH_3), 42.40 (CH_2), 107.81 (CH), 113.75 (CH), 116.73 (CH), 117.32 (C_q), 126.77 (CH), 142.71 (C_q), 155.13 (C_q), 155.22 (CO), 161.10 (C_q), 161.59 (CO), 163.12 (CO), 166.16 (CO).

*4.1.1.12 Coupling **70** to N-Boc-4-amino-3-hydroxybutyric acid*

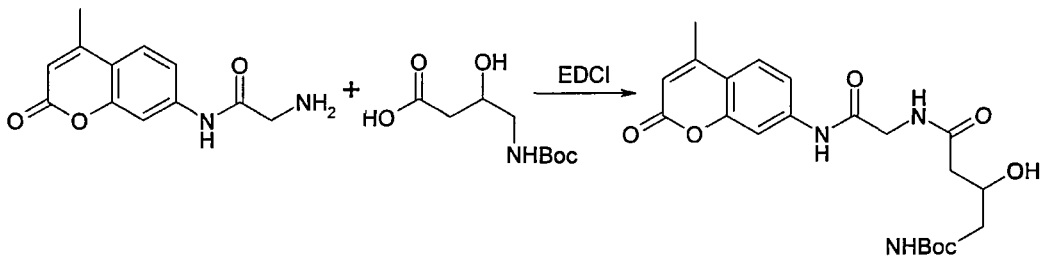

70 **55** **71**

70 (0.27 g, 1.2 mmol) was dissolved in water (10 mL), EDCI (0.26 g, 1.3 mmol, 1.1 eq) DIPEA (0.203 mL, 1.2 mmol, 0.15 g) and N-Boc-4-amino-3-hydroxybutyric acid (**55**) (0.25 g, 1.2 mmol) were added, and the solution was stirred at room temperature for 4 hours. The product precipitates out from the reaction mixture. When the reaction had reached completion the solid was

filtered off and washed thoroughly with water, DCM, dilute NaOH (1 M) and diethyl ether (20 mL each). The product (**71**), a white solid was isolated in 58% yield (0.29 g). MS: 432 $[M]^+$, 866 $[M+M+H+H]^+$; ^1H NMR (CD_3OD, δ): 1.34 (s, 9 H, CH_3), 2.18-2.31 (m, 1 H, CH_2-1), 2.35 (s, 3 H, CH_3), 2.90-3.14 (m, 6 H, overlapping CH_2's), 3.87 (m, 1 H, CH-O), 6.16 (s, 1 H, CH), 7.41-7.44 (m, 1 H, CH), 7.62-7.65 (m, 1 H, CH), 7.70 (s, 1 H, CH); ^{13}C NMR: 17.06 (CH_3), 27.53 (CH_3), 40.73 (CH_2), 42.48 (CH_2), 67.05 (CH), 105.58 (CH), 112.16 (CH), 115.00 (CH), 125.30 (CH), 141.51 (C_q), 153.79 (C_q), 168.29 (CO), 171.67 (CO).

*4.1.1.13 Removal of the Boc protection of **71***

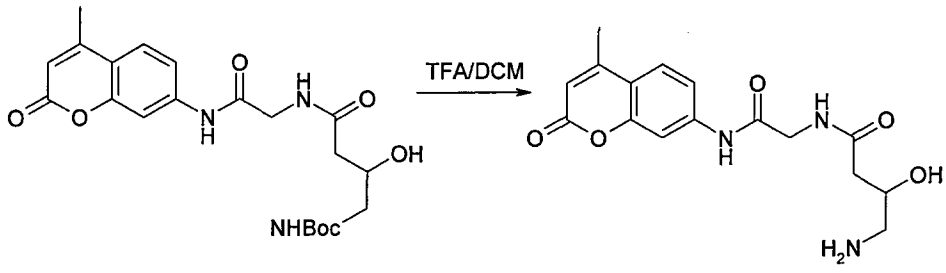

71 **72**

71 (0.27 g, 0.63 mmol) was dissolved in DCM (15 mL) and TFA (10 mL), and the solution was stirred at room temperature for 1 hour. The solvents were evaporated and the sample dried at reduced pressure for 24 hours to give the trifluoroacetate salt of **72**, a white solid, in quantitative yield. MS: 332 $[M]^+$, 667 $[M+M+H]^+$; ^1H NMR (CD_3OD, δ): 2.37 (s, 3 H, CH_3), 2.49-2.54 (m, 2 H, CH_2), 3.99-4.05 (d, 2 H, CH_2), 4.09-4.17 (m, 1 H, CH-O), 6.15 (s, 1 H, CH), 7.33-7.36 (m, 1 H, CH), 7.62-7.65 (m, 1 H, CH), 7.76 (s, 1 H, CH); ^{13}C NMR:18.49 (CH_3), 42.26 (CH_2), 44.06 (CH_2), 45.46 (CH_2), 66.26 (CH), 107.90 (CH), 113.59 (CH), 117.10 (CH), 126.74 (CH), 143.39 (C_q), 155.22 (CO), 170.12 (CO), 173.21 (CO).

4.1.1.14 *Coupling N-Boc-glycine to coumarin 151*

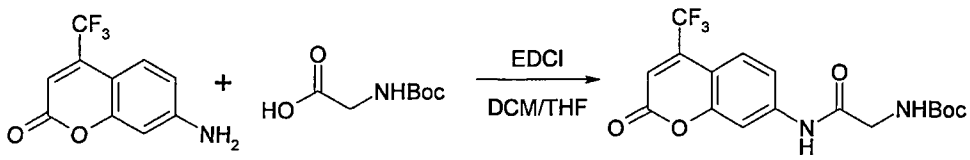

73 **68** **74**

Coumarin 151 (**73**) (0.53 g, 2.37 mmol) was dissolved in THF (15 mL) and DCM (10 mL), N-Boc-Glycine (**68**) (1.66 g, 9.46 mmol, 4 eq) and EDCI (1.82 g, 9.48 mmol, 4 eq) were added and the solution was stirred at room temperature for 3 days. The solvents were evaporated, the residue dissolved in DCM (30 mL) and water (30 mL), the phases were separated and the aqueous phase was extracted with DCM (2·30 mL). The combined organic phases were washed with water (2·30 mL), dried over $MgSO_4$, filtered and concentrated. The sample was applied onto a silica column and chromatographed with DCM / MeOH (1%) to give **74** in 51.5% yield (0.46 g). ^1H NMR (CD_3OD, δ): 1.46 (s, 3 H, CH_3), 3.89 (s, 2 H, CH_2), 6.65 (s, 1 H, CH), 7.49-7.52 (m, 1 H, CH), 7.67-7.69 (m, 1 H, CH), 7.93 (s, 1 H, CH); Sample solubility was too low to obtain a good ^{13}C NMR spetrum.

4.1.1.15 *Removal of the Boc protection from **74***

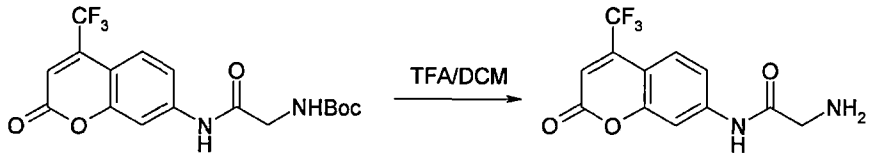

74 **75**

74 was dissolved in DCM (10 mL) and TFA (10 mL), and the solution was stirred at room temperature for 1 hour. The solvents were evaporated and the

sample dried at reduced pressure for 24 hours to give the trifluoroacetate salt of **75** in quantitative yield. MS: 232 $[M]^+$, 465 $[M+M+H]^+$; ^1H NMR (CD_3OD, δ): 3.90 (s, 2 H, CH_2), 6.71 (s, 1 H, CH), 7.38-7.41 (d, 2 H, CH), 7.88 (s, 1 H, CH); ^{13}C NMR: 42.44 (CH_2), 108.40 (CH), 110.71 (CH), 115.52 (CH), 117.23 (C_q), 126.96 (CH), 143.79 (C_q), 156.61 (C_q), 160.59 (CO), 166.44 (CO);

*4.1.1.16 Coupling **75** to **55***

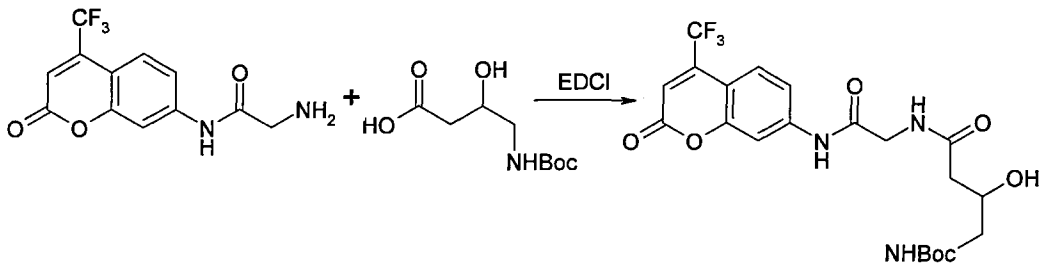

75 **55** **76**

75 (0.27 g, 0.94 mmol) was dissolved in water (10 mL), EDCI (0.26 g, 1.34 mmol, 1.4 eq) DIPEA (0.203 mL, 0.152 g, 1.1 mmol, 1.1 eq) and N-Boc-4-amino-3-hydroxybutyric acid (**55**) (0.25 g, 1.2 mmol, 1.2 eq) were added, and the solution was stirred at room temperature for 4 hours. The product precipitated out from the reaction mixture. When the reaction had reached completion the solid was filtered off and washed thoroughly with water, DCM, NaOH (1 M) and diethyl ether (20 mL each). The product (**76**), a white solid was isolated in 63% yield (0.29 g). MS: 487 $[M+H]^+$, 974 $[M+M+H]^+$; ^1H NMR (CD_3OD, δ): 1.38 (s, 9 H, Boc-CH_3), 2.26-2.43 (m, 2 H, CH_2), 2.98-3.16 (m, 2 H, CH_2), 3.95-3.99 (m, 3 H, CH + CH_2), 6.75 (s, 1 H, CH), 7.47 (dd, 1 H, CH, J_1 = 8.8 Hz, J_2 = 2.0 Hz), 7.62 (dd, 1 H, CH, J_1 = 8.0 Hz, J_2 = 1.7 Hz), 7.89 (d, 1 H, CH, J = 2.0 Hz); Sample solubility was too low to obtain a good ^{13}C NMR spetrum.

*4.1.1.17 Removal of the Boc protection of **76***

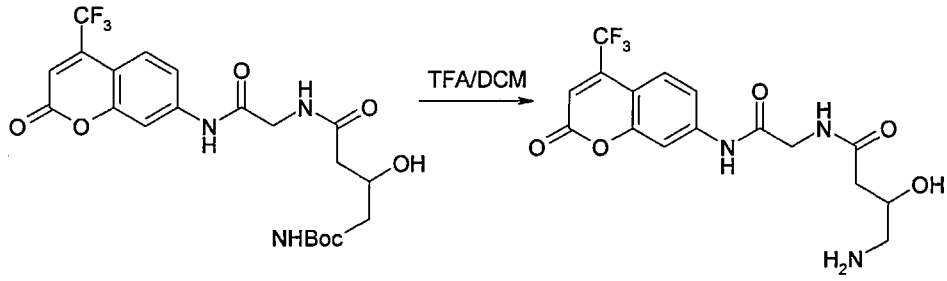

76 **77**

76 (0.11 g, 0.23 mmol) was dissolved in DCM (10 mL) and TFA (10 mL), and the solution was stirred at room temperature for 1 hour. The solvents were evaporated and the sample dried at reduced pressure for 24 hours to give the trifluoroacetate salt of **77** in quantitative yield. MS: 388 $[M+H]^+$, 755 $[M+H]^+$; ^1H NMR (CD_3OD, δ): 2.53 (d, 2 H, CH_2, J = 7.9 Hz), 2.90 (dd, 1 H, CH_2-1, J_1 = 12.7 Hz, J_2 = 9.2 Hz), 3.13 (dd, 1 H, CH_2-2, J_1 = 12.7 Hz, J_2 = 2.9 Hz), 4.01 (d, 2 H, CH_2, J = 4.6 Hz), 4.14-4.22 (m, 1 H, CH-O), 7.34 (dd, 1H, CH, J_1 = 8.8 Hz, J_2 = 2.0 Hz), 7.53 (dd, 1H, CH, J_1 = 9.0 Hz, J_2 = 1.9 Hz), 7.83 (d, 1H, CH, J = 2.0 Hz); ^{13}C NMR: 42.18 (CH_2), 44.19 (CH_2), 45.48 (CH_2), 60.30 (CH), 108.25 (CH), 110.28 (CH), 115.16 (CH), 117.29 (C_q), 126.70 (CH), 144.29 (C_q), 156.29 (CO), 160.72 (C_q), 170.30 (CO), 173.30 (CO).

4.1.1.18 Coupling N-Boc-glycine to coumarin 2

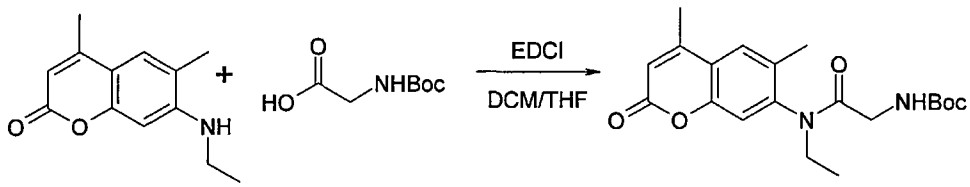

78 **68** **79**

Coumarin 2 (**78**) (0.22 g, 1 mmol) was dissolved in DCM (5 mL), N-Boc-glycine (**68**) (0.71 g, 4 mmol, 4 eq) and EDCI (0.79 g, 4 mmol, 4 eq) were added and the solution was stirred at room temperature for 3 days. The solvents were evaporated, the residue dissolved in DCM (30 mL) and water (30 mL), the phases were separated and the aqueous phase was extracted with DCM (2·30 mL). The combined organic phases were washed with water (2·30 mL), dried over $MgSO_4$, filtered and concentrated. The sample was applied onto a silica column and chromatographed with Et_2O to give **79** in 10% yield (0.04 g). MS: 374 $[M+H]^+$; ^1H NMR ($CDCl_3$, δ): 1.03-1.06 (t, 3 H, CH_3), 1.33 (s, 9 H, CH_3), 2.21 (s, 3 H, CH_3), 2.32 (s, 3 H, CH_3), 3.17-3.27 (sext., 1 H, CH_2-1), 3.44-3.46 (d, 2 H, CH_2), 4.02-4.14 (sext., 1 H, CH_2-1), 5.32 (br s, 1 H, NH), 6.25 (s, 1 H, CH), 7.02 (s, 1 H, CH), 7.45 (s, 1 H, CH); ^{13}C NMR: 12.76 (CH_3), 14.39 (CH_3), 17.18 (CH_3), 28.25 (CH_3), 38.18 (CH_2), 43.36 (CH_2), 79.65 (C_q), 109.14 (CH), 115.95 (C_q), 117.52 (CH), 118.41 (CH), 125.07 (CH), 127.34 (C_q), 132.08 (C_q), 149.57 (C_q), 152.94 (C_q), 154.73 (CO), 162.18 (CO), 167.80 (CO).

4.1.1.19 DL-4-Amino-3-hydroxybutyric acid ethyl ester

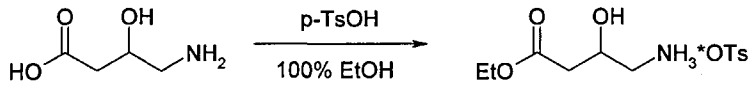

54 **80**

DL-4-amino-3-hydroxybutyric acid (**54**) (2.38 g, 20 mmol) was suspended in 100% EtOH (80 mL), p-TsOH monohydrate (4.18 g, 22 mmol, 1.1 eq) was added, and the solution was refluxed under argon for 24 hours. The ethanol was removed at reduced pressure and the residue triturated with diethyl ether (60 mL). After filtration the product (**80**), a white, crystalline solid, was isolated as the p-toluenesulfonate salt in 63% yield (3.99 g). MS: 147 $[M]^+$; ^1H NMR ($CDCl_3$, δ): 1.24 (dt, 3 H, CH_3, J_1 = 7.1 Hz, J_2 = 2.6 Hz), 2.36 (s, 3 H, CH_3), 2.53 (dd, 2 H, CH_2, J_1 = 9.2 Hz, J_2 = 3.1 Hz), 2.88 (dd, 2 H, CH_2, J_1 = 12.7 Hz, J_2 = 9.2 Hz), 3.10 (dd, 2 H, CH_2, J_1 = 12.7 Hz, J_2 = 3.1 Hz), 4.07-4.24 (m, 3 H, CH_2 + CH-O), 7.23 (d, 2 H, 2 CH, J = 7.9 Hz), 7.69 (d, 2 H, 2 CH, J = 8.3 Hz); ^{13}C NMR: 14.46 (CH_3), 21.30 (CH_3), 40.66 (CH_2), 45.36 (CH_2), 61.83 (CH_2-O), 65.57 (CH-OH), 126.92 (CH), 129.83 (CH), 141.76 (C_q), 143.41 (C_q), 172.18 (CO); mp: 73 °C, IR (ν_{max} / (cm^{-1}), KBr): 3338, 3099, 2971, 1740, 1621, 1504, 1456.

4.1.1.20 DL-N-Boc-4-amino-3-hydroxybutyric acid ethyl ester

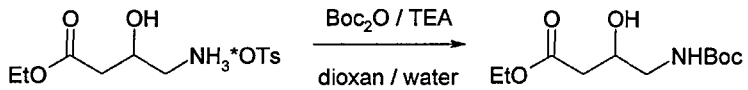

80 **81**

DL-4-amino-3-hydroxybutyric acid ethyl ester (**80**) (3.19 g, 10 mmol) was dissolved in DCM (17 mL), TEA (2.10 mL, 1.52 g, 15 mmol, 1.5 eq) and Boc_2O (2.42 g, 1.10 mmol, 1.1 eq) were added, and the reaction mixture was stirred at

room temperature for 24 hours. DCM (30 mL) and water (30 mL) were added, the phases were separated, and the aqueous phase was extracted with DCM (2·30 mL). The combined organic extracts were washed with water, 0.1 M HCl and 1 M $KHCO_3$, dried over $MgSO_4$, filtered, and the solvent was evaporated to afford the product (**81**) as a colourless oil in 80% yield (1.97 g). MS: 247 $[M]^+$; ^1H NMR ($CDCl_3$, δ): 1.20 (t, 3 H, CH_3, J = 7.1 Hz), 1.37 (s, 9 H, $3CH_3$), 2.41 (d, 1 H, CH_2-1, J = 3.1 Hz), 2.43 (s, 1 H, CH_2-2), 4.00-4.08 (m, 1 H, CH-O), 4.10 (q, 2 H, CH_2, J = 7.1 Hz), 5.01 (br s, 1 H, NH); ^{13}C NMR: 14.07 (CH_3), 28.30 (CH_3), 38.66 (CH_2), 45.48 (CH_2), 60.77 (CH_2-O), 67.00 (CH-OH), 79.52 (C_q), 156.49 (CO), 172.41 (CO); IR (ν_{max} / (cm^{-1}), paraffin): 3387, 2927, 2854, 1723, 1530, 1461.

*4.1.1.21 Coupling coumarin 343 to **80***

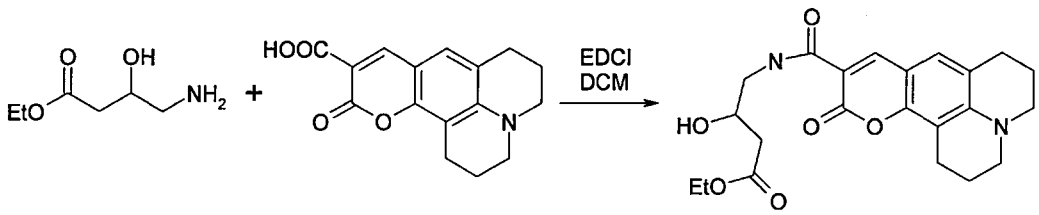

80 **82** **83**

80 (0.25 g, 0.77 mmol, TsOH-salt) was dissolved in DCM (6 mL), DIPEA (130 µL, 0.098 g, 0.77 mmol), coumarin 343 (**82**) (0.22 g, 0.77 mmol) and EDCI (0.16 g, 0.85 mmol, 1.1 eq) were added, and the solution was stirred at room temperature for 12 hours. DCM (30 mL) and water (30 mL) were added, the phases were separated, and the aqueous phase was extracted with DCM (2·20 mL). The combined organic phases were washed with water (30 mL), 1 M NaOH (30 mL), 1 M HCl (30 mL), dried over $MgSO_4$, filtered and evaporated to dryness. The product (**83**) was obtained in 60% yield (0.19 g) as an orange

solid. MS: 415 $[M+H]^+$, 829 $[M+M+H]^+$; ^1H NMR ($CDCl_3$, δ): 1.20 (t, 3 H, CH_3, J = 7.1 Hz), 1.87-1.95 (m, 4 H, 2 CH_2), 2.48 (d, 2 H, CH_2, J = 6.4 Hz), 2.70 (t, 2 H, CH_2, J = 6.1 Hz), 2.81 (t, 2 H, CH_2, J = 6.4 Hz), 3.24-3.29 (m, 4 H, CH_2), 3.39-3.48 (m, 1 H, CH_2-1), 3.55-3.62 (m, 1 H, CH_2-2), 4.07 (q, 2 H, CH_2, J = 7.1 Hz), 4.13-4.22 (m, 1 H, CH-OH), 6.92 (s, 1 H, CH), 8.50 (s, 1 H, CH), 9.13 (t, 1 H, NH, J = 5.7 Hz); ^{13}C NMR: 14.07 (CH_3), 19.95 (CH_2), 20.97 (CH_2), 27.33 (CH_2), 35.55 (CH_2), 39.23 (CH_2), 45.19 (CH_2), 49.72 (CH_2), 50.15 (CH_2), 60.59 (CH_2), 68.07 (CH), 105.51 (C_q), 108.05 (C_q), 119.63 (C_q), 126.59 (C_q), 126.99 (CH), 148.12 (CH), 148.27 (C_q), 152.63 (C_q), 162.81 (CO), 165.07 (CO), 171.98 (CO); mp: 123 °C; IR (ν_{max} / (cm^{-1}), KBr): 3321, 2937, 2849, 1734, 1693, 1618, 1586, 1520.

4.1.2 Triad synthesis with glutamic acid scaffold

4.1.2.1 Coupling coumarin 120 to N-Fmoc-γ-O-^{t}Bu glutamic acid

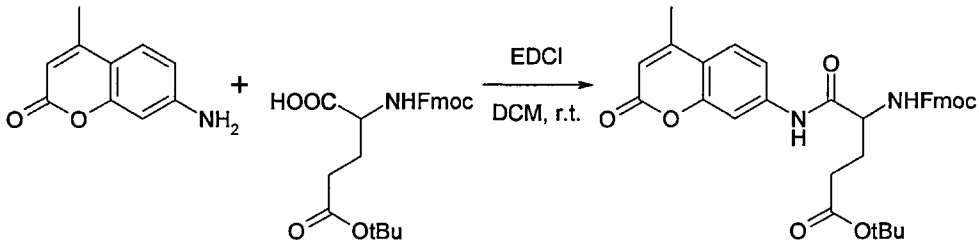

67 **84** **85**

Coumarin 120 (**67**) (0.50 g, 2.9 mmol) and N-Fmoc-γ-O-^{t}Bu glutamic acid (**84**) (1.27 g, 2.9 mmol) were dissolved in a mixture of 30 mL THF and 30 mL DCM, EDCI (0.60 g, 3.1 mmol, 1.1 eq) was added, and the solution was allowed to proceed at room temperature for 24 hours. The solvents were removed at reduced pressure, the residue dissolved in DCM (30 mL) and water (30 mL), the phases were separated, and the aqueous phase was extracted with DCM (2·25

mL). The combined extracts were washed with water (2·25 mL), dried over $MgSO_4$, filtered, and concentrated. The sample was purified on a silica column by elution with DCM / MeOH, to give the desired product (**85**) as a pale yellow solid in 64% yield (1.08 g). HR-ESMS ($C_{34}H_{34}N_2O_7$): calc: 583.2439 $[M+H]^+$, measured: 583.2441 $[M+H]^+$; Anal. calc. for $C_{34}H_{34}N_2O_7$: C: 70.09, H: 5.88, N: 4.81; Found: C: 68.27, H: 5.95, N: 4.49; ^1H NMR ($CDCl_3$): 1.34 (s, 9 H, CH_3-^{t}Bu), 1.91-2.46 (m, 7 H, CH_3 + 2·CH_2), 4.07-4.12 (m, 1 H, CH), 4.29-4.59 (m, 3 H, CH_2 + CH), 6.04 (s, 1 H, CH), 6.18 (br s, 1 H, NH), 7.16-7.69 (m, 11 H, CH), 9.33 (br s, 1 H, NH); ^{13}C NMR: 18.41 (CH_3), 27.74 (CH_2), 27.96 (CH_3), 31.76 (CH_2), 46.93 (CH), 55.32 (CH), 67.32 (CH_2), 81.17 (C_q), 100.89 (CH), 107.07 (CH), 111.68 (CH), 113.10 (CH), 115.59 (CH), 115.83, 119.89 (CH), 124.98 (CH), 125.67 (CH), 126.98 (CH), 127.03 (CH), 141.15 (C_q), 134.49 (C_q), 152.54 (C_q), 153.81 (C_q), 156.67 (CO), 161.14 (CO), 170.44 (CO), 172.82 (CO); mp: 112-113 °C; IR (ν_{max} / (cm^{-1}), KBr): 3309, 3066, 2978, 1698, 1618, 1583, 1525.

*4.1.2.2 Removal of the Fmoc protecting group from **85***

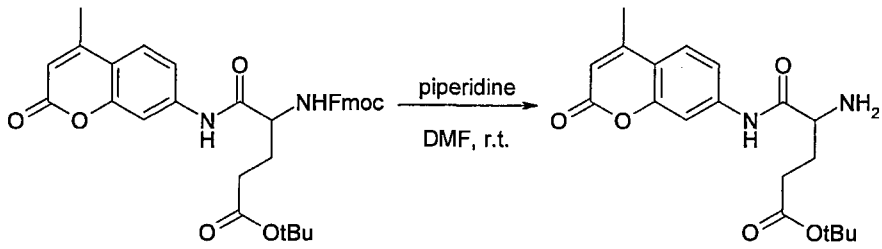

85 **86**

85 (0.38 g, 0.63 mmol) was dissolved in DMF (5 mL), piperidine (1.0 mL) was added, and the solution was stirred at room temperature for 1.5 hours. The DMF and the piperidine were removed at reduced pressure and the solid residue dissolved in DCM (3 mL). The product (**86**) was isolated as an off-white solid by chromatography on silica with DCM / MeOH in 79% yield (0.19 g). MS:

361 $[M+H]^+$, 722 $[M+M+H]^+$; ^1H NMR ($CDCl_3$): 1.38 (s, 9 H, $3CH_3$), 1.67 (s, 2 H, NH), 1.78-1.90 (m, 1 H, CH_2-1), 2.11-2.22 (m, 1 H, CH_2-2), 2.34 (s, 3 H, CH_3), 2.26-2.44 (m, 2 H, CH_2), 3.45-3.50 (m, 1 H, CH), 6.12 (s, 1 H, CH), 7.44-7.52 (2d, overlapping peaks, 2 H, CH), 7.57-7.58 (s, 1 H, CH), 9.73 (br s, 1 H, NH); ^{13}C NMR: 18.53 (CH_3), 28.05 (CH_3), 29.99 (CH_2), 32.14 (CH_2), 55.22 (CH), 80.86 (C_q), 106.77 (CH), 113.31 (CH), 115.29 (CH), 116.01 (C_q), 125.16 (CH), 141.02 (C_q), 152.13 (C_q), 154.30 (C_q), 161.03 (CO), 172.65 (CO), 173.12 (CO).

*4.1.2.3 Coupling coumarin 343 to **86***

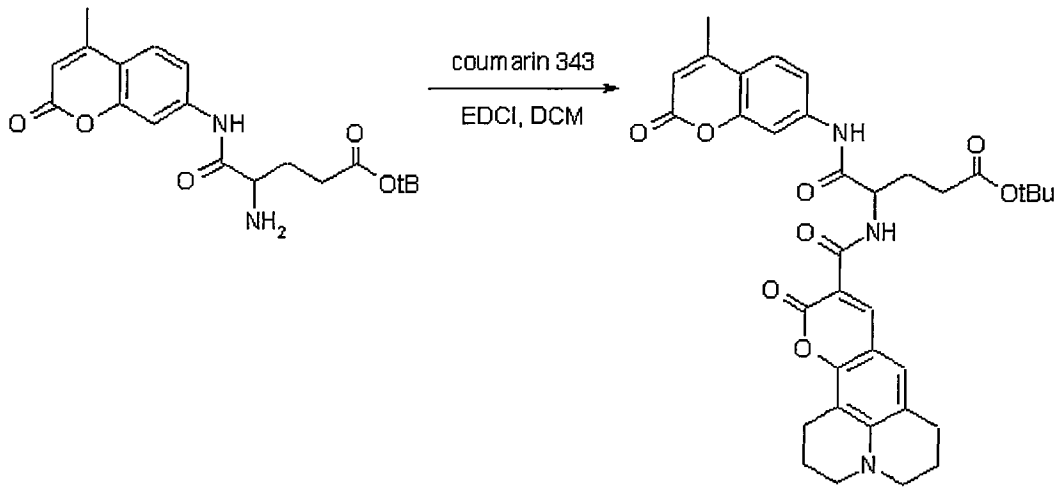

86 **87**

86 (1.33 g, 3.69 mmol) was dissolved in DCM (7 mL), coumarin 343 (**82**) (1.05 g, 3.69 mmol) and EDCI (0.78 g, 4.06 mmol, 1.1 eq) were added, and the reaction was allowed to proceed at room temperature for 24 hours. The reaction was stopped, DCM (20 mL) and water (30 mL) were added to the reaction mixture, the layers were separated and the aqueous phase was extracted with DCM (2·30 mL). The combined organic layers were washed with water (40 mL) and dilute NaOH (1 M, 40 mL), dried over $MgSO_4$, filtered, and concentrated *in vacuo*. The desired product (**87**) was isolated as a bright red solid in 50.5%

yield (1.17 g) by chromatography on silica with $CHCl_3$ / MeOH. HR-ESMS ($C_{35}H_{37}N_3O_8$): calc: 628.2653 $[M+H]^+$, measured: 628.2660 $[M+H]^+$; Anal. calc. for $C_{35}H_{37}N_3O_8$: C: 66.97, H: 5.94, N: 6.69; Found: C: 64.87, H: 6.02, N: 6.99; ^1H NMR ($CDCl_3$, δ): 1.32 (s, 9 H, CH_3), 1.88-1.90 (m, 4 H, CH_2), 2.02-2.17 (m, 1 H, CH_2-1), 2.23-2.51 (m, 6 H, CH_3 + CH_2-2, CH_2), 2.71 (t, 4 H, CH_2, J = 6.1 Hz), 2.81 (t, 4 H, CH_2, J = 6.2 Hz), 3.26-3.27 (m, 4 H, 2 CH_2), 4.68 (dd, 1 H, CH, J_1 = 13.7 Hz, J_2 = 7.1 Hz), 6.07 (d, 1 H, CH, J = 1.1 Hz), 6.95 (s, 1 H, CH), 7.11-7.30 (m, 2 H, 2 CH), 7.66 (s, 1 H, CH), 8.40 (s, 1 H, CH), 9.34-9.36 (d, 1 H, NH, J = 6.8 Hz), 9.97 (s, 1 H, CH); ^{13}C NMR: 18.25 (CH_3), 19.77 (CH_2), 19.86 (CH_2), 20.82 (CH_2), 26.83 (CH_2), 27.22 (CH_2), 27.89 (CH_3), 31.69 (CH_2), 49.69 (CH_2), 50.12 (CH_2), 53.35 (CH_2), 54.24 (CH), 80.51 (C_q), 105.38 (C_q), 106.86 (C_q), 107.10 (CH), 107.63 (C_q), 112.69 (CH), 115.21 (CH), 115.44 (C_q), 124.51 (CH), 127.11 (CH), 141.56 (C_q), 147.90 (C_q), 148.53 (C_q), 152.22 (C_q), 153.67 (C_q), 160.89 (CO), 162.66 (CO), 164.53 (CO), 170.30 (CO), 171.73 (CO); mp: 166-167 °C;

IR (ν_{max} / (cm^{-1}), KBr): 3299, 2936, 2849, 1698, 1618, 1583, 1562, 1516, 1445, 1416, 1390, 1368, 1310.

*4.1.2.4 Removal of the ^{t}Bu protection in **87***

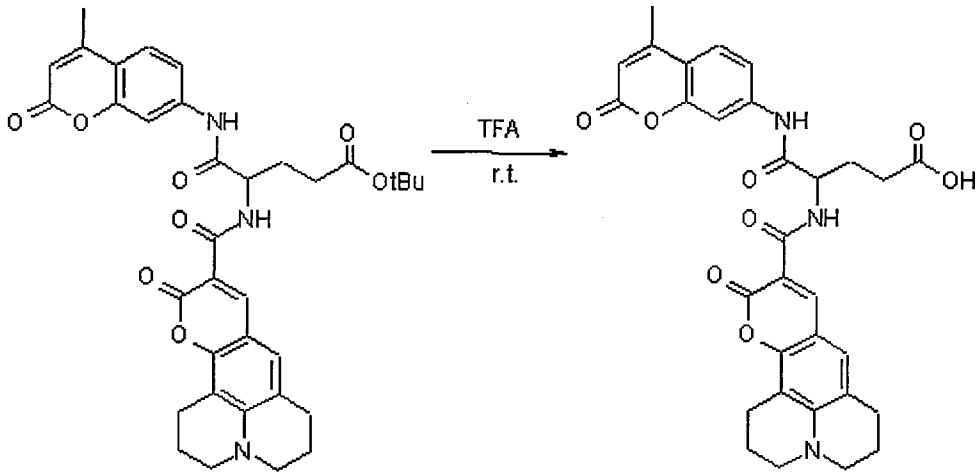

87 **88**

87 (0.43 g, 0.7 mmol) was dissolved in DCM (5 mL), TFA (5 mL) was added, and the solution was stirred at room temperature. The reaction was monitored by TLC on silica plates (developed in MeOH / DCM (1%)). When the transformation was complete, the volatile components were evaporated and the sample was dried *in vacuo* for 12 hours. The trifluoroacetate salt of **88** was obtained as a dark red solid in quantitative yield. MS: 571 $[M+H]^+$, 1142 $[M+M+H]^+$; ^{1}H NMR ($CDCl_3$, δ): 1.87 (br s, 4 H, $2CH_2$), 2.07-2.14 (m, 1 H, CH_2-1), 2.29 (s, 3 H, CH_3), 2.46-2.48 (m, 2 H, CH_2), 2.64-2.70 (m, 3 H, CH_2 + CH_2-2), 3.27 (br s (m), 4 H, CH_2), 4.72 (br s (m), 1 H, CH), 6.03 (s, 1 H, CH), 6.79 (s, 1 H, CH), 7.33 (d, 1 H, CH, J = 8.4 Hz), 7.40 (d, 1 H, CH, J = 8.4 Hz), 7.65 (s, 1 H, CH), 8.33 (s, 1 H, CH); ^{13}C NMR 17.98 (CH_3), 19.60 (CH_2), 20.56 (CH_2), 27.02 (CH_2), 27.33 (CH_2), 29.90 (CH_2), 49.50 (CH_2), 49.97 (CH_2), 53.57 (CH), 105.11 (C_q), 106.16 (C_q), 106.83 (C_q), 107.85 (CH), 112.36 (CH), 112.89 (C_q), 115.58 (CH), 115.77 (C_q), 116.68 (C_q), 119.99 (C_q), 124.85 (CH), 127.02 (CH), 141.41 (C_q), 147.98 (C_q), 148.75 (CH), 153.49 (C_q), 161.72 (CO), 162.86 (CO), 164.40 (CO), 170.47 (CO), 175.01 (CO).

*4.1.2.5 Coupling 2',3'-isopropylidene-5'-aminonucleotides to **88***

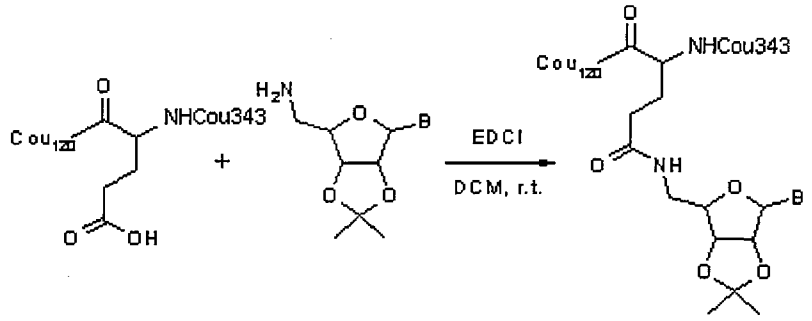

88 **89a-b** **90a-b**

88 (0.57 g, 1.0 mmol) was dissolved in DCM (10 mL). The pH of the solution was adjusted to 8.5 with TEA, and the 2',3'-isopropylidene-5'-aminonucleotide (**89a-b**) (1.1 mmol, 1.1 eq) was dissolved in this solution. EDCI (0.21 g, 1.1 mmol, 1.1 eq) was added, and the reaction mixture was stirred at room temperature for 24 hours. DCM (20 mL) and water (30 mL) were added to the solution, the phases were separated, and the aqueous phase was extracted with DCM (2·30 mL). The combined organic phases were washed with water (2·30 mL), dried over $MgSO_4$, concentrated, and chromatographed on silica with MeOH / DCM (0-5%) to give **90a** and **90b** as bright orange-coloured solids.

90a (B = U): Yield: 38% (0.32 g); HR-ESMS ($C_{43}H_{44}N_6O_{12}Na$): calc: 859.2909 $[M+Na]^+$, measured: 859.2897 $[M+Na]^+$; Anal. calc. for $C_{43}H_{44}N_6O_{12}$: C: 61.72, H: 5.30, N: 10.04; Found: C: 52.87, H: 5.00, N: 10.04; ^1H NMR ($CDCl_3$, δ): 1.24 (s, 3 H, OCH_3), 1.44 (s, 3 H, OCH_3), 1.87-1.89 (m, 4 H, 2 CH_2), 2.10-3.02 (m, 4 H, 2 CH_2), 2.20 (s, 3 H, CH_3), 3.68-3.73 (m, 1 H, CH), 2.26-3.39 (m, 19 H, CH_2), 4.15 (d, 1 H, CH, J = 4.0 Hz), 4.45 (dd, 1 H, CH, J_1 = 12.0 Hz, J_2 = 4.0 Hz), 4.58 (d, 1 H, CH, J = 5.9 Hz), 4.70 (d, 1 H, CH, J = 6.1 Hz), 4.76 (dd, 1 H, CH, J_1 = 11.3 Hz, J_2 = 5.3 Hz), 5.09 (d, 1 H, CH, J = 6.7 Hz), 5.63 (d, 1 H, CH, J = 8.1

Hz), 6.00 (s, 1 H, CH), 6.23 (s, 1 H, CH), 6.89 (s, 1 H, CH), 7.19 (s, 1 H, CH), 7.60 (s, 1 H, CH), 8.44 (d, 1 H, CH, J = 1.5 Hz), 8.63 (d, 1 H, CH, J = 7.1 Hz), 9.39 (d, 1 H, NH, J = 7.0 Hz), 9.93 (s, 1 H, NH), 10.55 (s, 1 H, NH); ^{13}C NMR: 18.36 (CH_3), 19.73 (CH_2), 19.96 (CH_2), 20.87 (CH_2), 24.60 (CH_3), 25.18 (CH_3), 26.25 (CH_3), 27.08 (CH_2), 27.26 (CH_3), 28.46 (CH_2), 33.25 (CH_2), 38.57 (CH_2), 40.58 (CH_2), 49.82 (CH_2), 50.18 (CH_2), 52.23 (CH_2), 53.39 (CH_2), 54.59 (CH), 68.09 (CH), 80.38 (CH), 83.63 (CH), 83.70 (CH), 85.17 (CH), 86.76 (CH), 87.91 (CH), 91.72 (CH), 97.00 (CH), 102.74 (CH), 105.63 (CH), 106.91 (C_q), 107.01 (C_q), 108.17 (CH), 111.99 (C_q), 112.75 (CH), 114.62 (C_q), 115.68 (C_q), 115.68 (CH), 119.92 (C_q), 124.75 (CH), 127.23 (CH), 141.71 (C_q), 143.62 (CH), 148.41 (C_q), 148.69 (CH), 150.89 (C_q), 151.11 (C_q), 152.37 (C_q), 152.59 (C_q), 153.79 (CO), 161.05 (CO), 163.25 (CO), 164.45 (CO), 167.86 (CO), 170.37 (CO), 172.91 (CO); mp: 172-174 °C; IR (ν_{max} / (cm^{-1}), KBr): 3320, 3081, 2987, 2940, 2851, 2361, 2342, 1696, 1617, 1583, 1560, 1516.

90b (B = A): Yield: 84% (0.72 g); HR-ESMS ($C_{44}H_{46}N_9O_{10}$): calc: 860.3362 [M+H^+], measured: 860.3350 [M+H^+]; Anal. calc. for $C_{44}H_{46}N_9O_{10}$: C: 61.39, H: 5.39, N: 14.64; Found: C: 56.56, H: 4.88, N:13.54; ^1H NMR ($CDCl_3$, δ): 1.29 (s, 3 H, OCH_3), 1.54 (s, 3 H, OCH_3), 1.86-1.88 (m, 4 H, CH_2), 2.25 (s, 3 H, CH_3), 2.18-2.26 (m, 1 H, CH_2-1), 2.39-2.46 (m, 1 H, CH_2-2), 2.57-2.66 (m, 4 H, 2 CH_2), 2.72 (d, 1 H, CH, J = 6.4 Hz), 3.21-3.25 (m, 4 H, CH_2), 4.01-4.04 (m, 1 H, CH), 4.42 (d, 1 H, CH, J = 2.4 Hz), 4.76-4.79 (m, 2 H, CH_2), 5.23-5.24 (m, 1 H, CH), 5.75 (d, 1 H, CH, J = 4.6 Hz), 6.01 (d, 1 H, CH, J = 1.1 Hz), 6.28 (br s, 2 H, NH_2), 6.83 (s, 1 H, CH), 7.30 (d, 1 H, CH, J = 8.8 Hz), 7.39 (d, 1 H, CH, J = 1.8 Hz), 7.60 (d, 1 H, CH, J = 1.8 Hz), 7.75 (s, 1 H, CH), 8.26 (s, 1 H, CH), 8.35 (d, 1 H, NH, J = 8.3 Hz), 8.39 (s, 1 H, NH), 9.42 (d, 1 H, NH, J = 7.3 Hz), 9.94 (s, 1

H, NH); ^{13}C NMR: 18.49 (CH_3), 19.96 (CH_2), 20.07 (CH_2), 21.03 (CH_2), 25.33 (CH_3), 27.35 (CH_2), 27.50 (CH_2), 28.10 (CH_3), 32.61 (CH_2), 41.11 (CH_2), 49.81 (CH_2), 50.23 (CH_2), 53.40 (CH), 54.00 (CH_3)?, 81.44 (CH), 82.45 (CH), 83.47 (CH), 92.32 (CH), 105.32 (CH), 105.58 (C_q), 107.11 (C_q), 107.68 (C_q), 108.11 (C_q), 112.97 (CH), 114.73 (C_q), 115.63 (C_q), 115.70 (CH), 119.66 (CH), 120.77 (C_q), 124.82 (CH), 127.15(CH), 140.09 (CH), 141.66 (C_q), 148.12 (C_q), 148.45 (CH), 148.70 (C_q), 152.27 (C_q), 152.70 (CH), 154.01 (C_q), 155.98 (C_q), 161.18 (CO), 162.66 (CO), 170.08 (CO), 172.96 (CO); mp: 193-195 °C; IR (ν_{max} / (cm^{-1}), KBr): 3325, 2938, 2361, 1698, 1636, 1617, 1582, 1560, 1516.

91 The major isolated product of the reaction:

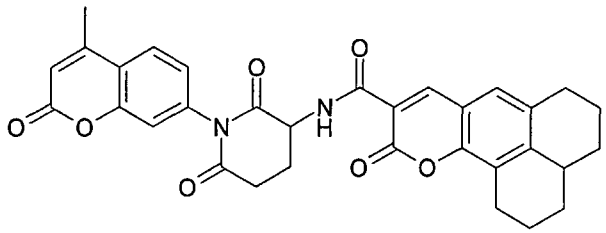

MS: 554 $[M+H]^+$, 1109 $[M+M+H]^+$; ^1H NMR ($CDCl_3$, δ): 1.61 (br s, 3 H, NH), 1.86-1.94 (m, 4 H, CH_2), 2.18-2.37 (m, 4 H, CH_2), 2.38 (s, 3 H, CH_3), 2.47-2.53 (m, 2 H, CH_2), 2.68-2.72 (m, 2 H, CH_2), 2.79-2.83 (m, 2 H, CH_2), 2.87-3.04 (m, 4 H, CH_2), 3.25-3.30 (m, 4 H, CH_2), 4.84-4.92 (m, 1 H, CH), 6.25 (d, 1 H, CH, J = 1.3 Hz), 6.94 (s, 1 H, CH), 7.03 (d, 1 H, CH, J = 2.0 Hz), 7.06 (d, 1 H, CH, J = 2.0 Hz), 7.12 (d, 1 H, CH, J = 2.0 Hz), 7.61 (d, 2 H, CH, J = 8.4 Hz), 9.50 (d, 1 H, NH, J = 6.9 Hz); ^{13}C NMR: 18.78 (CH_3), 20.15 (CH_2), 21.14 (CH_2), 24.30 (CH_2), 27.51 (CH_2), 32.22 (CH_2), 49.93 (CH_2), 50.35 (CH_2), 51.78 (CH), 105.77 (CH), 107.91 (CH), 108.25 (CH), 115.76 (C_q), 117.74 (CH), 119.86 (CH), 120.24 (C_q), 124.70 (C_q), 125.27 (C_q), 127.27 (C_q), 138.10 (C_q), 148.50 (C_q), 148.63

(C_q), 151.86 (C_q), 153.82 (C_q), 160.39 (CO), 162.98 (CO), 164.10 (CO), 171.15 (CO), 171.38 (CO).

4.1.2.6 Coupling coumarin 151 to N-Fmoc-γ-O-^{t}Bu glutamic acid

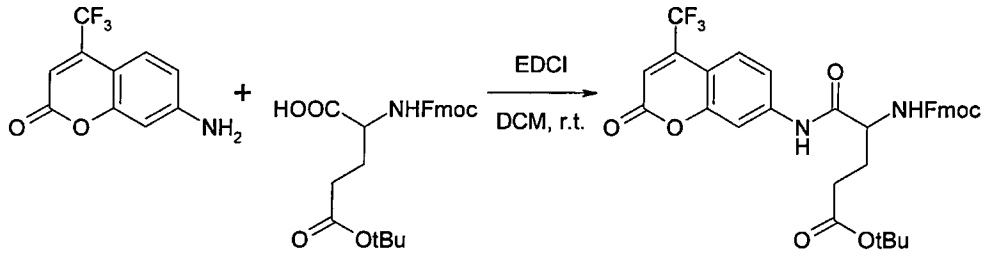

73 **84** **92**

Coumarin 151 (**73**) (0.47 g, 2.05 mmol) and N-Fmoc-γ-O-^{t}Bu glutamic acid (**84**) (0.87 g, 2.05 mmol) were dissolved in DCM (20 mL), EDCI (0.43 g, 2.26 mmol, 1.1 eq) was added, and the solution was allowed to proceed at room temperature for 3 days. Coumarin 151 is initially only partially dissolved, but gradually dissolves as the reaction proceeds. Water (30 mL) was added to the reaction mixture, the phases were separated, and the aqueous phase was extracted with DCM (2· 25 mL). The combined extracts were washed with water (2·30 mL), dried over $MgSO_4$, filtered, and concentrated. The sample was purified on a silica column by elution with Et_2O / Hexane (6:4), to give the desired product (**92**) as a white solid in 34% yield (0.44 g). HR-ESMS ($C_{34}H_{31}N_2O_7F_3$): calc: 637.2156 $[M+H]^+$, measured: 637.2157 $[M+H]^+$; Anal. calc. for $C_{34}H_{31}N_2O_7F_3$: C: 64.15, H: 4.91, N: 4.40; Found: C: 64.40, H: 5.02, N: 4.23; ^{1}H NMR ($CDCl_3$, δ): 1.37 (s, 9 H, 3 CH_3), 1.83-2.50 (m, 8 H, 2.5 CH_2 + CH_3), 4.10-4.15 (m, 1 H, CH), 4.32-4.35 (d, 2 H, CH_2), 6.03-6.08 (m, 2 H, 2 CH), 7.18-7.66 (m, 11 H, 11 CH), 9.26 (br s, ~1 H, NH); ^{13}C NMR: 27.72 (CH_2), 28.99 (CH_3), 46.92 (CH_2), 31.73 (CH_2), 55.18 (CH), 81.56 (C_q), 107.48 (CH), 109.27

(C_q), 113.77 (CH), 116.23 (CH), 119.97 (CH), 124.92 (CH), 127.01 (CH), 127.75 (CH), 141.18 (C_q), 141.20 (C_q), 142.20 (C_q), 143.42 (C_q), 143.48 (C_q), 155.00 (CF_3), 156.81 (CO), 159.12 (CO), 170.48 (CO), 173.15 (CO); mp: becomes glassy at 109-110 °C, complete melting at 129-130 °C; IR (ν_{max} / (cm^{-1}), KBr): 3285, 1733, 1698, 1669, 1618, 1583, 1524, 1419, 1408, 1369.

4.1.2.7 Removal of the Fmoc protecting group from ***92***

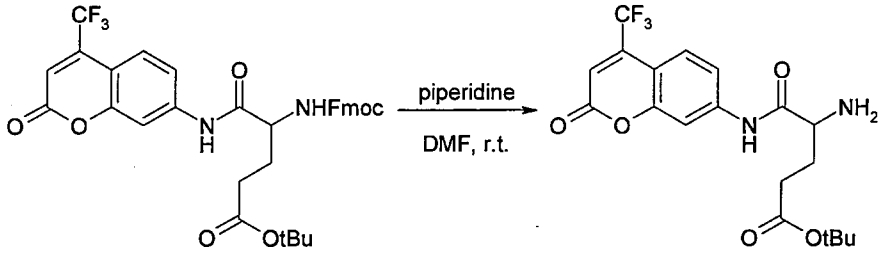

92 **93**

92 (0.41 g, 0.64 mmol) was dissolved in DMF (5 mL), piperidine (1 mL) was added, and the solution was stirred at room temperature for 1.5 hours. The volatile components were removed at reduced pressure and the solid residue dissolved in DCM (3 mL). The product (**93**) was isolated as a yellow solid by chromatography on silica with DCM / MeOH in 90% yield (0.24 g). MS: 415 $[M]^+$, 455 $[M+K]^+$, 828 $[M+M]^+$; ^1H NMR ($CDCl_3$, δ): 1.38 (s, 9 H, CH_3), 1.76-1.85 (m, 1 H, CH_2-1), 2.12-2.44 (2 m, 3 H, CH_2 + CH_2-1), 3.46-3.51 (m, 1 H, CH), 6.68 (s, 1 H, CH), 7.44-7.56 (m, 1 H, CH), 7.56-7.59 (m, 1 H, CH), 7.82 (s, 1 H, CH); ^{13}C NMR: 28.18 (CH_3), 30.06 (CH_2), 32.25 (CH_2), 55.37 (CH), 81.10 (C_q), 107.26 (CH), 113.78 (CH), 116.15 (C_q), 126.00, 142.29 (C_q), 155.50 (C_q), 162.69 (CO), 172.80 (CO), 173.53 (CO).

4.1.2.8 Coupling coumarin 343 to ***93***

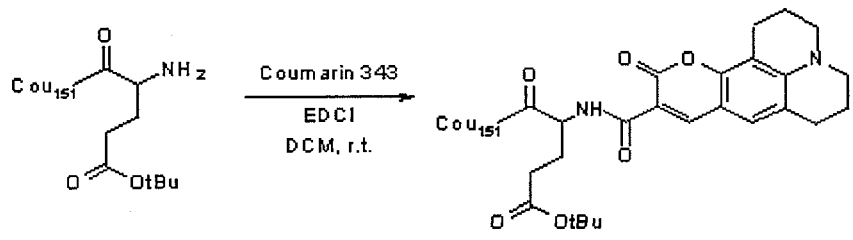

93 **94**

93 (0.33 g, 0.8 mmol) was dissolved in DCM (10 mL), coumarin 343 (**82**) (0.23 g, 0.8 mmol) and EDCI (0.17 g, 0.88 mmol, 1.1 eq) were added, and the reaction was allowed to proceed at room temperature for 24 hours. The reaction was stopped, DCM (20 mL) and water (30 mL) were added to the reaction mixture, the layers were separated and the aqueous phase was extracted with DCM (2·30 mL). The combined organic layers were washed with water (40 mL) and 1 M NaOH (40 mL), dried over $MgSO_4$, filtered, and concentrated *in vacuo*. The desired product (**94**) was isolated as a bright red solid in 50% (0.27 g) yield by chromatography on silica with $CHCl_3$ / MeOH. HR-ESMS ($C_{35}H_{34}N_3O_8F_3$): calc: 682.2371 $[M+H]^+$, measured: 682.2378 $[M+H]^+$; Anal. calc. for $C_{35}H_{34}N_3O_8F_3$: C: 61.67, H: 5.03, N: 6.16; Found: C: 60.86, H: 5.01, N: 6.10; ^1H NMR ($CDCl_3$, δ): 1.33 (s, 9 H, CH_3), 1.87-1.90 (t, 4 H, CH_2), 2.05-2.17 (m, 1 H, CH_2-1), 2.25-2.48 (m, 3 H, CH_2-2 + CH_2), 2.63-2.78 (m, 4 H, CH_2), 3.26-3.30 (m, 4 H, CH_2), 4.71 (dd, 1 H, CH, J_1 = 13.5 Hz, J_2 = 7.0 Hz), 6.47 (s, 1 H, CH), 6.84 (s, 1 H, CH), 7.30 (dd, 1 H, CH, J_1 = 8.9 Hz, J_2 = 1.8 Hz), 7.38 (d, 1 H, CH, J =7.5 Hz), 7.76 (d, 1 H, CH, J = 1.8 Hz), 8.36 (s, 1 H, NH), 9.35 (d, 1 H, NH, J_1 = 6.8 Hz), 10.04 (s, 1 H, NH); ^{13}C NMR: 19.76 (CH_2), 20.84 (CH_2), 26.70 (CH_2), 27.26 (CH_2), 27.91 (CH_3), 31.66 (CH_2), 49.73 (CH_2), 50.16 (CH_2), 54.28 (CH), 80.64 (C_q), 105.46 (C_q), 106.95 (C_q), 107.27 (C_q), 107.95 (C_q), 108.65 (CH),

113.11 (C_q), 116.31 (CH), 119.75 (CH), 123.17 (C_q), 125.25 (CH), 127.15 (CH), 140.71 (C_q), 141.14 (C_q), 142.88 (C_q), 147.95 (C_q), 148.62 (CH), 152.62 (C_q), 154.87 (C_q), 158.99 (CO), 162.73 (CO), 164.69 (CO), 170.55 (CO), 171.82 (CO); mp: 164-165 °C; IR (ν_{max} / (cm^{-1}), KBr): 3477, 3299, 3087, 2938, 2850, 2735, 1698, 1618, 1586, 1510, 1446, 1409, 1368, 1311.

4.1.2.9 Removal of the ^{t}Bu protection of ***94***

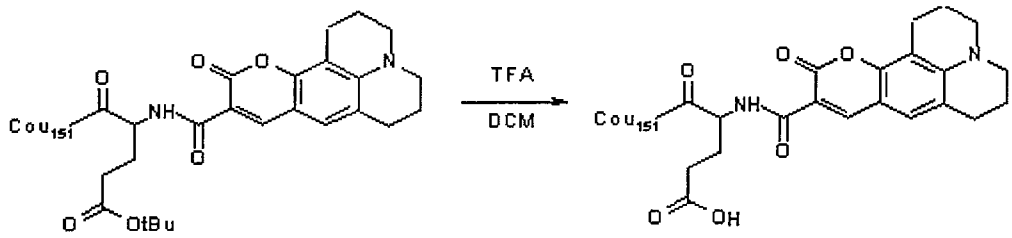

94 **95**

94 (0.25 g, 0.37 mmol) was dissolved in DCM (6 mL), TFA (6 mL) was added, and the solution was stirred at room temperature. The reaction was monitored by TLC. When the transformation was complete, the volatile components were evaporated and the sample was dried *in vacuo* for 12 hours. **95** Was obtained as a dark red solid in quantitative yield. MS: 571 $[M+H]^+$, 1142 $[M+M+H]^+$; ^{1}H NMR ($CDCl_3$, δ): 1.89 (m, 4 H, 2 CH_2), 2.24-2.69 (m, 2 H, CH_2), 3.32 (m, 4 H, 2 CH_2), 4.86-4.87 (m, 1 H, CH), 6.66 (s, 1 H, CH), 6.95 (s, 1 H, CH), 7.44 (dd, 1 H, CH, J_1 = 9.0 Hz, J_2 = 2.0 Hz), 7.58 (d, 1 H, CH, J = 7.3 Hz), 7.78 (d, 1 H, CH, J = 2.0 Hz), 8.40 (s, 1 H, CH), 9.31 (s, 1 H, NH), 9.58 (d, 1 H, NH, J = 7.5 Hz), 11.38 (s, 1 H, COOH); ^{13}C NMR: 27.71 (CH_2), 28.81 (CH_2), 31.05 (CH_2), 55.46 (CH), 108.36 (CH), 110.39 (C_q), 115.10 (CH), 117.49 (CH), 122.21 (C_q), 124.85 (C_q), 126.76 (C_q), 127.99 (CH), 144.09 (C_q), 149.42 (C_q), 156.29 (C_q), 160.46 (CO), 160.96 (CO), 162.38 (CF_3), 171.90 (CO), 176.09 (CO), 176.16 (CO).

*4.1.2.10 Coupling 2',3'-isopropylidene-5'-aminonucleotides to **95***

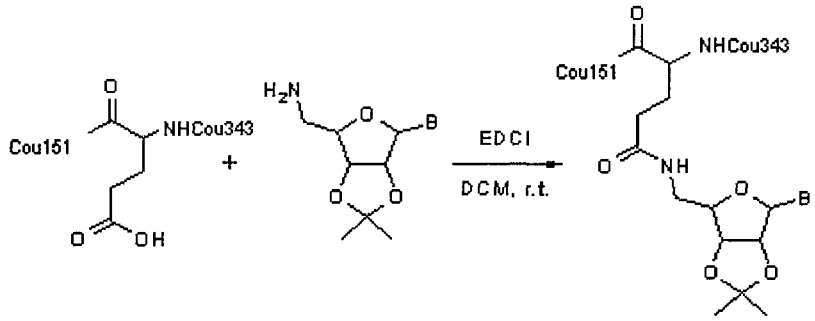

95 **89a-b** **96**

95 (0.57 g, 1.0 mmol) was dissolved in DCM (4 mL) and acetonitrile (1 mL). The pH of the solution was adjusted to 8.5 with TEA, and the 2',3'-isopropylidene-5'-aminonucleotide (**89a-b**) (2.0 mmol, 2 eq) was dissolved in this solution. EDCI (0.21 g, 1.1 mmol, 1.1 eq) was added, and the reaction mixture was stirred at room temperature for 48 hours. DCM (20 mL) and water (30 mL) were added to the solution, the phases were separated, and the aqueous phase was extracted with DCM (2·30 mL). The combined organic phases were washed with water (30 mL), dried over $MgSO_4$, concentrated, and chromatographed on silica to give **96a** and **96b** as bright yellow-coloured solids.

96a (B = U): Yield: 6% (0.05 g) HR-ESMS ($C_{43}H_{41}N_6O_{12}F_3$): calc: 891.2807 $[M+H]^+$, 891.2813 $[M+H]^+$; ^1H NMR ($CDCl_3$, δ): 1.28 (s, 3 H, OCH_3), 1.46 (s, 3 H, OCH_3), 1.90-1.92 (m, 6 H, 3 CH_2), 2.20-2.47 (m, 5 H, 2.5 CH_2), 2.67-2.71 (t, 2 H, CH_2), 2.86-2.89 (m, 2 H, CH_2), 3.34-3.40 (m, 6 H, 3 CH_2), 3.78-3.82 (m, 1 H, CH), 4.17-4.19 (d, 1 H, CH), ~4.70 (m / br s, 1 H, CH), 4.79-4.83 (t, 1 H, CH), 5.15 (dd, 1 H, CH, J_1 = 6.7 Hz, J_2 = 2.0 Hz), 5.22 (d, 1 H, CH, J = 2.0 Hz), 5.67 (dd, 1 H, CH, J_1 = 8.0 Hz, J_2 = 2.0 Hz), 6.52 (s, 1 H, CH), 6.95 (s, 1 H, CH), 7.13 (d, 1 H, CH, J = 8.3 Hz), 7.23 (s, 1 H, CH), 7.36 (dd, 1 H, CH, J_1 = 8.8 Hz, J_2 = 2.0 Hz), 7.45 (d, 1 H, CH, J = 7.3 Hz), 7.75 (d, 1 H, CH, J = 2.0 Hz), 8.51 (s, 1

H, NH), 9.42 (d, 1 H, NH, J = 6.8 Hz), 10.07 (s, 1 H, NH), 10.53 (s, 1 H, NH); ^{13}C NMR: 19.76 (CH_2), 20.06 (CH_2), 20.95 (CH_2), 25.25 (CH_3), 27.19 (CH_3), 27.40 (CH_2), 28.05 (CH_2), 33.65 (CH_2), 49.98 (CH_2), 50.31 (CH_2), 54.82 (CH), 80.13 (CH), 83.70, 85.18 (CH), 97.85 (CH), 103.02 (CH), 105.92 (CH), 106.77 (C_q), 107.42 (C_q), 108.34 (CH), 114.88 (CH), 116.45 (C_q), 120.16 (C_q), 125.53 (CH), 127.34 (CH), 142.93 (C_q), 143.70 (C_q), 148.69 (C_q), 148.98 (C_q), 151.16 (C_q), 152.75 (CO), 155.10 (CO), 159.21 (CO), 163.04 (CF_3), 163.59 (CO), 165.01 (CO), 170.42 (CO), 172.97 (CO); mp: decomposition above 157 °C; IR (ν_{max} / (cm^{-1}), KBr): 3429, 2939, 1697, 1617, 1584, 1560, 1517.

96b (B = A) : Yield: 15% (0.14 g); HR-ESMS ($C_{44}H_{43}N_9O_{10}F_3$): calc: 914.3079 $[M+H]^+$, 914.3078 $[M+H]^+$; Anal. calc. for $C_{44}H_{43}N_9O_{10}F_3$: C: 57.77, H: 4.74, N: 13.77; Found: C: 53.21, H: 4.31, N: 12.83; ^1H NMR ($CDCl_3$, δ): 1.30 (s, 3 H, OCH_3), 1.55 (s, 3 H, OCH_3), 1.88 (m, 4 H, 2 CH_2), 2.17-2.24 (m, 1 H, CH_2-1), 2.39-2.46 (m, 1 H, CH_2-2), 2.55-2.68 (m, 4 H, 2 CH_2), 2.75 (t, 2 H, CH_2, J = 6.4 Hz), 3.23-3.26 (m, 6 H, NH + 2 CH_2), 4.04-4.11 (m, 1 H, CH), 4.43 (d, 1 H, CH, J = 2.4 Hz), 4.75-4.79 (m, 1 H, CH), 4.78 (dd, 1 H, CH, J_1 = 6.2 Hz, J_2 = 2.2 Hz), 5.20-5.24 (m, 1 H, CH), 5.75 (d, 1 H, CH, J = 4.6 Hz), 6.07 (br s, 1 H, NH), 6.53 (s, 1 H, CH), 6.86 (s, 1 H, CH), 7.20 (s, 1 H, CH), 7.39 (dd, 1 H, CH, J_1 = 8.8 Hz, J_2 = 2.0 Hz), 7.45 (d, 1 H, CH, J = 1.8 Hz), 7.75 (s, 1 H, CH), 7.78 (d, 1 H, CH, J = 1.8 Hz), 8.29 (s, 1 H, CH), 8.40 (s, 1 H, NH), 9.42 (d, 1 H, NH, J = 7.1 Hz), 10.19 (s, 1 H, NH); ^{13}C NMR: 20.10 (CH_2), 20.20 (CH_2), 21.17 (CH_2), 25.46 (CH_3), 27.53 (CH_2), 27.66 (CH_3), 28.04 (CH_2), 32.78 (CH_2), 41.26 (CH_2), 49.97 (CH_2), 50.38 (CH_2), 53.53 (CH_2), 54.14 (CH), 81.57 (CH), 82.56 (CH), 83.57 (CH), 92.54 (CH), 105.80 (CH), 107.55 (C_q), 107.73 (C_q), 108.26 (C_q), 109.12 (C_q), 114.93 (C_q), 116.56 (CH), 119.84 (C_q), 121.04 (C_q), 125.68 (CH), 127.30

(CH), 140.41 (C_q), 142.96 (CH), 148.30 (C_q), 148.67 (CH), 148.88 (C_q), 152.90 (C_q), 155.29 (C_q), 155.94 (CO), 159.46 (CO), 162.84 (CF_3), 164.75 (CO), 170.36 (CO), 173.15 (CO); mp: decomposition above 148 °C; IR (ν_{max} / (cm^{-1}), KBr): 3333, 2939, 1738, 1695, 1636, 1616, 1583, 1516.

97 The major isolated component of the reaction mixture:

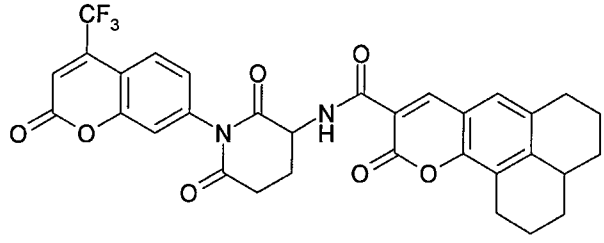

HR-ESMS ($C_{31}H_{24}N_3O_7F_3$): calc: 608.1639 $[M+H]^+$, measured: 608.1633 $[M+H]^+$; ^1H NMR ($CDCl_3$, δ): 1.84-1.91 (m, 4 H, $2CH_2$), 2.22-2.36 (m, 1 H, CH_2-1), 2.41-2.47 (m, 1 H, CH_2-2), 2.67 (t, 2 H, CH_2, J = 6.0 Hz), 2.77 (t, 2 H, CH_2, J = 6.2 Hz), 2.83-2.97 (m, 2 H, CH_2), 3.20-3.27 (m, 4 H, 2 CH_2), 4.91 (octet, 1 H, CH, J_1 = 12.4 Hz, J_2 = 6.1 Hz, J_3 = 5.3 Hz), 6.75 (s, 1 H, CH), 6.90 (s, 1 H, CH), 7.13 (dd, 1 H, CH, J_1 = 8.5 Hz, J_2 = 2.0 Hz), 7.24 (s, 1 H, CH), 7.70 (dd, 1 H, CH, J_1 = 8.6 Hz, J_2 = 1.7 Hz), 8.46 (s, 1 H, CH), 9.46 (d, 1 H, NH, J = 6.9 Hz); ^{13}C NMR: 19.93 (CH_2), 19.96 (CH_2), 20.92 (CH_2), 24.02 (CH_2), 27.29 (CH_2), 32.01 (CH_2), 49.72 (CH_2), 50.15 (CH_2), 51.48 (CH), 105.50 (C_q), 107.61 (C_q), 108.03 (C_q), 113.47 (C_q), 116.45 (CH), 118.31 (CH), 119.42 (C_q), 119.68 (C_q), 123.06 (C_q), 125.62 (CH), 125.72 (CH), 127.09 (CH), 139.44 (C_q), 148.27 (CH), 148.44 (CH), 152.74 (C_q), 154.35 (CO), 158.23 (CO), 162.74 (CF_3), 163.86 (CO), 170.99 (CO), 171.23 (CO); mp: decomposition above 188 °C; IR (ν_{max} / (cm^{-1}), KBr): 3432, 3091, 2942, 2852, 1747, 1699, 1618, 1585, 1652, 1519.

4.1.2.11 Coupling coumarin 2 to N-Fmoc-γ-O-^{t}Bu glutamic acid

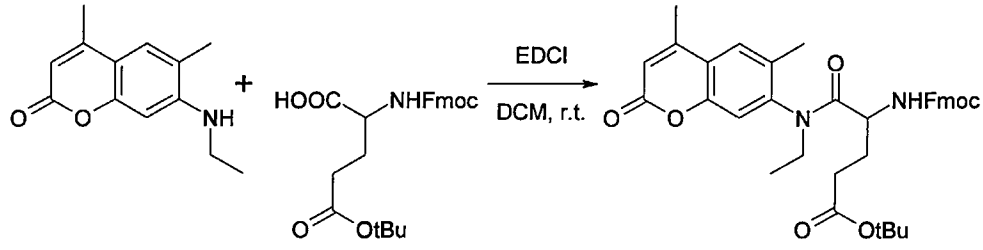

78 **84** **98**

Coumarin 2 (**78**) (0.21 g, 1.0 mmol) and N-Fmoc-γ-O-^{t}Bu glutamic acid (**84**) (0.43 g, 1.0 mmol) were dissolved in DCM (6 mL), EDCI (0.20 g, 1.1 mmol, 1.1 eq) was added, and the solution was allowed to proceed at room temperature for 1 week. Water (30 mL) and DCM (30 mL) were added to the reaction mixture, the phases were separated, and the aqueous phase was extracted with DCM (2·30 mL). The combined extractions were washed with water (2·30 mL), dried over $MgSO_4$, filtered, and concentrated. The sample was purified on a silica column by elution with EtOAc / hexane, to give the desired product (**98**) as a pale yellow solid in 15.6% yield (0.10 g). MS: 642 $[M+H]^+$; ^{1}H NMR ($CDCl_3$, δ): 1.08 (t, 3 H, CH_3, J = 6.8 Hz), 1.30 (s, 9 H, CH_3), 1.63-1.76 (m, 2 H, CH_2), 2.01-1.14 (m, 2 H, CH_2), 2.18 (s, 3 H, CH_3), 2.37 (s, 3 H, CH_3), 3.41-3.48 (m, 1 H, CH_2-1), 3.82-3.99 (m, 2 H, CH_2), 4.08-4.12 (m, 1 H, CH), 5.55-5.58 (m, 1 H, CH_2), 6.26 (s, 1 H, CH), 6.38 (s, 1 H, CH), 7.14 (s, 1 H, CH), 7.19-7.70 (m, 8 H, CH); ^{13}C NMR: 12.81 (CH_3), 14.43 (CH_3), 17.30 (CH_3), 18.54 (CH_3), 27.99 (CH_3), 30.49 (CH_2), 31.55 (CH_2), 38.17 (CH_2), 44.04 (CH_2), 47.10 (CH), 51.26 (CH), 66.88 (CH_2), 80.49 (C_q), 96.20 (CH), 109.24 (CH), 115.82 (CH), 117.34 (CH), 118.32 (C_q), 119.94 (CH), 120.19 (CH), 125.07 (CH), 127.03 (CH), 141.24 (CO), 143.71 (CO), 149.58 (CO), 171.60 (CO).

4.1.2.12 5'-Mesyl-2'3'-isopropylideneadenosine

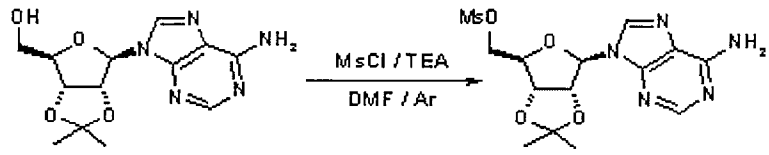

99 **100**

2',3'-Isopropylideneadenosine (**99**) (2.17 g, 7.1 mmol) was dissolved in dry DMF (15 mL) and TEA (3 mL, 2.14 g, 21.2 mmol, 3 eq). The solution was cooled in an ice-water bath, and MsCl (602 μL, 0.89 g, 7.8 mmol, 1.1 eq) was added in small portions. The reaction mixture was allowed to warm to room temperature, and the stirring continued for a further 12 hours. The DMF was removed *in vacuo*, and the residue was dissolved in DCM (40 mL) and water (40 mL). The phases were separated and the aqueous phase was extracted with DCM (2·40 mL). The combined organic phases were washed with water (2·30 mL), dried over $MgSO_4$, filtered, and concentrated to ~2 mL. The sample was applied onto a silica chromatographic column and purified by elution with DCM / MeOH (0-2%). The product (**100**) was obtained as a white solid in 70% yield. MS: 385 $[M+H]^+$, ^1H NMR ($CDCl_3$, δ): 1.33 (s, 3 H, OCH_3), 1.55 (s, 3 H, OCH_3), 2.92 (s, 3 H, SCH_3), 4.33-4.49 (m, 4 H, CH_2 + CH), 5.08-5.11 (m, 1 H, CH), 5.39-5.42 (m, 1 H, CH), 5.87 (br s, 2 H, NH_2), 6.07 (d, 1 H, CH, J = 2.0 Hz), 7.91 (s, 1 H, CH), 8.48 (s, 1 H, CH); ^{13}C NMR: 24.85 (CH_3), 27.12 (OCH_3), 62.99 (CH_2), 81.39 (CH), 83.14 (CH), 85.78 (CH), 93.22 (CH), 113.82 (CH), 139.95 (CH), 152.38 (CH_3);

4.1.2.13 5'-Azido-2'3'-isopropylideneadenosine

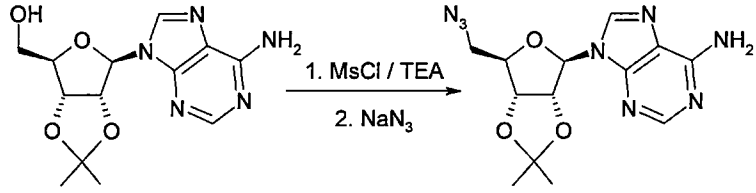

99 **101**

2'3'-Isopropylideneadenosine (**99**) (6.01 g, 19.6 mmol) was dissolved in DMF (15 mL) and TEA (8.23 mL, 5.90 g, 58.7 mmol, 3 eq) was added. The solution was cooled in an ice-water bath and a solution of methanesulfonyl chloride (3.03 mL, 4.49 g, 39.2 mmol, 2 eq) was added in small portions, while the solution was stirred vigorously. The reaction mixture was allowed to reach room temperature, and the stirring was continued for 12 hours. NaN_3 (3.82 g, 58.8 mmol, 3 eq) was added in small portions, and the temperature was raised to 45 °C. The reaction was continued for 48 hours. The solvents were removed *in vacuo*, the residue dissolved in a mixture of DCM (40 mL) and water (20 mL), the phases were separated, and the aqueous phase was extracted with DCM (2·30 mL). The combined organic layers were washed with water (30 mL), dried over $MgSO_4$, concentrated, and purified on a silica column to give **101** as a yellow solid in 12% yield (0.80 g). MS: 332 $[M]^+$; ^1H NMR ($CDCl_3$, δ): 1.33 (s, 3 H, OCH_3), 1.55 (s, 3 H, OCH_3), 3.50-3.53 (m, 2 H, CH_2), 4.29-4.34 (m, 1 H, CH), 5.00 (dd, 1 H, CH, J_1 = 6.4 Hz, J_2 = 3.5 Hz), 5.41 (dd, 1 H, CH, J_1 = 6.4 Hz, J_2 = 2.2 Hz), 5.70 (s, 2 H, NH_2), 6.05 (d, 1 H, CH, J = 2.2 Hz), 7.20 (s, 1 H, NH), 7.86 (s, 1 H, NH), 8.43 (s, 1 H, NH); ^{13}C NMR: 25.32 (OCH_3), 27.12 (OCH_3), 52.30 (CH_2), 82.03 (CH), 84.60 (CH), 85.64 (CH), 90.63 (CH), 114.73 (C_q), 120.27 (C_q), 139.89 (C_q), 149.18 (CH), 155.09 (C_q), 162.54 (CH); mp: decomposition

with gas evolution above 136 °C; IR (ν_{max} / (cm^{-1}), paraffin): 3317, 2922, 2853, 2096, 1641, 1596, 1575, 1465, 1377.

4.1.2.14 5'-Amino-2'3'-isopropylidene-adenosine

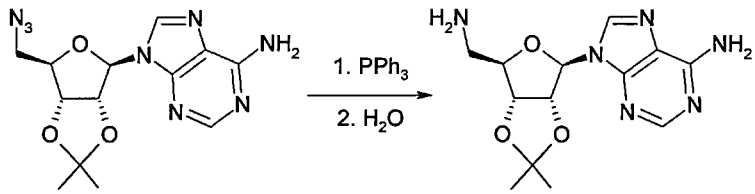

101 **89b**

101 (0.42 g, 1.27 mmol) was dissolved in dry THF (10 mL), PPh_3 (0.33 g, 1.27 mmol) was added, and the solution was stirred at room temperature for 2 hours. Water (35 μL, 35 mg, 1.91 mmol, 1.5 eq) was added, and the reaction was allowed to proceed overnight. The THF was removed at reduced pressure, the residue dissolved in water (30 mL) and DCM (30 mL), the phases were separated, the organic layer was extracted with water (3·30 mL). The combined aqueous phases were washed with DCM (30 mL), and the water was removed *in vacuo*. The sample was dried and **89b** was crystallised by the addition of diethyl ether (40 mL). After filtration, **89b** was obtained as a white solid in 72% yield (0.29 g). MS: 307 $[M+H]^+$; ^1H NMR ($CDCl_3$, δ): 1.32 (s, 3 H, OCH_3), 1.53 (s, 3 H, OCH_3), 2.79 (s, 2 H, NH_2), 2.94 (d, 2 H, CH_2, J = 5.7 Hz), 2.98 (s, 2 H, NH_2), 4.24 (dt, 1 H, CH, J_1 = 5.7 Hz, J_2 = 3.3 Hz), 5.01 (dd, 1 H, CH, J_1 = 6.4 Hz, J_2 = 3.3 Hz), 5.45 (dd, 1 H, CH, J_1 = 6.4, Hz, J_2 = 2.9 Hz), 6.14 (d, 1 H, CH, J = 2.9 Hz), 8.21 (s, 1 H, NH), 8.30 (s, 1 H, NH); ^{13}C NMR: 25.57 (CH_3), 27.49 (CH_3), 44.37 (CH_2), 83.23 (CH), 84.91 (CH), 88.04 (CH), 91.64 (CH), 115.69 (C_q), 120.72 (C_q), 141.93 (CH), 150.24 (C_q), 153.97 (CH), 157.42 (C_q), 164.82

(C_q); mp: decomposition above 183 °C; IR ((ν_{max} / (cm^{-1}), paraffin): 3551, 2923, 2853, 2730, 2678, 1675, 1603, 1569, 1512, 1463, 1371.

4.1.2.15 2',3'-Isopropylideneuridine

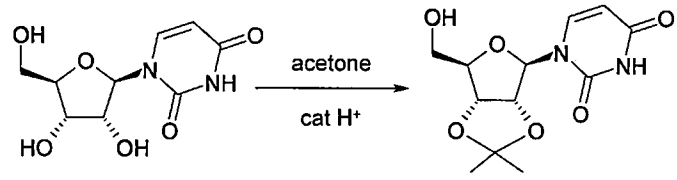

102 **103**

Uridine (**102**) (0.49 g, 2.01 mmol) was suspended in acetone (100 mL), conc. HCl (2 mL) was added, and the mixture was stirred at room temperature overnight. As the reaction proceeds the solid gradually dissolves. After the completion of the reaction anhydrous K_2CO_3 (10 g) was added, the stirring was continued for a further 10 minutes, and the K_2CO_3 was filtered out. The acetone was removed at reduced pressure, and **103** was isolated as a white solid in 90% yield (0.51 g). MS: 284 $[M+H]^+$, 568 $[M+H]^+$, 869 $[M+M+M+H]^+$; ^1H NMR (d_6-Acetone, δ): 1.33 (s, 3 H, OCH_3), 1.52 (s, 3 H, OCH_3), 3.79 (dd, 2 H, CH_2, J_1 = 5.7 Hz, J_2 = 3.5 Hz), 4.19 (dd, 1 H, CH, J_1 = 7.0 Hz, J_2 = 3.5 Hz), 4.89 (dd, 1 H, CH, J_1 = 6.2 Hz, J_2 = 2.8 Hz), 4.95 (dd, 1 H, CH, J_1 = 6.2 Hz, J_2 = 3.3 Hz), 5.62 (d, 1 H, CH, J = 8.1 Hz), 5.92 (d, 1 H, NH, J = 2.8 Hz), 7.84 (d, 1 H, CH, J = 8.1 Hz); ^{13}C NMR: 25.54 (OCH_3), 27.58 (OCH_3), 62.79 (CH_2), 81.61 (CH), 85.16 (CH), 87.64 (CH), 93.03 (CH), 102.70 (CH), 114.31 (C_q), 142.67 (CH); mp: 154-155 °C; IR ((ν_{max} / (cm^{-1}), KBr): 3246, 2986, 2935, 2901, 2359, 1776, 1704, 1675, 1619, 1519, 1468.

4.1.2.16 5'-Mesyl-2'3'-isopropylideneuridine

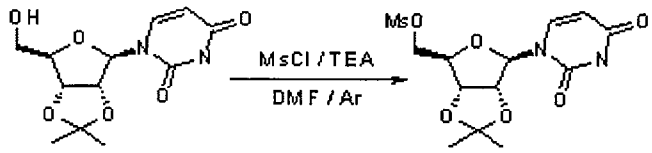

103 **104**

2',3'-Isopropylideneuridine (**103**) (2.98 g, 10.5 mmol) was dissolved in dry DMF (15 mL) and TEA (4.42 mL, 3.18 g, 31.5 mmol, 3 eq). The solution was cooled in an ice-water bath, and MsCl (1.62 mL, 2.40 g, 21.0 mmol, 2 eq) was added in small portions. The reaction mixture was allowed to warm to room temperature, and the stirring continued for a further 12 hours. The DMF was removed *in vacuo*, and the residue was dissolved in DCM (40 mL) and water (40 mL). The phases were separated and the aqueous phase was extracted with DCM (2·40 mL). The combined organic phases were washed with water (2·30 mL), dried over $MgSO_4$, filtered, and concentrated to ~ 2 mL. The sample was applied onto a silica chromatographic column and purified by elution with DCM/MeOH (0-5%). The product (**104**) was obtained as an off-white solid in 80% yield (3.04 g). ^{1}H NMR ($CDCl_3$, δ): 1.33 (s, 3 H, OCH_3), 1.54 (s, 3 H, OCH_3), 3.02 (s, 3 H, SCH_3), 4.34-4.39 (m, 1 H, CH), 4.44 (d, 2 H, CH_2, J = 5.0 Hz), 4.86 (dd, 1 H, CH, J_1 = 6.5 Hz, J_2 = 3.4 Hz), 5.03 (dd, 1 H, CH, J_1 = 6.4 Hz, J_2 = 1.8 Hz), 5.58 (d, 1 H, CH, J = 1.8 Hz), 5.75 (d, 1 H, CH, J = 7.9 Hz), 8.05 (d, 1 H, CH, J = 8.1 Hz); ^{13}C NMR: 26.98 (CH_3), 31.39 (CH_3), 68.91 (CH_2), 81.01 (CH), 84.26 (CH), 85.55 (CH), 95.86 (CH), 102.85 (CH), 114.65 (CH), 142.82 (CH), 162.52 (CO).

4.1.2.17 5'-Azido-2'3'-isopropylidene-uridine

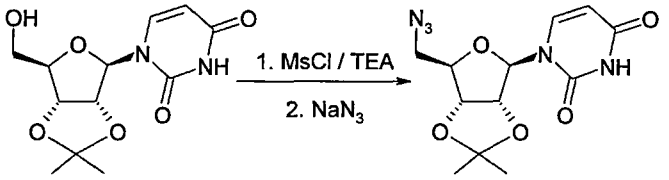

103 **105**

103 (4.29 g, 15.1 mmol) was dissolved in DMF (15 mL) and TEA (6.40 mL, 4.60 g, 45.3 mmol, 3 eq) was added. The solution was cooled in an ice-water bath and a solution of methanesulfonyl chloride (2.34 mL, 3.46 g, 30.2 mmol, 2 eq) was added in small portions, while the solution was stirred vigorously. The reaction mixture was allowed to reach room temperature, and the stirring was continued for 12 hours. NaN_3 (4.91 g, 75.5 mmol, 5 eq) was added in small portions, and the temperature was raised to 45 °C. The reaction was continued for 48 hours. The solvents were removed *in vacuo*, the residue dissolved in a mixture of DCM (40 mL) and water (20 mL), the phases were separated, and the aqueous phase was extracted with DCM (2·30 mL). The combined organic layers were washed with water (30 mL), dried over $MgSO_4$, concentrated, and purified on a silica column to give **105** as a yellow solid in 85% yield (3.98 g). MS: ^{1}H NMR ($CDCl_3$, δ): 1.29 (s, 3 H, OCH_3), 1.56 (s, 3 H, OCH_3), 3.58 (d, 2 H, CH_2, J = 7.3 Hz), 4.17 (dd, 1 H, CH, J_1 = 9.5 Hz, J_2 = 5.1 Hz), 4.76 (dd, 1 H, CH, J_1 = 6.4 Hz, J_2 = 4.2 Hz), 4.95 (dd, 1 H, CH, J_1 = 6.4 Hz, J_2 = 2.0 Hz), 5.56 (d, 1 H, CH, J = 2.0 Hz), 5.70 (d, 1 H, CH, J = 8.0 Hz), 7.24 (d, 1 H, CH, J = 8.0 Hz), 9.94 (br s, 1 H, NH); ^{13}C NMR: 25.16 (CH_3), 27.01 (CH_3), 52.28 (CH_2), 81.47 (CH), 84.25 (CH), 85.81 (CH), 94.79 (CH), 102.79 (CH), 114.67 (CH), 142.45 (CH), 162.55 (CO), 163.49 (CO); mp: 68-69 °C, gas evolution above 87 °C; IR (ν_{max} / (cm^{-1}), paraffin): 2927, 2854, 2104, 1692, 1461, 1378, 1273, 1214.

4.1.2.18 5'-Amino-2'3'-isopropylidene-uridine

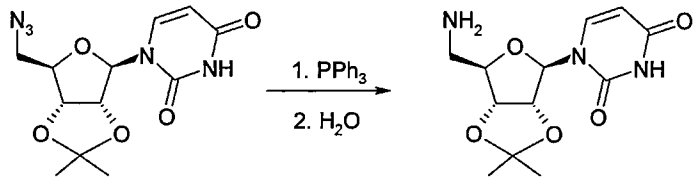

105 **89a**

105 (2.15 g, 6.96 mmol) was dissolved in dry THF (10 mL), PPh_3 (1.82 g, 6.96 mmol) was added, and the solution was stirred at room temperature for 2 hours. Water (150 µL, 150 mg, 8.35 mmol, 1.2 eq) was added, and the reaction was allowed to proceed overnight. The THF was removed at reduced pressure, the residue dissolved in water (30 mL) and DCM (30 mL), the phases were separated, the organic layer was extracted with water (3·30 mL). The combined aqueous phases were washed with DCM (20 mL), and the water was removed *in vacuo*. The sample was dried and **89a** was crystallised by the addition of diethyl ether (40 mL). After filtration the product was obtained as a white solid in 79% yield (1.56 g). MS: 284 $[M+H]^+$, 566 $[M+M+H]^+$, 850 $[M+M+M+H]^+$; ^1H NMR (CD_3OD, δ): 1.25 (s, 3 H, OCH_3), 1.45 (s, 3 H, OCH_3), 2.85 (d, 2 H, CH_2, J = 4.6 Hz), 4.05 (dd, 1 H, CH, J_1 = 10.4 Hz, J_2 = 5.7 Hz), 4.68-4.80 (m, 2 H, 2 CH), 5.03 (dd, 1 H, CH, J_1 = 6.6 Hz, J_2 = 2.4 Hz), 5.68 (d, 1 H, CH, J = 7.9 Hz), 5.73 (d, 1 H, NH, J = 2.6 Hz), 7.64 (d, 1 H, CH, J = 8.1 Hz); ^{13}C NMR: 24.28 (CH_3), 25.95 (CH_3), 51.95 (CH_2), 68.09 (CH), 83.57 (CH), 86.76 (CH), 87.78 (CH), 91.59 (CH), 111.96 (CH), 151.48 (CO), 168.59 (CO); mp: melting accompanied by gas evolution at 94-95 °C; IR (ν_{max} / (cm^{-1}), KBr): 3364, 3207, 3061, 2988, 2939, 1698.

4.1.2.19 5'-Azido-2'3'-isopropylidene-guanosine

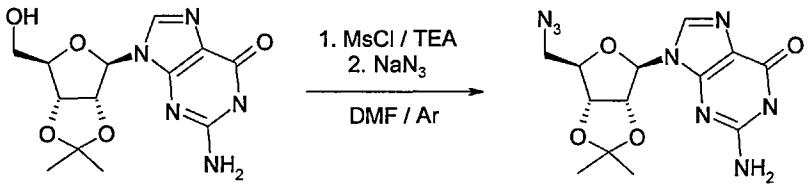

106 **107**

2',3'-Isopropylideneguanosine (**106**) (7.24 g, 22.4 mmol) was dissolved in dry DMF (50 mL) and TEA (3 eq, 67.2 mmol, 9.4 mL, 6.8 g). The solution was cooled in an ice-water bath, and MsCl (1.91 mL, 2.82 g, 24.6 mmol, 1.1 eq) was added in small portions. The reaction mixture was allowed to warm to room temperature, and the stirring continued for a further 12 hours. NaN_3 (8.74 g, 134.4 mmol, 6 eq) was added, and the temperature was raised to 45 °C. The reaction was continued for 48 hours. The DMF was removed *in vacuo*, and the residue was suspended in DCM (50 mL). After filtration the sample was dried over $MgSO_4$, filtered again, and concentrated to ~8 mL. The sample was applied onto a silica chromatographic column and purified by elution with DCM/MeOH (0-15%). The product (**107**) was obtained as an off-white solid in 21% yield. ^1H NMR ($CDCl_3$, δ): 1.27 (s, 3 H, OCH_3), 1.47 (s, 3 H, OCH_3), 3.49-3.53 (m, 2 H, CH_2), 4.10 (dd, 1 H, CH, J_1 = 8.2 Hz, J_2 = 5.1 Hz), 4.95 (m, 1 H, CH), 5.03 (t, 1 H, CH, J = 5.1 Hz), 5.30 (dd, 1 H, CH, J_1 = 6.3 Hz, J_2 = 2.8 Hz), 6.56 (s, 1 H, NH), 7.94 (s, 1 H, CH), 10.68 (s, >1 H, NH_2); ^{13}C NMR: 25.23 (OCH_3), 27.06 (OCH_3), 61.60 (CH_2), 81.18 (CH), 83.57 (CH), 86.63 (CH), 88.42 (CH), 113.04 (C_q), 135.86 (CH), 150.73 (C_q), 153.69 (C_q), 156.72 (C_q), 162.31 (CH).

4.1.2.20 2'3'-Isopropylidene-cytidine

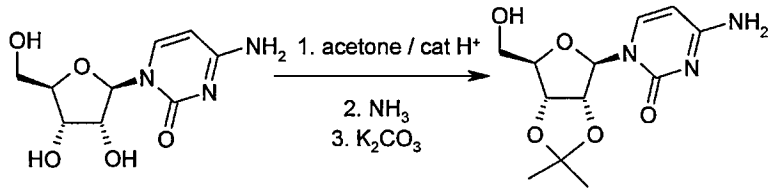

108 **109**

Cytidine (**108**) (7.00 g, 28.8 mmol) was suspended in acetone (300 mL), conc. $HClO_4$ (4 mL) was added, and the reaction mixture was stirred at room temperature overnight. Concentrated aqueous NH_3 (5 mL) was added to the mixture, and the stirring was continued for ten minutes, after which anhydrous K_2CO_3 (10 g) was added, and the mixture was stirred for a further 10 minutes. The solid was removed by filtration, and the volatile components were evaporated *in vacuo*. **109** was obtained as a white solid in 87% yield (7.12 g). ^1H NMR ($CDCl_3$, δ): 1.04 (s, 3 H, OCH_3), 1.26 (s, 3 H, OCH_3), 3.48 (dd, 1 H, CH_2-1, J_1 = 11.9 Hz, J_2 = 4.0 Hz), 3.57 (dd, 1 H, CH_2-2, J_1 = 11.9 Hz, J_2 = 3.5 Hz), 3.95 (dd, 1 H, CH, J_1 = 7.1 Hz, J_2 = 3.5 Hz), 4.68 (dd, 1 H, CH, J_1 = 6.3 Hz, J_2 = 3.5 Hz), 4.75 (dd, 1 H, CH, J_1 = 6.3 Hz, J_2 = 2.6 Hz), 5.55 (d, 1 H, CH, J = 2.4 Hz), 5.74 (d, 1 H, CH, J = 7.5 Hz), 6.96 (br s, > 1 H, NH_2), 7.58 (d, 1 H, CH, J = 7.3 Hz); ^{13}C NMR: 25.64 (CH_3), 27.66 (CH_3), 54.38 (CH_2), 81.69 (CH), 85.56 (CH), 88.27 (CH), 95.59 (CH), 114.00 (C_q), 144.52 (CH), 156.89 (C_q), 167.57 (CO).

4.1.2.21 5'-Mesyl-2',3'-isopropylidenecytidine

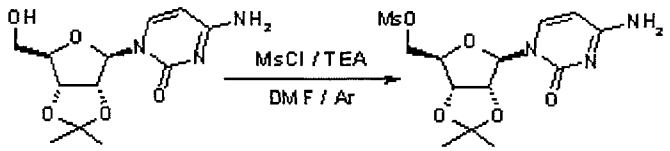

109 **110**

2',3'-Isopropylidenecytidine (**109**) (8.64 g, 30.5 mmol) was dissolved in dry DMF (20 mL) and TEA (12.8 mL, 9.24 g, 91.5 mmol, 3 eq). The solution was cooled in an ice-water bath, and MsCl (2.60 mL, 3.84 g, 33.55 mmol, 1.1 eq) was added in small portions. The reaction mixture was allowed to warm to room temperature, and the stirring continued for a further 12 hours. The DMF was removed *in vacuo*, and the residue was dissolved in DCM (40 mL) and water (40 mL). The phases were separated and the aqueous phase was extracted with DCM (2·40 mL). The combined organic phases were washed with water (2·30 mL), dried over $MgSO_4$, filtered, and concentrated to ~ 2 mL. The sample was applied onto a silica chromatographic column and purified by elution with DCM / MeOH (0-5%). The product (**110**) was obtained as an off-white solid in 60% yield. ^1H NMR ($CDCl_3$, δ): 1.27 (s, 3H, OCH_3), 1.47 (s, 3H, OCH_3), 2.98 (s, 3H, SO_3CH_3), 4.30-4.32 (m, 1H, CH), 4.42 (d, 2H, CH_2, J = 5.3 Hz), 4.82-4.85 (m, 1H, CH), 5.03 (d, 1H, CH, J = 6.4 Hz), 5.53 (s, 1H, CH), 5.95 (d, 1H, CH, J = 7.3 Hz), 7.35 (d, 1H, CH, J = 7.7 Hz); ^{13}C NMR: 25.18 (OCH_3), 26.98 (OCH_3), 69.43 (CH_2), 81.33 (CH), 84.65 (CH), 85.63 (CH), 95.85 (CH), 114.15 (C_q), 144.30 (CH), 155.28 (C_q), 165.68 (CO).

4.1.2.22 5'-Azido-2',3'-isopropylidene-cytidine

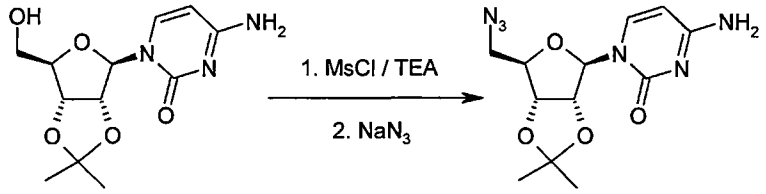

109 **111**

2',3'-Isopropylidenecytidine (**109**) (6.64 g, 23.5 mmol) was dissolved in DMF (15 mL) and TEA (9.90 mL, 7.11 g, 70.4 mmol, 3 eq) was added. The solution was cooled in an ice-water bath and solution of methanesulfonyl chloride (2.00 mL, 2.96 g, 25.8 mmol, 1.1 eq) was added dropwise while stirring vigorously. The reaction mixture was allowed to reach room temperature, and the stirring was continued for 12 hours. NaN_3 (9.20 g, 141.0 mmol, 6 eq) was added in small portions, and the temperature was raised to 45 °C. The reaction was continued for 48 hours. The solvents were removed *in vacuo*, the residue dissolved in a mixture of DCM and water (40 mL each), the phases were separated, and the aqueous phase was extracted with DCM (2·30 mL). The combined organic layers were washed with water (30 mL), dried over $MgSO_4$, concentrated, and purified on a silica column to give **111** as a yellow solid in 14% yield (1.01 g). MS: 330 $[M+Na]^+$, 617 $[M+M+H]^+$; ^1H NMR ($CDCl_3$, δ): 1.19 (s, 3 H, OCH_3), 1.50 (s, 3 H, OCH_3), 3.39-3.66 (m, 1 H, CH), 4.17 (dd, 1 H, CH, J_1 = 12.7 Hz, J_2 = 6.4 Hz), 4.77 (dd, 1 H, CH, J_1 = 6.4 Hz, J_2 = 4.2 Hz), 4.98 (dd, 1 H, CH, J_1 = 6.4 Hz, J_2 = 1.8 Hz), 5.56 (d, 1 H, CH, J = 1.8 Hz), 5.85 (d, 1 H, CH, J = 7.3 Hz), 7.35 (d, 1 H, CH, J = 7.0 Hz), 7.94 (s, 1 H, NH); ^{13}C NMR: 25.23 (CH_3), 27.07 (CH_3), 52.48 (CH_2), 81.80 (CH), 84.77 (CH), 86.15 (CH), 95.59 (CH), 95.79 (CH), 114.27 (C_q), 143.65 (CH), 155.33 (C_q), 166.19 (CO).

4.2 Lanthanide triads

4.2.1 Lanthanide ligand synthesis from protected cyclen derivatives

4.2.1.1 N^7-Boc-cyclen-1,4-oxamide

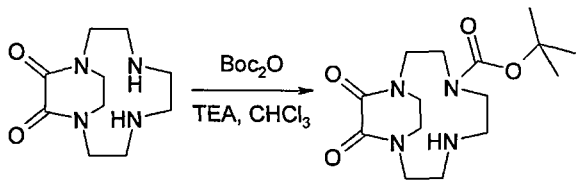

112 **113**

To a solution of the cyclen oxalamide (**112**) (0.22 g, 1 mmol in 12 mL chloroform) was added triethylamine (183 μL, 0.24 g, 2.4 mmol) was added and the mixture was vigorously stirred at room temperature. Di-tert-butyl dicarbonate (0.24 g, 1.1 mmol) was dissolved in chloroform (10 mL) and this solution was added dropwise (in 4 hours) to the solution of the cyclen diamide. The mixture was stirred for 24 hours, concentrated, and chromatographed ($CHCl_3$ / $^iPrNH_2$ = 95:5) to yield 0.44 g (70%) of the title product (**113**) as a yellow solid. HR-ESMS ($C_{15}H_{26}N_4O_4$): calc: 327.2027 $[M+H]^+$, measured: 327.2024 $[M+H]^+$; ^1H NMR ($CDCl_3$, δ) 1.42 (s, 9 H, CH_3 Boc), 2.43-4.41 (m, 16 H, CH_2 macrocycle), the NH protons were not seen in the spectrum; ^{13}C NMR: 28.41 (CH_3, Boc), 45.33 (CH_2), 47.58 (CH_2), 49.81 (CH_2), 55.07 (CH_2), 80.58 (C_q), 156.38 (CO), 158.98 (CO); mp: 109-110 °C; IR (ν_{max} / (cm^{-1}), KBr): 3565, 3324, 2975, 2937, 2821, 1685.

4.2.1.2 Coupling NMA to chloroacetic acid with EDCI

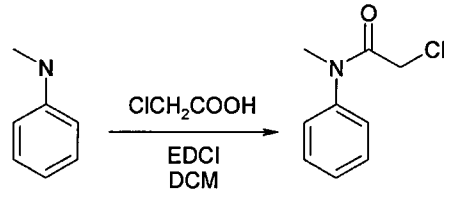

57 **114**

NMA (**57**) (112 µL, 0.11 g, 1 mmol) was dissolved in DCM (10 mL), chloroacetic acid (0.13 g, 1.3 mmol, 1.3 eq) and EDCI (0.19 g, 1 mmol, 1 eq) were added and the solution was stirred at room temperature for three days. DCM (15 mL) and water (25 mL) were added, the phases were separated, the aqueous phase was extracted with DCM (2·30 mL). The combined organic phases were washed with dilute acid (0.1 M HCl, 25 mL), dilute NaOH (0.1 M, 30 mL) and water (25 mL). The organic phase was dried over $MgSO_4$, filtered, and evaporated to dryness. The product (**114**) was isolated as an off-white solid in 79% yield (0.14 g). ^{1}H NMR ($CDCl_3$, δ): 3.25 (s, 3 H, NCH_3), 3.78 (s, 2 H, CH_2), 7.16-7.20 (m, 2 H, CH-ar), 7.30-7.42 (m, 3 H, CH-ar); ^{13}C NMR: 37.98 (N-CH_3), 41.49 (CH_2Cl), 127.05 (CH-ar), 128.56 (CH-ar), 130.06 (CH-ar), 142.67 (C_{ar}-N), 166.26 (CO).

*4.2.1.3 Alkylation of **113** with **114***

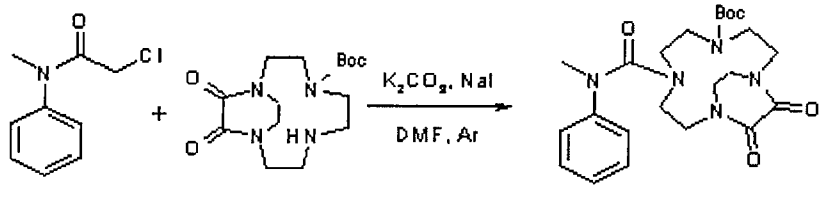

114 **113** **115**

Triprotected cyclen (**113**) (0.18 g, 0.55 mmol) and **114** (0.10 g, 0.55 mmol) were dissolved in DMF (5 mL), K_2CO_3 (0.5 g) and NaI (0.5 g) were added to the

solution and the reaction mixture was stirred under an argon atmosphere at 80 °C for 3 days. The DMF was removed *in vacuo*, the residue dissolved in DCM (40 mL) and water (40 mL), the phases were separated, and the aqueous phase was extracted with DCM (2·30 mL). The combined organic phases were washed with water (2·30 mL), dried over $MgSO_4$, filtered, and concentrated. The sample was chromatographed on silica with DCM / $^{i}PrNH_2$. The desired product (**115**) was obtained in 51% yield (0.12 g) as a pale yellow solid. MS: 474 $[M+H]^+$; ^1H NMR (400 MHz, $CDCl_3$, δ): 1.30 (s, 9 H, Boc), 2.48-4.72 (m, 21 H, CH_2 + NCH_3), 7.23-7.43 (m, 5 H, CH); ^{13}C NMR: 28.53 (CH_3), 37.35 (NCH_3), several peaks around 47.46 (CH_2), 80.81 (C_q), 127.30 (CH), 130.30 (CH), 156.63 (C_q), 158.75 (CO), 159.00 (CO); mp: 114 °C; IR (ν_{max} / (cm^{-1}), KBr): 3509, 2975, 2937, 1685, 1596, 1479, 1433, 1408;

4.2.1.4 Coupling coumarin 2 to chloroacetic acid

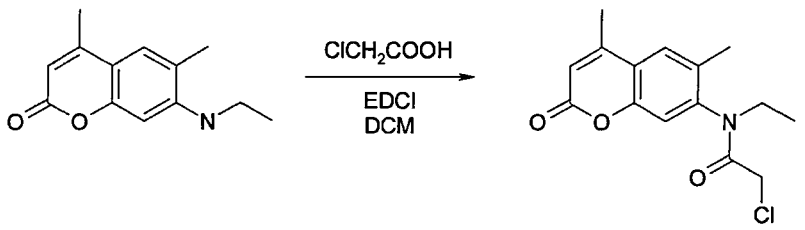

78 **116**

Coumarin 2 (**78**) (0.21 g, 1 mmol) was dissolved in DCM (10 mL), chloroacetic acid (0.13 g, 1.3 mmol) and EDCI (0.19 g, 1 mmol) were added and the solution was stirred at room temperature for three days. DCM (15 mL) and water (25 mL) were added, the phases were separated, the water phase was extracted with DCM (2·30 mL). The combined organic phases were washed with dilute NaOH (30 mL) and water (25 mL). The organic phase was dried over $MgSO_4$, filtered, concentrated to ~2 mL, and applied onto a silica column. Elution with

ethyl acetate / hexane (1:1) gave recovered coumarin 2 (0.07 g, 33%) and the product (**116**) as a white, crystalline solid in 67% yield (0.20 g). HR-ESMS ($C_{15}H_{16}NO_3Cl$): calc: 294.0891 $[M+H]^+$, measured: 294.0891 $[M+H]^+$; Anal. calc. for $C_{15}H_{16}NO_3Cl$: C: 61.33, H: 5.49, N: 4.77; Found: C: 60.08, H: 5.53, N: 4.78; ^1H NMR ($CDCl_3$, δ): 1.11 (t, 3 H, CH_3, J = 7.0 Hz), 2.27 (s, 3 H, CH_3), 2.39 (s, 3 H, CH_3), 3.14-3.26 (m, 1 H, CH_2-1), 3.67 (s, 2 H, CH_2Cl), 4.04-4.18 (m, 1 H, CH_2-2), 6.28 (s, 1 H, CH-ar), 7.08 (s, 1 H, CH-ar), 7.48 (s, 1 H, CH-ar); ^{13}C NMR: 13.04 (CH_3), 17.94 (CH_3), 19.17 (CH_3), 42.05 (CH_2), 44.54 (CH_2), 116.62 (CH-ar), 118.16 (CH-ar), 120.88 (C_q), 127.75 (CH-ar), 132.51 (C_q), 142.55 (C_q), 151.96 (C_q), 152.78 (C_q), 160.55 (CO), 165.86 (CO); mp: 172 °C; IR (ν_{max} / (cm^{-1}), KBr): 1722, 1678, 1626, 1615, 1558, 1502, 1444, 1402.

4.2.1.5 Coupling coumarin 2 to bromoacetic acid

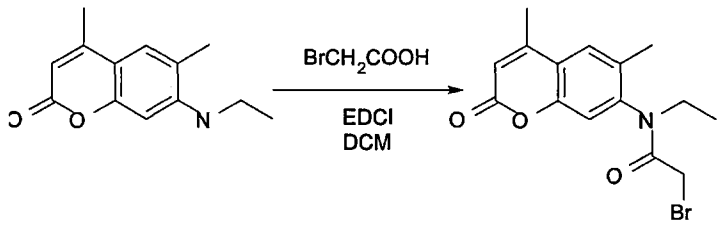

78 **117**

Coumarin 2 (**78**) (4.06 g, 18.7 mmol) and bromoacetic acid (10.40 g, 74.8 mmol, 4 eq) were dissolved in DCM (30 mL), and EDCI (14.36 g, 74.8 mmol, 4 eq) was added in small portions to the vigorously stirred solution. The reaction was allowed to proceed for 24 hours at room temperature. Water (50 mL) and DCM (30 mL) were added to the solution, the phases were separated and the product was extracted into DCM (2·30 mL). The combined organic phases were washed with water (40 mL) and 2 M NaOH (50 mL), dried over $MgSO_4$, filtered, and the DCM was evaporated *in vacuo* to. The product (**117**) was isolated as a white

solid in 84% yield (5.28 g) in high purity. Analytically pure samples were obtained by chromatography on silica with EtOAc / DCM (1:9). HR-ESMS ($C_{15}H_{16}NO_3Br$): calc: 338.0386 $[M+H]^+$, measured: 338.0389 $[M+H]^+$; Anal. calc. for $C_{15}H_{16}NO_3Br$: C: 53.27, H: 4.77, N: 4.14; Found: C: 60.34, H: 5.44, N: 4.72; ^1H NMR ($CDCl_3$, δ): 1.07-1.12 (t, 3 H, CH_3), 2.27 (s, 3 H, CH_3); 2.40 (s, 3 H, CH_3), 3.13-3.23 (m, 1 H, CH_2-1), 3.61 (s, 2 H, $BrCH_2$), 4.08-4.18 (m, 1 H, CH_2-2), 6.28 (s, 1 H, CH), 7.09 (s, 1 H, CH), 7.49 (s, 1 H, CH); ^{13}C NMR: 12.49 (CH_3), 17.38 (CH_3), 18.64 (CH_3), 41.54 (CH_2), 43.99 (CH_2), 116.04 (CH), 117.58 (CH), 120.38 (C_q), 127.24 (CH), 131.97 (C_q), 142.17 (C_q), 151.29 (C_q), 152.02 (C_q), 159.96 (CO), 165.45 (CO); mp: 171 °C, IR (ν_{max} / (cm^{-1}), KBr): 1723, 1676, 1626, 1614, 1558, 1502, 1444.

4.2.1.6 Coupling bromoacetic acid to coumarin 120

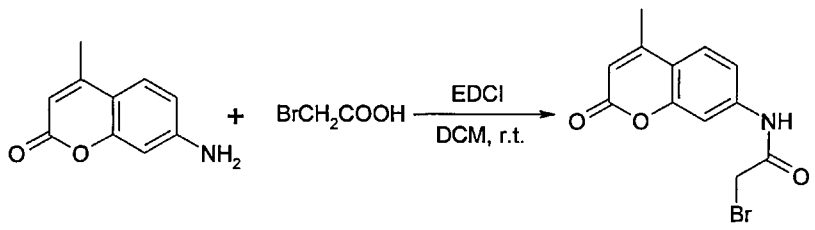

67 **118** **119**

Coumarin 120 (**67**) (1.10 g, 6.3 mmol), bromoacetic acid (0.87 g, 6.3 mmol) and EDCI (1.33 g, 6.93 mmol, 1.1 eq) were suspended in a mixture of THF and DCM (20 mL each). The product started to form immediately, as indicated by the appearance of a white precipitate. After 12 hours the solid was filtered off and washed on the filter with several small portions of DCM. The product (**119**) was obtained in 75% yield (1.39 g). ^1H NMR (DMSO, δ): 2.39 (s, 3 H, CH_3), 4.31 (s, 2 H, CH_2), 6.27 (s, 1 H, CH), 7.44-7.49 (m, 1 H, CH), 7.71-7.77 (m, 2 H, CH), 10.71 (s, <1 H, NH); ^{13}C NMR: 17.95 (CH_3), 43.56 (CH_2), 105.86 (CH), 112.57

(CH), 115.28 (CH), 115.47 (C_q), 126.07 (CH), 141.68 (C_q), 153.00 (C_q), 153.56 (C_q), 159.89 (CO), 165.32 (CO).

4.2.1.7 Coupling chloroacetic acid to N-Methyl-L-glucamine

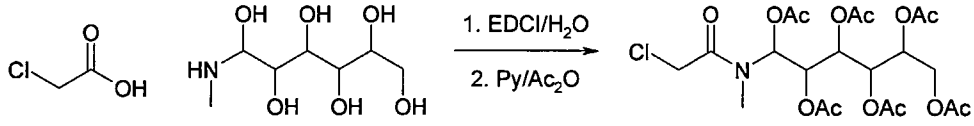

120 **121** **122**

Chloroacetic acid (**120**) (0.95 g, 1 mmol) and N-methyl-L-glucamine (**121**) (1.95 g, 1 mmol) were dissolved in 15 mL water, EDCI (3.84 g, 2 mmol, 2 eq) was added to the solution, and the reaction was allowed to proceed for 12 hours at room temperature. The water was removed at reduced pressure, the residue (colourless oil) was dissolved in dry pyridine (12 mL), and the solution was cooled in an ice-water bath for ten minutes. The solution was stirred vigorously while acetic anhydride (15 mL) was added to the solution in small portions. The reaction mixture was allowed to reach room temperature and the stirring was continued for another 12 hours. The excess acetic anhydride was consumed by the addition of water (10 mL). DCM (30 mL) and water (40 mL) were afterwards added to the mixture, the phases were separated and the aqueous phase was extracted with DCM (3·30 mL). The combined organic phases were washed with water (2·30 mL) and dilute acid (1 M HCl, 1·40 mL), dried over $MgSO_4$, filtered and the DCM was removed *in vacuo*. The product (**122**) was isolated as a colourless solid in 42% yield (2.06 g). ^{1}H NMR ($CDCl_3$, δ): 2.04-2.10 (m, 15 H, CH_3CO), 2.16 (s, 3 H, NCH_3), 3.07 (s, 2 H, $ClCH_2$), 3.56-3.57 (m, 2 H, CH_2), 4.03-4.16 (m, 1 H, CH), 4.27-4.31 (m, 1 H, CH), 5.04 (br s / m, 1 H, CH), 5.30-5.37 (m, 1 H, CH); ^{13}C NMR: 19.88 (CH_3), 19.99 (CH_3), 20.07 (CH_3), 20.21

(CH_3), 22.13 (CH_3), 36.84 (NCH_3), 47.33 (CH_2), 60.99 ($ClCH_2$), 68.24(CH), 68.33 (CH), 68.65 (CH), 68.50 (CH), 168.94 (CO), 169.20, (CO) 169.34 (CO), 169.59 (CO), 169.98 (CO), 170.67 (CO).

4.2.1.8 Coupling bromoacetic acid to N-Methyl-L-glucamine

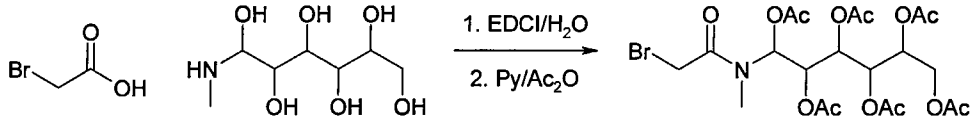

118 **121** **123**

Bromoacetic acid (**118**) (1.38 g, 1 mmol) and N-methyl-L-glucamine (**121**) (1.95 g, 1 mmol) were dissolved in 15 mL water, EDCI (3.84 g, 2 mmol, 2 eq) was added to the solution, and the reaction was allowed to proceed for 12 hours at room temperature. The water was removed at reduced pressure, the residue (colourless oil) was dissolved in dry pyridine (12 mL), and the solution was cooled in an ice-water bath for ten minutes. The solution was stirred vigorously while acetic anhydride (15 mL) was added to the solution in small portions. The reaction mixture was allowed to reach room temperature and the stirring was continued for another 12 hours. The excess acetic anhydride was consumed by the addition of water (10 mL). DCM (30 mL) and water (40 mL) were afterwards added to the mixture, the phases were separated and the aqueous phase was extracted with DCM (3·30 mL). The combined organic phases were washed with water (2·30 mL) and dilute acid (1 M HCl, 1·40 mL), dried over $MgSO_4$, filtered and the DCM was removed *in vacuo*. The product (**123**) was isolated as a colourless solid in 34% yield (1.80 g). ^1H NMR ($CDCl_3$, δ): 2.00-2.05 (m, 15 H, CH_3), 2.09 (s, 3 H, NCH_3), 2.94 (s, 2 H, $BrCH_2$), 3.46-3.60 (m, 2 H, CH_2), 3.98-4.09 (m, 1 H, CH), 4.20-4.25 (m, 1 H, CH), 4.95-4.99 (m, 1 H, CH), 5.23-5.28

(m, 1 H, CH), 5.38-5.41 (m, 1 H, CH); ^{13}C NMR: 20.31 (CH_3), 20.44 (CH_3), 20.52 (CH_3), 20.65 (CH_3), 20.69 (CH_3), 21.09 (CH_3), 21.43 (CH_3), 33.56 (CH_3), 37.20 (CH_3), 47.77 (CH_2), 50.69 (CH_2), 61.29 (CH_2), 61.46 (CH_2), 67.61 (CH), 68.50 (CH), 68.59 (CH), 68.65 (CH), 68.74 (CH), 69.08 (CH), 69.20 (CH), 69.50 (CH), 169.39 (CO), 169.76 (CO), 169.87 (CO), 170.16 (CO), 170.56 (CO), 171.55 (CO).

*4.2.1.9 Alkylation of **113** with **116***

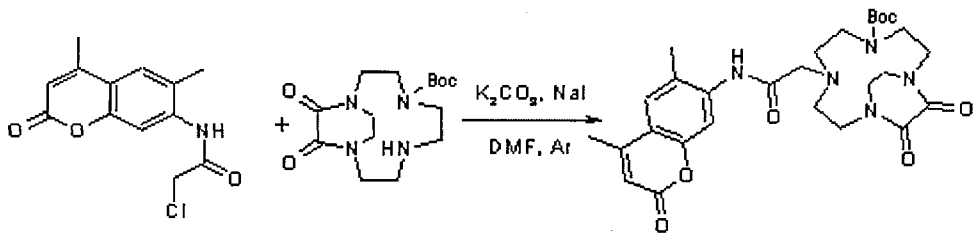

116 **113** **124**

Triprotected cyclen (**113**) (0.18 g, 0.55 mmol) and **116** (0.16 g, 0.37 mmol) were dissolved in DMF (10 mL), K_2CO_3 (2 g) and NaI (2 g) were added to the solution and the reaction mixture was stirred under an argon atmosphere at 80 °C for 3 days. The DMF was removed *in vacuo*, the residue dissolved in DCM (40 mL) and water (40 mL), the phases were separated, and the aqueous phase was extracted with DCM (2·30 mL). The combined organic phases were washed with water (2·30 mL), dried over $MgSO_4$, filtered, and concentrated. The sample was chromatographed on silica with DCM / $^{i}PrNH_2$. The desired product (**124**) was obtained in 45% yield (0.12 g) as a pale yellow solid. MS: 584 $[M+H]^+$; ^1H NMR ($CDCl_3$, δ): 1.08 (t, 3 H, CH_3, J = 7.1 Hz), 1.40 (s, 9 H, $3CH_3$), 2.18 (s, 3 H, CH_3), 2.40 (s, 3 H, CH_3), 2.61-4.62 (m, 24 H, CH_2), 6.28 (s, 1 H, CH), 7.04 (s, 1 H, CH), 7.57 (s, 1 H, CH); ^{13}C NMR: 12.69 (CH_3), 46.61 (CH_3), 48.04 (CH_3),

50.68 (CH_3), 53.48 (CH_3), 62.36 (CH_3), 80.64 (C_q), 116.00 (CH), 117.36 (CH), 120.44 (C_q), 125.39 (CH), 127.39 (C_q), 141.11 (C_q), 152.02 (C_q), 156.31 (CO), 159.18 (CO), 159.93 (CO), 166.34 (CO).

Side-product (**125**):

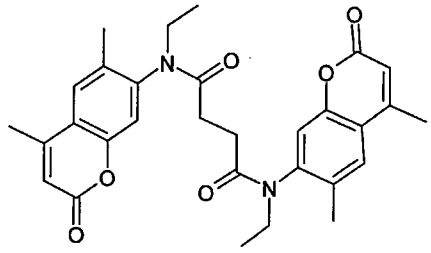

MS: 513 $[M+H]^+$; ^1H NMR ($CDCl_3$, δ): 1.11 (t, 6 H, 2 CH_3, J = 7.1 Hz), 2.23 (s, 6 H, 2 CH_3), 2.39 (s, 6 H, 2 CH_3), 3.20-3.31 (m, 2 H, 2 CH_2-1), 3.45 (d, 2 H, 2 CH_2-1, J = 15.8 Hz), 3.74 (d, 2 H, 2 CH_2-2, J = 15.8 Hz), 4.07-4.19 (m, 2 H, 2 CH_2-2), 6.28 (s, 2 H, 2 CH), 7.03 (s, 2 H, 2 CH), 7.53 (s, 2 H, 2 CH); ^{13}C NMR: 12.76 (CH_3), 17.12 (CH_3), 18.65 (CH_3), 30.29 (CH_2), 43.67 (CH_2), 60.66 (CH_2), 116.18 (CH), 117.58 (CH), 120.56 (C_q), 132.01 (CH), 140.39 (C_q), 151.24 (C_q), 152.20 (C_q), 159.79 (CO), 171.14 (CO); mp: 133-134 °C;

IR (ν_{max} / (cm^{-1}), KBr): 3450, 3066, 2983, 2930, 1728, 1662, 1611, 1557, 1499, 1448.

*4.2.1.10 Removal of the Boc protection **124***

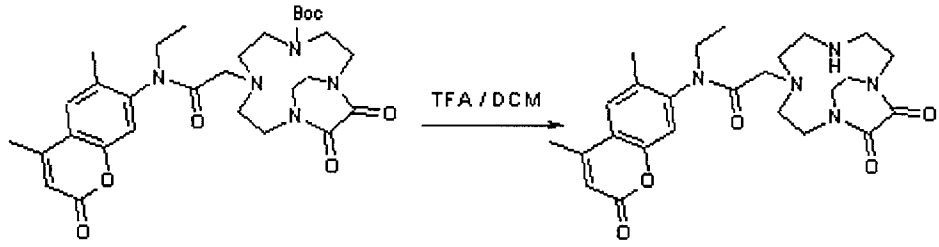

124 **126**

124 (0.06 g, 0.11 mmol) was dissolved in a mixture of DCM (10 mL) and TFA (10 mL), and the solution was stirred at room temperature for 1 hour. The solvents were evaporated, and the yellow residue was dissolved in DCM (40 mL) and NaOH (2 M , 40 mL). The phases were separated and the product was extracted from the aqueous phase with DCM (3·40 mL). The combined organic phases were dried over $MgSO_4$, filtered and evaporated to dryness to give **126** as a pale yellow solid in 75% yield (0.04 g). ^1H NMR (CD_3OD, δ): 1.08 (t, 3 H, CH_3, J = 6.8 Hz), 2.30 (s, 3 H, CH_3), 2.42 (s, 3 H, CH_3), 3.14-4.37 (m, 20 H, CH_2), 6.30 (s, 1 H, CH), 7.24 (s, 1 H, CH), 73 (s, 1 H, CH); ^{13}C NMR: 12.91 (CH_3), 17.25 (CH_3), 18.67 (CH_3), 44.66-55 several peaks (CH_2), 64.29 (CH_2), 116.46 (CH), 117.92 (C_q), 118.57 (CH), 122.00 (C_q), 125.75 (CH), 129.16 (C_q), 139.10 (C_q), 153.32 (C_q), 154.50 (C_q), 162.30 (CO), 164.35 (CO), 168.99 (CO).

*4.2.1.11 Alkylation of **113** with **119***

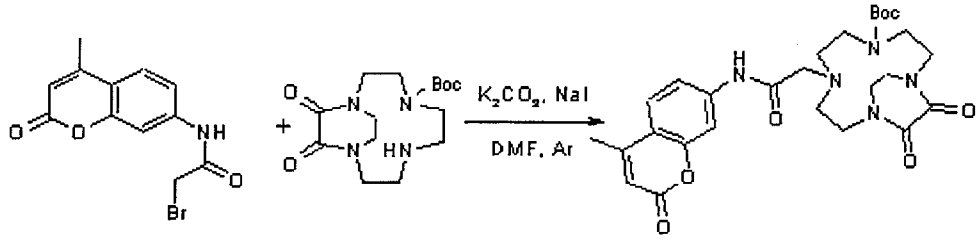

119 **113** **127**

Triprotected cyclen (**113**) (0.70 g, 2.15 mmol) and **119** (0.63 g, 2.15 mmol) were dissolved in DMF (20 mL), K_2CO_3 (2 g) and NaI (2 g) were added to the solution and the reaction mixture was stirred under an argon atmosphere at 80 °C for 3 days. The DMF was removed *in vacuo*, the residue dissolved in DCM (40 mL) and water (40 mL), the phases were separated, and the aqueous phase was extracted with DCM (2·30 mL). The combined organic phases were washed with water (2·30 mL), dried over $MgSO_4$, filtered, and concentrated. The sample was chromatographed on silica with DCM / MeOH (0-5%). **127** was obtained in 29% yield (0.34 g) as a pale yellow solid. MS: 542 $[M+H]^+$, 1082 $[M+H]^+$; ^1H NMR (CD_3OD / $CDCl_3$, δ): 1.39 (s, 9 H, CH_3-Boc), 2.13 (s, 3 H, CH_3), 2.55-4.84 (m, 18 H, CH_2) 3.94 (s, 2 H, CH_2), 5.24 (s, 1 H, CH), 6.11 (s, 1 H, CH), 7.44-7.52 (m, 2 H, CH), 7.82 (br s, <1 H, NH); ^{13}C NMR 18.12 (CH_3), 28.03 (CH_3), 46.79 (CH_2), several peaks at 47-53 ppm (CH_2), 53.18 (CH_2), 61.73 (CH_2), 80.91 (C_q), 106.91 (CH), 112.63 (CH), 115.66 (CH), 115.94 (C_q), 124.83 (CH), 140.61 (C_q), 141.16 (C_q), 152.92 (C_q), 153.61 (CO), 153.75(CO), 156.53 (CO), 161.63 (CO), 171.47 (CO).

4.2.1.12 Removal of the Boc protection ***127***

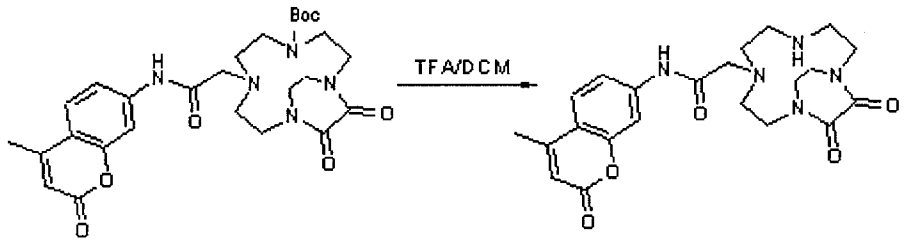

127 **128**

127 (0.10 g, 0.18 mmol) was dissolved in a mixture of DCM (10 mL) and TFA (10 mL), and the solution was stirred at room temperature for 1 hour. The solvents were evaporated, and the yellow residue was dissolved in DCM (40 mL) and NaOH (2 M , 40 mL). The phases were separated and the product was extracted from the aqueous phase with water (3·40 mL). The combined organic phases were dried over $MgSO_4$, filtered and evaporated to dryness to give **128** as a pale yellow solid in 92% yield (0.08 g). MS: 441 $[M+H]^+$, 474 $[M+H+MeOH]^+$, 883 $[M+M+H]^+$, 915 $[M+M+MeOH]^+$; ^1H NMR (CD_3OD, δ): 2.32 (s, 3 H, CH_3), 2.78-3.65 (m, 18 H, CH_2), 6.12 (s, 1 H, CH), 7.47 (d, 1 H, CH, J = 8.6 Hz), 7.94 (d, 1 H, CH, J = 8.4 Hz), 7.81 (s, 1 H, CH), 8.13 (br s, 1 H, NH), 9.24 (br s, 1 H, NH); ^{13}C NMR: 18.52 (CH_3), several peaks at 45-52 ppm (CH_2), 54.09 (CH_2), 57.32 (CH_2), 62.71 (CH_2), 107.08 (CH), 113.49 (CH), 115.76 (C_q), 116.27 (CH), 125.19 (CH), 141.48 (C_q), 152.50 (C_q), 153.86 (C_q), 159.75 (CO), 161.28 (CO), 166.79 (CO).

*4.2.1.13 Alkylation of **128** with N-Boc bromoethylamine*

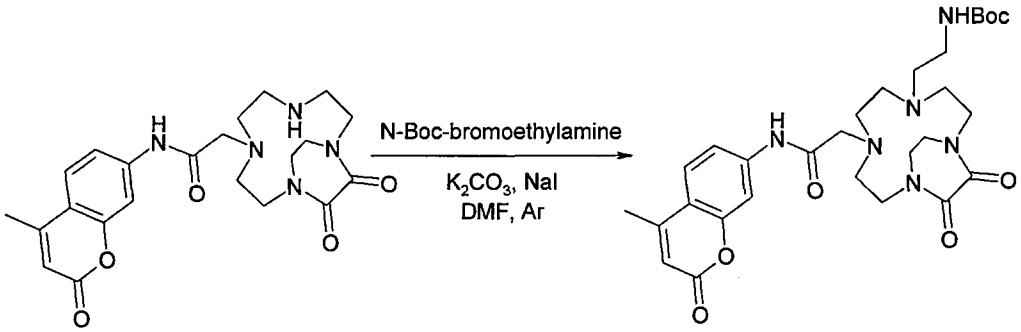

128 **129**

128 (0.28 g, 0.64 mmol) was dissolved in DMF (8 mL), K_2CO_3 (0.53 g, 3.81 mmol, 6 eq), NaI (0.57 g, 3.81 mmol, 6 eq) and N-Boc-bromoethylamine (**131**) (0.71 g, 3.12 mmol, 5 eq) were added, and the mixture was stirred at 80 °C under argon atmosphere for 24 hours. The DMF was removed *in vacuo*, the residue dissolved in a mixture of DCM and water (40 mL each), the phases were separated, and the aqueous phase was extracted with DCM (2·30 mL). The combined organic phases were washed with water (2·30 mL), dried over $MgSO_4$, filtered, and concentrated to ~5 mL. The product (**129**) was isolated as a pale yellow solid after purification on a silica column by elution with DCM / $^iPrNH_2$ in 12% yield. MS: 622 $[M+K]^+$; ^1H NMR (CD_3OD, δ): 1.32 (s, 9 H, Boc), 2.15-2.48 (m, 10 H, CH_3 + CH_2), 2.33 (s, 3 H, CH_3), 2.70-3.02 (m, 10 H, CH_2), 4.28-4.62 (m, 3 H, CH_2), 6.09 (s, 1 H, CH), 7.49 (d, 1 H, CH, J = 8.6 Hz), 7.89 (dd, 1 H, CH, J_1 = 2.0 Hz, J_2 = 8.8 Hz), 8.15 (d, 1 H, CH, J = 1.5 Hz), 9.37 (s, 1H, NH); ^{13}C NMR: 18.50 (CH_3), 28.27 (CH_3), 43.73 (CH_2), 44.34 (CH_2), 46.71 (CH_2), 48.16 (CH_2), 53.07 (CH_2), 53.40 (CH_2), 54.24 (CH_2), 61.52 (CH_2), 107.70 (CH), 112.89 (CH), 115.56 (C_q), 116.85 (CH), 124.65 (CH), 142.12 (C_q), 152.38 (CO), 154.05 (CO), 160.20 (CO).

4.2.1.14 *N-Boc Bromoethylamine*

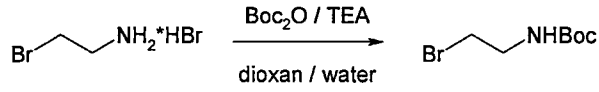

130 **131**

Bromoethylamine hydrobromide (**130**) (2.05 g, 10 mmol) was dissolved in a mixture of dioxan and water (6 mL each), TEA (4.20 mL, 3.02 g, 30 mmol, 3 eq,) and Boc_2O (2.3 g, 11 mmol, 1.1 eq) were added, and the solution was stirred at room temperature for three hours. DCM and water (30 mL each) were added, the phases were separated, and the aqueous phase was extracted with DCM (2·20 mL). The combined organic extracts were washed with water (40 mL) and dilute acid (0.1 M HCl, 40 mL), were dried over $MgSO_4$, filtered and concentrated to ~3 mL. Purification of the sample by column chromatography (silica column, elution with ether / hexane (2:8)) gave the product (**131**) as a colourless oil in 48% yield (1.02 g). MS: 223 $[M+H]^+$, 241 $[M+H+H_2O]^+$; ^1H NMR ($CDCl_3$, δ): 1.38 (s, 9 H, CH_3), 3.38-3.55 (m, 4 H, $2CH_2$), 4.96 (br s, ~1 H, NH); ^{13}C NMR: 28.30 (CH_3), 32.73 (CH_2), 42.32 (CH_2), 79.75 (C_q), 155.55 (CO); IR (ν_{max} / (cm^{-1}), paraffin): 3347, 2924, 2854, 2361, 2342, 1725, 1709, 1503, 1462.

4.2.1.15 *N-Boc Ethanolamine methanesulphonate*

65 **132**

N-Boc Ethanolamine (**65**) (3.60 g, 22.5 mmol) was dissolved in DCM (20 mL), TEA (9.5 mL, 6.84 g, 67.7 mmol, 3 eq) was added, and the reaction mixture was cooled in an ice-water bath. MsCl (1.75 mL, 2.58 g, 22.5 mmol) was added, and the solution was allowed to reach room temperature. The reaction was

allowed to proceed overnight, then water (20 mL) was added to the mixture, the phases were separated and the aqueous phase was extracted with DCM (2·20 mL). The combined organic phases were washed with water (40 mL), dried over $MgSO_4$, filtered, and concentrated. Column chromatography on silica with DCM gave **132** in 58% yield (3.09 g) as a colourless, viscous oil. ^1H NMR ($CDCl_3$, δ): 1.41 (s, 9 H, CH_3), 2.94 (s, 3 H, CH_3), 3.40-3.47 (m, 2 H, CH_2), 4.24 (t, 2 H, CH_2, J = 5.1 Hz), 4.95 (br s, 1 H, NH); ^{13}C NMR: 28.35 (CH_3), 37.43 (CH_3), 65.86 (CH_2), 68.94 (CH_2) 79.97 (C_q), 156.90 (CO).

*4.2.1.16 Removal of the Boc protection from **129***

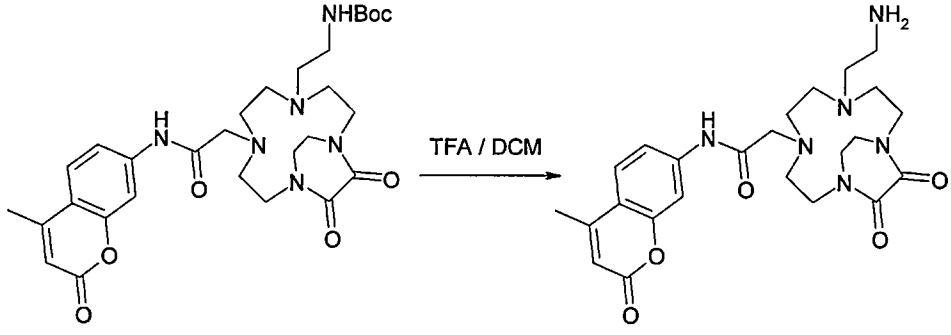

129 **133**

129 (0.10 g, 0.17 mmol) was dissolved in DCM (10 mL), TFA (5 mL) was added to the solution, and the reaction was allowed to proceed for 30 minutes. The solvents were removed at reduced pressure, the residue neutralised with saturated aqueous $KHCO_3$ solution (25 mL), and the product was extracted into DCM (4·30 mL). The combined organic phases were dried over $MgSO_4$, filtered, and evaporated to dryness to afford the desired product (**133**) as a yellow solid in 78% yield (0.065 g). ^1H NMR ($CDCl_3$, δ): 2.32 (s, 3 H, CH_3), 2.50-4.00 (m, 18 H, CH_2), 4.05-4.63 (m, 3 H, CH_2), 6.09 (s, 1 H, CH), 7.45-8.00 (m, 3 H, CH), 9.20 (br s, 1 H, NH), 9.86 (br s, 1 H, NH); ^{13}C NMR: 18.62 (CH_3), 43.03 (CH_2),

46.21 (CH_3), 47.51 (CH_3), 53.50 (CH_3), 113.12 (CH), 116.26 (CH), 117.10 (CH), 124.89 (CH), 141.99 (C_q), 152.46 (CO), 154.26 (CO), 161.39 (CO), 169.84 (CO).

4.2.1.17 Uridine-5'-carboxylic acid pentafluorophenyl ester

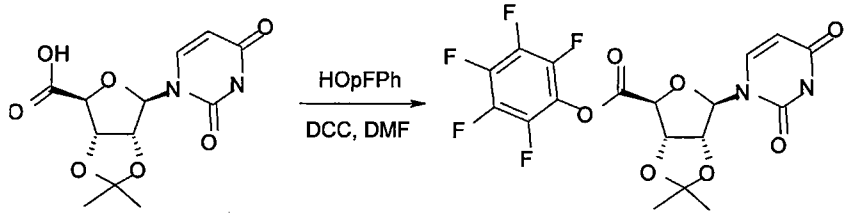

134 **135**

Uridine-5'-COOH (0.37 g, 1.30 mmol) was dissolved in DMF (5 mL), pentafluorophenol (0.24 g, 1.30 mmol) and DCC (0.27 g, 1.30 mmol) were added, and the reaction mixture was stirred at room temperature for 24 hours. The urea was removed by filtration to the activated ester was isolated as colourless crystals (0.68 g crude product, >90% purity). ^{1}H NMR ($CDCl_3$, δ): 1.21 (s, 1 H, OCH_3), 1.47 (s, 1 H, OCH_3), 5.00 (s, 1 H, CH), 5.20 (t, 1 H, CH, J = 6.1 Hz), 5.48 (s, 1 H, CH), 5.55 (d, 1 H, CH, J = 6.0 Hz), 5.68 (d, 1 H, CH, J = 7.9 Hz), 7.20 (d, 1 H, CH, J = 7.9 Hz); ^{13}C NMR: 24.81 (CH_3), 25.64 (CH_3), 84.76 (CH), 88.31 (CH), 99.28 (CH), 103.03 (CH), 113.91 (CH), 143.95 (CH), 150.80 (C_q), 162.76 (CO), 163.19 (CO).

4.2.1.18 Coupling uridine-5'-carboxylic to bromethylamine

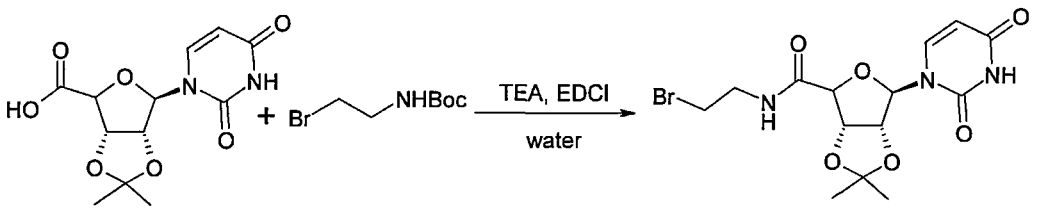

134 **130** **136**

Uridine-5'-COOH (**134**) (0.64 g, 2.0 mmol) was dissolved in water (20 ml), TEA (301 μL, 0.22 g, 2.1 mmol, 1.05 eq), 2-bromoethylamine hydrobromide (**130**) (0.44 g, 2 mmol) and EDCI (0.84 g, 4.0 mmol, 2 eq) were added, and the reaction mixture was stirred at room temperature for 3 hours. The product was extracted into EtOAc (4·25 mL), the combined organic phases were washed with dilute acid (0.01 M p-TsOH, 30 mL), and dried over $MgSO_4$. The product (**136**) was isolated in 12% yield (0.10 g) as a pale yellow solid. ^1H NMR ($CDCl_3$, δ): 1.29 (s, 3 H, OCH_3), 1.48 (s, 3 H, OCH_3), 3.29-3.59 (m, 4 H, 2 CH_2), 4.55 (d, 1 H, CH, J = 2.8 Hz), 5.08 (dd, 1 H, CH, J_1 = 6.4 Hz, J_2 = 1.5 Hz), 5.25 (dd, 1 H, CH, J_1 = 6.4 Hz, J_2 = 2.6 Hz), 5.45 (d, 1 H, CH, J = 1.5 Hz), 5.70 (d, 1 H, CH, J = 7.9 Hz), 6.73 (br s, 1 H, NH), 7.18 (d, 1H, C H, J = 8.8 Hz), 8.91 (br s, 1 H, NH); ^{13}C NMR: 24.71 (OCH_3), 26.53 (OCH_3), 32.28 (CH_2), 40.43 (CH_2), 83.37 (CH), 83.54 (CH), 88.14 (CH), 98.11 (CH), 102.69 (CH), 113.77 (C_q), 143.86 (CH), 150.13 (CO), 163.62 (CO), 169.31 (CO).

4.2.2 Ligand synthesis from unprotected cyclen

*4.2.2.1 Alkylation of cyclen with **119***

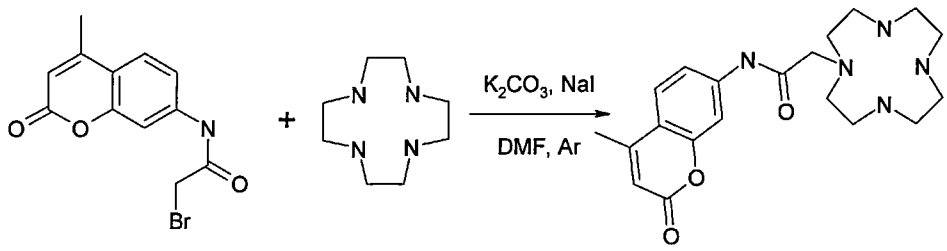

119 **137** **138**

Cyclen (**137**) (0.61 g, 3.55 mmol, 1.2 eq) and coumarin 120 bromoacetate (**119**) (0.70 g, 3.0 mmol) were dissolved in dry DMF (5 mL), K_2CO_3 (1.3 g, 9 mmol, 3 eq) and NaI (1.35 g, 9 mmol, 3 eq) were added to the solution and the reaction mixture was stirred at 80 °C under argon atmosphere for 3 days. The DMF was removed at reduced pressure, the residue was dissolved in water (40 mL) and DCM (40 mL) the phases were separated and the aqueous phase was extracted with DCM (2·30 mL). The combined organic phases were washed with water (30 mL), dried over $MgSO_4$, filtered, and concentrated. The sample was applied onto a silica column and eluted with chloroform containing isopropylamine. The product (**138**) was obtained after the evaporation of the solvent as pale yellow solid in 33.5% yield (0.46 g). MS: 388 $[M+H]^+$; ^1H NMR ($CDCl_3$, δ): 2.29 (s, 3 H, CH_3), 2.49-2.80 (m, 16 H, CH_2), 3.32 (s, 2 H, CH_2), 6.04 (s, 1 H, CH), 7.37-7.40 (m, 1 H, CH), 7.63-7.66 (m, 1 H, CH), 7.78 (s, 1 H, CH); ^{13}C NMR: 18.37 (CH_3), 42.60 (CH_2), 46.05 (CH_2), 46.57 (CH_2), 47.33 (CH_2), 53.45 (CH_2), 60.18 (CH_2), 106.65 (CH), 112.70 (CH), 115.40 (CH), 115.48 (C_q), 124.87 (CH), 141.86 (C_q), 152.33 (C_q), 153.71 (C_q), 153.91 (C_q), 161.91 (CO), 170.75 (CO).

*4.2.2.2 Alkylation of **138** with ethyl bromoacetate*

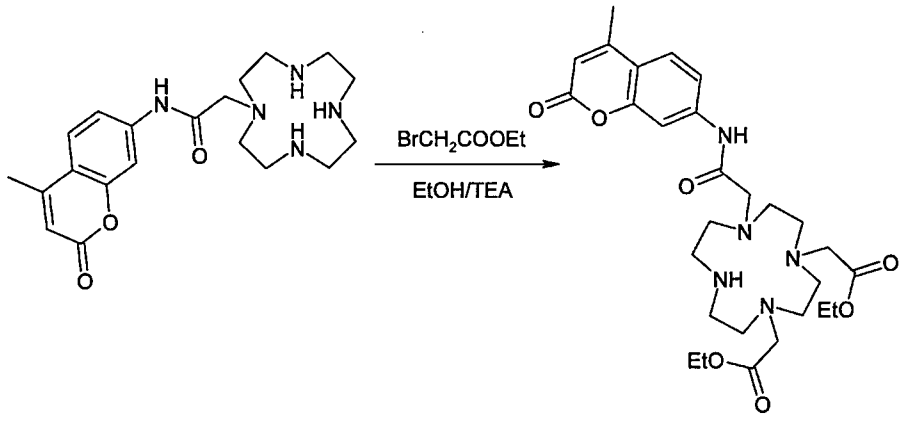

138 **139**

138 (0.41 g, 1.06 mmol) was dissolved in 100% EtOH (10 mL), TEA (372 μL, 2.64 eq) and ethyl bromoacetate (244 μL, 0.38g, 2.32 mmol, 2.2 eq) were added, and the solution was refluxed under argon for 4 days. The ethanol was evaporated at reduced pressure and, the residue was dissolved in a mixture of DCM and water (30 mL each). The phases were separated and the aqueous phase was extracted with DCM (2·30 mL). The combined organic phases were washed with water (40 mL) and dried over $MgSO_4$. The sample was concentrated to ~5 mL and **139** was isolated by silica column chromatography (DCM / $^{i}PrNH_2$, 0-10%) to afford the product in 21% yield (0.12 g). ^{1}H NMR ($CDCl_3$, δ): 1.12 (t, 3 H, CH_3, J = 7.1 Hz), 1.21 (td, 3 H, CH_3, J_1 = 7.1 Hz, J_2 = 2.4 Hz), 2.34 (d, 3 H, CH_3, J = 0.9 Hz), 2.40-3.32 (m, 17 H, CH_2), 3.25 (s, 2 H, CH_2), 3.31 (s, 2 H, CH_2), 3.99 (q, 2 H, CH_2, J = 7.1 Hz), 4.09 (q, 2 H, CH_2, J = 7.1 Hz), 6.11 (d, 1 H, CH, J = 1.3 Hz), 7.42 (d, 1 H, CH, J = 7.7 Hz), 7.70 (d, 1 H, CH, J = 2.0 Hz), 7.73 (dd, 1 H, CH, J_1 = 5.1 Hz, J_2 = 2.0 Hz); ^{13}C NMR: 14.24 (CH_3), 14.29 (CH_3), 18.60 (CH_3), 46.32 (CH_2), 47.01 (CH_2), 51.10 (CH_2), 51.17 (CH_2), 51.56 (CH_2), 51.89 (CH_2), 52.10 (CH_2), 53.07 (CH_2), 53.47 (CH_2), 54.62 (CH_2), 56.01 (CH_2), 56.51 (CH_2), 60.20 (CH_2), 60.35 (CH_2), 60.49 (CH_2), 106.96

(CH), 113.22 (CH), 115.62 (CH), 115.91 (C_q), 125.11 (CH), 141.77 (C_q), 152.17 (C_q), 154.31 (C_q), 161.08 (CO), 170.72 (CO), 170.94 (CO), 171.33 (CO).

*4.2.2.3 Alkylation of cyclen with **116***

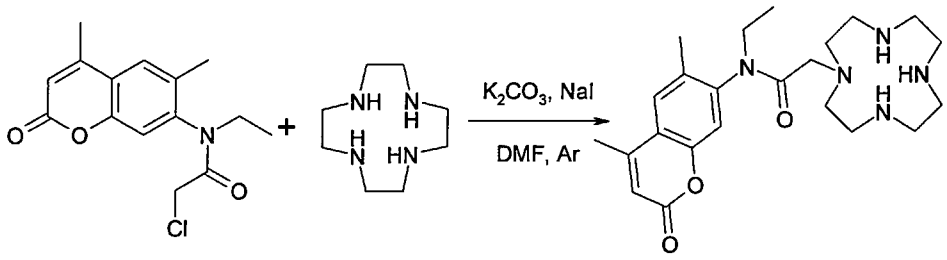

116 **137** **140**

Cyclen (**137**) (2.52 g, 14.7 mmol, 1.5 eq) and coumarin 2 chloroacetate (**116**) (2.87 g, 9.78 mmol) were dissolved in dry DMF (30 mL), K_2CO_3 (3 g, 22 mmol, 2.2 eq) and NaI (3 g, 20 mmol, 2 eq) were added to the solution and the reaction mixture was stirred at 80 °C under argon atmosphere for 24 hours. The DMF was removed at reduced pressure, the residue was dissolved in 40 mL water and 40 mL DCM the phases were separated and the aqueous phase was extracted with 2·30 mL DCM. The combined organic phases were washed with 30 mL water, dried over $MgSO_4$, filtered, and evaporated to dryness. The residue, a dark yellow oil was dissolved in minimum amount of methanol and triturated with ether. The crystals were filtered and washed with small portions of cold diethyl ether. The product (**140**) was isolated as pale yellow crystals in 87% yield (3.65 g). Lower yields, but very high purity can be achieved by alkylation in refluxing 100% EtOH (25 mL), in the presence of TEA (3 eq), in 24 hours, under inert atmosphere. Removal of the ethanol and the TEA, followed by chromatography on basic alumina (pH 9.5) with DCM / MeOH gave the product in 45% yield. HR-ESMS ($C_{23}H_{35}N_5O_3$): calc: 430.2813 $[M+H]^+$,

measured: 430.2814 $[M+H]^+$; ^1H NMR ($CDCl_3$, δ): 1.11-1.16 (t, 3 H, 3 CH_3, J = 6.8 Hz), 2.27 (s, 3 H, CH_3), 2.40 (s, 3 H, CH_3), 2.66-3.32 (m, 17 H, CH_2), 3.38-3.44 (q, 2 H, CH_2), 3.99-4.11 (m, 1 H, CH_2-2), 6.26 (s, 1 H, CH), 7.04 (s, 1 H, CH), 7.50 (s, 1 H, CH); ^{13}C NMR: 12.80 (CH_3), 15.22 (CH_3), 17.53 (CH_3), 18.69 (CH_3), 43.36 (CH_2), 45.33 (CH_2), 46.40 (CH_2), 47.65 (CH_2), 51.87 (CH_2), 65.79 (CH_2), 115.81 (CH), 117.27 (CH), 120.21 (C_q), 127.48 (CH), 131.95 (C_q), 142.23 (C_q), 151.58 (C_q), 152.07 (C_q), 160.10 (CO), 169.88 (CO).

*4.2.2.4 Alkylation of **140** with 2',3'-isopropylidene-5'-O-Ms-uridine*

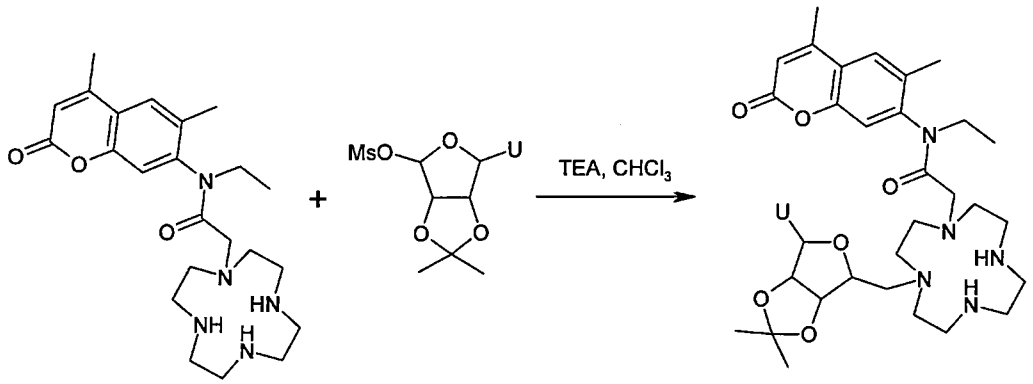

140 **104** **141**

140 (0.37 g, 1.26 mmol) was dissolved in dry chloroform (10 mL), TEA (1.77 mL, 1.27 g, 12.6 mmol, 10 eq) was added, and the solution was flushed with argon for 10 minutes. **104** (0.45 g, 1.26 mmol, dissolved in 10 mL dry chloroform) was added dropwise, and the reaction was allowed to proceed for 18 hours. The volatile components were removed *in vacuo*, and the sample was purified by column chromatography (alumina, pH = 9.5, DCM / MeOH). The product (**141**) was isolated in 41% yield (0.36 g) as a pale yellow solid. ^1H NMR ($CDCl_3$, δ): 1.09 (t, 3 H, CH_3, J = 7.1 Hz), 1.29 (s, 3 H, OCH_3), 1.46 (s, 3 H, OCH_3), 2.25 (d, 1.5 H, 0.5 CH_3, J = 5.0 Hz), 2.29 (s, 1.5 H, 0.5 CH_3), 2.39 (s, 3

H, CH_3), 2.67-3.32 (m, 19 H, CH_2's), 3.97-4.10 (m, 1 H, CH_2-1), 4.33 (t, 1 H, CH, J = 4.6 Hz), 4.40 (d, 2 H, CH_2, J = 4.6 Hz), 4.82 (dd, 1 H, CH, J_1 = 6.4 Hz, J_2 = 3.8 Hz), 5.00 (dd, 1 H, CH, J_1 = 6.4 Hz, J_2 = 1.7 Hz), 5.55 (d, 1 H, CH, J = 1.8 Hz), 5.68 (dd, 1 H, NH, J_1 = 8.0 Hz, J_2 = 0.9 Hz), 6.26 (s, 1 H, CH), 7.00 (d, 0.5 H, 0.5 CH, J = 6.2 Hz), 7.14 (d, 0.5 H, 0.5 CH, J = 6.2 Hz), 7.21 (d, 1 H, NH, J = 8.0 Hz), 7.48 (s, 1 H, CH), 7.51 (d, 1 H, NH, J = 3.8 Hz); ^{13}C NMR: 12.70 (CH_3), 17.53 (CH_3), 18.68 (CH_3), 25.17 (CH_3), 27.00 (CH_3), 37.70 (CH_2), 43.64 (CH_2), 44.68 (CH_2), 45.85 (CH_2), 46.66 (CH_2), 51.92 (CH_2), 53.41 (CH_2), 68.86 (CH_2), 80.97 (CH), 84.26 (CH), 85.42 (CH), 95.69 (CH), 102.88 (CH), 114.70(CH), 115.85 (CH), 117.48 (C_q), 120.26 (C_q), 127.40 (CH), 132.05 (C_q), 142.73 (CH), 151.56 (CO), 152.07 (CO), 160.13 (CO), 170.20 (CO).

*4.2.2.5 Alkylation of **140** with 2',3'-isopropylidene-5'-O-Ms-adenosine*

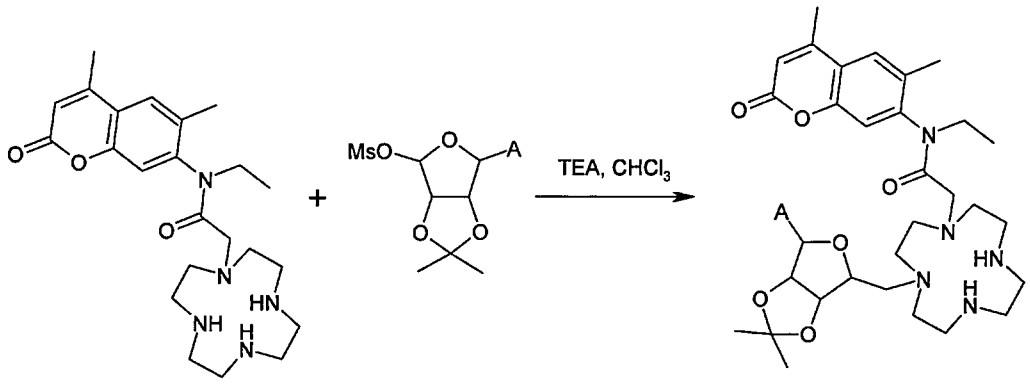

140 **100** **142**

140 (1.34 g, 3.12 mmol) was dissolved in dry chloroform (20 mL), TEA (4.38 mL, 3.15 g, 31.20 mmol, 10 eq) was added, and the solution was flushed with argon for 10 minutes. **100** (1.20 g, 3.12 mmol, dissolved in 10 mL dry chloroform) was added dropwise, and the reaction was allowed to proceed for 18 hours. The volatile components were removed *in vacuo*, and the sample was

purified by column chromatography (alumina, pH = 9.5, DCM / MeOH). The product (**142**) was isolated in 32% yield (0.71 g) as a pale yellow solid. MS: 716 $[M]^+$; ^1H NMR ($CDCl_3$, δ): 1.06 (t, 3 H, CH_3, J = 7.1 Hz), 1.31 (s, 3 H, OCH_3), 1.58 (s, 3 H, OCH_3), 2.22 (s, 3 H, CH_3), 2.39 (s, 3 H, CH_3), 2.21-3.15 (m, 27 H, CH_2's), 3.72 (d, 1 H, CH, J = 12.5 Hz), 3.90 (d, 1 H, CH, J = 12.8 Hz), 4.05 (m, 1 H, CH_2-2), 4.47 (s, 1 H, CH), 5.04 (d, 1 H, CH, J = 5.9 Hz), 5.14 (t, 1 H, CH, J = 5.5 Hz), 5.89 (d, 1 H, CH, J = 5.0 Hz), 6.01 (br s, ~ 2 H, NH, J_1 = 8.0 Hz, J_2 = 0.9 Hz), 6.26 (s, 1 H, CH), 7.00 (s, 1 H, CH), 7.45 (s, 1 H, CH), 8.24 (d, 1 H, CH, J = 2.4 Hz); ^{13}C NMR: 12.83 (CH_3), 17.33 (CH_3), 18.65 (CH_3), 25.20 (OCH_3), 27.61 (OCH_3), 42.98 (CH_2), 50.64 (CH_2), 53.40 (CH_2), 54.67 (CH_2), 55.21 (CH_2), 58.36 (CH_2), 63.32 (CH_2), 81.66 (CH), 82.98 (CH), 86.06 (CH), 94.16 (CH), 113.94 (CH), 115.76(CH), 117.42 (CH), 119.98 (C_q), 127.05 (CH), 131.84 (C_q), 140.20 (CH), 148.38(C_q), 151.43 (C_q), 152.09 (C_q), 152.60 (C_q), 155.99 (C_q), 160.15 (CO), 170.22 (CO).

*4.2.2.6 Alkylation of **140** with ethyl bromoacetate*

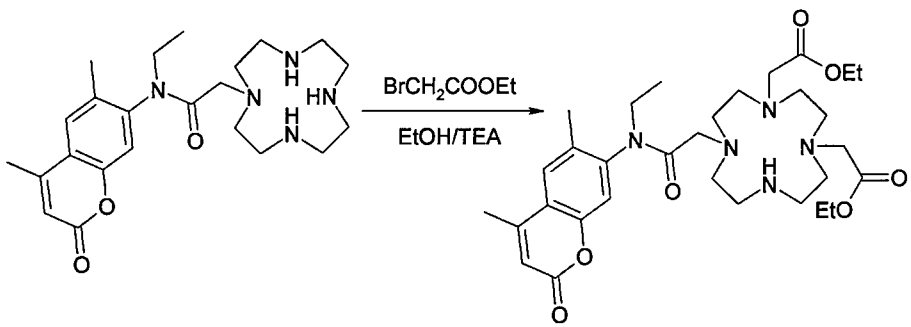

140 **143**

140 (0.92 g, 2.1 mmol) was dissolved in absolute ethanol (12 mL), TEA (902 µL, 0.65 g, 6.4 mmol, 3 eq) was added, and the solution was flushed with argon for 10 minutes. Bromoacetic acid ethyl ester (513 µL, 0.77 g, 4.6 mmol, 2.2 eq) was

added to the solution and the reaction mixture was refluxed under an argon atmosphere for 5 days. The ethanol was evaporated, the residue was dissolved in 30 mL water and 30 mL DCM the phases were separated and the aqueous phase was extracted with 2·30 mL DCM. The combined organic phases were washed with 30 mL water, dried over $MgSO_4$, filtered, and concentrated to ~ 2 mL. The sample was chromatographed on a silica column with DCM containing 2-5% isopropylamine. After evaporation of the solvent the desired product (**143**) was obtained in 15% yield (0.22 g) as an off-white solid. MS: 601 $[M+H]^+$; ^1H NMR ($CDCl_3$, δ): 0.97-1.26 (m, 9 H, 3·CH_3), 2.35 (m, 3 H, CH_3), 2.40 (m, 3 H, CH_3), 2.55-3.32 (m, 23 H, CH_2), 3.99-4.11 (m, 5 H, CH_2), 6.25 (s, 1 H, CH), 7.03 (s, 1 H, CH), 7.47 (s, 1 H, CH); ^{13}C NMR: 12.70 (CH_3), 14.17 (CH_3), 14.21 (CH_3), 17.19 (CH_3), 18.55 (CH_3), 25.97 (CH_2), 42.81 (CH_2), 42.92 (CH_2), 46.86 (CH_2), 47.33 (CH_2), 50.53 (CH_2), 50.98 (CH_2), 51.74 (CH_2), 51.88 (CH_2), 55.39 (CH_2), 55.96 (CH_2), 56.41 (CH_2), 56.82 (CH_2), 59.93 (CH_2), 60.01 (CH_2), 60.09 (CH_2), 115.65 (CH), 117.33 (CH), 119.90 (CH), 127.07 (C_q), 142.73 (C_q), 151.35 (C_q), 152.04 (C_q), 159.98 (C_q), 169.76 (CO), 171.06 (CO), 171.24 (CO), 171.38 (CO).

Isolated side-products

(**144**) Symmatric trisubstituted:

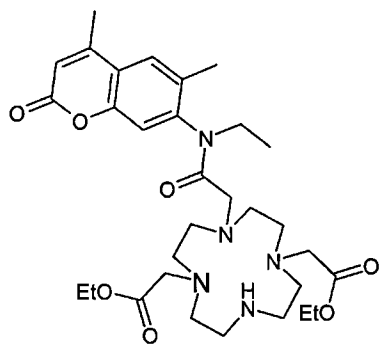

^{1}H NMR ($CDCl_3$, δ): 1.03-1.05 (t, 3 H, CH_3, J = 4.1 Hz), 1.17-1.21 (t, 3 H, CH_3, J = 7.1 Hz), 2.25 (s, 3 H, CH_3), 2.36 (s, 3 H, CH_3), 2.31-2.92 (m, 19 H, CH_2), 3.21 (s, 4 H, CH_2), 3.23-3.37 (m, 1 H, CH_2-2), 4.06 (q, 4 H, 2·CH_2, J = 7.1 Hz), 6.26 (s, 1 H, CH), 7.03 (s, 1 H, CH), 7.49 (s, 1 H, CH); ^{13}C NMR: 12.54 (CH_3), 13.91 (CH_3), 14.01 (CH_3), 17.08 (CH_3), 18.43 (CH_3), 42.65 (CH_2), 46.50 (CH_2), 50.32 (CH_2), 51.25 (CH_2), 51.77 (CH_2), 52.04 (CH_2), 55.68 (CH_2), 55.68 (CH_2), 59.81 (CH_2), 115.41 (CH), 117.15 (CH), 119.77 (CH), 127.00 (C_q), 131.42 (C_q), 142.54 (C_q), 151.35 (C_q), 152.85 (C_q), 159.90 (C_q), 170.19 (CO), 171.21 (CO).

(**145**) Fully substituted:

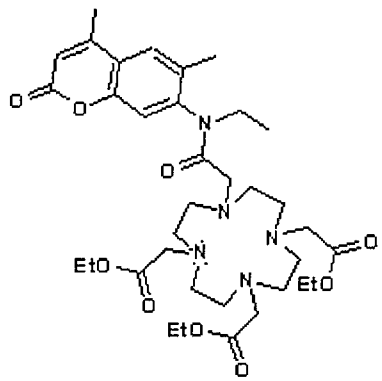

MS: 689 $[M+H]^+$, 706 $[M+H_2O]^+$; ^{1}H NMR ($CDCl_3$, δ): 1.03-1.30 (m, 12 H, 4·CH_3), 2.22-3.71 (m, 31 H, 2· CH_3 + CH_2's), 3.99-4.16 (m, 7 H, CH_2's), 6.25 (s, 1 H, CH), 6.94 (s, 1 H, CH), 7.63 (s, 1 H, CH); ^{13}C NMR: 13.83 (CH_3), 13.87 (CH_3), 18.78 (CH_3), 31.09 (CH_2), 36.27 (CH_2), 43.32 (CH_2), several minor peaks at ~ 50 ppm, 54.67 (CH_2), 54.86 (CH_2), 60.95 (CH_2), 61.01 (CH_2), 115.35 (CH), 116.62 (CH), 120.12 (CH), 127.76 (C_q), 131.65 (C_q), 141.69 (C_q), 151.68 (C_q), 159.91 (C_q), 162.19 (C_q), 170.15 (CO), 173.22 (CO), 173.37 (CO).

*4.2.2.7 Alkylation of **143** with N-Boc ethanolamine methanesulphonate*

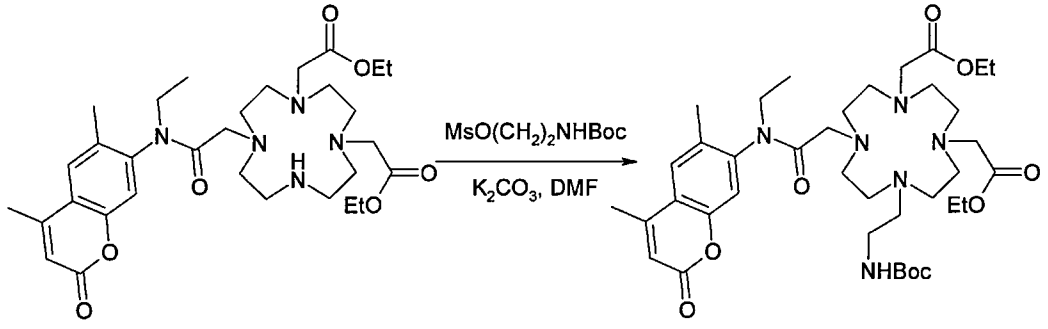

143 **146**

143 (0.39 g, 0.57 mmol) was dissolved in DMF (8 mL), potassium carbonate (0.45 g, 3.24 mmol, 5.7 eq) and N-Boc-ethanolaminemethanesulfonate (0.39 g, 1.63 mmol, 2.9 eq) were added, and the mixture was stirred at 80 °C under argon for 24 hours. The DMF was removed at reduced pressure, the residue suspended in DCM (30 mL), water was added to the suspension (30 mL), and the phases were separated. The aqueous phase was extracted with DCM (2·30 mL), the combined organic extracts were washed with water (2·25 mL), were dried over $MgSO_4$, and after filtration the sample was concentrated to ~3 mL. The product (**146**) was isolated as an off-white solid after chromatography on silica with DCM / $^{i}PrNH_2$ (2-5%) in 12% yield (0.06 g). MS: 746 $[M+H]^+$; ^1H NMR ($CDCl_3$, δ): 1.04-1.38 (18 H, m, 6·CH_3), 2.10-3.40 (m, 33 H, 16.5·CH_2), 3.58-4.09 (m, 5H, 2.5·CH_2), 6.26 (s, 1 H, CH), 7.04 (s, 1 H, CH), 7.48 (s, 1 H, CH); ^{13}C NMR: 12.76 (CH_3), 14.20 (CH_3), 17.37 (CH_3), 18.63 (CH_3), 28.36 (Boc-CH_3), 24.99 (CH_2), 42.97 (CH_2), 43.25 (CH_2), 43.43 (CH_2), 45.43 (CH_2), 51.26 (CH_2), 51.65 (CH_2), 52.34 (CH_2), 52.74 (CH_2), 52.84 (CH_2), 58.25 (CH_2), 60.21 (CH_2), 77.21 (C_q), 115.69 (CH), 117.21 (CH), 117.69, 120.06 (CH), 127.02 (C_q), 127.25 (C_q), 131.75 (C_q), 151.48 (C_q), 151.53 (C_q), 151.99 (C_q), 152.17 (CO), 160.27 (CO), 171.03 (CO), 171.20 (CO), 171.34 (CO).

*4.2.2.8 Alkylation of **143** with **100***

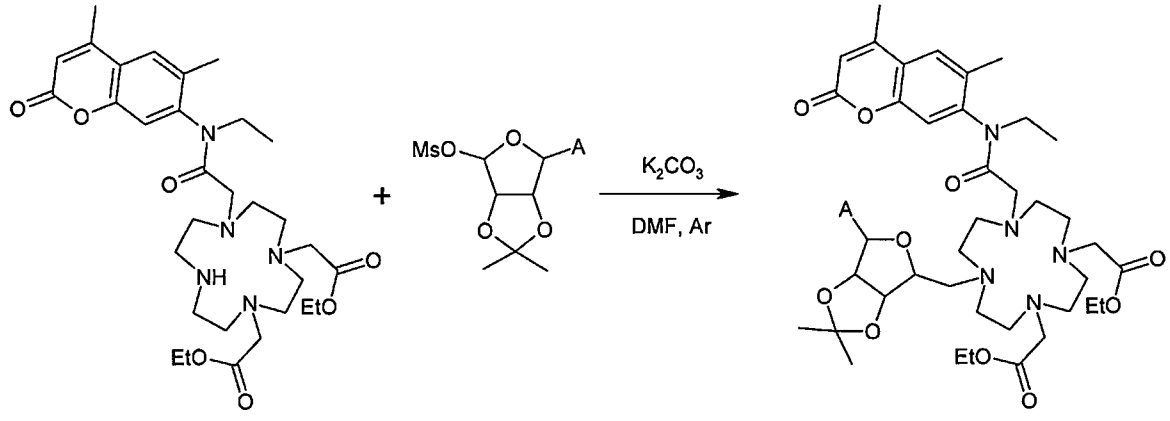

143 **100** **147**

143 (0.75 g, 1.25 mmol) was dissolved in DMF (6 mL), K_2CO_3 (3 g) and **100** (0.96 g, 2.49 mmol, 2 eq) were added, and the mixture was stirred at 80 °C under argon for 24 hours. The DMF was removed at reduced pressure, the residue dissolved in a mixture of DCM and water (30 mL each), and the phases were separated. The aqueous phase was extracted with DCM (3·30 mL), the combined organic phases were washed with water (1·30 mL), dried over $MgSO_4$, filtered, and concentrated. After extensive chromatography on silica (DCM / $^{i}PrNH_2$, 0-20%) and alumina (DCM / MeOH, 0-5%) **147** was isolated as a pale pink solid in 3.5% yield (40 mg). MS: 906 $[M+H_2O]^+$; ^1H NMR ($CDCl_3$, δ): 1.06 (t, 3 H, CH_3, J = 7.0 Hz), 1.10-1.24 (m, 6 H, 2 CH_3), 1.27 (s, 3 H, OCH_3), 1.48 (s, 3 H, OCH_3), 2.23 (s, 3 H, CH_3), 2.35 (s, 3 H, CH_3), 2.54-3.69 (m, 23 H, CH_2's), 3.97-4.11 (m, 6 H, CH_2's), 4.51 (d, 1 H, CH, J = 5.7 Hz), 4.63 (br s, 1 H, CH), 4.93 (d, 1 H, CH, J = 5.5 Hz), 5.76 (s, 1 H, CH), 6.26 (s, 1 H, CH), 7.04 (s, 1 H, CH), 7.47 (s, 1 H, CH), 7.87 (s, 1 H, CH); ^{13}C NMR: 12.83 (CH_3), 14.24 (CH_3), 17.35 (CH_3), 18.65 (CH_3), 24.41 (OCH_3), 26.01 (OCH_3), 42.63 (CH_2), 43.03 (CH_2), 47.25 (CH_2), 49.68 (CH_2), 51.83 (CH_2), 52.02 (CH_2), 52.13 (CH_2), 52.52 (CH_2), 53.02 (CH_2), 53.40 (CH_2), 54.46 (CH_2), 55.28 (CH_2), 55.74 (CH_2),

56.33 (CH_2), 60.21 (CH_2), 60.38 (CH_2), 82.17 (CH), 85.49 (CH), 85.74 (CH), 90.89 (CH), 112.76 (CH), 115.76 (CH), 117.52 (CH), 119.98 (C_q), 127.06 (CH), 131.10 (CH), 131.79 (C_q), 132.01 (C_q), 142.9 (CH)7, 152.13 (C_q), 160.18 (C_q), 163.36 (C_q), 164.97 (CO), 169.88 (CO), 171.09 (CO), 171.25 (CO).

*4.2.2.9 Alkylation of **140** with N-Boc-bromoethylamine*

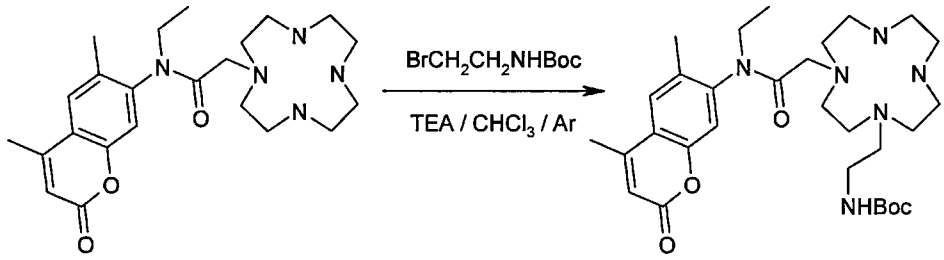

140 **148**

140 (3.10 g, 7.23 mmol) was dissolved in chloroform (100 mL), TEA (10.20 mL, 7.40 g, 72.3 mmol, 10 eq) was added, and the solution was flushed with argon for ten minutes. N-Boc-Bromoethylamine (**131**) (1.77 g, 7.95 mmol, 1.1 eq), dissolved in chloroform (20 mL) was added dropwise to the solution (the addition took approximately 1 hour) and the reaction was allowed to continue for 24 hours. The solvents were removed under reduced pressure and the residue was chromatographed on silica with DCM / $^{i}PrNH_2$ (0-20%) to give **148** in 29% (1.21 g) yield as a pale yellow solid. HR-ESMS ($C_{30}H_{48}N_6O_5$): calc: 573.3759 $[M+H]^+$, measured: 573.3765 $[M+H]^+$; ^1H NMR ($CDCl_3$, δ): 1.06 (t, 3 H, CH_3, J = 7.1 Hz), 1.22 (s, 9 H, $3CH_3$), 2.24 (s, 3 H, CH_3), 2.39 (s, 3 H, CH_3), 2.38-3.23 (m, 24 H), 4.02 (dt, 1 H, 0.5 CH_2, J_1 = 13.5 Hz, J_2 = 7.3 Hz), 6.26 (s, 1 H, CH), 7.00 (s, 1 H, CH), 7.48 (s, 1 H, CH); ^{13}C NMR: 12.72 (CH_3), 17.22 (CH_3), 18.55 (CH_3), 28.19 (CH_3), 38.79(CH_2), 43.09 (CH_2), 45.96 (CH_2), 47.41 (CH_2), 47.63 (CH_2), 51.49 (CH_2), 51.75 (CH_2), 51.98 (CH_2), 53.16 (CH_2), 53.35 (CH_2), 77.98

(C_q), 115.67 (CH), 117.07 (CH), 120.02 (C_q), 127.25 (CH), 131.65 (C_q), 142.70 (C_q), 151.44 (C_q), 152.05 (C_q), 156.07 (C_q), 159.96(CO), 169.56(CO), 172.73 (CO); mp: 55 °C; IR (ν_{max} / (cm^{-1}), KBr): 3368, 2975, 2933, 2824, 1703, 1664, 1626, 1614, 1559, 1502.

*4.2.2.10 Alkylation of **148** with ethyl bromoacetate*

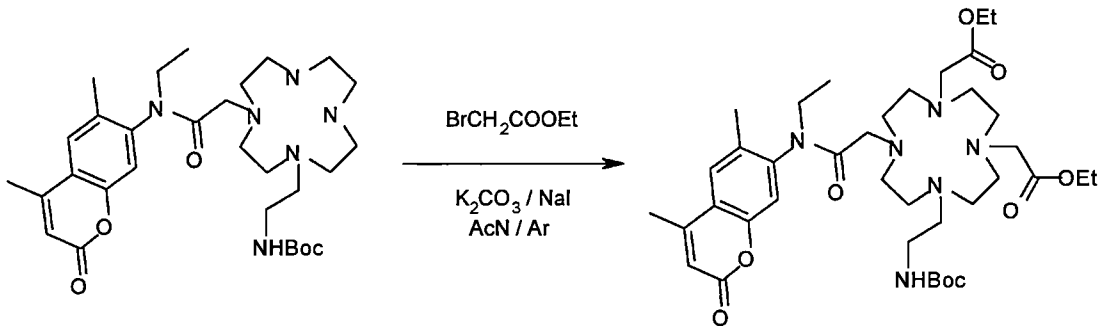

148 **146**

148 (1.09 g, 1.91 mmol) was dissolved in AcN (6 mL), K_2CO_3 (4.25 g, 30.6 mmol, 8 eq), NaI (4.58 g, 30.6 mmol, 8 eq) and ethyl bromoacetate (2118 µL, 3.19 g, 19.1 mmol, 5 eq) were added, and the mixture was stirred at 80 °C under argon for 24 hours. The DMF was removed *in vacuo*, the residue dissolved in water (40 mL) and DCM (40 mL), the phases were separated and the aqueous phase was extracted with DCM (2·30 mL). The combined organic phases were washed with water (2·30 mL), dried over $MgSO_4$, filtered, and the sample was concentrated to 3 mL. The desired product (**146**) was obtained by purification with silica column chromatography using DCM / $^iPrNH_2$ eluants (0-5%). Yield: 70% (0.99 g); MS: 743 $[M+H]^+$, 765 $[M+Na]^+$; ^1H NMR ($CDCl_3$, δ): 1.12 (m, 3 H, CH_3), 1.25 (m, 6 H, 2 CH_3), 1.38(s, 9 H, 3 CH_3), 2.32 (s, 3 H, CH_3), 2.45 (s, 3 H, CH_3), 2.00-3.21 (m, 33 H), 4.15 (m, 1 H, CH), 6.29 (s, 1 H, CH), 6.95 (s, 1 H, CH), 7.62 (s, 1 H, CH); ^{13}C NMR: 12.58 (CH_3), 14.06 (CH_3),

14.12 (CH_3), 17.53 (CH_3), 18.87 (CH_3), 28.38 (CH_3), 43.48 (CH_2), 43.71 (CH_2), 50.52 (CH_2), 53.40 (CH_2), 55.10 (CH_2), 55.73 (CH_2), 56.27 (CH_2), 61.23 (CH_2), 61.36 (CH_2), 67.74 (CH_2), 79.98 (C_q), 105.01 (C_q), 115.84 (CH), 116.78 (CH), 117.10 (CH), 120.49 (C_q), 127.99 (CH), 141.48 (C_q), 141.55 (C_q), 151.86 (CO), 160.06 (CO), 170.64 (CO), 173.24 (CO);

*4.2.2.11 Removal of the Boc protection from **146***

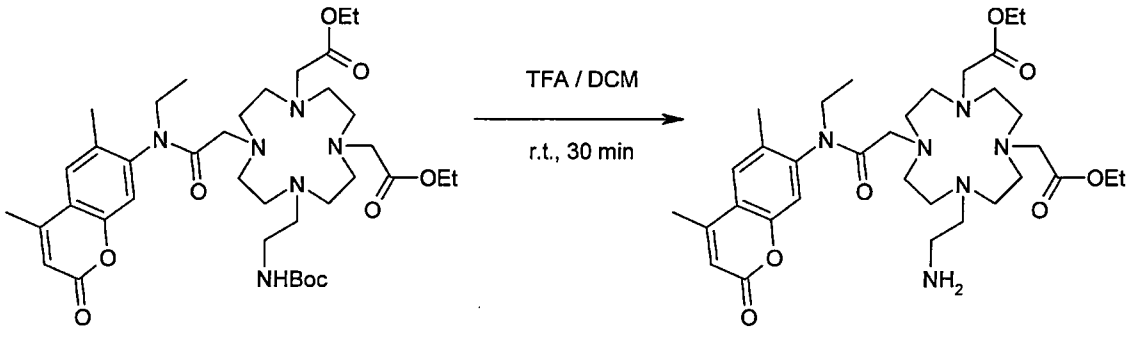

146 **149**

146 (0.99 g, 1.33 mmol) was dissolved in DCM (10 mL), TFA (5 mL) was added to the solution, and the reaction mixture was stirred vigorously at room temperature for 30 minutes. The volatile components were removed at reduced pressure and the residue dissolved in DCM (30 mL). Concentrated aqueous solution of $KHCO_3$ was added in small portions until the pH of the solution reached 8. The aqeous phase was extracted with DCM (2·30 mL), and the combined organic phases were washed with water (40 mL). The organic phase was dried over $MgSO_4$, filtered, and the DCM was evaporated, to give **149** in 84% yield (0.72 g) as a pale yellow solid. MS: 643 $[M+H]^+$, 686 unassigned; ^1H NMR ($CDCl_3$, δ): 1.07 (t, 3 H, CH_3, J = 6.9 Hz), 1.13-1.26 (m, 6 H, $2CH_3$), 2.25 (s, 3 H, CH_3), 2.39 (s, 3 H, CH_3), 2.32-3.74 (m, 27 H, CH_2), 4.04-4.17 (m, 5 H, CH_2), 6.26 (s, 1 H, CH), 7.00 (s, 1 H, CH), 7.50 (s, 1 H, CH), 7.95 (s, 1 H, NH),

8.01 (br s, 1 H, NH); ^{13}C NMR: 12.63 (CH_3), 14.00 (CH_3), 17.20 (CH_3), 18.64 (CH_3), 43.22 (CH_2), 49.16 (CH_2), 49.82 (CH_2), 50.95 (CH_2), 51.88 (CH_2), 53.39 (CH_2), 54.95 (CH_2), 60.42 (CH_2), 63.99 (CH_2), 115.74 (CH), 117.11 (CH), 127.47 (CH), 151.99 (C_q), 160.09 (C_q), 162.44 (CO), 164.67 (CO), 166.44 (CO), 171.38 (CO).

*4.2.2.12 Coupling 5'-carboxylic nucleotides to **149***

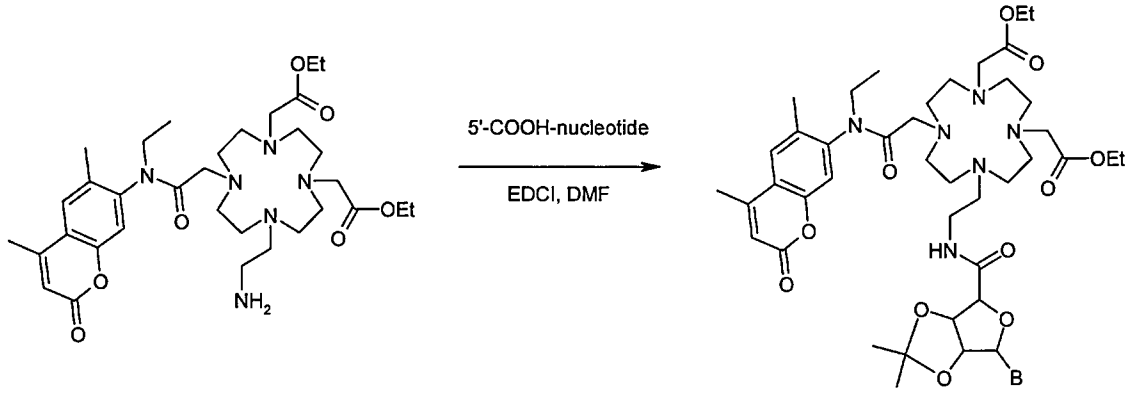

149 **150a-b**

149 (0.65 g, 1.0 mmol) was dissolved in DMF (5 mL), and a solution of the 5'-carboxylic nucleotide (2.0 mmol, 2 eq) and EDCI (0.43 g, 2.2 mmol, 2.2 eq) was added. The reaction mixture was stirred at room temperature for 24 hours. The DMF was removed at reduced pressure and the sample was dissolved in a mixture of DCM and water (40 mL each). The phases were separated and the aqueous phase was extracted with DCM (2·40 mL). The combined organic phases were washed with water (2·25 mL), dried over $MgSO_4$, filtered, and concentrated to 3 mL. Purification of the sample by silica column chromatography (DCM / $^{i}PrNH_2$, 0-20%) gave the products **150a** and **150b**.

150a (B = U): Yield: 84% (0.78 g); HR-ESMS ($C_{45}H_{64}N_8O_{13}$): calc: 947.4485 [M+Na^+], measured: 947.4477 [M+Na^+]; Anal. calc. for $C_{45}H_{64}N_8O_{13}$: C: 58.43,

H: 6.97, N: 12.11; Found: C: 56.25, H: 6.86, N: 11.58; ^{1}H NMR ($CDCl_3$, δ): 1.06 (t, 3 H, CH_3, J = 7.1 Hz), 1.17 (t, 6 H, 2 CH_3, J = 7.1 Hz), 1.28 (s, 3 H, OCH_3), 1.51 (s, 3 H, OCH_3), 2.23 (d, 3 H, CH_3, J = 1.7 Hz), 2.35 (s, 3 H, CH_3), 2.17-3.35 (t, 33 H, CH_2), 3.22 (s, 4 H, arms-NCH_2), 4.05 (q, 4 H, arms-CH_2, J = 7.1 Hz), 4.01-4.15 (m, 1 H, coumarin-CH_2-1), 4.53 (dd, 1 H, C^1H, J_1 = 7.1 Hz, J_2 = 2.0 Hz), 4.92-4.98 (m, 2 H, C^2H and C^3H), 5.66 (dd, 1 H, CH, J_1 = 6.0 Hz, J_2 = 1.8 Hz), 5.74 (dd, 1 H, CH, J_1 = 9.9 Hz, J_2 = 2.2 Hz), 6.26 (d, 1 H, CH, J = 0.9 Hz), 7.03 (d, 1 H, CH, J = 4.0 Hz), 7.48 (s, 1 H, CH), 7.66 (dd, 1 H, CH, J_1 = 8.1 Hz, J_2 = 7.7 Hz), 7.80 (br s, 1 H, NH); ^{13}C NMR: 12.62 (CH_3), 13.93 (CH_3), 14.10 (CH_3), 17.19 (CH_3), 17.30 (CH_3), 18.55 (CH_3), 25.00 (OCH_3), 26.94 (OCH_3), 37.00 (CH_2), 43.00 (CH_2), 51.82 (CH_2), 52.57 (CH_2), 53.35 (CH_2), 54.86 (CH_2), 55.48 (CH_2), 59.94 (CH_2), 60.02 (CH_2), 82.99 (CH), 83.97 (CH), 102.44 (CH), 113.81 (C_q), 115.48 (CH), 117.20 (CH), 119.84 (C_q), 127.11 (CH), 131.72 (C_q), 142.27 (CH), 151.54 (C_q), 151.85 (C_q), 160.09 (CO), 169.00 (CO), 169.64 (CO), 169.64 (CO), 169.76 (CO), 171.27 (CO); mp: turns glassy at 87 °C, gas evolution at 110 °C, complete melting at 122 °C; IR (ν_{max} / (cm^{-1}), KBr): 2983, 2938, 2826, 1729, 1697, 1669, 1627, 1614, 1558, 1526, 1455.

150b (B = A): Yield: 47% (0.45 g); HR-ESMS ($C_{46}H_{66}N_{11}O_{11}$): calc: 948.4938 $[M+H]^+$, measured: 948.4947 $[M+H]^+$; Anal. calc. for $C_{46}H_{66}N_{11}O_{11}$: C: 58.21 H: 7.01 N: 16.23; Found: C: 56.15 H: 6.82 N: 15.35; ^{1}H NMR ($CDCl_3$, δ): 1.05 (t, 3 H, CH_3, J = 7.1 Hz), 1.12-1.21 (m, 6 H, 2CH_3), 1.33 (s, 3 H, OCH_3), 1.54 (s, 3 H, OCH_3), 2.22 (s, 3 H, CH_3), 2.40 (s, 3 H, CH_3), 2.15-3.34 (m, 33 H, CH_2's), 4.01-4.07 (m, 4 H, CH_2), 5.34-5.36 (m, 1 H, CH), 5.40 (m, 1 H, CH), 5.84 (br s, 2 H, NH_2), 6.15 (d, 1 H, CH), 6.25 (s, 1 H, CH), 7.10 (d, 1 H, CH, J = 11.34 Hz), 7.47 (s, 1 H, CH), 8.03 (d, 1 H, CH, J = 1.5 Hz), 8.22 (d, 1 H, CH, J = 1.5 Hz); ^{13}C

NMR: 12.79 (CH_3), 14.24 (CH_3), 14.27 (CH_3), 17.35 (CH_3), 18.67 (CH_3), 25.04 (OCH_3), 26.83 (OCH_3), 43.15 (CH_2), 51.45 (CH_2), 51.58 (CH_2), 51.80 (CH_2), 52.41 (CH_2), 55.15 (CH_2), 56.32 (CH_2), 56.51 (CH_2), 60.21 (CH_2), 83.56 (CH), 84.07 (CH), 86.78 (CH), 91.43 (CH), 113.85 (C_q), 115.70 (CH), 117.48 (CH), 117.61 (C_q), 119.75 (C_q), 119.98 (C_q), 127.05 (CH), 131.86 (C_q), 140.19 (CH), 149.50 (C_q), 151.54 (C_q), 151.60 (C_q), 152.03 (CH), 153.09 (CO), 155.54 (CO), 160.24 (CO), 168.77 (CO), 171.48 (CO); mp: turns glassy at 105 °C, gas evolution at 114 °C, complete melting at 137 °C; IR (ν_{max} / (cm^{-1}), KBr): 2981, 2828, 2361, 2341, 1654, 1577, 1559, 1541, 1522, 1507, 1498.

*4.2.2.13 Complexation of europium with **150a** and **150b***

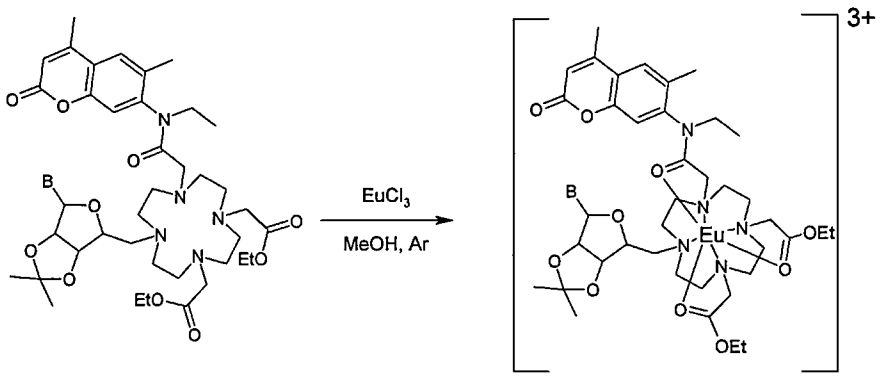

150a-b **151a-b**

The ligands (**150a** and **150b**), (74 mg and 71 mg, 0.074 mmol, 1.1 eq) were dissolved in HPLC-grade methanol (0.5 mL), anhydrous europium chloride (17.5 mg, 0.067 mmol) was added, and the solution was refluxed under argon overnight. The reaction mixture was allowed to cool back to room temperature and was pored into cold diethyl ether (5 mL). The mixture was centrifuged and the ether was poured off the white precipitate. The solid was suspended in 5 mL of ether, and centrifuged again. The ether was poured off again, the residue dissolved in distilled water (1 mL), filtered through a plug of cotton wool and the

sample was freeze-dried. The complexes (**151a** and **151b**) were obtained as white solids. The purity of the samples were checked by TLC (alumina plates, DCM / MeOH).

151a (B = U): Yield: 74% (60 mg); MS: 897 [Ligand-2 Et]$^+$; ^{1}H NMR (CD_3OD, δ): 9.23, 9.97, 12.02, 13.42, 15.81, 17.28, 18.53, 19.70, 20.94, 21.41, 22.58;

151b (B = A): Yield: 76% (63 mg); MS: 920 [Ligand-2 Et]$^+$, 1043 [M-Et_2]$^+$; ^{1}H NMR (CD_3OD, δ): several peaks between 1.63 and 8.40, 10.84, 18.01;

*4.2.2.14 Complexation of terbium with **150a** and **150b***

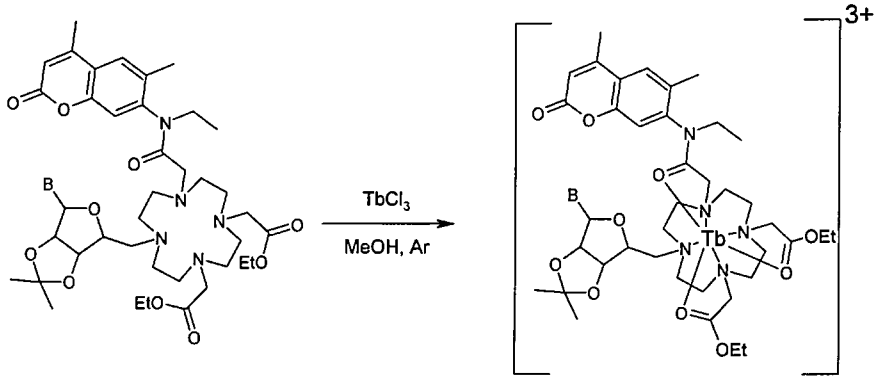

150a-b **152a-b**

The ligands (**150a** and **150b**), (74 mg and 71 mg, 0.074 mmol, 1.1 eq, respectively) were dissolved in HPLC-grade methanol (0.5 mL), anhydrous terbium chloride (19 mg, 0.67 mmol, 0.9 eq) was added, and the solution was refluxed under argon overnight. The reaction mixture was allowed to cool back to room temperature and was poured into cold diethyl ether (5 mL). The mixture was centrifuged and the ether was poured off the white precipitate. The solid was suspended in 5 mL of ether, and centrifuged again. The ether was poured off again, the residue dissolved in distilled water (1 mL), filtered through a plug of cotton wool and the sample was freeze-dried. The complexes (**152a** and

152b) were obtained as white solids. The purity of the samples were checked by TLC (alumina plates, DCM / MeOH).

152a (B = U): Yield: 78% (63 mg); MS: 1101 $[M+H_2O]^+$, 897 [Ligand-2 Et]$^+$; NMR could not be obtained.

152b (B = A): Yield: 80% (66 mg); MS: 920 [Ligand-2 Et]$^+$; ^{1}H NMR (CD_3OD, δ): 10.76, 13.85, 16.05, 18.04, 20.91; NMR could not be obtained.

4.2.2.15 Alkylation of cyclen with N-Boc bromoethylamine

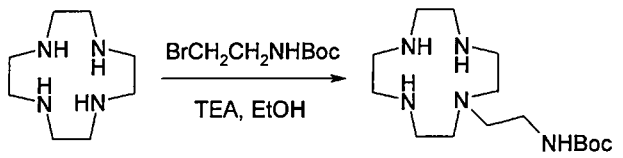

137 **153**

Cyclen (**137**) (7.60 g, 60.3 mmol, 1.1 eq) was dissolved in 100% EtOH (30 mL), TEA (16.92 mL, 12.18 g, 120.6 mmol, 3 eq) and N-Boc bromoethylamine (8.93 g, 40.2 mmol) were added, and the solution was refluxed under argon atmosphere for 24 hours. The ethanol and the triethylamine were evaporated, the residue dissolved in DCM (40 mL), and the solution was washed with 1 M NaOH (30 mL). The aqueous phase ws extracted with DCM (2·30 mL), the combined organic phases were dried over $MgSO_4$, filtered, concentrated to ~5 mL, and purified by column chromatography on a basic alumina column (pH 9.5) by elution with DCM / MeOH (0.2-4%). The product (**153**) was isolated as a white solid in 23% yield (4.27 g). MS: 315 $[M+H]^+$; ^{1}H NMR ($CDCl_3$, δ): 1.37 (s, 9 H, CH_3), 2.48-2.78 (m, 18 H, CH_2), 3.14-3.22 (m, 4 H, CH_2), 5.54; ^{13}C NMR: 28.42 (CH_3), 46.08 (CH_2), 47.04 (CH_2), 47.80 (CH_2), 51.95 (CH_2), 54.20 (CH_2), 78.76(C_q), 155.98 (CO); mp: 119-120°C; IR (ν_{max} / (cm^{-1}), KBr): 3344, 3269, 3186, 2956, 2803, 2700, 1697, 1566.

4.2.2.16 *Alkylation of **153** with coumarin 2 bromoacetate (**117**)*

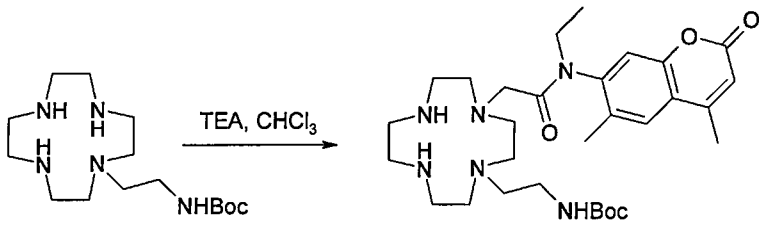

153 **148**

153 (1.54 g, 4.90 mmol) was dissolved in dry chloroform (100 mL), TEA (3.44 mL, 2.47 g, 24.5 mmol, 5 eq) was added to the solution, and the mixture was flushed with argon for 10 minutes. Coumarin 2 bromoacetate (1.66 g, 4.90 mmol) in chloroform (23 mL) was added dropwise (in 1 hour) to the reaction mixture, and the stirring was continued for 36 hours at room temperature. Water (40 mL) was added, the phases were separated, and the organic phase was washed with water again (40 mL). The organic phase was dried over $MgSO_4$, filtered, and concentrated to ~5 mL. The desired product (**148**) was isolated by silica column chromatography by elution with DCM / $^{i}PrNH_2$ (2.5-10%) as a pale yellow solid in 13% yield (0.37 g). Data equal to those reported at *4.2.2.9*.

4.2.2.17 *N-Fmoc Bromoethylamine*

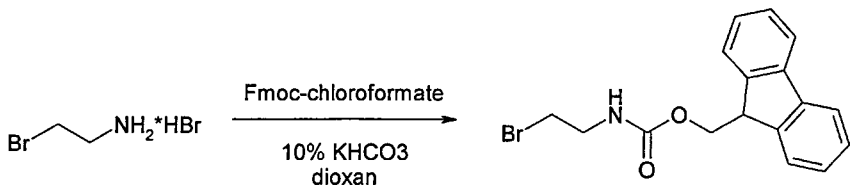

130 **154**

Bromoethylamine hydrobromide (**130**) (4.10 g, 20 mmol) was dissolved in 10% $KHCO_3$ solution (20 mL), dioxin (20 mL) was added, and the solution was cooled in an ice-water bath. In small portions Fmoc-chlorocarbonate (5.20 g, 20

mmol) was added, and the mixture was stirred at ice-water temperature for 4 hours and room temperature for 12 hours. DCM and water (30 mL each) were added to the reaction mixture, the phases were separated, and the aqueous phase was extracted with DCM (12·30 mL). The combined organic phases were washed with water (30 mL) and dilute acid (0.5 M HCl, 50 mL). The DCM solution was dried over $MgSO_4$, filtered, concentrated to ~ 5 mL, and chromatographed on silica with Et_2O / Hexane (2 : 8). After evaporation of the solvents N-Fmoc bromoethylamine (**154**) was obtained in 23% yield (1.60 g) as a shiny white, fluffy solid. MS: 345 [$M+H^+$], 363 [$M+H_3O^+$]; ^1H NMR (δ, $CDCl_3$): 3.43-3.47 (m, 2 H, CH_2), 3.53-3.69 (m, 2 H, CH_2), 4.09-4.13 (m, 1 H, CH), 4.40-4.42 (m, 2 H, CH_2), 7.27-7.77 (m, 8 H, CH); ^{13}C NMR: 32.48 (CH_2), 42.73 (CH_2), 47.17 (CH_2), 66.88 (CH), 120.00 (CH), 124.99 (CH), 127.05 (CH), 127.72 (CH), 141.31 (C_q), 143.77 (C_q); mp: 86-87 °C; IR (ν_{max} / (cm^{-1}), KBr): 3330, 1699, 1608, 1547, 1477.

4.2.2.18 Alkylation of cyclen with t-Butyl bromoacetate

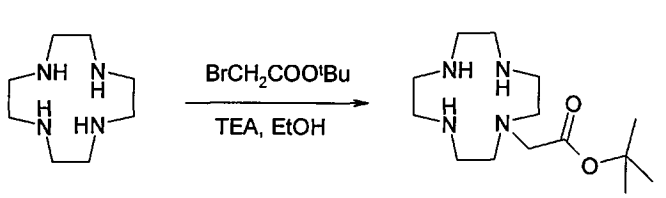

137 **155**

Cyclen (**137**) (10.00 g, 58.1 mmol, 1.5 eq) was dissolved in 100% EtOH (45 mL), TEA (16.3 mL, 11.7 g, 116.2 mmol, 3 eq) and tert-butyl bromoacetate (6.30 mL, 7.56 g, 38.8 mmol) were added, and the solution was refluxed under argon for 24 hours. The ethanol and the triethylamine were evaporated, and the residue dissolved in DCM (30 mL). The solution was washed with water (30

mL), and the aqueous phase was extracted with DCM (2·30 mL). The combined organic phases were washed with water (30 mL), dried over $MgSO_4$, filtered, and concentrated to ~5 mL. The crude sample was purified on a basic alumina column (pH 9.5) by elution with DCM / MeOH (0.2-4%) to give the monoalkylated product (**155**) in 45% yield (5.00 g) as an off-white, viscous liquid. MS: 286 $[M+H]^+$; ^1H NMR (CD_3OD, δ): 1.40 (s, 9 H, CH_3), 2.54-2.86 (m, 16 H, CH_2), 3.14-3.31 (m, 2 H, CH_2); ^{13}C NMR: 28.14 (CH_3), 45.23 (CH_2), 45.98 (CH_2), 46.93 (CH_2), 51.68 (CH_2), 56.94 (CH_2), 80.85 (C_q), 170.70 (CO); IR (ν_{max} / (cm^{-1}), KBr): 2923, 2853, 2360, 1735, 1462.

*4.2.2.19 Alkylation of **151** with tBu bromoacetate*

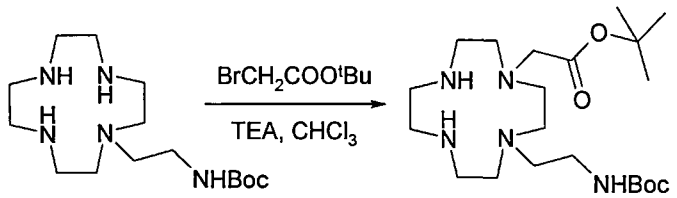

151 **156**

151 (3.00 g, 9.6 mmol) was dissolved in dry chloroform (120 mL), TEA (13.40 mL, 9.65 g, 95.5 mmol, 10 eq) was added to the solution, which was then flushed with argon for 10 minutes. ^{t}Butyl bromoacetate (1.55 mL, 1.86 g, 9.6 mmol) in chloroform (29 mL) was added dropwise (in 1 hour) to the vigorously stirred reaction mixture, and the reaction was allowed to proceed for 36 hours at room temperature. Water (40 mL) was added to the solution, the phases were separated, and the organic phase was washed with water (40 mL). The organic phase was dried over $MgSO_4$, filtered, and concentrated to ~5 mL. The desired product (**156**) was isolated by silica column chromatography by elution with DCM / $^i PrNH_2$ (2.5-10 %) in 25% yield (1.01 g) as a white solid. ^1H NMR

(CD_3OD, δ): 1.37 (s, 9 H, CH_3), 1.39 (s, 9 H, CH_3), 2.43-3.42 (m, 24 H, CH_2), inside the multiplet: 3.29 (s, 2 H, $C\underline{H_2}COO^tBu$); ^{13}C NMR: 28.07 (CH_3), 28.39 (CH_3), 38.85 (CH_2), 45.57 (CH_2), 46.18 (CH_2), 47.65 (CH_2), 47.96 (CH_2), 50.91 (CH_2), 51.73 (CH_2), 51.85 (CH_2), 52.52 (CH_2), 53.40 (CH_2), 54.28 (CH_2), 78.39 (C_q), 80.84 (C_q), 156.12 (CO), 170.53 (CO).

*4.2.2.20 Alkylation of **156** with ethyl bromoacetate*

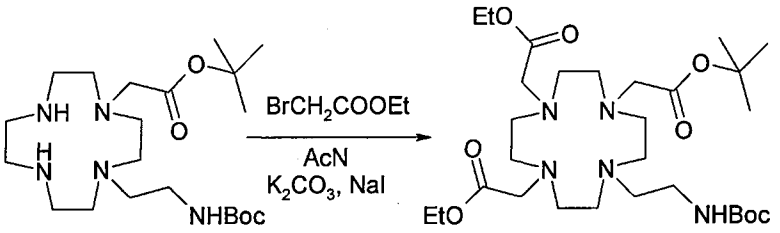

156 **157**

156 (1.01 g, 2.36 mmol) was dissolved in acetonitrile (10 mL), K_2CO_3 (4.80 g, 37.7 mmol, 8 eq), NaI (5.66 g, 37.7 mmol, 8 eq) and ethyl bromoacetate (2617 μL, 3.94 g, 23.6 mmol, 5 eq) were added, and the mixture was stirred at 80 C under argon for 24 hours. The acetonitrile was removed *in vacuo*, the residue dissolved in water (40 mL) and DCM (40 mL), the phases were separated and the aqueous phase was extracted with DCM (2·30 mL). The combined organic phases were washed with water (2·30 mL), dried over $MgSO_4$, filtered, and the sample was concentrated to 3 mL. The desired product (**157**) was obtained by purification with silica column chromatography using DCM / MeOH eluants. Yield: 0.97 g (69%); ^1H NMR (CD_3OD, δ): 1.11-1.23 (m, 6 H, CH_3), 1.34 (s, 9 H, Boc-CH_3), 1.43 (s, 9 H, CH_3), 2.32-3.47 (m, 25 H, CH_2), 4.00-4.23 (m, 5 H, CH_2); ^{13}C NMR: 14.04 (CH_3), 14.13 (CH_3), 27.97 (CH_3), 28.31 (CH_3), 37.81 (CH_2), 50.24 (CH_2), 51.14 (CH_2), 54.04 (CH_2), 55.04 (CH_2), 55.84 (CH_2), 56.57

(CH_2), 61.37 (CH_2), 61.69 (CH_2), 79.23 (Boc-C_q), 82.86 (C_q), 173.31 (CO), 173.92 (CO).

*4.2.2.21 Removal of the Boc protection from **157***

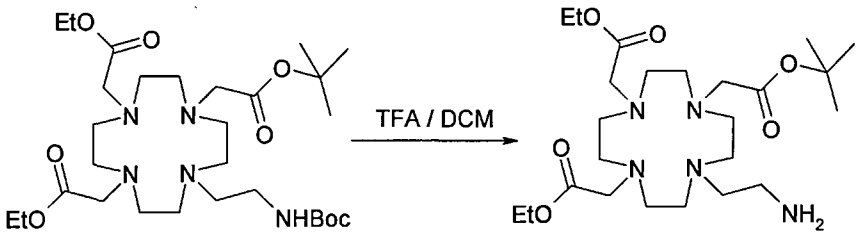

157 **158**

157 (0.97 g, 1.63 mmol) was dissolved in DCM (10 mL), TFA (5 mL) was added to the solution, and the reaction mixture was stirred vigorously at room temperature for 30 minutes. The volatile components were removed at reduced pressure and the residue dissolved in DCM (30 mL). Concentrated aqueous solution of $KHCO_3$ was added in small portions until the pH of the solution reached 8. The aqeous was extracted with DCM (2·30 mL), and the combined organic phases were washed with water (40 mL). The organic phase was dried over $MgSO_4$, filtered, and the DCM was evaporated, to give **158** in 84% (0.68 g) yield as an off-white solid. ^{1}H NMR ($CDCl_3$, δ): 0.96-1.01 (m, 6 H, CH_3), 1.39 (s, 9 H, CH_3), 2.53-2.75 (m, 21 H, CH_2), 3.21 (s, 2 H, CH_2), 3.32-3.36 (m, 4 H, CH_2), 3.98-4.11 (m, 4 H, CH_2); ^{13}C NMR: 14.17 (CH_3), 14.21 (CH_3), 28.14 (CH_3), 51.17 (CH_2), 51.82 (CH_2), 55.34 (CH_2), 56.20 (CH_2), 60.20 (CH_2), 60.35 (CH_2), 81.03 (C_q), 171.15 (CO), 171.54 (CO), 171.69 (CO).

*4.2.2.22 Attachment of adenosine to the **158***

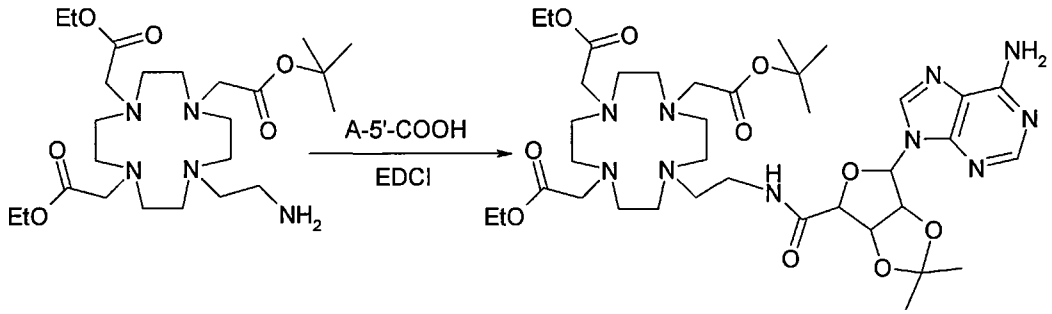

158 **159**

158 (0.47 g, 0.94 mmol) was dissolved in DMF (6 mL), and a solution of the 5'-carboxylic adenosine (2 eq, 1.88 mmol, 0.60 g) and EDCI (2 eq, 1.88 mmol, 0.36 g) was added. The reaction mixture was stirred at room temperature for 24 hours. The DMF was removed at reduced pressure and the sample was dissolved in a mixture of DCM and water (40 mL each). The phases were separated and the aqueous phase was extracted with DCM (2·40 mL). The combined organic phases were washed with water (2·25 mL), dried over $MgSO_4$, filtered, and concentrated to 3 mL. Purification of the sample by silica column chromatography (DCM / $^{i}PrNH_2$) gave the product **159** in 25% yield (0.19 g). ^{1}H NMR ($CDCl_3$, δ): 1.16-1.23 (m, 6 H, CH_3), 1.33 (s, 3 H, OCH_3), 1.38 (s, 9 H, Boc-CH_3), 1.55 (s, 3 H, OCH_3), 2.10-3.38 (m, 25 H, CH_2), 4.03-4.12 (m, 4 H, CH_2), 5.33 (d, 1 H, CH, J = 6.0 Hz), 5.40 (d, 1 H, CH, J = 6.0 Hz), 5.77-5.81 (m, 1 H, CH), 6.18 (s, 1 H, CH), 7.18 (br s, NH_2), 8.06 (s, 1 H, NH), 8.16 (s, 1 H, CH); ^{13}C NMR: 14.35 (CH_3), 14.38 (CH_3), 25.14 (OCH_3), 26.94 (OCH_3), 28.28 (Boc-CH_3), 31.48 (CH_2), 36.53 (CH_2), 51.96 (CH_2), 52.47 (CH_2), 52.89 (CH_2), 55.54 (CH_2), 56.40 (CH_2), 60.21 (CH_2), 60.30 (CH_2), 80.93 (CH_2), 80.93 (C_q), 83.70 (CH), 84.34 (CH), 86.80 (CH), 91.58 (CH), 113.96 (CH), 119.84, 140.29 (CH), 149.64 (C_q), 153.21 (C_q), 155.56 (C_q), 168.87 (CO), 170.90 (CO), 171.55 (CO), 171.72 (CO).

*4.2.2.23 Removal of the tBu protection from **159***

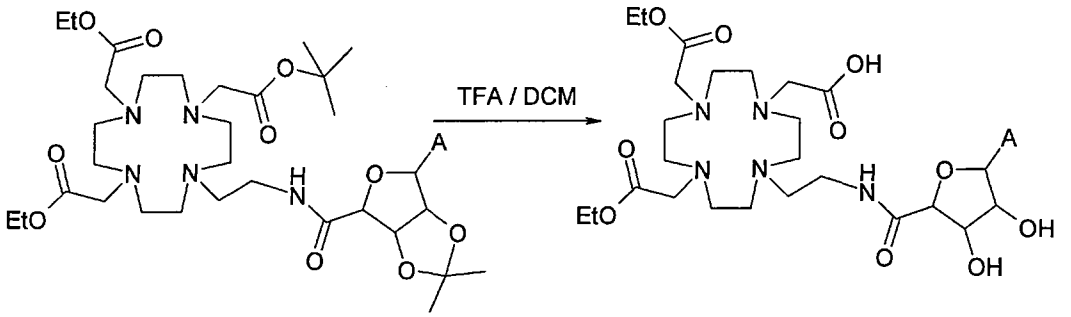

159 **160**

159 (0.19 g, 0.24 mmol) was dissolved in DCM (6 mL), TFA (6 mL) was added to the solution, and the reaction mixture was stirred vigorously at room temperature for 2 hours. The volatile components were removed at reduced pressure and the sample was dried at reduced pressure overnight to give **160** in quantitative yield as a pale brown solid. ^{1}H NMR (CD_3OD, δ): 1.28,-1.41 (m, 6 H, CH_3), 2.89-3.67 (m, 6 H, CH_3), 4.19-4.31 (m, 22 H, CH_2), 4.45-4.47 (m, 8 H, CH_2), 4.58-4.60 (m, 1 H, CH), 4.65-4.70 (m, 1 H, CH), 6.17-6.21 (m, 1 H, CH), 7.98 (br s, 2 H, NH_2), 8.74 (s, 1 H, CH), 8.85 (m, 1 H, CH); ^{13}C NMR: 14.13 (CH_3), 14.27 (CH_3), 31.79 (CH_2), 37.05 (CH_2), 45.79 (CH_2), 50.77 (CH_2), 51.18 (CH_2), 52.28 (CH_2), 53.50 (CH_2), 53.73 (CH_2), 54.25 (CH_2), 55.07 (CH_2), 62.42 (CH_2), 63.49 (CH_2), 74.11 (CH_2), 83.95 (CH), 84.14 (CH), 84.98 (CH), 90.19 (CH), 110.62 (C_q), 114.43 (CH), 118.23 (CH), 122.04 (C_q), 144.94 (C_q), 160.38 (CO), 160.89 (CO), 164.89 (CO), 172.28 (CO).

*4.2.2.24 Attachment of rhodamine B to **147***

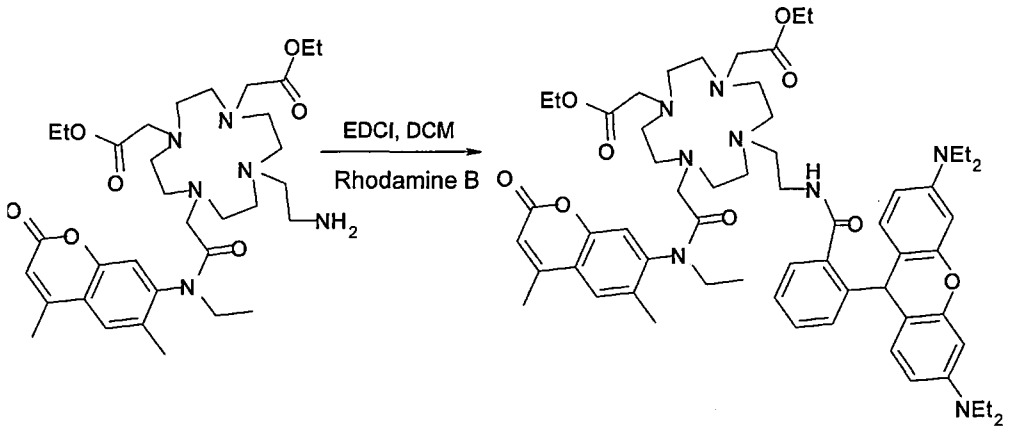

147 (0.65 g, 1.01 mmol) was dissolved in DCM (10 mL), rhodamine B (0.73 g, 1.52 mmol, 1.5 eq) and EDCI (0.29 g, 1.52 mmol, 1.5 eq) were added, and the solution was stirred at room temperature for 24 hours. Water (30 mL) and DCM (20 mL) were added to the solution, and the phases were separated. The aqueous phase was extracted with DCM (3·30 mL), and the combined organic phases were washed with water (50 mL). The organic phase was dried over $MgSO_4$, filtered, and concentrated to ~5 mL. The crude sample was purified by silica column chromatography by elution with DCM containing 2.5% isopropylamine to yield the **161** in 65% yield (0.70 g) as a deep purple solid. MS: 1046 [M, one ethyl ester cleaved]$^+$; 1070 $[M+H]^+$; ^1H NMR ($CDCl_3$, δ): 1.04-1.15 (m, 21 H, 7 ethyl CH_3), 2.09-3.31 (m, 45 H, CH_2), 4.01-4.06 (m, 3 H, 1.5 CH_2), 6.16-6.36 (m, 6 H, CH), 7.01-7.02 (m, 1 H, CH), 7.14 (d, 1 H, CH, J = 7.5 Hz), 7.35-7.37 (m, 2 H, CH), 7.49-7.56 (m, 3 H, CH), 7.89 (m, 1 H, CH), 7.91 (d, 1 H, J = 7.5 Hz); ^{13}C NMR: 12.44 (CH_3), 12.52 (CH_3), 12.73 (CH_3), 14.09 (CH_3), 14.20 (CH_3), 14.23 (CH_3), 18.60 (CH_3), 18.84 (CH_3), 42.97 (CH_2), 44.25 (CH_2), 44.35 (CH_2), 45.15 (CH_2), 50.67 (CH_2), 51.73 (CH_2), 52.08 (CH_2), 53.36 (CH_2), 55.00 (CH_2), 56.31 (CH_2), 59.94 (CH_2), 61.33 (CH_2), 97.50 (CH), 97.61 (CH),

105.57 (C_q), 107.84 (CH), 107.95 (CH), 115.44 (C_q), 115.71 (C_q), 117.49 (C_q), 119.79 (C_q), 122.42 (C_q), 123.73 (C_q), 124.05 (C_q), 124.52 (C_q), 125.37 (CH), 127.71 (CH), 128.79 (CH), 129.03 (CH), 131.55 (C_q), 131.97 (CH), 132.12 (C_q), 134.34 (CH), 148.67 (C_q), 149.31 (C_q), 153.04 (C_q), 153.20 (C_q), 153.23 (CO), 160.20 (CO), 167.33 (CO), 169.75 (CO), 171.40 (CO).

*4.2.2.25 Complexation of neodymium with **161***

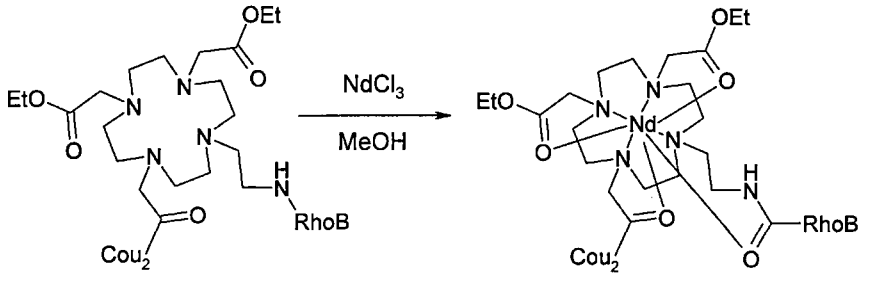

161 **162**

161 (200 mg, 0.19 mmol) was dissolved in HPLC-grade methanol (3 mL), anhydrous neodymium chloride (42 mg, 0.17 mmol, 0.9 eq) was added, and the solution was refluxed under argon overnight. The reaction mixture was allowed to cool back to room temperature and was poured into cold diethyl ether (15 mL). The mixture was centrifuged and the ether was poured off the dark purple precipitate. The solid was suspended in 5 mL of ether, and centrifuged again. The ether was poured off again, the residue dissolved in distilled water (5 mL), filtered through a plug of cotton wool and the sample was freeze-dried. The complex (**162**) was obtained as a dark purple solid in 70% yield. The purity of the sample was checked by TLC (alumina plates, DCM / MeOH, various ratios, up to 20% MeOH). MS: 1157 $[M(\text{-ethyl esters})+H]^+$; ^1H NMR (CD_3OD, δ): 0.75-1.45 (m), 3.29-3.73 (m, approximately 22 H), 6.42-6.46 (br m, 2 H), 6.97 (br s 2 H), 7.06-7.09 (br m, 3 H), 7.60 (br m, 2 H) 7.83 (br m, 1 H) 9.01 (br m, 2 H); ^{13}C

NMR: 12.65, 12.94, 38.00, 45.08, 46.62, 66.60, 73.92, 78.07, 87.93, 97.28, 113.32, 115.62, 157.00, 160.14, 162.11.

*4.2.2.26 Complexation of ytterbium with **161***

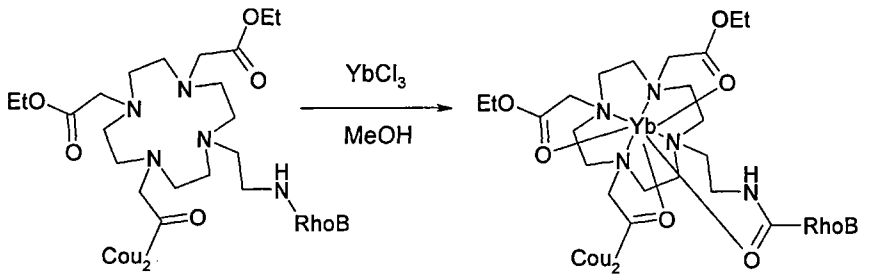

161 **163**

161 (200 mg, 19 mmol) was dissolved in HPLC-grade methanol (3 mL), anhydrous ytterbium chloride (0.044 g, 0.17 mmol, 0.9 eq) was added, and the solution was refluxed under argon overnight. The reaction mixture was allowed to cool back to room temperature and was poured into cold diethyl ether (15 mL). The mixture was centrifuged and the ether was poured off the white precipitate. The solid was suspended in 5 mL of ether, and centrifuged again. The ether was poured off again, the residue dissolved in distilled water (4 mL), filtered through a plug of cotton wool and the sample was freeze-dried. The complex was obtained as purple solids in 85% yield. The purity of the sample was checked by TLC (alumina plates, DCM / MeOH, 0%, 2%, 10%). MS: 1189 $[M(\text{-ethyl esters})+H]^+$.

4.2.2.27 Reaction of bromoethylamine with rhodamine B

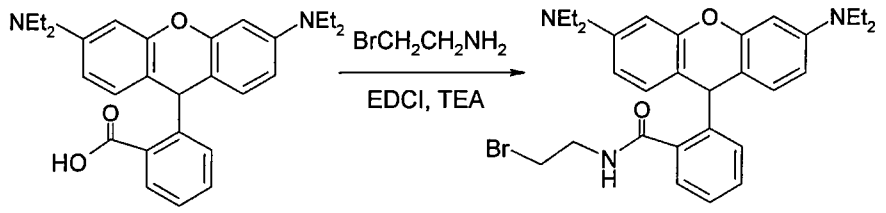

164 **165**

Rhodamine B (**164**) (14.24 g, 30 mmol) was dissolved in DCM (40 mL), EDCI (5.73 g, 30 mmol) was added to the solution, and the carboxylic acid was pre-activated for 10 minutes. Bromoethylamine hydrobromide (6.15 g, 30 mmol) and TEA (4.21 mL, 3.03 g, 30 mmol) were added, and the reaction was allowed to proceed for 24 hours. Water (40 mL) was added to the solution, the phases were separated, and the aqueous phase was extracted with DCM (2·40 mL). The combined organic phases were washed with water (50 mL) and dilute acid (0.1 M HCl, 40 mL), dried over $MgSO_4$, filtered, and concentrated. The sample was purified by chromatography on silica by elution with DCM / MeOH (0-1%). The product (**165**) was obtained as a pale pink solid in 41% yield (7.08 g). MS: 550 $[M+H]^+$; ^1H NMR (δ, $CDCl_3$): 1.10 (t, 12 H, 4 CH_3, J = 7.0 Hz), 2.91 (t, 2 H, CH_2, J = 7.3 Hz), 3.26 (q, 8 H, CH_2, J = 7.0 Hz), 3.45 (t, 2 H, CH_2, J = 7.3 Hz), 6.18 (d, 1 H, CH, J = 2.8 Hz), 6.21 (d, 1 H, CH, J = 2.6 Hz), 6.31 (d, 1 H, CH, J = 2.6 Hz), 6.34 (s, 1 H, CH), 6.37 (s, 1 H, CH), 6.96-7.02 (m, 1 H, CH), 7.33-7.39 (m, 2 H, CH), 7.80-7.86 (m, 1 H, CH); ^{13}C NMR: 12.54 (CH_3), 41.76 (CH_2), 44.31 (CH_2), 64.65 (CH_2), 97.72 (CH), 105.07 (CH), 108.12 (CH), 122.89 (CH), 123.77 (CH), 128.04 (CH), 128.64 (CH), 130.50 (C_q), 132.64 (CH), 148.84 (C_q), 153.15 (C_q), 153.54 (CO).

*4.2.2.28 Alkylation of cyclen with **165***

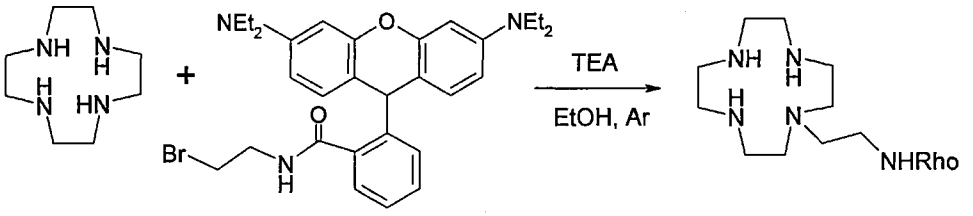

137 **165** **166**

Cyclen (**137**) (3.21 g, 18.66 mmol, 1.5 eq) was dissolved in 100% EtOH (25 mL), TEA (5.24 mL, 3.77 g, 37.33 mmol, 3 eq) and (**165**) (7.08 g, 12.44 mmol) were added, and the solution was refluxed under argon for 24 hours. The ethanol and the triethylamine were evaporated, and the residue dissolved in DCM (30 mL). The solution was washed with water (30 mL), and the aqueous phase was extracted with DCM (2·30 mL). the combined organic phases were washed with water (30 ml), dried over $MgSO_4$, filtered, and concentrated to ~5 mL. The crude sample was purified on a basic alumina column (pH 9.5) by elution with DCM / MeOH (0.2-4%) to give the monoalkylated product (**166**) in 39% yield (3.12 g) as a pale pink solid. MS: 641 $[M+H]^+$; ^1H NMR (δ, $CDCl_3$): 1.10 (t, 12 H, 4 CH_3, J = 7.0 Hz), 2.17-3.37 (m, 28 H, 14 CH_2), 6.17-6.21 (m, 2 H, CH), 6.31-6.41 (m, 5 H, CH), 6.97-7.01 (m, 1 H, CH), 7.32-7.36 (m, 1 H, CH), 7.44-7.47 (m, 1 H, CH), 7.80-7.86 (m, 1 H, CH); ^{13}C NMR: 12.56 (CH_3), 37.83 (CH_2), 41.76 (CH_2), 44.32 (CH_2), 45.36 (CH_2), 46.32 (CH_2), 47.18 (CH_2), 51.13 (CH_2), 52.05 (CH_2), 64.78 (CH_2), 97.83 (CH), 105.68 (CH), 108.00 (CH), 122.57 (CH), 123.68 (CH), 127.87 (CH), 128.84 (CH), 131.41 (C_q), 132.11 (CH), 148.67 (C_q), 153.34 (C_q), 153.45 (CO), 167.61 (C_q).

*4.2.2.29 Alkylation of **166** with N-Boc bromoethylamine*

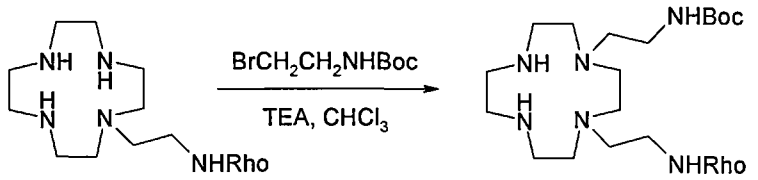

166 **167**

166 (3.12 g, 4.73 mmol) was dissolved in dry chloroform (55 mL), TEA (6.64 mL, 4.80 g, 47.3 mmol, 10 eq) was added to the solution, and the mixture was flushed with argon for 10 minutes. N-Boc Bromoethylamine (1.06 g, 4.73 mmol) in chloroform (15 mL) was added dropwise (in 1 hour) to the reaction mixture, and the stirring was continued for 36 hours at room temperature. Water (35 mL) was added, the phases were separated, and the organic phase was washed with water again (40 mL). The organic phase was dried over $MgSO_4$, filtered, and concentrated to ~ 5 mL. The desired product (**167**) was isolated by silica column chromatography by elution with DCM / $^{i}PrNH_2$ (2.5-10%) as an off-white solid in 20% yield (0.75 g). MS: 784 $[M+H]^+$; ^1H NMR (δ, $CDCl_3$): 1.10 (t, 12 H, 4 CH_3, J = 7.0 Hz), 1.29 (s, 9 H, Boc), 2.08-2.64 (m, 20 H, 10 CH_2), 2.92-3.30 (m, 12 H, 6 CH_2) 6.18 (d, 1 H, CH, J = 2.7 Hz), 6.21 (d, 1 H, CH, J = 2.7 Hz), 6.30-6.35 (m, 5 H, CH), 6.44 (br s, 1 H, NH), 6.99-7.04 (m, 1 H, CH), 7.34-7.40 (m, 2 H, CH), 7.80-7.84 (m, 1 H, CH); ^{13}C NMR: 12.62 (CH_3), 28.50 (CH_3), 34.79 (CH_2), 38.76 (CH_2), 44.31 (CH_2), 45.28 (CH_2), 45.36 (CH_2), 46.75 (CH_2), 47.46 (CH_2), 48.11 (CH_2), 50.73 (CH_2), 51.38 (CH_2), 51.63 (CH_2), 52.39 (CH_2), 53.26 (CH_2), 64.79 (CH_2), 97.54 (CH), 105.61 (CH), 108.03 (CH), 122.53 (CH), 123.79 (CH), 128.05 (CH), 129.11 (CH), 131.81 (C_q), 132.17 (CH), 148.75 (C_q), 153.11 (C_q), 153.49 (CO), 167.36 (C_q).

*4.2.2.30 Alkylation of **167** with ethyl bromoacetate*

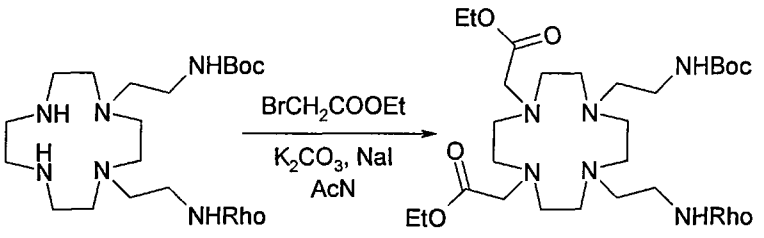

167 **168**

167 (1.08 g, 1.56 mmol) was dissolved in AcN (8 mL), K_2CO_3 (3.50 g, 25.0 mmol, 8 eq), NaI (3.74 g, 25.0 mmol, 8 eq) and ethyl bromoacetate (1733 µL, 2.61 g, 15.6 mmol, 5 eq) were added, and the mixture was stirred at 80 °C under argon for 24 hours. The AcN was removed *in vacuo*, the residue dissolved in water (40 mL) and DCM (40 mL), the phases were separated and the aqueous phase was extracted with DCM (2·30 mL). The combined organic phases were washed with water (2·30 mL), dried over $MgSO_4$, filtered, and the sample was concentrated to 3 mL. The desired product (**168**) was obtained by purification with silica column chromatography using DCM / MeOH eluants (0-2.5%). Yield: 83% (1.24 g); MS: 957 $[M+H]^+$; ^1H NMR (δ, $CDCl_3$): 1.07-1.25 (m, 18 H, 6 CH_3), 1.34 (s, 9 H, Boc), 2.18-3.58 (m, 36 H, CH_2), 4.00-4.53 (m, 4 H, CH_2), 6.18 (d, 1H, CH, J = 2.6 Hz), 6.21 (d, 1H, CH, J = 2.6 Hz), 6.26-6.37 (m, 4 H, CH), 7.01-7.04 (m, 1 H, CH), 7.36-7.39 (m, 2 H, CH), 7.80-7.83 (m, 1 H, CH); ^{13}C NMR: 12.61 (CH_3), 14.24 (CH_3), 14.27 (CH_3), 28.48 (CH_3), 44.32 (CH_2), 50.75 (CH_2), 51.27 (CH_2), 51.91 (CH_2), 52.41 (CH_2), 53.40 (CH_2), 60.18 (CH_2), 97.62 (CH), 105.57 (CH), 108.02 (CH), 122.58 (CH), 123.79 (CH), 128.04 (CH), 129.00 (CH), 148.76 (C_q), 153.46 (C_q), 156.23 (CO), 167.47 (CO), 171.39 (CO).

(**169**) Side-product isolated:

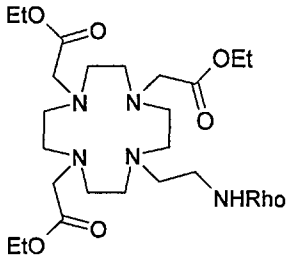

MS: 899 $[M+H]^+$; ^1H NMR (δ, $CDCl_3$): 1.09-1.29 (m, 21 H, CH_3), 2.10-2.82 (m, 22 H, CH_2), 2.81 (s, 1 H, CH_2-1), 2.89 (s, 1 H, CH_2-2), 3.07-3.17 (m, 2 H, CH_2), 3.23-3.39 (m, 12 H, CH_2), 4.00-4.14 (m, 6 H, CH_2), 6.18 (d, 1 H, CH, J = 2.6 Hz), 6.21 (d, 1 H, CH, J = 2.6 Hz), 6.30-6.36 (m, 3 H, CH), 7.01-7.03 (m, 1 H, CH), 7.33-7.39 (m, 2 H, CH), 7.79-7.82 (m, 1 H, CH); ^{13}C NMR: 12.58 (CH_3), 14.27 (CH_3), 14.31 (CH_3), 44.31 (CH_2), 50.74 (CH_2), 51.85 (CH_2), 51.93 (CH_2), 52.11 (CH_2), 52.56 (CH_2), 55.80 (CH_2), 60.03 (CH_2), 64.78 (CH_2), 97.68 (CH), 105.72 (C_q), 108.02 (CH), 122.57 (CH), 123.77 (CH), 127.96 (CH), 128.98 (CH), 131.70 (C_q), 132.13 (C_q), 148.72 (CH), 153.19 (C_q), 153.41 (C_q), 167.47 (CO), 171.67 (CO).

*4.2.2.31 Removal of the Boc protection from **168***

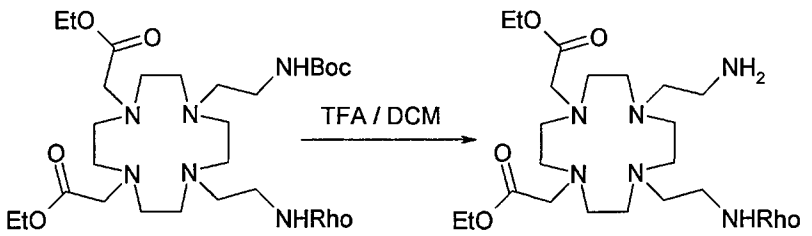

168 **170**

168 (1.24 g, 1.30 mmol) was dissolved in DCM (12 mL), TFA (6 mL) was added to the solution, and the reaction mixture was stirred vigorously at room temperature for 30 minutes. The volatile components were removed at reduced pressure and the residue dissolved in DCM (30 mL). Concentrated aqueous

solution of $KHCO_3$ was added in small portions until pH 8 was reached. The aqeous was extracted with DCM (2·30 mL), and the combined organic phases were washed with water (40 mL). The organic phase was dried over $MgSO_4$, filtered, and the DCM was evaporated, to give **170** in 84% yield as an pale purple solid. MS: 856 $[M+H]^+$, 428 $[M+H+H]^{2+}$; ^1H NMR (δ, $CDCl_3$): 1.07-1.23 (m, 18 H, 6 CH_3), 2.10-3.39 (m, 36 H, 18 CH_2), 3.98 (q, 2 H, CH_2, J = 7.2 Hz), 4.07-4.14 (m, 2 H, CH_2), 6.20 (d, 1 H, CH, J = 2.6 Hz), 6.23 (d, 1 H, CH, J = 2.6 Hz), 6.30-6.37 (m, 4 H, CH), 7.01-7.04 (m, 1 H, CH), 7.35-7.40 (m, 2 H, CH), 7.81-7.84 (m, 1 H, CH), 8.07 (br s, 2 H, NH_2); ^{13}C NMR: 12.58 (CH_3), 14.01 (CH_3), 34.87 (CH_2), 37.00 (CH_2), 44.31 (CH_2), 49.13 (CH_2), 49.59 (CH_2), 49.92 (CH_2), 50.79 (CH_2), 51.33 (CH_2), 52.35 (CH_2), 55.62 (CH_2), 60.35 (CH_2), 60.91 (CH_2), 64.93 (CH_2), 97.51 (CH), 105.50 (CH), 108.10 (CH), 122.69 (CH), 123.77 (C_q), 128.12 (CH), 129.06 (CH), 131.45 (CH), 132.33 (C_q), 148.80 (C_q), 152.95 (C_q), 153.46 (C_q), 167.61 (CO), 171.35 (CO), 171.89 (CO).

*4.2.2.32 Attachment of 5'-COOH-nucleosides to **170***

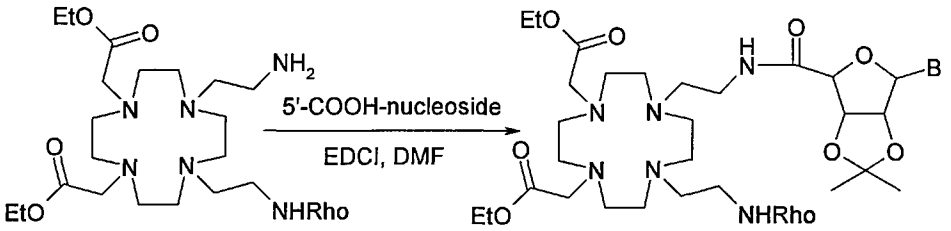

170 **171a-b**

170 (0.86 g, 1.0 mmol) was dissolved in DMF (7 mL), and a solution of the 5'-carboxylic nucleotide (1.1 mmol, 1.1 eq) and EDCI (0.23 g, 1.2 mmol, 1.2 eq) was added. The reaction mixture was stirred at room temperature for 24 hours. The DMF was removed at reduced pressure and the sample was dissolved in a mixture of DCM and water (40 mL each). The phases were separated and the

aqueous phase was extracted with DCM (2·40 mL). The combined organic phases were washed with water (2·25 mL), dried over $MgSO_4$, filtered, and concentrated to 3 mL. Purification of the sample by silica column chromatography (DCM / $^{i}PrNH_2$, 0-20%) gave the products **171a** and **171b**.

171a (B = U): Yield: 48% (0.54 g); MS: 1140 $[M+H]^+$; ^1H NMR (δ, $CDCl_3$): 1.07-1.21 (m, 18 H, 6 CH_3), 1.25 (s, 3 H, OCH_3), 1.48 (s, 3 H, OCH_3), 1.87-3.31 (m, 39 H, CH + CH_2), 4.01-4.10 (m, 5 H, CH + CH_2), 4.55 (br s, 1 H, NH), 5.63 (d, 2 H, 2 CH, J = 8.1 Hz), 6.18-6.23 (m, 2 H, CH), 6.30-6.35 (m, 3 H, CH), 7.02-7.05 (m, 1 H, CH), 7.38-7.41 (m, 2 H, CH), 78.2-7.85 (m, 1 H, CH); ^{13}C NMR: 12.60 (CH_3), 14.20 (CH_3), 24.52 (OCH_3), 26.96 (OCH_3), 33.52 (CH_2), 44.35 (CH_2), 45.25 (CH_2), 50.66 (CH_2), 50.74 (CH_2), 51.91 (CH_2), 52.48 (CH_2), 52.17 (CH_2), 60.48 (CH_2), 77.93 (CH), 84.21 (CH), 89.70 (CH), 97.61 (CH), 102.67 (CH), 108.09 (CH), 109.86 (CH), 122.79 (CH), 123.86 (C_q), 125.49 (C_q), 128.94 (CH), 129.05 (C_q), 132.48 (C_q), 132.92 (C_q), 148.85 (C_q), 153.48 (CO), 171.31 (CO), 173.66 (CO).

171b (B = A): Yield: 40% (0.46 g); MS: 1163 $[M+H]^+$; ^1H NMR (δ, $CDCl_3$): 1.06-1.22 (m, 18 H, 6 CH_3), 1.30 (s, 3 H, OCH_3), 1.52 (s, 3 H, OCH_3), 1.87-3.29 (m, 39 H, CH + CH_2), 4.01-4.10 (m, 5 H, CH + CH_2), 5.89 (br s, 2 H, NH_2), 6.17-6.22 (m, 2 H, CH), 6.29-6.37 (m, 3 H, CH), 7.01-7.04 (m, 1 H, CH), 7.36-7.39 (m, 2 H, CH), 7.80-7.83 (m, 1 H, CH), 8.06 (s, 1 H, CH), 8.22 (s, 1 H, CH); ^{13}C NMR: 12.59 (CH_3), 14.24 (CH_3), 14.30 (CH_3), 25.11 (OCH_3), 26.83 (OCH_3), 44.33 (CH_2), 45.24 (CH_2), 51.54 (CH_2), 52.09 (CH_2), 55.23 (CH_2), 55.34 (CH_2), 60.03 (CH_2), 60.11 (CH_2), 64.87 (CH_2), 83.70 (CH), 84.33 (CH), 87.07 (CH), 91.51 (CH), 97.62 (CH), 97.71 (CH), 105.61 (CH), 108.01 (CH), 113.72 (CH), 119.75 (C_q), 122.60 (CH), 123.80 (CH), 128.04 (CH), 128.97 (CH), 129.14 (C_q), 132.21

(C_q), 140.34 (C_q), 148.74 (CH), 149.49 (C_q), 153.08 (C_q), 153.43 (C_q), 155.50 (C_q), 167.43 (CO), 168.60 (CO), 171.48 (CO), 171.59 (CO).

*4.2.2.33 Complexation of neodymium with **171a** and **171b***

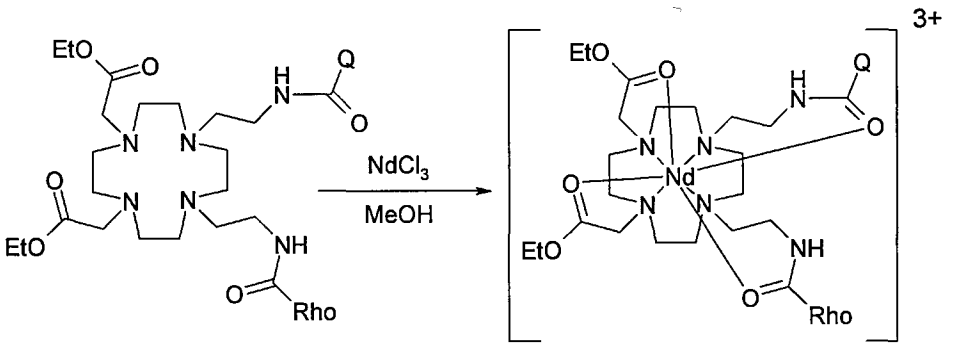

171a-b **172a-b**

171a and **171b** (75 mg and 80 mg, 0.066 mmol and 0.069 mmol) were dissolved in HPLC-grade methanol (0.5 mL), anhydrous neodymium chloride (15.7 mg and 16.4 mg, 0.95 eq) was added, and the solution was refluxed under argon overnight. The reaction mixture was allowed to cool back to room temperature and was poured into cold diethyl ether (20 mL). The mixture was centrifuged and the ether was poured off the white precipitate. The solid was suspended in 5 mL of ether, and centrifuged again. The ether was poured off again, the residue dissolved in distilled water (3 mL), filtered through a plug of cotton wool and the sample was freeze-dried. The complexes were obtained as pink solids. The purity of the samples were checked by TLC (alumina plates, DCM / MeOH).

172a (Q = uridine): Yield: 82% (62.5 mg); MS: 1183 [Ligand – Both ethyl esters+H]$^+$, 1111 unassigned; ^{1}H NMR (δ, CD_3OD): 0.82-0.88 (m), 1.07-1.09 (m), 1.19 (br s), 1.42 (br s), 1.07-1.59 (m), 2.56-3.61 (m), 3.04 (s), 4.11-4.13 (m), 5.08 (br s), 5.18 (br s), 5.61 (br s), 6.32-6.37 (m), 7.00 (br s), 7.48-7.81 (m).

172b (Q = adenosine): Yield: 58% (49.5 mg); MS: 630 $[M]^{2+}$, 1261 $[M]^{+}$, 1135 [Ligand – Both ethyl esters+H]$^{+}$; ^{1}H NMR (δ, CD_3OD): 1.13-1.19 (m, 12 CH_3, Rhodamine ethyl), 1.40 (s, 3 H, OCH_3), 1.58 (s, 3 H, OCH_3), 2.15 (s, 2 H, CH_2), 2.41-2.96 (m, CH_2), 3.35-3.40 (m, CH_2), 3.67 (s), 3.69 (s), 4.70 (br s), 5.45-5.47 (m), 5.61 (m), 6.36-6.45 (m), 7.10-7.12 (m), 7.56-7.60 (m), 7.88-7.90 (m), 8.17 (m), 8.25 (m).

*4.2.2.34 Complexation of ytterbium with **171a** and **171b***

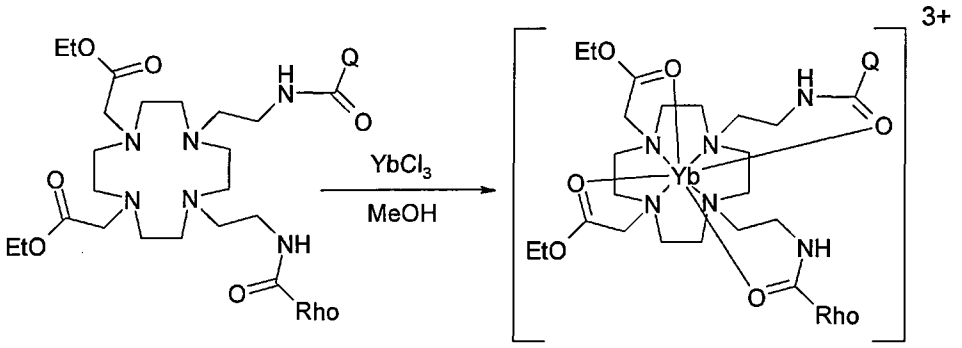

171a-b **173a-b**

171a and **171b** (75 mg and 80 mg, 0.066 mmol and 0.069 mmol) were dissolved in HPLC-grade methanol (0.5 mL), anhydrous ytterbium chloride (17.5 mg and 18.3 mg, 0.95 eq) was added, and the solution was refluxed under argon overnight. The reaction mixture was allowed to cool back to room temperature and was poured into cold diethyl ether (20 mL). The mixture was centrifuged and the ether was poured off the white precipitate. The solid was suspended in 5 mL of ether, and centrifuged again. The ether was poured off again, the residue dissolved in distilled water (3 mL), filtered through a plug of cotton wool and the sample was freeze-dried. The complexes were obtained as white solids in 30-50% yields. The purity of the samples were checked by TLC (alumina plates, DCM / MeOH).

173a (Q = uridine): MS: 1183 [Ligand – Both ethyl esters+H]$^{+}$, 1111 unassigned; 879 [M+M]$^{3+}$; ^{1}H NMR (δ, CD_3OD): 1.14 (br s, Rhodamine ethyl CH_3), 1.39 (br s, OCH_3), 1.57 (br s, OCH_3), 2.67-3.36 (m, cyclen), 3.69 (br s, Rhodamine, ethyl CH_2), 5.46 (br s), 5.61 (br s), 6.36 (br s), 6.42 (br s), 7.06 (br s), 7.58 (br s), 7.95 (br s), 8.17 (br s), 8.26 (br s).

173b (Q = adenosine): MS: 1135 [Ligand – Both ethyl esters+H]$^{+}$; ^{1}H NMR (δ, CD_3OD): 1.07-1.16 (m), 1.25 (s), 1.42 (s), 2.55-3.60 (m), 4.05 (br s), 4.48 (br s), 5.10 (br s), 5.16 (br s), 5.62 (br s), 6.32-6.37 (m), 7.00 (m), 7.47 (m), 7.61 (m), 7.77 (m).

5 RESULTS AND DISCUSSION

5.1 Synthesis of the coumarin 343 acceptor-containing triads

5.1.1 Functionalising the 4-amino-3-hydroxybutyric acid

5.1.1.1 Amide bond formation between the coumarin 2 donor and the carboxylic acid of the scaffold molecule

The first target triad consisted of a coumarin 2 donor, a coumarin 343 acceptor and a uridine quencher. The three functional units would be held together by a 4-amino-3-hydroxybutyric acid scaffold (*Figure 17*).

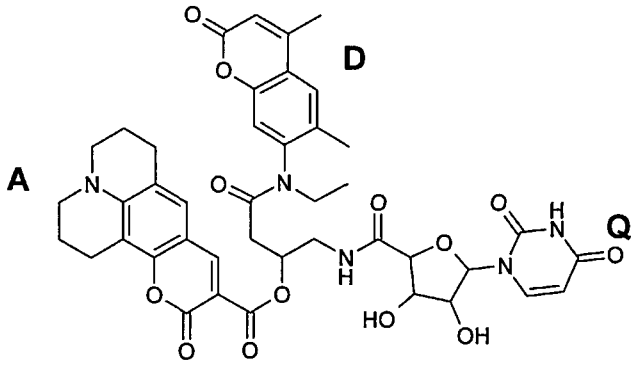

*Figure 17. The first target molecule (**50**), consisting of coumarin 2 donor, coumarin 343 acceptor and uridine quencher, held together by 4-amino-3-hydroxybutyric acid.*

The proposed reaction route to the synthesis of **50** is shown in *Scheme 2*. Coumarin 2 is attached to the carboxylic acid *via* an amide bond through its amino group. Coumarin 343 esterifies the 3-hydroxyl group of the scaffold, while uridine is oxidised to its 5'-carboxylic acid derivative, and coupled to the 4-amino group of the HBA.

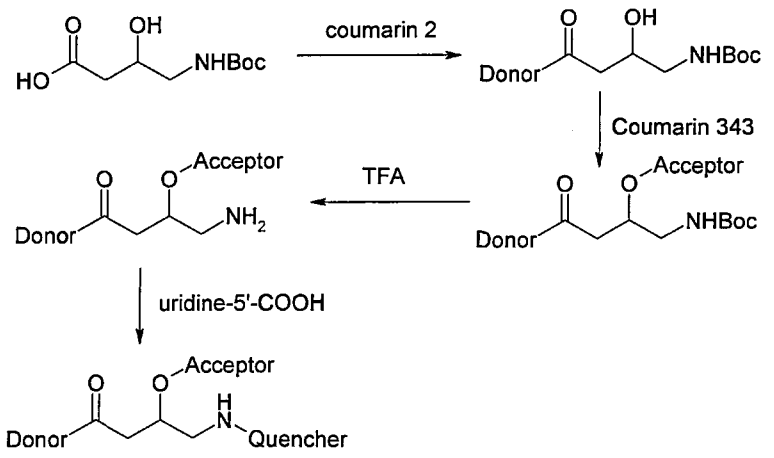

*Scheme 2. Synthetic route to **50**.*

Our initial attempts were directed at the formation of a peptide bond between the secondary amino group of coumarin 2 and the carboxylic acid function of the 4-amino-3-hydroxybutyric acid. Test reactions were carried out using N-methylaniline as a model compound for coumarin 2. Like coumarin 2, NMA is an aromatic secondary amine. Its main advantage is its easy availability and low price.

The amino group of the HBA was protected by reaction with Boc carbonate under standard conditions used in peptide chemistry.[81] The desired N-protected product was isolated in high yield and purity, and was reacted with NMA in the presence of EDCI coupling reagent (*Scheme 3*).

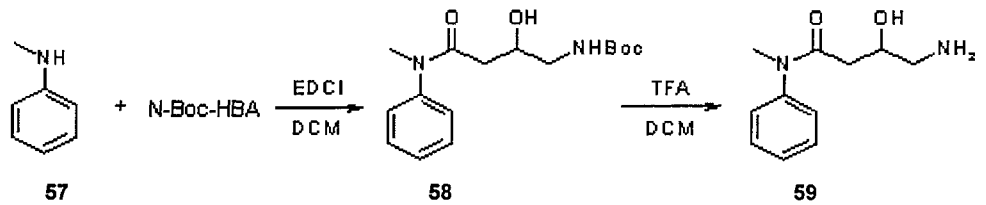

Scheme 3. Test reaction between N-methylaniline and N-Boc-hydroxybutyric acid, followed by removal of the Boc protection.

The expected product was formed in moderate yields under mild conditions and was isolated by means of silica column chromatography. Removal of the Boc

protecting group by TFA in DCM proceeded smoothly and gave the unprotected amine in quantitative yields.

In the reaction between the N-Boc-HBA and coumarin 2 under the same conditions no product formation was observed.

When reactions were allowed to proceed for several days, on TLC the formation of several highly fluorescent compounds was seen. Attempts at isolating these showed that they were present in < 1% each, and due to the small amounts NMR-analysis could not be performed. Mass spectrometric analysis suggested, that loss of the N-ethyl substituent could have happened. There are also examples in the literature for the photodimerization and subsequent cleavage for coumarin derivatives.[82]

Therefore it is possible that the observed compounds were various coumarin 2 dimers and cleavage products. Unfortunately the ES-MS system routinely produces cluster ions of two or three molecules, and it could not be determined, whether the 434 M / z peak corresponding to 2·MW(coumarin 2) was a dimer or an aggregate. The formation of the new fluorescent compounds could be efficiently suppressed when reactions were conducted in the dark, and exposure to light was reduced during the work-up and purification steps, which further supports the proposal that the side-products were formed by photodimerization.

As coumarin 2 did not react at room temperature in dichloromethane in the presence of EDCI, a range of reaction conditions were explored (*Table 1*). As reaction rates are strongly dependent on the stabilities of the transition state, solvents of different polarities and boiling points were tried, to facilitate the formation of the transition complex. A range of solvents and solvent mixtures

were explored to enhance the solubility of the protected amino acid. Dichloromethane was replaced by high boiling point solvents, which enabled the increase of the reaction temperature.

Reactant	Coupling agent	Solvent	T	*t*	Yield (%)
N-Boc-AA	EDCI	DCM	25°C	3 days	0
N-Boc-AA	DCC	THF	25°C	3 days	0
N-Boc-AA	DCC	ACN	25°C	3 days	0
N-Boc-AA	EDCI	DMF	25°C	3 days	0
N-Boc-AA	EDCI	DMSO	25°C	3 days	0
N-Boc-AA	EDCI	Water/DCM	25°C	3 days	0
N-Boc-AA	EDCI	Water/DMF	25°C	3 days	0
N-Boc-AA	EDCI	DCM	Reflux	3 days	0
N-Boc-AA	DCC	DMF	40°C	3 days	0
N-Boc-AA	EDCI	DMSO	60°C	3 days	0
N-Boc-AA	EDCI	THF	Reflux	3 days	0
N-Boc-AA	EDCI	ACN	Reflux	3 days	0
N-Boc-AA	DCC/HOBt	THF	25°C	2 days	0
N-Boc-AA	EDCI/HOBt	THF	25°C	2 days	0
N-Boc-AA-OPFP	-	DCM	25°C	1 day	0
N-Boc-AA chloride	-	DCM	25°C	1 day	0

Table 1. Test reactions for the peptide bond formation between the amino group of coumarin 2 and the carboxylic acid function of the N-Boc-protected HBA-derivatives.

The lack of reaction in all cases suggests that the coumarin 2 has a very low reactivity. The non-bonding pair of the amino group will be delocalised and in conjugation with the coumarin aromatic system. The carbonyl group has an electron-withdrawing effect not present in the NMA, making the non-bonding pair less available. Although the N-ethyl substituent of the coumarin 2 is not

expected to cause a much more significant steric hindrance than the N-methyl group of NMA, it probably contributes to the slowing down of the reaction.

Although the reaction was attempted in a range of solvents, in neither case was product formation seen. As in more polar solvents the transition state would be more stable, and this would help advance the reaction, and no such advancement was observed, it is possible that the coupling stops at the activated ester stage. This supports the theory that it is the lack of reactivity of the coumarin 2 that forbids the product formation.

5.1.1.2 Protection of the 3-hydroxyl of HBA

Mass spectrometric analysis of the reaction mixtures of the coupling reactions between N-Boc-HBA and coumarin 2 showed M / z peaks at 619. This is equivalent to the M / z of the product of the esterification reaction between three N-Boc-HBA molecules. Two water molecules have been eliminated, as indicated by the weigth loss of 36 from the 657, which 3·M(N-Boc-HBA). This suggested a side reaction occurring between the secondary hydroxyl group of the HBA and the carboxylic acid of another HBA molecule. Further evidence came from the NMR spectra of the samples, where the signals of the hydrogens of the secondary and tertiary carbons became indistinguishable from each other, resulting in a series of overlapping, broad multiplets. In the proton NMR spectrum of the pure N-Boc-HBA the hydrogens are well separated and it is even possible to distinguish between the two C^3H_2-signals.

To eliminate the esterification reaction protection of the hydroxyl group was attempted. Surprisingly, applications of standard and widely used methods gave the O-protected products in poor yields. Attempts at acetylating the hydroxyl

functionality with acetic anhydride / pyridine produced the O-acetyl derivative (**174**) in approximately 20-30% yields (*Scheme 4*). Furthermore, significant losses in the Boc protection occurred during the acidic workup.

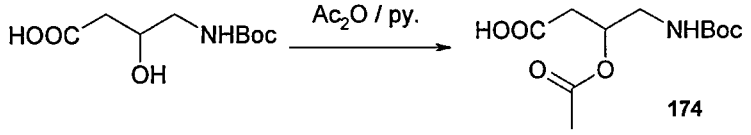

Scheme 4. Acetylation of the 3-hydroxyl group of N-Boc-HBA with acetic anhydyde / pyridine.

When the N-Boc HBA was reacted with two equivalents of sodium hydride followed by benzyl bromide in DMF, only traces of the O-benzyl (**175**) derivative were isolated (*Scheme 5*).

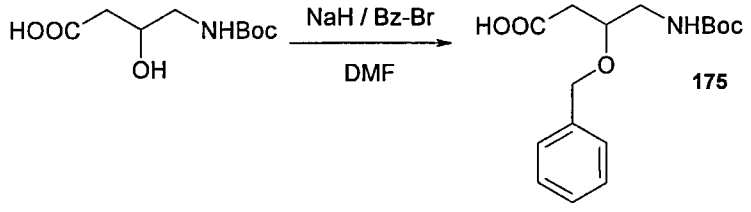

Scheme 5. Alkylation of the 3-hydroxyl group with benzyl bromide.

As the O-acetylation route seemed promising, and a large part of the losses were due to the cleavage of the Boc during the work-up, an acid-resistant N-protecting group was introduced instead of the Boc protection. The N-Fmoc HBA derivative was synthesised by the reaction of the HBA and Fmoc-chloroformate in a mixture of 10% potassium hydrogencarbonate and dioxan. O-actylation in acetic anhydryde / pyridine provided the N-Fmoc-O-Acetyl HBA derivative in ~40% yield. Separation of the product from the unreacted starting material proved inefficient and time-consuming and reduced the yields significantly.

Both N-Fmoc-HBA and N-Fmoc-O-acetyl-HBA were reacted with coumarin 2. Various coupling reagents were tested, but neither using DCC, nor the similar, but water-soluble EDCI, nor the more potent PyBop resulted in product formation. The usually harsher carboxylic acid-activation methods, such as acid chloride formation, *in situ* and isolated hydroxysuccinimide activated esters were also unsuccessful. In order to be able to increase the concentration of the reagents and conduct the reactions at higher temperatures, the coupling reaction was attempted in several solvents and solvent mixtures, as shown in *Table 2*. In neither reaction was formation of the product observed.

Reactant	Coupling agent	Solvent	T	*t*	Yield (%)
N-Fmoc-O-Ac-AA	EDCI	DCM	25 °C	1 week	0
N-Fmoc-O-Ac-AA	EDCI/HOBt	DCM	25 °C	1 week	0
N-Fmoc-O-Ac-AA	*	DCM	25 °C	3 days	0
N-Fmoc-O-Ac-AA	*	THF	Reflux	3 days	0
N-Fmoc-O-Ac-AA	N-HOSu	DCM	25 °C	1 week	0
N-Fmoc-O-Ac-AA	N-HOSu	THF	Reflux	1 week	0

*Table 2. Tested condition for the peptide bond formation reaction between coumarin 2 and N-Fmoc- and O-acetyl protected HBA. * acid chloride formation*

The lack of reaction between either of the HBA-derivatives and coumarin 2 indicates that the poor nucleophilicity of coumarin 2 is a major problem. In addition to this, the low yields for the O-protecting reactions for the N-protected HBA suggests that the position of the carboxylic acid and the hydroxyl group of the HBA is hindering the reactions involving the COOH group. As the OH and COO^- moieties can form a six-membered ring (*Figure 18*) via hydrogen bonds, it is likely that the stability of that ring is reducing the reactivity of the carboxylic acid.

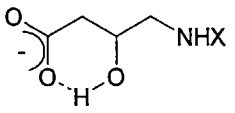

Figure 18. Possible structure of the HBA. X = Fmoc of Boc

To further investigate this hypothesis, other organic acids were brought into peptide bond formation reactions with coumarin 2.

5.1.2 Amide bond formation between coumarin 2 and haloacetic acids

Results of the peptide coupling reactions suggested that coumarin 2 has a very low nucelophilicity. Curious to find out if it is possible to engage the amino group of coumarin 2 in amide bond formation, coumarin 2 was reacted with chloroacetic acid in DCM in the presence of EDCI coupling reagent at room temperature (*Scheme 6*).

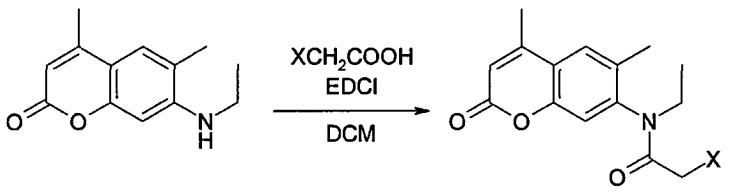

Scheme 6. Coupling coumarin 2 to chloracetic acid (X = Cl) or bromoacetic acid (X = Br).

When fourfold excess of acid and coupling reagent were used, the coumarin 2 chloroacetate was isolated in 60-70% yield after 3 days. Replacement of chloroacetic acid with bromoacetic acid brought the reaction to completion overnight under the same conditions. The coumarin 2 chloroacetate and bromomoacetate found use during the synthesis of the cyclen-based ligands (**150a-b** and **161**, described later in this thesis). The reactions between NMA or coumarin 2 and chloro- or bromoacetic acid are summarised in *Table 3*.

Amine	X	Coupling agent	Solvent	T	*t*	Yield (%)
NMA	Cl	EDCI	DCM	25°C	3 days	79
Coumarin 2	Cl	DCC	AcN	25°C	3 days	64
Coumarin 2	Cl	EDCI	THF	25°C	5 days	88
Coumarin 2	Cl	EDCI	DCM	25°C	3 days	86
Coumarin 120	Cl	EDCI	DCM	25°C	overnight	60
Coumarin 120	Br	EDCI	DCM	25°C	overnight	75
Coumarin 2	Br	EDCI	DCM	25°C	overnight	>98

Table 3. Reactions of XCH_2COOH with coumarin 2, coumarin 120 and NMA. X = Cl or Br.

Attempts to alkylate either the secondary oxygen in the N-Boc-HBA, or the primary amino group in the unprotected HBA with coumarin chloroacetate resulted in the complete decomposition of the alkylating agent to coumarin 2 within a short time. The same result was obtained in a range of solvents such as acetonitrile, ethanol, or DMF, and in the presence of both potassium carbonate and TEA bases. Sodium iodide was not necessary for the reaction to occur, therefore halogen exchange is not a key step in the mechanism.

5.1.3 Alkylation of the secondary amine of coumarin 2

In order to overcome the difficulties associated with amide bond formation in this case, alternative means were sought to functionalise coumarin 2.

There are examples available in the literature of alkylation of coumarin 2 on the amino group with benzyl-bromide-type reagents in acetonitrile.[83] Reaction of coumarin 2 with ethyl bromoacetate in acetonitrile in the presence of potassium carbonate and sodium iodide gave small amounts of the alkylated derivative,

but the reaction was difficult to reproduce. No reaction occured between coumarin 2 and N-Boc-bromoethylamine under similar conditions.

Attempts to alkylate coumarin 2 with N-Boc-ethanolamine in a Mitsunobu reaction[84,85] to introduce a masked primary amine functionality were unsuccessful under various conditions (*Table 4*).

Amine	Reagent	Solvent	T	Amine : alcohol : TPP : DEAD	Yield (%)
NMA	DEAD	THF	25 °C	1:1:1:1	0
NMA	DEAD	THF	Reflux	1:1:1:1	0
NMA	DEAD	dioxan	Reflux	1:1:1:1	0
NMA	DEAD	THF	Reflux	1:2:2:2	6
NMA	DEAD	dioxan	Reflux	1:2:2:2	9
NMA*	DEAD	dioxan	Reflux	1:2:2:2	~2
Coumarin 2	DIAD	THF	Reflux	1:1:1:1	0
Coumarin 2	DEAD	THF	Reflux	1:2:2:2	0
Coumarin 2	DEAD	dioxan	Reflux	1:1:1:1	0
Coumarin 2	DEAD	dioxan	Reflux	1:2:2:2	0

*Table 4. Mitsunobu reactions of NMA or C2 with N-Boc-ethanolamine. * Alcohol: N-Boc-HBA.*

Neither replacement of the DEAD with DIAD, nor changing of the THF to dioxane, nor increasing the reaction temperature resulted in product formation. Varying the ratio of the reagents did not help product formation either. If the NMA test compound was used instead of coumarin 2, small amounts of alkylated product were isolated, albeit rather forcing conditions were needed, such as large excess of reagents and refluxing dioxane. Also, long reaction times were necessary, whereas the Mitsunobu reaction on primary aliphatic amines usually proceeds swiftly, and affords the product in a matter of hours. Alkylation of NMA with N-Boc-HBA in a Mitsunobu reaction through the

secondary hydroxyl group of the HBA was successful, but afforded the product in very low yields. (~2%)

5.1.4 Attachment of the donor through a glycine linker

To suppress the side-reaction between the secondary hydroxyl group of HBA and its carboxylic acid, coumarin 2 was reacted with N-Boc glycine first. Glycine has only a COOH group and no side reactions were possible. It was expected that the primary amino group of the glycine would afterwards react with the carboxylic acid of the HBA. The glycine would become a linker in the final product. Peptide bond formation between a primary aliphatic amine and a carboxylic acid is usually much faster than esterification of the COOH with a secondary hydroxyl group, so introduction of the glycine would reduce the significance of the self-esterificaion.

Unfortunately the desired product was obtained in ~15% yield after a week-long reaction in the presence of excess N-Boc glycine and EDCI (*Scheme 7*).

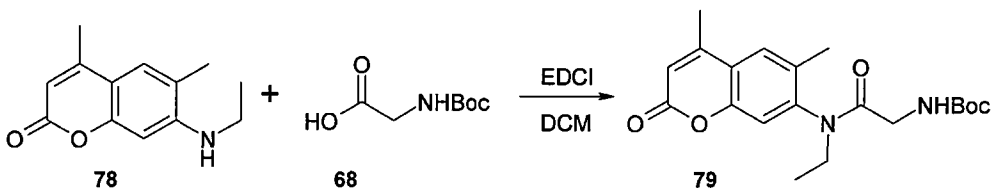

Scheme 7. Amide bond formation between coumarin 2 and N-Boc glycine.

The low yield of the peptide bond formation reation between coumarin 2 and glycine has proved that the major obstacle is the poor nucleophilicity of the coumarin 2. Therefore other donors, with better reactivities were sought.

5.1.5 The coumarin 120 and coumarin 151 donors.

Replacement of coumarin 2 was required and two new donors were introduced. Both coumarin 120 and coumarin 151 are primary amines, and were thought to be more reactive than coumarin 2. Both have excitation and emission wavelengths close to those of coumarin 2, therefore RET between the new donors and the coumarin 343 acceptor is possible (*Table 5*).

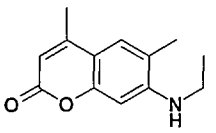

coumarin 2

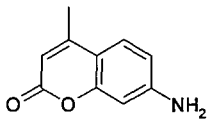

coumarin 120

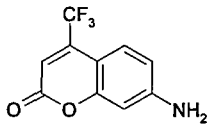

coumarin 151

	coumarin 2	coumarin 120	coumarin 151
λ_{max} (absorption)	366 nm	343 nm	377 nm
ε	$2.1 \cdot 10^5$	$2.2 \cdot 10^5$	$2.1 \cdot 10^5$
λ_{max} (emission)	432 nm	433 nm	487 nm

Table 5. Photophysical properties of coumarin 2, coumarin 120[86] and coumarin 151.[87] Spectra were recorded in methanol, and the data are for underivatized compounds.

Neither coumarin 120, nor coumarin 151 reacted with HBA, but both formed amide bonds readily with N-Boc glycine, affording the corresponding products in high and moderate yields, respecitvely. The Boc protection of the glycine was removed in both cases by cleavage with 33% TFA in DCM, and the free amino groups were coupled to the carboxylic acid of N-Boc-HBA. Deprotection of the amino groups gave the donors attached to the HBA scaffold through a glycine linker. The products thus obtained were insoluble in most solvents, which prohibited further reactions, and coupling of coumarin 343 to the scaffold was unsuccessful (*Scheme 8*).

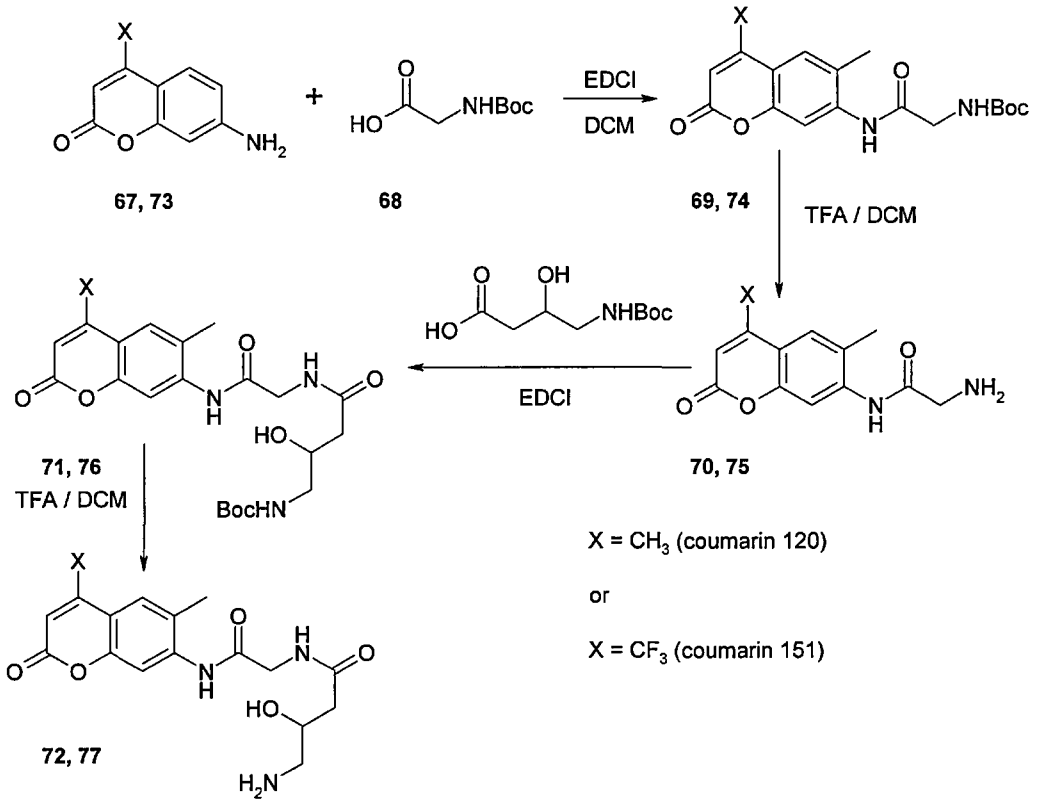

*Scheme 8. Attachment of coumarin 120 (**67**) and coumarin 151 (**73**) to the HBA scaffold molecule through a glycine linker.*

Another approach to the synthesis of the donor-acceptor diad held together by glycine-HBA involved coupling coumarin 343 to the free amino group of HBA ethyl ester (*Scheme 9*) followed by saponification of the ethyl ester using 1 M NaOH solution in methanol.

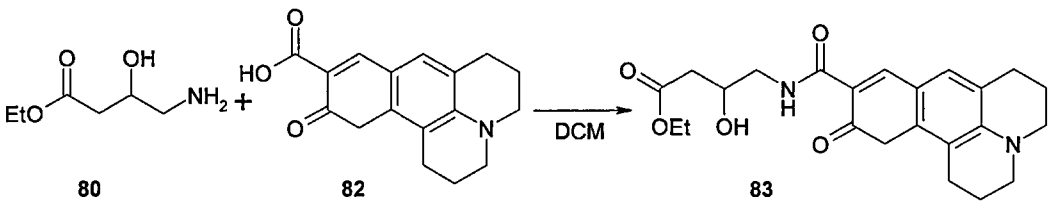

Scheme 9. Reaction of coumarin 343 with ethyl ester protected HBA.

Although the ester hydrolysis went to completion under mild conditions, isolation and purification of the free acid was problematic, as the product is water-

soluble, and attempts of its extraction into organic solvents were unsuccessful. Chromatography on either silica or alumina was hindered by its zwitterionic nature, and in particular its ionisable carboxylic acid functionality.

Reduced solubility of the donor-glycine-HBA and the acceptor-HBA was possibly due to the rigid structure of the HBA scaffold, which probably helped π-π stacking of the donors. Therefore replacement of the HBA with a more flexible 'backbone' was necessary. The commercially available N-Fmoc-γ-O-^{t}Butyl glutamic acid was chosen, as apart from a free carboxylic acid to which the donor could be coupled, a second carboxyl group and an amino group are present in orthogonally protected forms.

5.1.6 Synthesis of the organic triad held together by a glutamic acid scaffold

Coumarin 120 was reacted with N-Fmoc-γ-O-^{t}Butyl glutamic acid in DCM at room temperature in the presence of 10% excess of EDCI coupling reagent for two days. After acidic workup and silica column chromatography the product was isolated in high yields. The Fmoc protecting group was removed by cleavage with piperidine or diethyl amine, the latter being preferred for its lower boiling point and easier removal. α-Amino acids with free amino groups are known to undergo diketopiperazine formation, therefore it is essential to reduce the isolation and purification time to the minimum, and avoid high temperatures. Removal of the solvent and the nucleophile was followed by silica column chromatography to separate the free amine from the high boiling point solvent residues and the dibenzofulvene. The isolated product was reacted immediately with the coumarin 343 acceptor in DCM at room temperature in the presence of 10% excess of EDCI. After 24 hours the reaction was stopped. Removal of the

EDCI, the residual free amine and coumarin 343 by aqueous, acidic and basic washings respectively gave the donor-acceptor-scaffold product in > 95% purity. Analytically pure compound was obtained after subjecting the crude sample to silica column chromatography (*Scheme 10*).

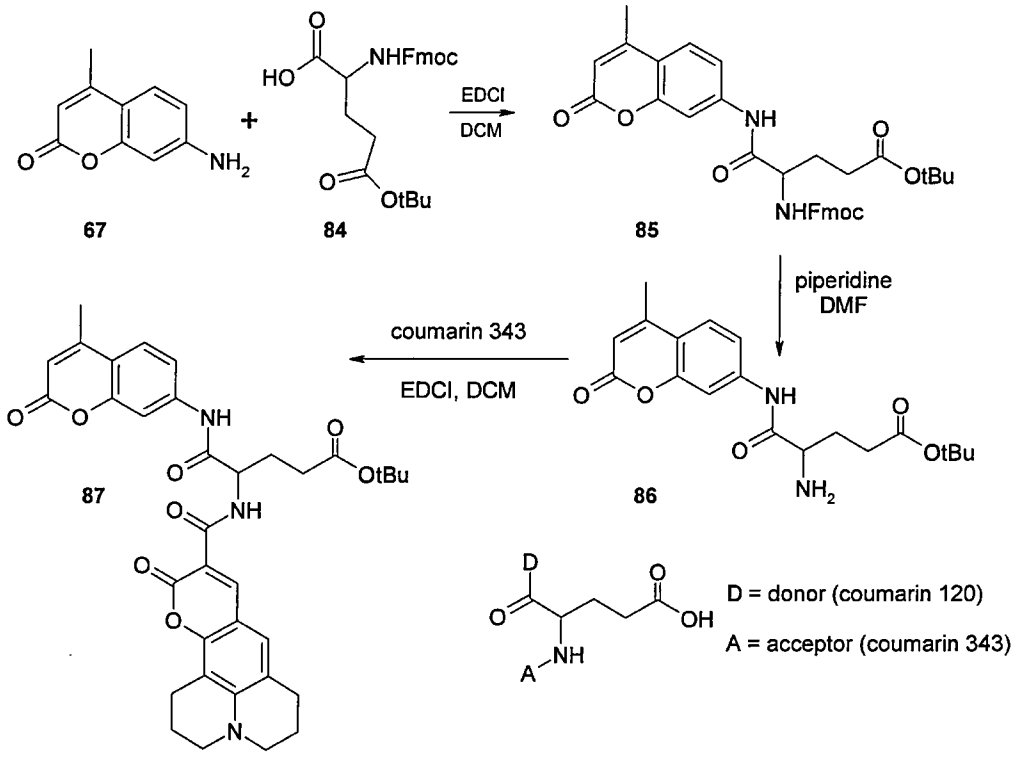

*Scheme 10. Synthesis of the organic diad **87**. The donor and the acceptor are attached to a tert-butyl ester protected glutamic acid backbone.*

Cleavage of the ^{t}Butyl ester with 50% TFA in DCM afforded the free acid in quantitative yields after evaporation of the solvents. This work-up afforded the free acid diad with the tertiary amino group of the coumarin 343 protonated. After neutralising the TFA salt with triethylamine, the carboxylic acid was reacted with the 5'-hydroxyl group of uridine. The esterification reaction proceeded smoothly and afforded the desired triad in the presence of EDCI and catalytic amount of DMAP. Although after aqueous workup TLC, mass spectrometry and NMR spectroscopy suggested almost complete

transformation of the reactants into the product, removal of the remaining starting materials via column chromatography was necessary. This resulted in the hydrolysis of the ester bond between the diad and the quencher. As the ester bond proved unstable under the chromatographic conditions, a more stable attachment method was sought. It is possible to transform the 5'-hydroxyl group of the nucleoside into an amino group, offering the possibility of an amide bond formation between the scaffold and the quencher. Therefore the nucleoside was transformed into the 5'-amino derivative.

5.1.7 Synthesis of the 5'-aminonucleosides

There are a number of routes available in the literature to the synthesis of 5'-aminonucleosides. The synthetic strategy presented below is based on known transformations of various other types of molecules. It utilises readily available chemicals, our target being a fast, effective route for the production of at least one 5'-aminonucleoside.

The 5'-hydroxyl group of the 2',3'-isopropylidene-protected nucleoside was activated *in situ* by methanesulphonyl chloride in the presence of three equivalents of triethylamine under argon atmosphere, and was replaced by an azido group derived from sodium azide. The 5'-azido nucleosides were purified by column chromatography. Reduction of the azido group was attempted initially in dry DCM with lithium aluminium hydride, but even at room temperature a mixture of decomposition products were formed.

The azides were successfully reduced in dry THF with triphenylphosphine to the corresponding P=N compounds, which were hydrolysed *in situ* by the addition of water (*Scheme 11*). After evaporation of the THF, the 5'-aminonucleosides

were dissolved in water, and the triphenylphosphine oxide was removed by washing with DCM. The products were isolated by evaporation of the water, and pure samples were obtained by trituration with diethyl ether. This method was applicable for the synthesis of 5'-aminouridine and 5'-aminoadenosine. Both 5'-azidocytidine and 5'-azidoguanosine were also synthesised, albeit in poor yields. Reduction of these compounds produced a mixture of compounds, among them substantial amounts of decomposed material.

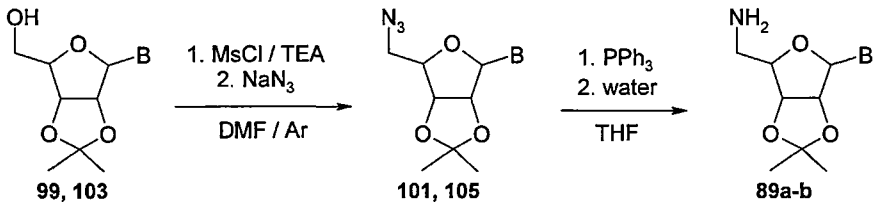

99, 103 **101, 105** **89a-b**

*Scheme 11. Synthesis of 5'-aminouridine (**89a**) (B = U) and 5'-aminoadenosine (**89b**) (B = A). Activation of the 5'-hydroxyl group of the 2',3'-protected ribose is followed by substitution with azide. The azide is reduced by a combination of triphenylphosphine and water.*

5.1.8 Synthesis of the triads

The 5'-aminonucleoside was coupled to the γ-carboxylic acid of the donor-acceptor diad in DCM with EDCI and the product was isolated after silica column chromatography in moderate yields (*Scheme 12*). The major product of the reaction was the cyclised compound **91** that presumably formed after activation of the carboxylic acid with EDCI. Its production was facilitated by the removal of the amide proton by the triethylamine, making it prone to an attack by the activated carboxylic acid. The molecule also contains a stable six-membered diamide ring. The triad with uridine quencher was isolated in 38% yield, while the one with adenosine quencher in 84% yield after silica column chromatography.

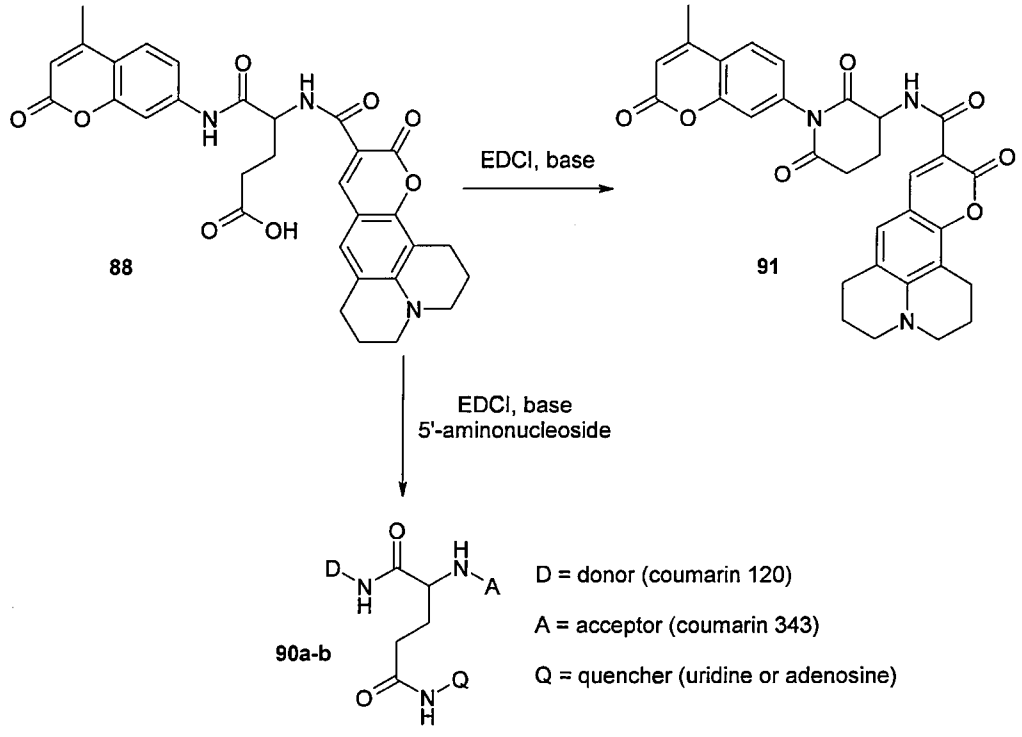

*Scheme 12. Synthesis of the coumarin 120-coumarin 343-uridne and coumarin 120-coumarin 343-adenosine triads (**90a-b**) from the corresponding diad.*

5.1.9 Coumarin 151 donor

Triads bearing coumarin 151 donors and uridine or adenosine quenchers were prepared in syntheses analogous to those of the coumarin 120-donor triads. The reaction between the diprotected glutamic acid and the coumarin 151 was slower and less efficient than in the case of the coumarin 120, due to the lower reactivity and poorer solubility of the coumarin 151. The corresponding diad was isolated in good yields, and removal of the ^{t}butyl ester was unproblematic (*Scheme 13*).

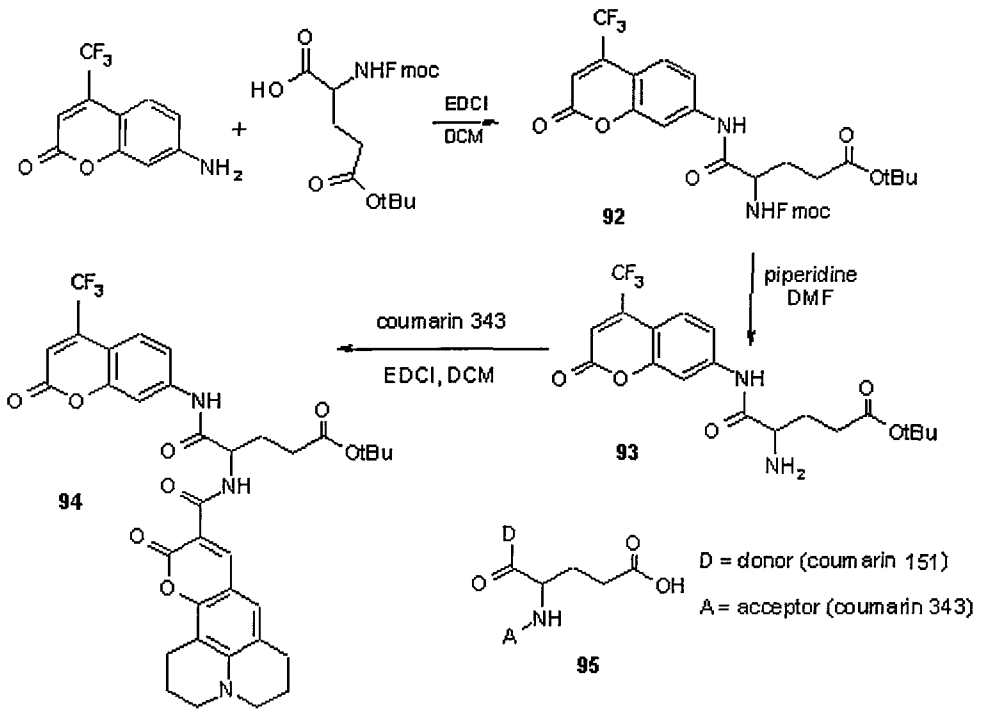

*Scheme 13. Synthesis of the organic diad **95**. The donor and the acceptor are attached to a tert-butyl ester protected glutamic acid backbone.*

The reaction between the free acid diad and the 5'-aminonucleosides produced almost uniquely the cyclised side-product. The target C151-C343-A and C151-C343-U triads (**96a-b**) were isolated in 15% and 6% yields, respectively (*Scheme 14*).

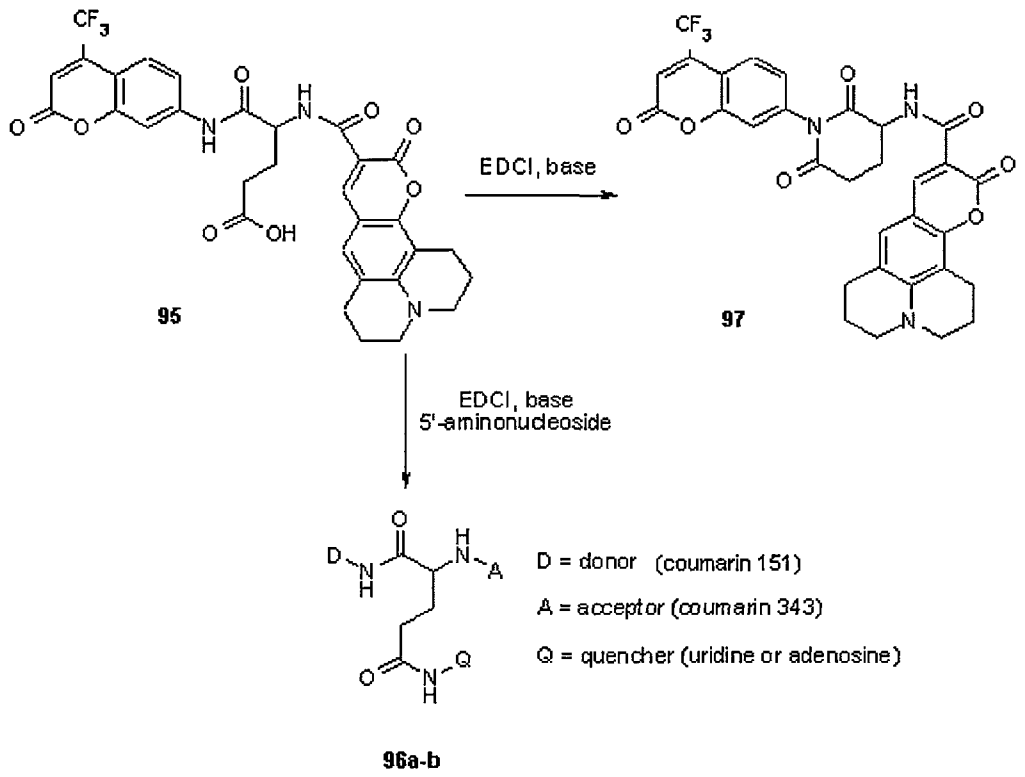

*Scheme 14. Synthesis of the coumarin 151-coumarin 343-uridne and coumarin 151-coumarin 343-adenosine triads (**96a-b**) from the corresponding diad.*

5.2 Characterisation of the organic triads

Measurements concerning the organic diads and triads were carried out in methanol, while those on the lanthanides were performed in water, buffered to pH 7.4 with MOPS. Adenosine was dissolved in DMSO and uridine in water. DNA was dissolved in pH 7.4 water. Sample concentrations were 0.3-1.0 mM, and absorptions were in the 0.2-0.5 AU range.

Our attempts to titrate organic diads and triads in aqueous solutions failed due to the low solubility of the compounds in pH 5.5 water and the quenching of the sample luminescence caused by the medium (*Figure 19*). The latter is probably due to a protonation of the coumarin 343 tertiary nitrogen. At pH 7.4 the solubility of the diads and triads was even lower, because of the lack of ionisation on the acceptor. Therefore in neutral or basic solutions measurements could not be carried out.

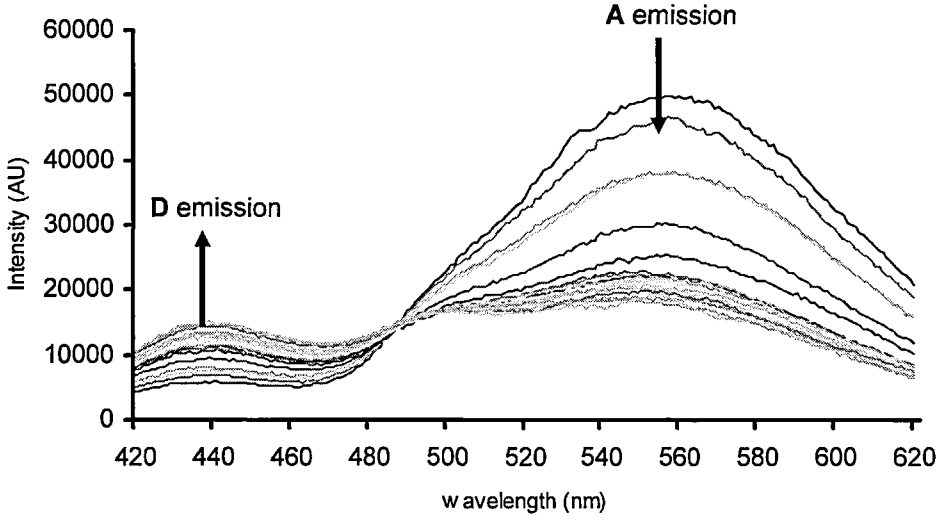

Figure 19. Changes in the emission spectrum of the c120-c343 diad in distilled water / DMSO upon the addition of uridine in DMSO. The maximum at 560 nm decreased, that at 440 nm increased during the titration.

In pH 5.5 water the emission spectrum had a maximum around 560 nm, which rapidly decreased in intensity during the measurement, independent of the amount of nucleoside present. The fluorescence quenching by the water is supported by NMR-measurements in d_6-DMSO / D_2O, where the chemical shifts and multiplicities of the aromatic C-H hydrogen signals remained unchanged. There was no sign of decomposition either in the ^1H or the ^{13}C spectrum. Protonation of the tertiary amino group of the coumarin 343 reduces the fluorescence quantum yield of the acceptor and also shifts the emission wavelength of the **A**, together with its absorption wavelength. This makes RET from the **D** less efficient, and the new peak, centred around 440 nm is likely to be the donor emission. As the amide-bound c120 and c151 have no easily protonable sites, their photophysical properties are unaffected by the medium. As RET becomes less efficient, emission from the donor becomes more and more pronounced.

Attempts at determining the donor lifetime by direct excitation of the donor and monitoring emission at 440 nm was not possible, as the donor emission intensity was not high enough in a mixture of DMSO and water. A lifetime of 3.63 ns was measured by detection at 475 nm, emission of the unprotonated acceptor, which is slightly longer than the 3.31 ns measured in methanol for the diad lifetime, although it is still within experimental error. The acceptor lifetime was 4.03 ns upon direct excitation (@ 440 nm, detection @ 540 nm), while excitation of the donor with emission from the acceptor yielded a lifetime of 4.11 ns. The increase of the acceptor lifetime might be due to the protonation of the amino group, which, when unprotonated could act as an electron donor in PET, and shorten τ. Similar measurements for the diad with c151 **D** could not be

carried out, as the emission wavelength for the c151 is at longer wavelengths, and is buried under the acceptor absorption band even in aqueous solutions.

5.2.1 Organic diads

The organic diads, having no quencher moiety in the molecule, could not be measured against the complementary base of the **Q**.

The organic diads were titrated in methanol with salmon testis DNA. The interaction between DNA and both diads was strong ($K > 10^4$). The binding constant could not be determined more accurately because of the inaccuracies caused by the low concentrations of the samples. In the case of the coumarin 120 – coumarin 343 diad, initially only inconsistent results were obtained, as neither quenching nor increase in the luminescence intensity was observed. If the samples were allowed at least 24 hours between preparation and measurement, the reproducibility of the results increased significantly. It is possible that the complete dissolution of the compounds is not instantaneous, despite the clear solutions obtained.

In the presence of DNA, the coumarin 120 – coumarin 343 diad (**87**) was 'turned on' (*Figure 20*).

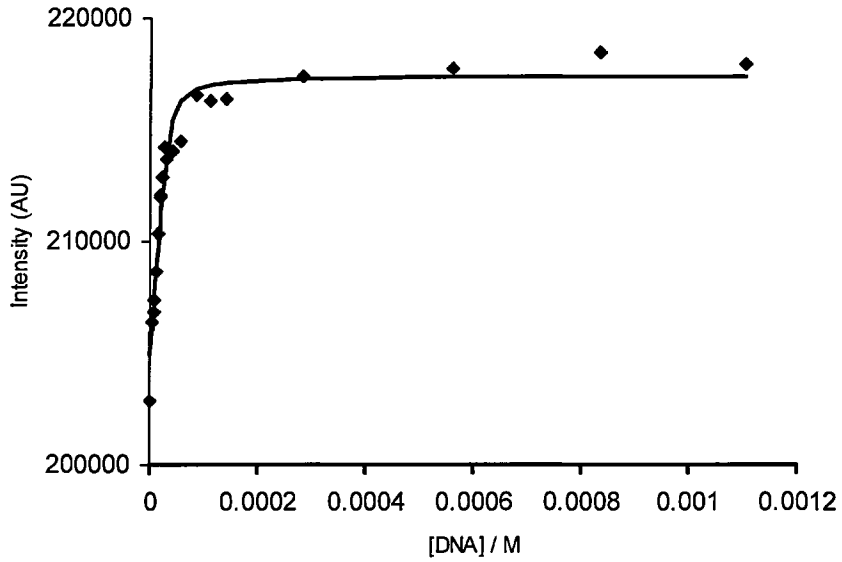

*Figure 20. Increase in the emission intensity of the coumarin 120-coumarin343 diad (**87**) in methanol, upon addition of double stranded DNA (dissolved in pH 7.4 water).*

The coumarin 151 – coumarin 343 diad (**94**) was quenched by DNA. In both cases the donor is possibly intercalating between the DNA base pairs, causing the effects. While the coumarin 120, substituted with a methyl group in the 4 position is an electron-donating moiety, the coumarin 151 is strongly electron-withdrawing. If the quenching of the donor by the DNA occurs through electron transfer, intercalation of the coumain 120 means that the excited state donor is in an electron-rich environment, and cannot be readily oxidised, and thus quenched. The oxidising coumain 151 on the other hand is placed in the electron-rich environment of the negatively charged phosphate backbone, and can be reduced easily. Thus in the case of coumarin 151 it is probably reductive electron transfer that quenches the fluorescence.

When comparing the excitation and emission spectra of the two diads, a striking difference between the fluorescence intensity is seen (*Figure 21 and Figure 22*).

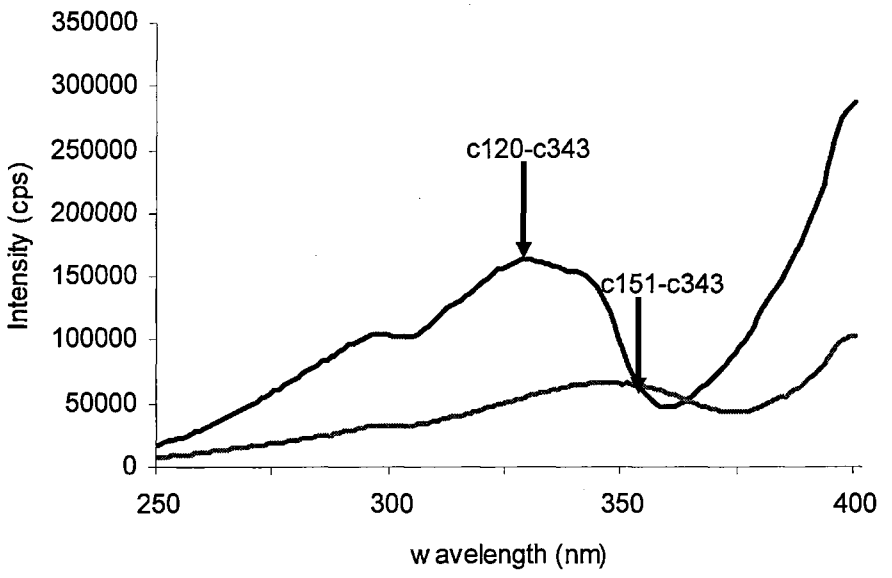

*Figure 21. Excitation spectra of the diads in methanol (emission detected @ 480 nm). Emission from the diad **87** is much more intense than emission form diad **94**.*

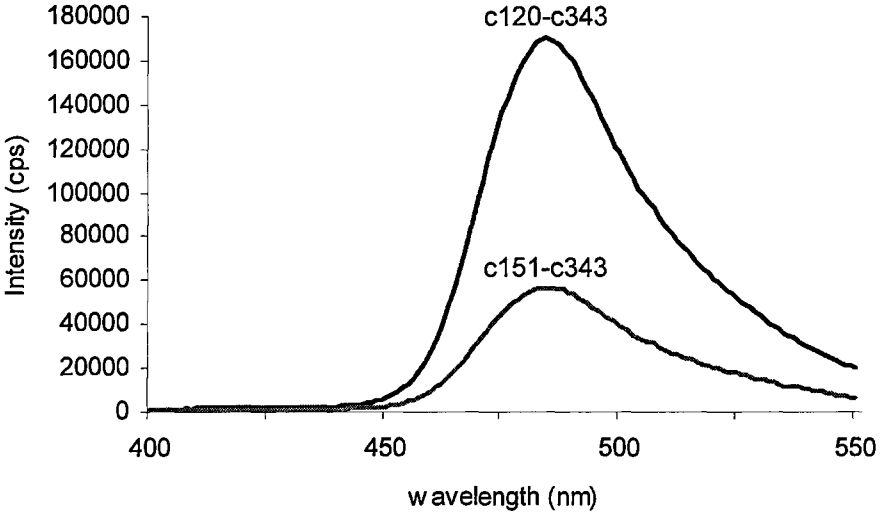

Figure 22. Emission spectra of the diads in methanol (excitation wavelength 328 nm).

The UV-Vis spectra of the organic diads and triads were recorded in methanol containing 3% DCM. The absorption spectra of the two compounds are very

similar, showing a strong absorption band with a maximum at 440 nm, due to the coumarin 343, and a smaller band at 336 nm (coumarin 151) or 326 nm (coumarin 150). The donor absorption bands are of similar intensities, and according to the data available in the literature, both compounds emit in the 430-450 nm range (*Figure 23*).

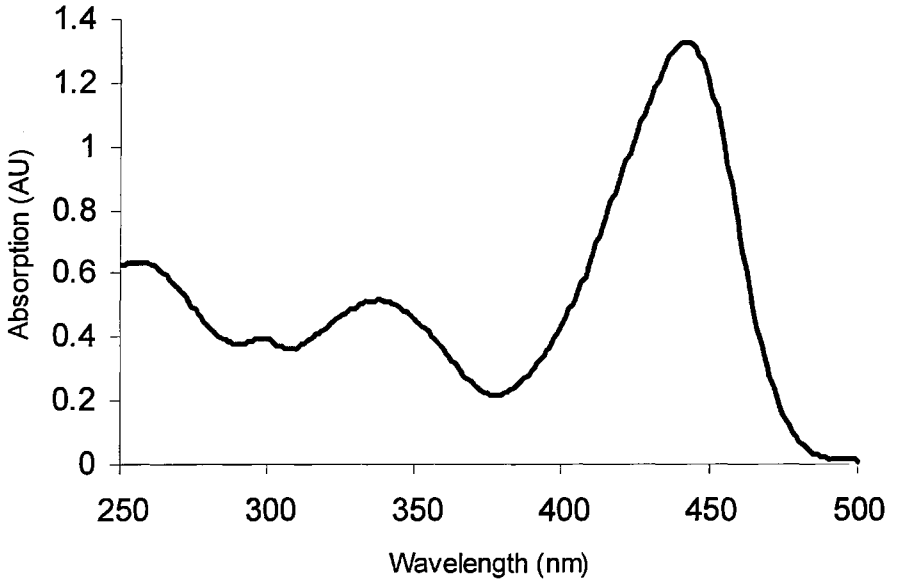

Figure 23. Absorption spectrum of the coumarin 151-coumarin 343-uridine triad in methanol (0.033 mM). The maximum at 340 nm corresponds to the donor absorption, the one at 440 nm is that of the acceptor. Similar spectra were obtained for the other organic diads and triads.

The UV-Visible spectroscopic properties of the organic diads and triads are summarised in *Table 6*. The absorption maxima and absorption coefficients for the nucleosides were similar to those found in the literature. Thus, both uridine and adenosine absorbed strongly at around 260 nm, with absorption coefficients in the 10^4 range. As excitation of the compounds was performed at wavelengths exceeding 300 nm, this is not a problem.

	c120-c343	c151-c343	c120-c343-U	c120-c343-A	c151-c343-U	c151-c343-A
$A_{max(D)}$	325 nm	334 nm	325 nm	325 nm	334 nm	334 nm
ε	$1.1 \cdot 10^4$	$1.2 \cdot 10^4$	$1.1 \cdot 10^4$	$1.1 \cdot 10^4$	$1.2 \cdot 10^4$	$1.2 \cdot 10^4$
$A_{max(A)}$	441 nm					
ε	$3.1 \cdot 10^4$					

Table 6. Absorption maxima and ε of the organic diads and triads.

The shifts in the absorption bands, compared to those of the free coumarins, to shorter wavelengths by 20-40 nm is due to the participation of the primary amino groups in the amide bonds of the diads. It is likely that the emission maximum of the coumarin 120 is exactly at the absorption maximum of the coumarin 343, or immediately below it, while that of the coumarin 151 is slightly over 440 nm. This could account for a difference in the efficiency of the resonance energy transfer between the donor and the acceptor, and the resulting variations in the donor fluorescence (*Figure 24a and 24b*).

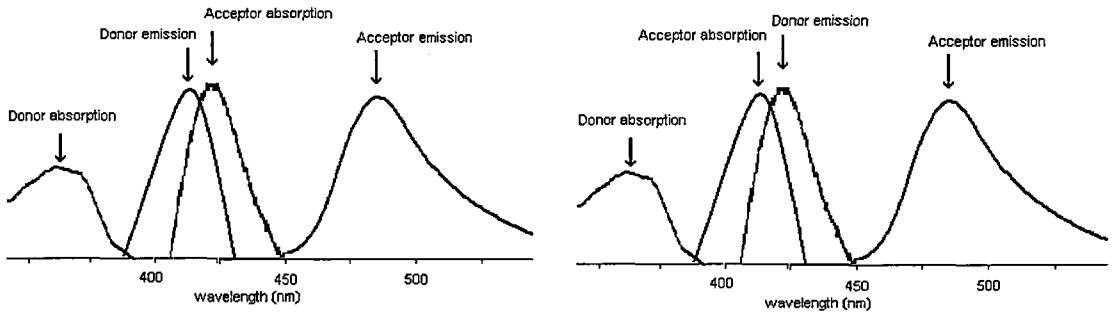

Figure 24a and b. Possible explanation of the differences in the luminescence intensity of the diads with different donors. The emission maximum of coumarin 120 is below the absorption maximum of the acceptor, making the RET very efficient, while that of the coumarin 151 is possibly marginally over the c343 absorption, making RET difficult.

5.3 Organic triads and complementary bases

5.3.1 Coumarin 120 donor and uridine quencher

The fluorescence of the organic triad consisting of coumarin 120 donor, coumarin 343 acceptor and uridine quencher (**90a**) in methanol showed no changes when small quantities of the complementary base (adenosine) were added. At adenosine concentrations hugely exceeding the triad concentrations (50-100-fold), luminescence intensity decreased (*Figure 25*).

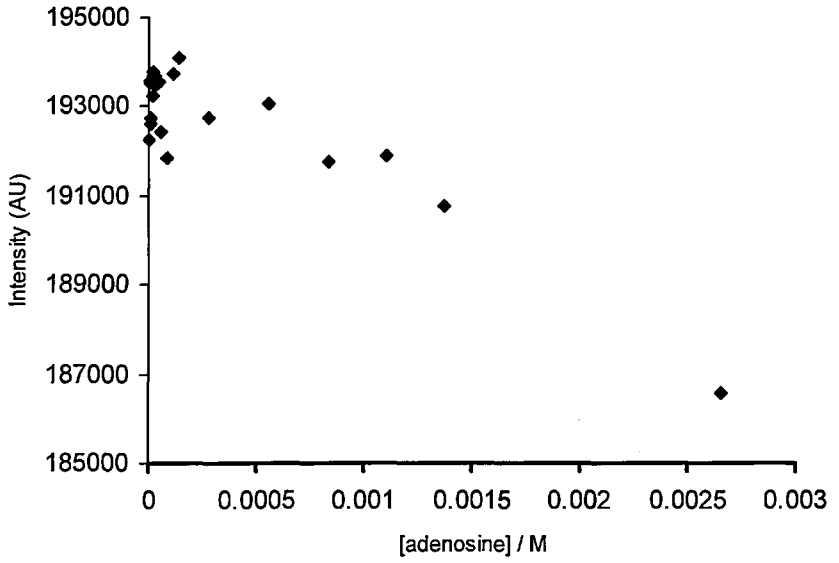

*Figure 25. Decrease in the emission intensity of the triad **90a** in methanol, upon addition of the complementary base adenosine.*

This might be due either to the adenosine, or the solvent in which the adenosine was dissolved (1:1 mixture of DMSO and water). A 100-fold excess in adenosine means the introduction of 236 μL of DMSO : water, about 7% of the total volume. This could account for the change, as the coumarin 343 emission is very sensitive to solvent polarity. On the other hand, the presence of a 100-fold excess means that it is more likely that the adenosine is quenching the

donor directly. The scattering of the data points does not allow the calculation of a binding constant.

In acetonitrile the association between the triad and the complementary base was indicated by decrease of fluorescence (*Figure 26*). Acetonitrile, being polar but aprotic, can only act as an acceptor in hydrogen bonding, thus facilitating the interaction between the host and the guest.

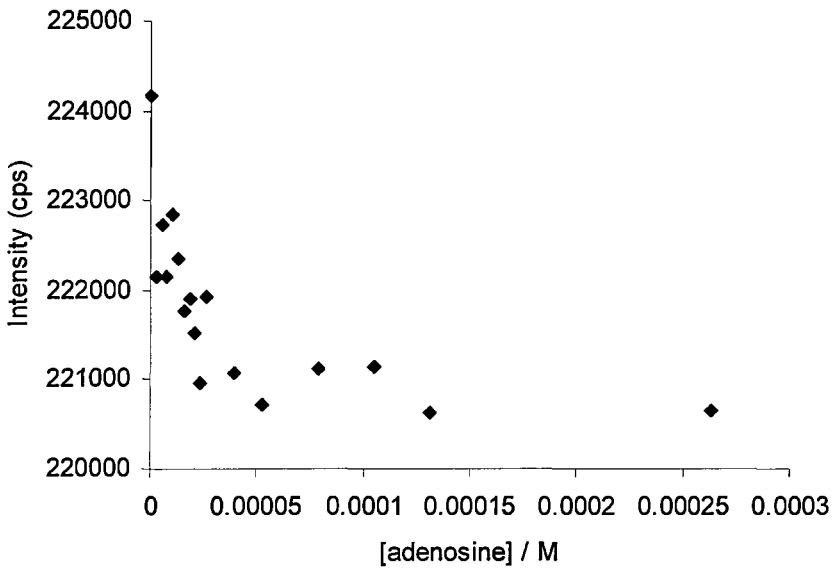

*Figure 26. Decrease in the emission intensity of the **90a** in acetonitrile, upon addition of the complementary base adenosine.*

5.3.2 Coumarin 120 donor and adenosine quencher

Addition of the complementary base uridine to **90b** (coumarin 120 – coumarin 343 - adenosine) resulted in increased fluorescence intensity (*Figure 27*). The effect was more pronounced in acetonitrile, where the final intensity was 15% higher than the initial intensity. In methanol the increase was only 3% (*Figure 28*).

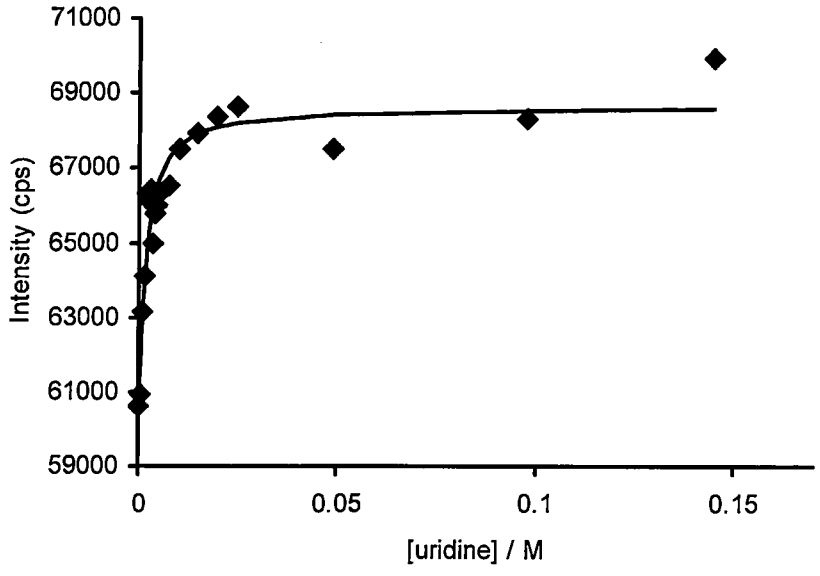

*Figure 27. Increase in the emission intensity of the triad **90b** in acetonitrile, upon addition of the complementary base uridine. The intensity change corresponds to approximately 15%.*

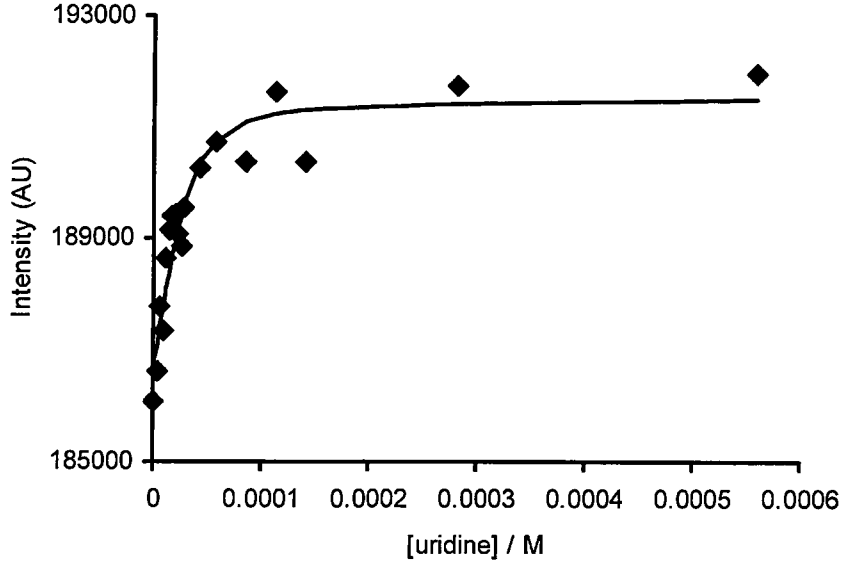

*Figure 28. Increase in the emission intensity of **90b** triad in methanol, upon addition of the complementary base uridine. The intensity change corresponds to approximately 3%.*

The difference could be caused by the weaker interaction in the highly polar and protic methanol. **90b** was the only one of the four organic triads that behaved in the way predicted originally. Although the fluorescence of the donor – acceptor diad is not turned completely off, it is decreased considerably. Addition of the substrate of the quencher (the complementary base uridine) reduces the quenching. According to the data available, quenching of the coumarins by nucleosides happens *via* electron transfer.[75] Base pairing between the adenosine and the uridine could change the redox potential of the quencher by affecting the electron distibution of the heterocycle. This in turn could reduce the rate of the electron transfer, resulting in an increase in luminescence intensity.

5.3.3 Coumarin 151 donor and uridine quencher

The coumarin 151 – coumarin 343 – uridine triad (**96a**) was titrated with adenosine in methanol. Addition of the complementary base quenched the emission from the acceptor. The interaction between the host and the guest was strong, as indicated by a 13% change in the luminescence intensity upon addition of 1 equivalent of the complementary base. The intensity changes induced by adding more adenosine were small. The binding constant could not be determined unambiguously because of the low concentration of both compounds.

This triad was also titrated with uridine, guanosine and cytidine, to determine if it is possible to distinguish between them. In DNA, base pairing is strictly controlled, but the free nucleosides can form hydrogen bonds freely with each other in any combination. Adding solutions of the nucleosides resulted invariably in quenching of the luminescence. The degree of the quenching was

of the same order of magnitude in all four cases, therefore it was not possible to distinguish between the four nucleosides this way.

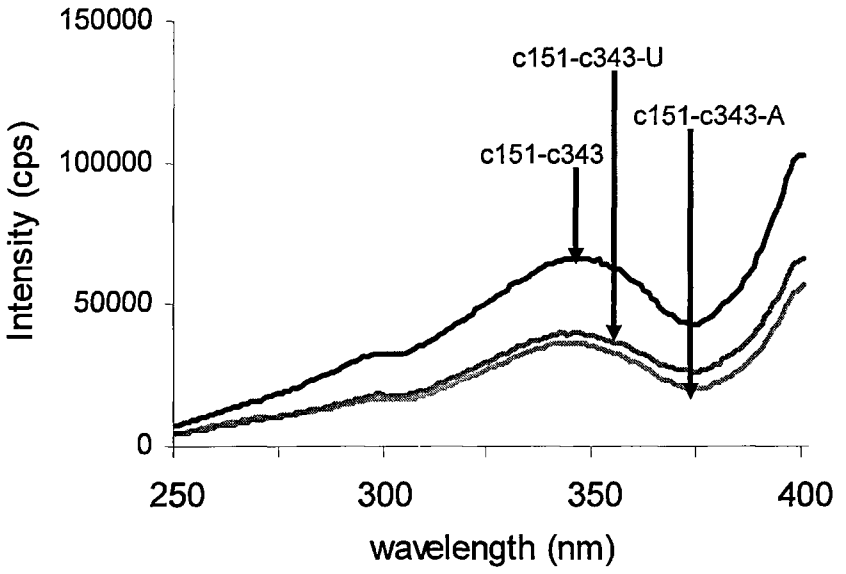

*Figure 29. Excitation spectra of the diads and triads (**D** = c151) in methanol (det: 480 nm). Above 350 nm direct excitation of the acceptor becomes significant.*

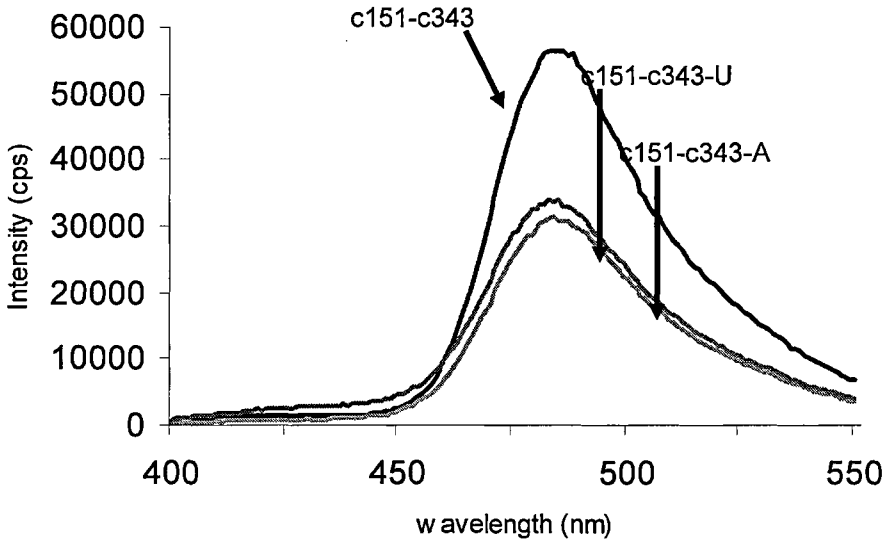

Figure 30. Emission spectra of the organic diads and triads in methanol (excitation: 328 nm). Only emission from the coumarin 343 donor is observed (484 nm).

Under identical experimental conditions the excitation and emission spectra of the c151-c343 diad and the corresponding triads were compared (*Figure 29* and *30*). The triad fluorescence is effectively quenched by the nucleosides in both cases. As the addition of the complementary bases caused further quenching, it is possible that the base pairs can quench the coumarin 151 more effectively than the unpaired nucleoside (*Figure 31*), or they are quenching the donor directly.

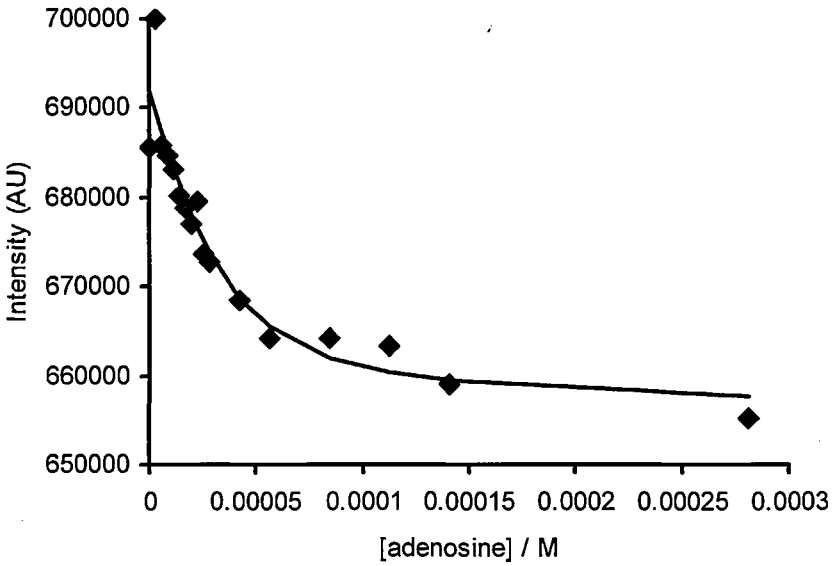

Figure 31. Quenching of the triad ***96a*** *by the addition of adenosine. (Methanol, c(triad) = 0.033 mM, excitation @ 328 nm)*

5.3.4 Coumarin 151 donor and adenosine quencher

The triad consisting of coumarin 151 donor, coumarin 343 acceptor and adenosine quencher (**96b**) was less luminescent than its corresponding diad. Addition of the complementary base uridine induced further quenching, which

might be due to the increased quenching ability of the base pair compared to the adenosine (*Figure 32*) or direct quenching of the donor by the uridine.

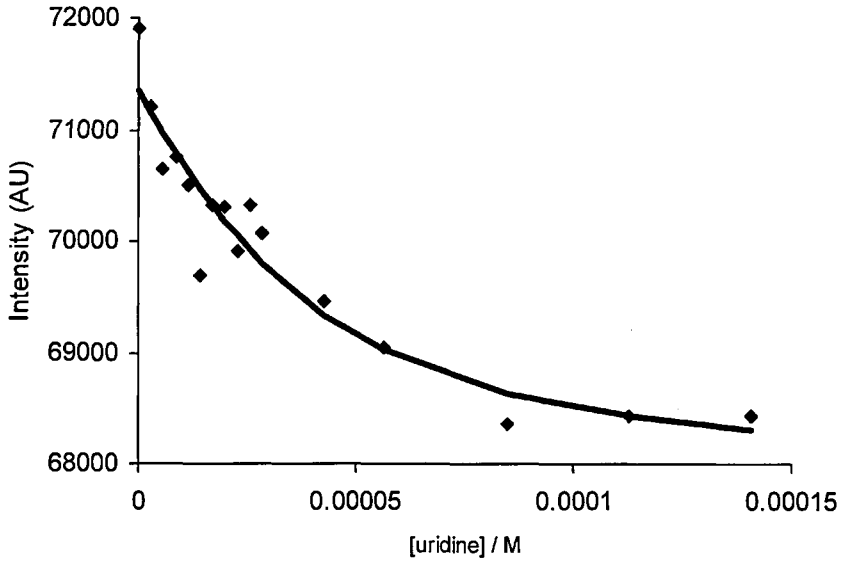

*Figure 32. Quenching of the c151-c343-A triad (**96b**) by the addition of uridine. (Methanol, c(triad) = 0.033 mM, excitation @ 328 nm)*

5.4 Organic triads and DNA

5.4.1 Coumarin 120 donor

Both coumarin 120 – donor bearing triads dissolved in methanol were titrated with DNA. In neither case were consistent and reproducible data obtained. At high DNA excess a slight decrease in fluorescence intensity was observed, but this was not significant until the DNA was in ~100-fold excess (*Figure 33*).

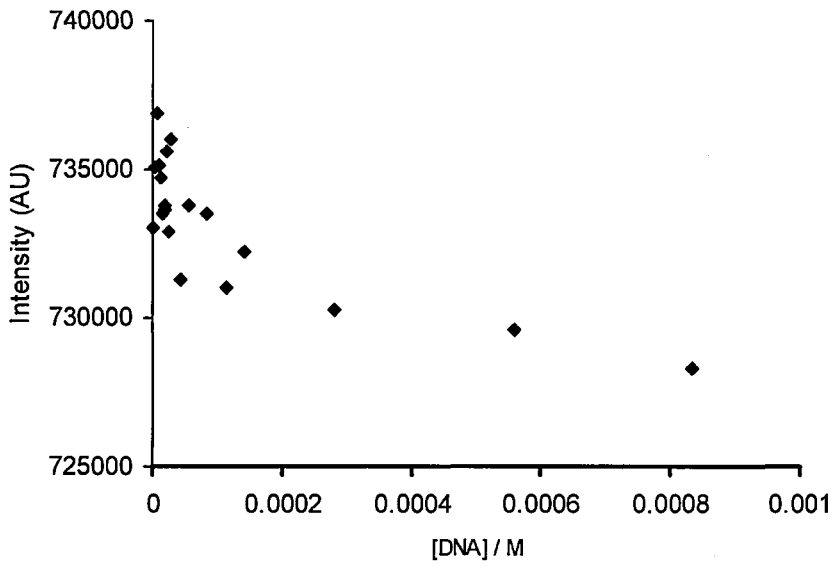

*Figure 33. Quenching of **90b** by DNA. (MeOH, c(triad) = 0.033 mM, excitation @ 328 nm)*

5.4.2 Coumarin 151 donor

The triads equipped with coumarin 151 donors displayed strong interaction with DNA. Both triads were efficiently quenched by DNA, which is probably the result of the intercalation of the donor with the double strand. It is possible, that the previously mentioned increase in the quenching of the coumarin 151 by base pairs plays a role in this case too, and contributes to the quenching.

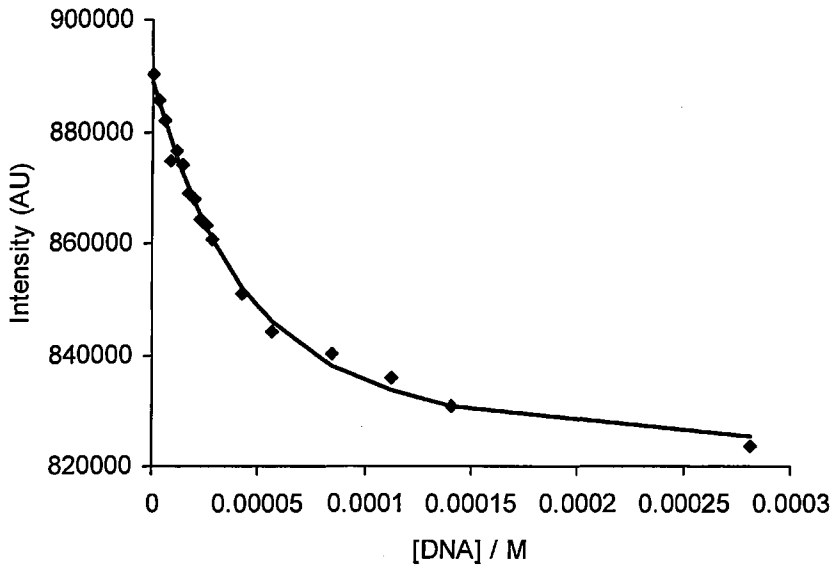

*Figure 34. Quenching of the c151-c343-A (**96b**) triad by the addition of DNA. (Methanol, c(triad) = 0.033 mM, excitation @ 328 nm)*

A summary of luminescent properties, the binding constants of the triads and their complementary bases, the triads and the diads with DNA, and the effects of the targets on the probe luminescence is shown in *Table 7*.

	c120-c343	c151-c343	c120-c343-U	c120-c343-A	c151-c343-U	c151-c343-A
c.b.	-	-	*	increase	decrease	decrease
K	-	-	*	$> 10^4$	$> 10^4$	$> 10^4$
DNA	increase	decrease	*	*	decrease	decrease
K	$> 10^4$	$> 10^4$	*	*	$> 10^4$	10^4
o.b.	-	-	decrease[a]	increase[a]	decrease[b]	
K	-	-	$\sim 10^3$	$\sim 10^3$	$> 10^4$	

*Table 7. All measurements were conducted in methanol, unless stated otherwise. *no consistent data were obtained, [a]measurement in acetonitrile, [b]measurement with C, G, A and U separately, c.b. complementary base, o.b. own base, increase = increase in fluorescence intensity, decrease = decrease in fluorescence intensity.*

5.5 Stern-Volmer constants for the quenching of the triads

In most cases the data obtained from the fluorescence titrations of the triads did not allow the calculation of a binding constant for the nucleosides. The apparent constants obtained were significantly higher than those found in the literature, typically 70 M^{-1} in DMSO, for the association of the adenine-uridine base pair.[88] Although the triad – nucleoside systems are different from the free A – U base pair, the association constant should be of a similar magnitude, given the number of possible hydrogen bonds between the two heterocycles.

Plotting I_0 / I versus the quencher concentration gives information about the nature of the quenching procedure. The c120-c343-U (**90a**) triad was quenched both in methanol and acetonitrile by adenosine, but it was not possible to fit a binding curve to the data. The Stern-Volmer plot revealed that until the 1 : 1 ratio of the [**Q**] : [triad] was reached, the quenching of the triad was increasing with the concentration. In the presence of excess **Q** the quenching did not become more efficient, as shown by a break in the curve drawn over the data points. Similar results were obtained for the c151-c343 diad with DNA and the c151-donor triads with both their complementary bases and DNA (*Figure 35*).

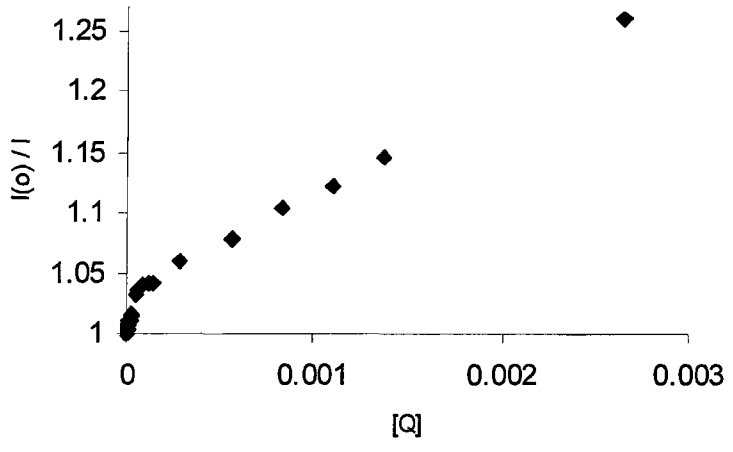

*Figure 35. Quenching of the c120-c343 (**87**) diad by dsDNA.*

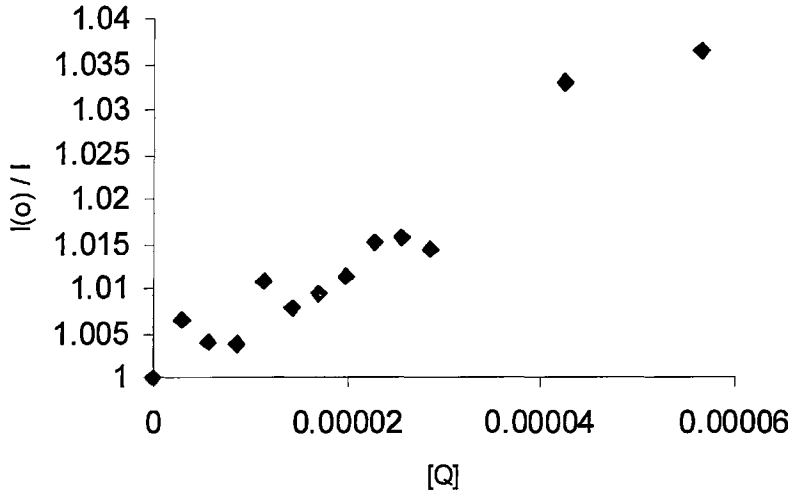

Figure 36. The initial section of the Stern-Volmer plot in Figure 35.

Stern-Volmer constants were calculated by fitting a straight line to the initial section of the plot. If the quenching obeys Stern-Volmer kinetics the intercept should be at $b = 1$, x is the concentration of the quencher, and the slope of the curve (m) gives the Stern-Volmer constant (*Eq 3*).

$$y = mx + b \qquad \textit{Eq. 3}$$

The constants obtained for the organic diads and triads for the quenching by their complementary bases and DNA are summarised below (*Table 8*).

	c120-c343	c151-c343	c120-c343-A	c120-c343-U	c151-c343-U	C151-c343-A
c.b.	-	-	*	12	$7.5 \cdot 10^2$	$3.2 \cdot 10^2$
DNA	**	$6.5 \cdot 10^2$	**	11	$7.3 \cdot 10^2$	$7.4 \cdot 10^2$

*Table 8. Stern-Volmer constants. *The c120-c343-A triad behaved in the predicted way, i.e. its fluorescence intensity was increased by addition of its complementary base. **The Stern-Volmer constant for its quenching by DNA could not be calculated.*

5.6 *Determination of τ of the organic diads and triads*

The luminescent lifetimes of the triads and the diads were determined in the presence of their complementary bases, the solutions of their own quenchers, and DNA (*Table 9*).

	87	94	97	90a	90b	96a	96b
τ	3.52 ns	1.33 ns	1.71 ns	3.38 ns	3.46 ns	1.33 ns	1.40 ns
c.b.[a]	-	-	-	3.36 ns	3.48 ns	1.39 ns	1.40 ns
c.b.[b]	-	-	-	3.40 ns	3.51 ns	1.30 ns	1.33 ns
DNA[a]	3.51 ns	1.27 ns	1.86 ns	3.38 ns	3.51 ns	1.32 ns	1.43 ns
DNA[b]	3.55 ns	1.14 ns	1.73 ns	3.40 ns	3.51 ns	1.29 ns	1.30 ns
o.b.[a]	-	-	-	3.38 ns	3.50 ns	1.33 ns	1.45 ns
o.b[b]	-	-	-	3.50 ns	3.47 ns	1.39 ns	1.29 ns

Table 9. The lifetimes of the organic diads and triads in methanol. [a]one equivalent, [b]ten equivalents, c.b. complementary base, o.b. same base as quencher base. Lifetimes can be measured with ± 10% accuracy.

Excitation of the samples was performed at 320 nm, which is close to the excitation maximum of the donor, and is at sufficiently short wavelength to avoid direct excitation of the acceptor. The two triads bearing c120 donors were also excited at 310 nm, without significant changes in τ. Direct excitation of the acceptor at 450 nm did not change the τ, indicating, that in the case of these two triads, RET is fast and the rate determining step is the fluorescence emission.

The luminescent lifetimes seem to be dependent on the donor, which is somewhat contradictory with the results obtained by direct excitation of the acceptor. A possible explanation is that in the case of coumarin 151 there are several vibronic levels in the excited state that are slightly below the excited

state of the coumarin 343, and the the acceptor can thermally repopulate the donor excited state (*Figure 37*).

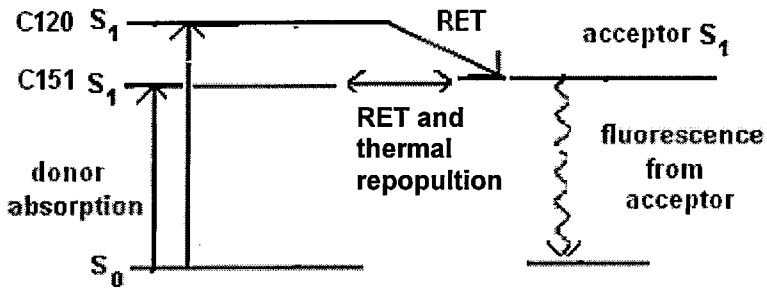

Figure 37. Energy levels of the donors and the acceptor.

This would open up a deactivation pathway for the [c151-c343]* system, which could compete with the fluorescence emission from the acceptor. If we assume that (a) no such repopulation occurs for the c120-donor bearing species, and (b) the only de-activation pathways significantly contributing to the de-excitation of the acceptor, *Eq 4.* describes the concentration of A* at any given time after excitation.

$$[A^*]_t = [A^*]_0 \cdot e^{-tk_1} + [A^*]_0 \cdot e^{-tk_2} \qquad \text{Eq 4.}$$

The rate constants of the luminescent decay and repopulation are k_1 and k_2, respectively, t is the time, $[A^*]_0$ and $[A^*]_t$ are the concentrations of the A* at $t = 0$ and $t = t$. As the concentration of A* is reduced by an additional non-radiative process, its observed lifetime decreases.

The luminescent lifetimes of the triads are longer than the lifetimes of the corresponding diads. Addition of one equivalent of the complementary base of the quencher increases τ in both measured cases. Adding the **Q** nucleotide to the solution resulted in increase of the lifetime, probably because base pairing is possible in other combinations than the Watson-Crick base pairs. The drop in

the τ when 10 equivalents of the nucleotides were added can be a solvent effect, or due to a competitive reaction, for example association of the free bases, or direct quenching of the donor.

DNA decreased the luminescent lifetime in the case of the c151-c343-A (**96b**) triad, and increased marginally that of the c120-c343-U triad (**90a**).

When uridine was added in small portions to **96b** a gradual increase in the τ of the triad was observed, in accordance with the changes seen in the luminescent intensity (*Figure 38*). Although it was not possible to fit a binding curve to the data points, the increase in the lifetime suggests that in the triad the quencher is disrupting the RET, which is aprtially restored upon the addition of the complementary base.

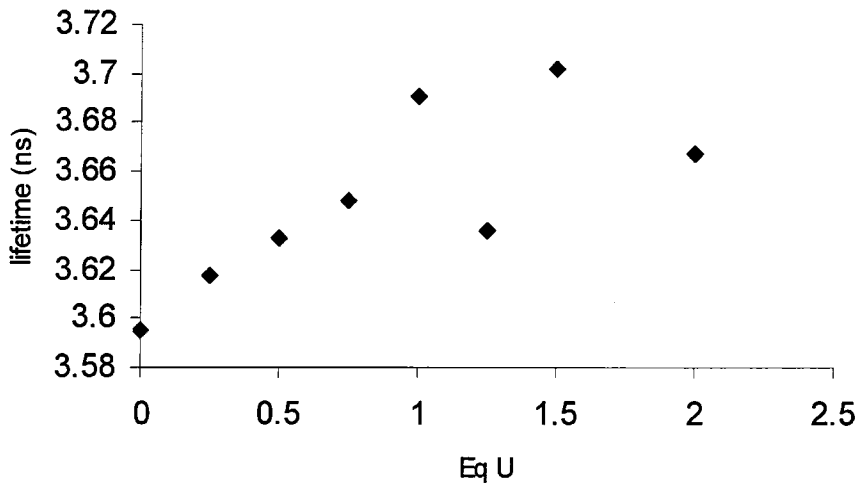

*Figure 38. Changes of τ for the triad **90b** upon addition of uridine. The scattering of the data points is caused by the inaccuracies of the determination of the τ, usually ±10%.*

Addition of uridine to the triad **96b** and addition of DNA to the diad **94** resulted in a decrease in their luminescent lifetimes (*Figure 39*).

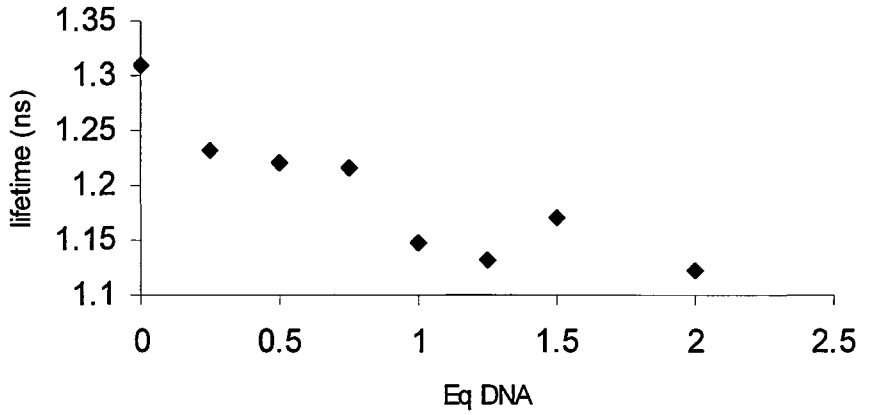

*Figure 39. Changes of τ for the triad **96b** upon addition of DNA.*

The lifetime of the cyclic side-product with c151 **D** (**97**) was measured and was significantly higher than that of the corresponding diads and triads. As the amide group through which the c151 is attached to the scaffold is replaced by a diamide bond, the absorption and excitation maxima of the c151 are shifted to shorter wavelengths, to approximately 320 nm. This means an increase in the S_1 state energy of the donor, which reduces the efficiency of thermal re-population of the donor S_1 from the excited-state acceptor. Addition of DNA to this compound increased the τ. The DNA is probably acting as an electron donor to the electron-withdrawing coumarin 151. If quenching of the diamide-bound **D** occurs through oxidative PET, electron donation from the DNA could decrease its rate.

5.7 Lanthanide ligands

A series of lanthanide complexes were designed to serve as luminescent probes using triggered resonance energy transfer. The mechanism of sensing and reporting is similar to the one exploited in the organic triads. A donor transfers its energy to an acceptor moiety. The transfer is inhibited by a quencher, possessing a recognition unit. Binding of a substrate to the **Q** recognition site disrupts the quenching, and energy transfer between the **D** and the **A** can take place.

The **D** of the lanthanide complexes is coumarin 2, which can serve as an antenna for the metal ions Eu and Tb. This is essential for overcoming the barrier of the low absorption coefficients of the lanthanides. The **Q** is a nucleotide. The various functional units are held together by a cyclen scaffold. Unlike the organic triads, the lanthanide complexes have an inorganic reporter. The line-like, long wavelength lanthanide emission (*Figure 40* and *Figure 41*) makes detection easy as most of the interference from biological samples is < 500 nm. Further improvement in the sensitivity can be achieved by filtering out short-lived signals (for example τ < 500 ns). The intensity ratios of the transitions also give information about the symmetry of the complex. Changes upon addition of a substrate indicate significant conformational changes. The spectra shown in *Figures 40* and *41* belong to highly asymmetric complexes.

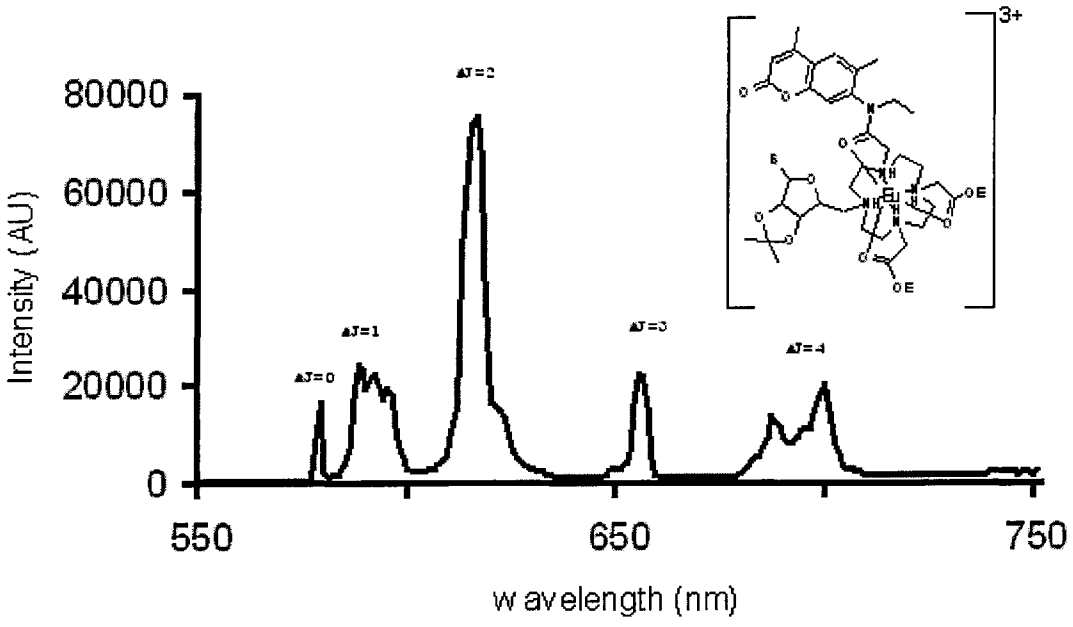

*Figure 40. Emission spectrum of **151a** in methanol. Excitation @ 328 nm.*

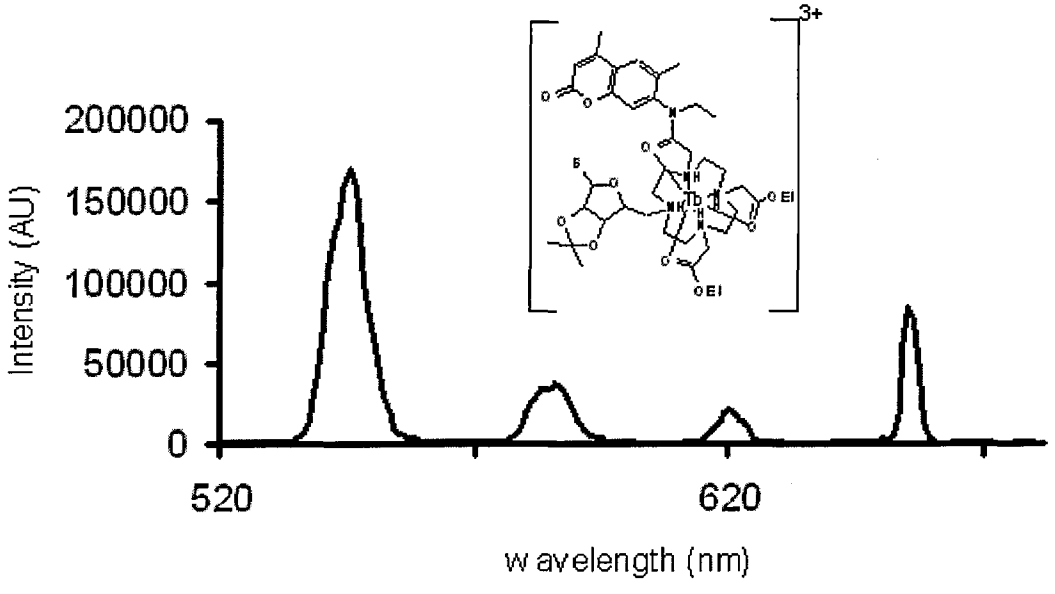

*Figure 41. Emission spectrum of **151b** in methanol. Excitation @ 328 nm.*

5.7.1 Attachment of the coumarin 2 antenna to the cyclen

To enable attachment of the coumarin 2 antenna to the cyclen scaffold, coumarin 2 was reacted with chloroacetic acid (*Scheme 6*). The reaction proceeded smoothly, and with excess chloroacetic acid and EDCI provided the coumarin 2 chloroacetate (**116**) in very good yields. The excess EDCI and

chloroacetic acid were removed by aqueous and basic washings. The residual coumarin 2 (typically < 5%) could be easily separated from the product by silica column chromatography.

Although the coumarin 2 chloroacetate (**116**) proved an excellent reagent for our purposes, replacement of chloroacetic acid with bromoacetic acid increased both yields and reaction rates, therefore in the final synthetic procedure coumarin 2 bromoacetate (**117**) was used instead of the chloroacetate.

5.7.2 Cyclen derivatisation starting from the bis-protected cyclen-oxalamide

Simultaneous protection of the N1,N4 nitrogen atoms of cyclen is known from the literature. The oxalamide protecting group can be hydrolysed by 10 M aqueous NaOH, or refluxing concentrated hydrochloric acid.

The third nitrogen was reacted with di-tert Butyl dicarbonate at room temperature in chloroform in the presence of 1.5 equivalent triethylamine. The formation of fully protected (bis-Bocced) cyclen was not seen, and the triprotected cyclen was easily separated from the unreacted oxalamide. Typical yields were between 70-80% (*Scheme 15*).

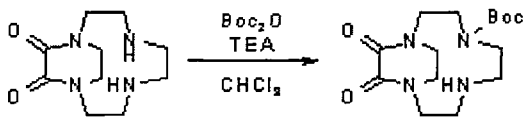

113

*Scheme 15. Synthesis of the triprotected cyclen (**113**).*

Alkylation of the free fourth nitrogen was unsuccessful (*Scheme 16*). Using the model molecules, NMA chloroacetate (**114**) and coumarin 120 bromoacetate

(**119**) instead of the coumarin 2 analogue a series of reaction were conducted to find the optimal conditions for the alkylation (*Table 9*).

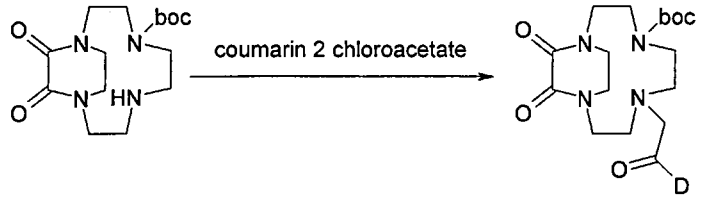

*Scheme 16. Alkylation of N10 of **113**. **D** = coumarin 2, coumarin 120 or NMA.*

Reagent	base	NaI	solvent	T	Yield (%)
NMA-chloroacetate	K_2CO_3	+	DMF	100 °C	50
C2-chloroacetate	K_2CO_3	+	AcN	Reflux	0
C2-chloroacetate	TEA	-	EtOH	Reflux	6
C2-chloroacetate	K_2CO_3	+	DMF	80 °C	45
C120-bromoacetate	K_2CO_3	+	DMF	80 °C	29

*Table 9. Optimisation reactions for the alkylation of the triprotected cyclen derivative **113**. In the test reactions, the readily available coumarin 120 and NMA replaced coumarin 2.*

The coumarin 2–equipped triprotected cyclen (**124**) was isolated in low yields. This was due to the poor nucleophilicity of the fourth nitrogen atom under relatively mild conditions (warm acetonitrile, 3-5 equivalents of potassium carbonate).

At more forcing conditions (refluxing acetonitrile or DMF at 80-90 °C, large excess of potassium or cesium carbonate, sodium iodide) the decomposition of the chloroacetate occurred. Both coumarin 2 and a dimerised product of the coumarin 2 chloroamide (**125**) were isolated and characterised. A similar dimerisation reaction was seen when the alkylation was performed with the NMA-chloroacetate, indicated by the appearance of the 2 (*m* / *z*) = 594 peak in

the mass spectrum of the reaction mixture. The dimerisation of the coumarin 2 chloroacetate is probably initiated by sodium iodide. In a halogen exchange, the chlorine is replaced by iodine. Molecules containing carbon-iodine bonds are known to undergo homogeneous bond fission, forming the reactive radical, which in this system formed a carbon-carbon bond with an identical radical. It is also possible that the base in the reaction mixture deprotonates the electron-deficient α-carbon of **116**, and this species reacts further to form the dimer.

After acidolysis of the Boc protection the second substitution reaction was carried out with a series reagents. Direct amide bond formation between uridine 5'-carboxylic acid and the secondary nitrogen atom of the cyclen was impossible either with DCC or EDCI in DMF or THF. Therefore introduction of a linker moiety to provide a masked primary amine to facilitate the attachment of the 5'-COOH-U was necessary. Alkylation of the cyclen nitrogen with either N-Boc-bromoethylamine or N-Boc-ethanolamine methanesulfonate were attempted, but gave the desired products in low (10-12%) yields (*Scheme 17*).

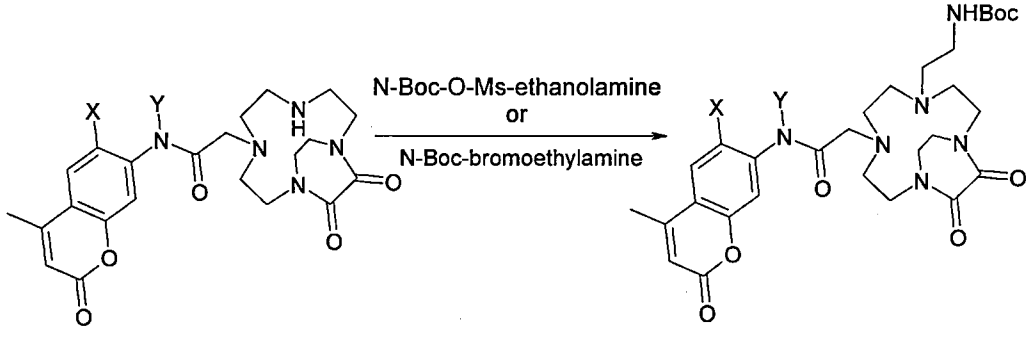

Scheme 17. Alkylation of the monosubstituted cyclen oxalamide. X = H or Me, Y = H or Et.

5.7.2.1 Sequential synthesis of the asymmetric trisubstituted cyclen

As alkylation of the triprotected cyclen (**113**) afforded the product in very low yields, selective monoalkylation of one of the nitrogen atoms of unprotected

cyclen was attempted. Reacting coumarin 2 chloroacetate with 1.5 equivalents of cyclen in DMF in the presence of potassium carbonate base and sodium iodide catalyst resulted in the formation of the monoalkylated derivative (*Scheme 18*).

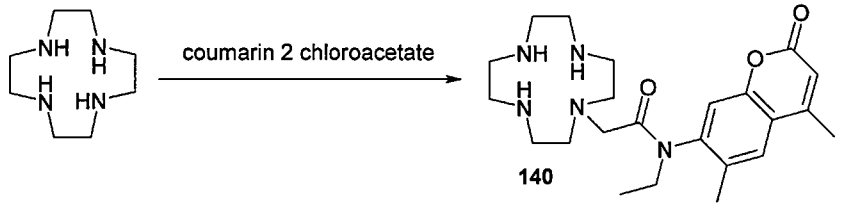

*Scheme 18. Attachment of the coumarin 2 antenna to the cyclen.The major product is monosubstituted cyclen (**140**) (solvent: 100% ethanol, base: TEA).*

The major side-products were disubstituted cyclen and dimerised coumarin 2 chloroacetate (**125**). Replacement of DMF with 100% ethanol and potassium carbonate with triethylamine facilitated the purification of the product. When the coumarin 2 bromoacetate (**117**) was used for the alkyaltion the disubstituted derivative formed in somewhat larger quantities (5-10%). This is only a minor drawback, as the synthesis of the bromoacetate is considerably faster and more efficient than that of the chloroacetate.

Previous experimental data suggested that under standard alkylation conditions (dipolar solvents, high temperatures) the second substitution step occurs at the N7 position. Therefore a bis-alkylation reaction was devised, where the stabilising 'arms' would be attached to the cyclen scaffold simultaneously. The first arm will predominantly alkylate the N7 nitrogen, leaving both nitrogens *cis* to the donor free. The second arm would substitute the hydrogen atom of one of the remaining nitrogens. The crucial aspect of this step is the possibility of

halting the reaction in the trisubstituted cyclen phase, without the formation of large quantities of fully substituted cyclen (*Scheme 19*).

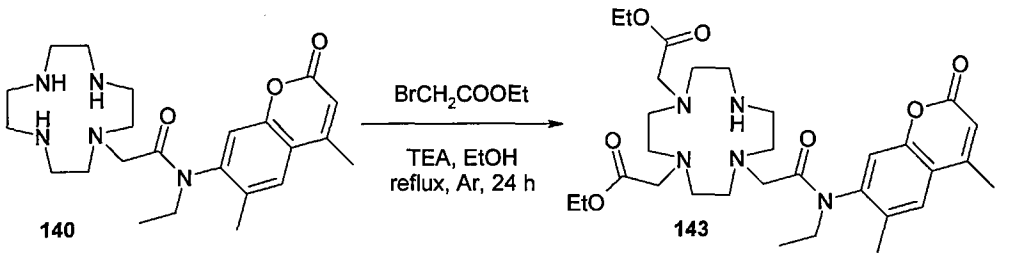

*Scheme 19. Alkylation of monosubstituted cyclen (**140**) with ethyl bromoacetate.*

After optimisation the ideal conditions for the bis-alkylation were found to be refluxing 100% ethanol solvent, 3 equivalents of TEA base and 2.2 equivalents of ethyl bromoacetate. These relatively mild conditions still yielded the tetrasubstituted cyclen (**145**) as the major product, but sufficient quantities (typically 500 mg for 2.00 g of starting material **140**) of the asymmetric **143** were isolated. A small amount (~2%) of the symmetric trisubstituted derivative (**144**) was found and purified, along with some disubstituted compound. When DMF or acetonitrile were used instead of ethanol, only disubstituted and fully substituted derivatives were isolated.

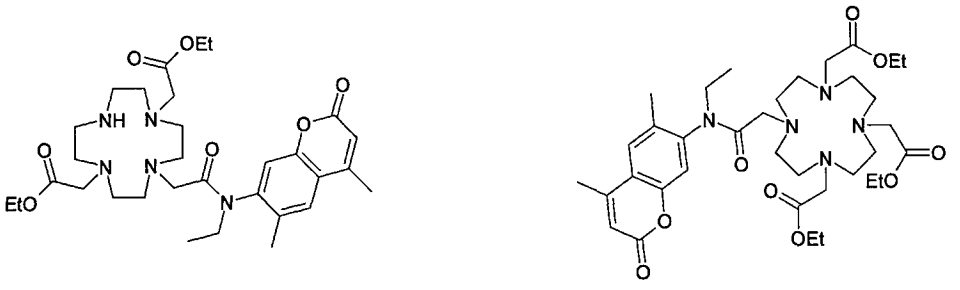

144 **145**

*Figure 42. Side-products isolated during the synthesis of the asymmetric cyclen-derivative **143**. The symmetric **144** was isolated in <5% yields, but **145** was formed in 30-40% yields.*

Alkylation of the last secondary nitrogen atom has proved difficult in the oxalamide approach. As in this case the N10 nitrogen substitution would be the final step, relatively low yields would have been acceptable, as all the previous

steps proceeded with moderate to good yields. The electron withdrawing effect of the 'arms' and the steric hindrance were both assumed to be lower in the trisubstituted cyclen than in the triprotected compound, which both suggested that in this case the substitution reaction might be more efficient.

Alkylation of the N10 nitrogen was carried out under a number of different conditions with both 5'-mesyl-nucleosides and N-Boc bromoethylamine or N-Boc-ethanolamine methanesulphonate. The latter two could serve as linkers to which the nucleosides could be coupled. Unfortunately the products were formed in very low yields even under rather forcing conditions (*Table 10*).

Reagent	base	Solvent	T	*t*	Yield (%)
$BrCH_2CH_2NHBoc$	TEA	EtOH	reflux	24 h	15
$MsOCH_2CH_2NHBoc$	K_2CO_3	DMF	80 °C	24 h	12
MsO-2',3'-isopropylidene-U	K_2CO_3	DMF	80 °C	36 h	0
MsO-2',3'-isopropylidene-A	K_2CO_3	DMF	80 °C	24	3.5

Table 10. Alkylation of the N10 nitrogen of the trisubstituted cyclen ***143****. Although various reaction conditions and reagents were explored, yields remained low.*

The ligand **147**, containing coumarin 2 donor and adenosine acceptor (*Figure 43*) was successfully synthesised and characterised, albeit in very low yields and after extensive chromatography. The analogous reaction with uridine-5'-methanesulphonate was not successful, and formation of the desired product was not observed.

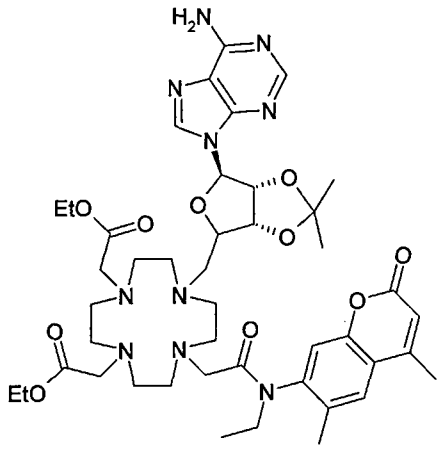

*Figure 43. The ligand (**147**) was successfully prepared. The corresponding uridine-containing molecule could not be synthesised.*

5.7.2.2 Sequential synthesis of the asymmetric ligand

The experimental results obtained so far enabled us to draw a number of conclusions. Monoalkylation of cyclen is easily accomplished under mild conditions, and purification of the product is straightforward by chromatography. Substitution of at least two further nitrogens is similarly simple, furthermore, the substitution of the third and the fourth nitrogen atoms seems to occur almost simultaneously. On the other hand, the reactivity of the N10 nitrogen in an already trialkylated cyclen derivative is poor.

Therefore, the optimal reaction sequence would be the following. Monoalkylation with the donor (coumarin 2 bromoacetate, **117**) followed by selective alkylation of the N4 nitrogen atom, either with a linker, or directly with a suitably activated quencher. A final alkylation step would furnish the scaffold with the 'arms'. In the case where the quencher was attached to the scaffold *via* a linker, the last alkylation would be followed by attachment of the quencher to the linker (*Scheme 20*).

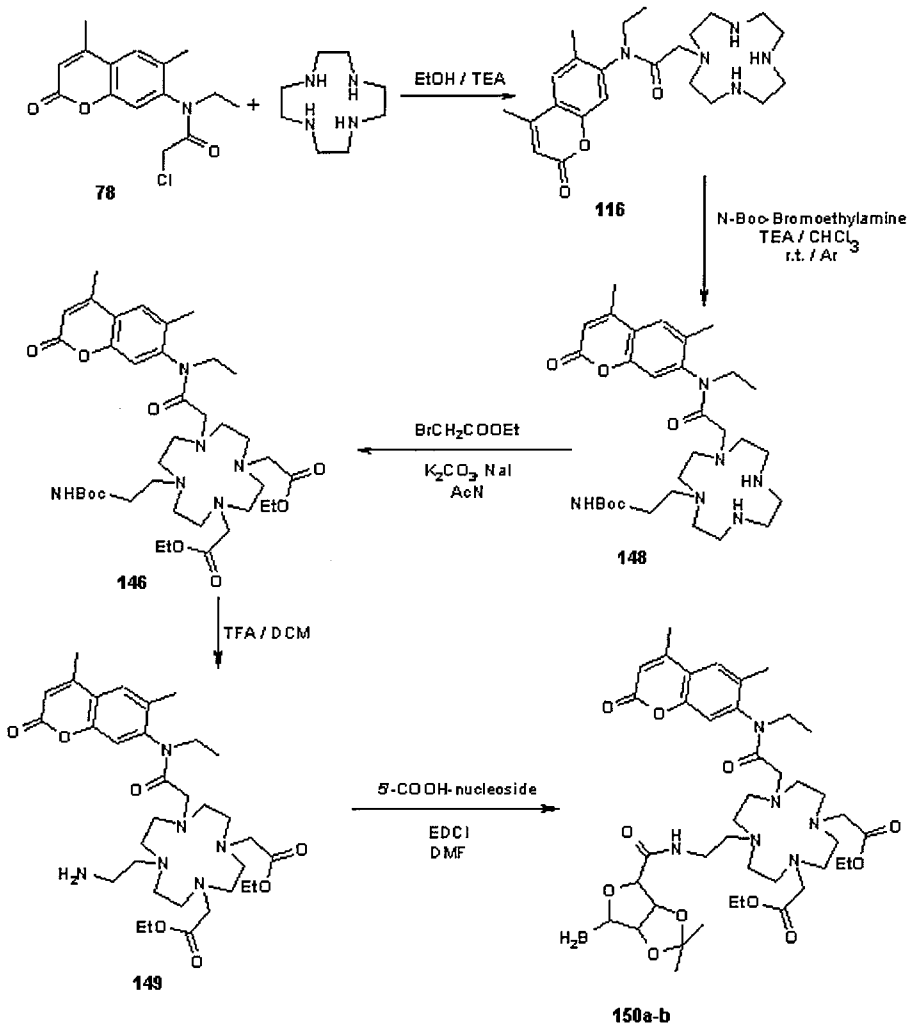

*Scheme 20. The synthesis route leading to the asymmetric, tetrasubstituted cyclen-based ligands (**150a-b**) for the complexation of europium and terbium.*

Recently it has been found that N1,N4 bis-alkylated cyclen derivatives can be synthesised in good yields and without the formation of the N1,N7 isomer, when the reaction is carried out in apolar solvents (chloroform) in the presence of triethylamine base.[89]

Based on this, a similar reaction was carried out. Monosubstituted cyclen was alkylated with N-Boc-bromoethylamine in freshly distilled chloroform in the

presence of 10 equivalents of base. The concentration of the reagents was kept at 50 mM, as at higher concentrations significant amounts of tri- and tetrasubstituted derivatives formed. Apart from these two side-products, only the *cis* disubstituted compound was isolated. Neither NMR, nor TLC indicated the presence of the N1,N7 isomer.

The alkylation reaction was carried out with 5'-mesyl-activated nucleosides. Under the same conditions the N1,N4-substituted derivatives formed in low yields. Most of the starting material was recovered intact. Increasing the reaction times or the concentrations did not increase the yield. It is interesting that O-mesyl-N-Boc-bromoethanol gave the corresponding disubstituted product in similarly low yields. It is possible that the methanesulfonyl group, while being an excellent leaving group is too large, and hinders attack of the nitrogen lone pair of the cyclen on the electrophile (*Table 11*).

Reagent	eqiuvalent base	Time	Yield (%)
$BrCH_2CH_2NHBoc$*	5	24 h	29
$MsOCH_2CH_2NHBoc$*	5	24 h	14
MsO-2',3'-isopropylidene-U*	10	36 h	41
MsO-2',3'-isopropylidene-A*	10	24	32
Coumarin 2 chloroacetate**	10	36 h	7
Coumarin 2 bromoacetate**	10	36 h	13

*Table 11. Alkylation of the N4 nitrogen of the monosubstituted cyclen. * N1-substituent: acetoxy coumarin 2, N1-substituent: N-Boc-2-aminoethyl. Solvent: chloroform.*

Alkylation first with N-Boc-bromoethylamine, followed by the coumarin 2 bromoacetate is also possible, but gives the desired product in lower yields (*Scheme 21*). The reaction gives rise to the coumarin 2 dimer (**125**), which cannot be recovered for further use. As sodium iodide was not present in the

reaction mixture, this can be explained either by homogeneous breaking of the Br-C bond, or by base-induced α-elimination of hydrogen bromide from the coumarin 2 bromoacetate. Because of the better yields, the initial approach, where N-Boc bromoethylamine is used for the second alkylation step is preferred.

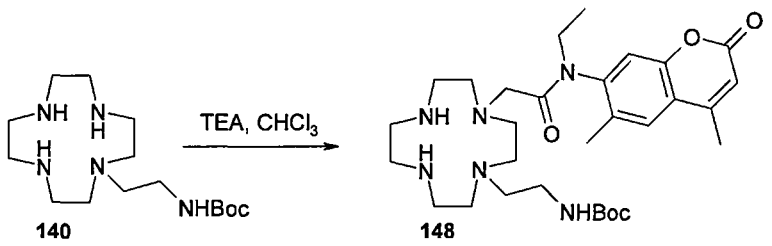

140 148

*Scheme 21. Alkylation of N1-monosubstituted cyclen (**140**) on the N4 nitrogen. The N1,N7-isomer was not formed.*

The disubstituted cyclen (**148**) was reacted with excess ethyl bromoacetate in refluxing dry acetonitrile in the presence of potassium carbonate and sodium iodide. The conversion to the fully alkylated derivative (**146**) (*Scheme 20*) was complete in 24 hours, and only mechanical losses reduced the yield.

Removal of the Boc protection from the linker by acidolysis revealed a primary amine to which 5'-oxidised nucleosides could be attached. Ligands **150a** and **150b** (*Figure 44*) were synthesised in good yields.

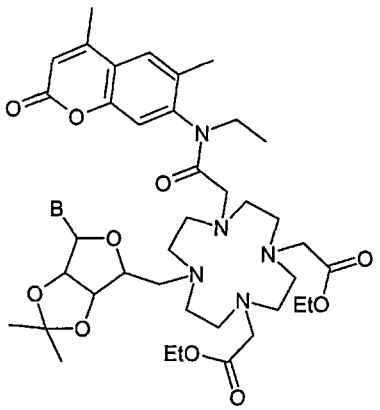

*Figure 44. The ligands (**150a-b**) of the lanthanide triads. B = uracil or adenine*

*5.7.2.3 Complexation of **150a** and **150b** with europium and terbium*

Complexations of **150a** and **150b** with the lanthanides europium and terbium were carried out in refluxing methanol under inert atmosphere. The ligands were added in slight excess to the anhydrous lanthanide chlorides. The reactions were allowed to proceed overnight, the solutions were cooled back to room temperature and poured into tenfold volumes of diethyl ether. The precipitate was centrifuged and the solvent was decanted. The solid residue was suspended in ether and the procedure was repeated. The solid was dissolved in the minimum amount of water, filtered through a plug of cotton wool to remove the free ligand residues and the complex was freeze dried.

Thin layer chromatography on both silica and alumina plates showed that the sample was free from the uncomplexed ligand. The proton NMR of the complexes provided spectra showing signals in the 10-35 ppm region, a clear indication of complex formation. Although only some of the peaks could be resolved, loss of the ethyl esters was suggested. This finding was supported by the mass spectrometric analysis of the samples, where molecular ions corresponding to the mono and di-deesterified complexes (with the resulting decrease in the overall charges of the complexes) were seen. This is probably caused by the presence of the lanthanide ion, which can act as a Lewis acid, and catalytically hydrolyse the ethyl esters.

5.8 Determination of the hydration state of the Eu and Tb complexes

The lanthanide ions in the complexes have nine co-ordination sites. Saturation of the co-ordination sphere is essential for the stability of the complexes. Also, in solvents with O-H and N-H oscillators, and to a much lesser extent, with C-H oscillators, the solvent molecules binding to the unfilled co-ordination sites can quench the lanthanide emission. Therefore it is essential to know the number of solvent molecules bound to the solvated complexes. The ligands offer eight co-ordinating atoms, four nitrogens on the cyclen ring, and four carbonyl oxygens on the substrates. In solution the ninth site is expected to be occupied by one solvent molecule, although, as the solvent molecules surrounding the complex can also have an effect on the lanthanide luminescence, it is possible that the effective number is more than one, and it does not have to be an integer.

To determine the number of co-ordinating water molecules the lanthanide luminescent lifetime has to be measured in water and deuterated water. The D-O oscillators have different vibrational energies than the O-H oscillators, and their quenching of the lanthanide is less efficient, which is indicated by an increase in the luminescence lifetimes. With the formula in *Eq 5* the number of bound water molecules can be calculated.

$$q = A\left(k_{H2O} - k_{D2O}\right) \qquad \textit{Eq 5}$$

In the equation q stands for the number of water molecules bound to the central atom, A is an experimental value, which is 0.525 ms^{-1} in the case of europium per OH oscillator and 2.1 ms^{-1} for terbium. The rate constants, assuming first-order decays are the reciprocals of the experimentally determined lifetimes. The charge and geometry of the complex can also be taken into account when determining the q values.

The lifetimes of the Eu and Tb complexes have been determined in both distilled water and deuterated water, and their hydration states have been calculated (*Table 12*).

	Eu(**150a**)	Tb(**150a**)	Eu(**150b**)	Tb(**150b**)
$\tau(D_2O)$	2.70 ms	0.35 ms	3.11 ms	0.56 ms
$\tau(H_2O)$	0.61 ms	0.27 ms	0.49 ms	0.40 ms
q	1.34	1.72	1.67	1.47

Table 12. The lifetimes of the Eu and Tb complexes in H_2O and D_2O, and their hydration states.

The number of bound water molecules are > 1 in all cases. As there are eight possible co-ordinating atoms in each complex, it is natural that the ninth co-ordination site is filled by a solvent molecule. The accuracy of lifetime measurements is ±10%, and that of the q is ±0.5. Therefore the variation in the calculated q values is within the experimental error.

The complexes equipped with uridine quenchers have shorter luminescent lifetimes than their adenosine-bearing analogues. In the case of the Tb complexes Tb(**150a**) and Tb(**150b**) the variation is as high as 38%. This can be explained by the differences in the abilities of the quenchers to stop RET from the antenna to the metal, uridine being a more efficient quencher of coumarin 2 than adenosine.

5.9 Luminescent properties of the Eu and Tb complexes

5.9.1 Europium complexes

5.9.1.1 Changes in the luminescence intensity

Measurements of the luminescent intensities of the europium complexes of the ligands **150a** and **150b** in pH 7.4 aqueous solutions, in the presence of increasing amounts of the complementary bases of the quenchers did not give reproducible results. In methanol, and mixtures of methanol and unbuffered water, and methanol and acetonitrile, addition of adenosine to **151a** resulted in the increase in the intensity of the peaks at 588 nm and 613 nm. The increase of luminescence intensity is caused by removal of the quencher from the **D-Q** interaction, and an increase in the efficiency of the energy transfer from the antenna to the lanthanide (*Figure 45*).

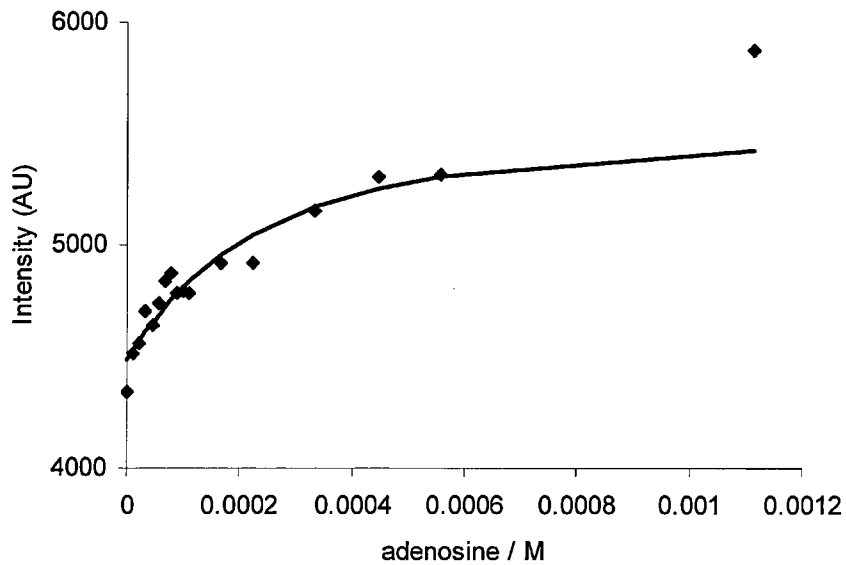

*Figure 45. Changes in the luminescent lifetime of the europium in the complex **151a** upon the addition of the complementary base adenosine. (methanol / acetonitrile, excitation @ 328 nm, detection @ 588 nm)*

5.9.1.2 Changes in the luminescent lifetime

The luminescent lifetimes of both **151a** and **151b** have been determined in the presence of increasing levels of the complementary bases. In both cases an increase of ~0.05 ms in the europium lifetime was observed (*Figure 46 and Figure 47*). The reason for this is the same as for the increase in the luminescent intensity in methanolic solutions, namely base-pairing between the quencher and its complementary base. It is not likely that the complementary base is increasing the lifetime of the lanthanide ion by replacing the co-ordinated water molecules, as in the case of the terbium complexes both an increase and a decrease in τ was seen (See *5.9.2.2*).

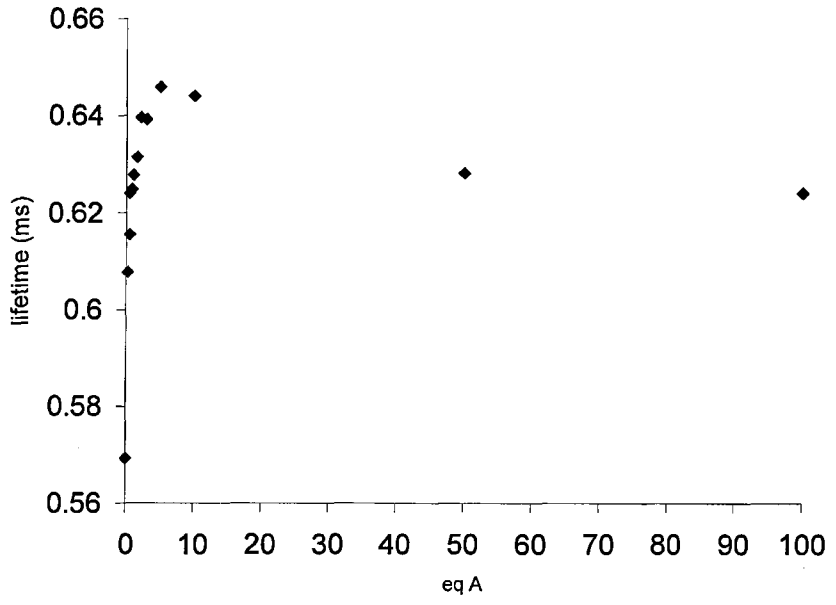

*Figure 46. Changes in the luminescent lifetime of the europium in **151a** upon the addition of the complementary base adenosine. (pH 7.4 aqueous MOPS buffer, excitation @ 328 nm, detection @ 615 nm)*

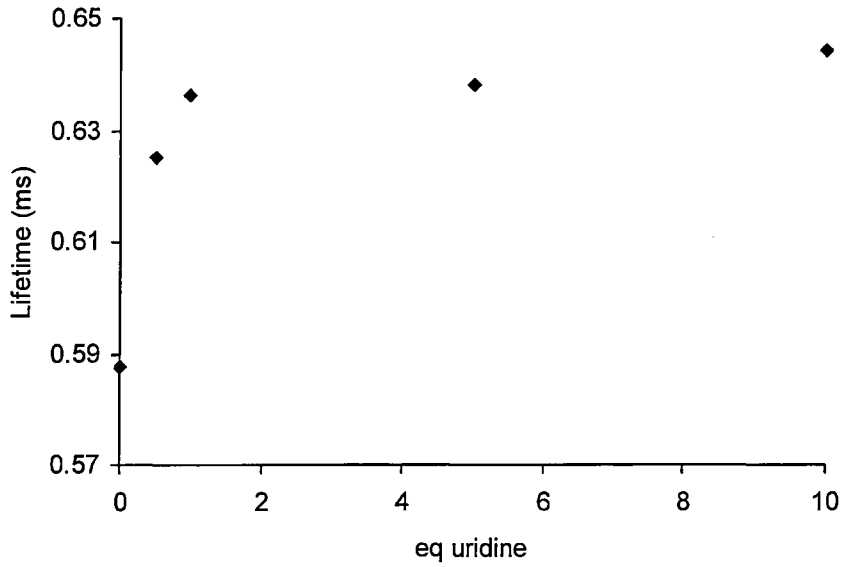

*Figure 47. Changes in the luminescent lifetime of the europium in **151b** upon the addition of the complementary base uridine (pH 7.4 aqueous MOPS buffer, excitation @ 328 nm, detection @ 615 nm).*

Direct quenching of the antenna by the added nucleoside is possible, but in the case of the europium complexes its lifetime-diminishing effect is compensated for by the lifetime increase caused by base pairing between the quencher and the complementary base.

The deviations in the initial lifetimes can be caused by the differences in the pH of the aqueous solutions (non-buffered *vs* pH 7.4), in addition to the inherent imprecision of the lifetime determination.

5.9.2 Terbium complexes

5.9.2.1 Changes in the luminescence intensity

The luminescence intensities of both terbium complexes (**152a** and **152b**) decreased upon titration with their complementary bases. One equivalent of

adenosine decreased the luminescence of the coumarin 2 – uridine – Tb (**152a**) complex by 37%. One hundredfold excess of adenosine resulted in only 7% further loss, suggesting a strong interaction between the complex and the nucleoside.

Similar results were obtained for the coumarin 2 – adenosine – Tb complex (**152b**), the intensity loss induced by one equivalent of uridine being 20% (*Figure 48*).

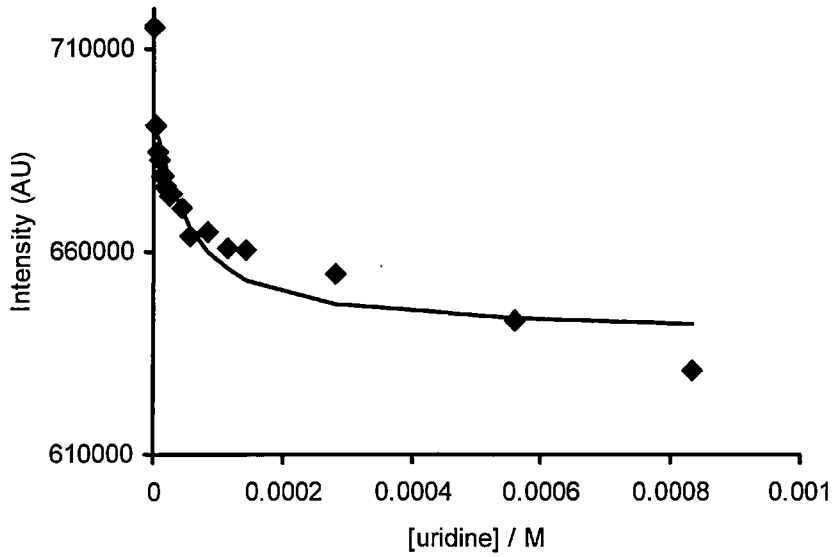

*Figure 48. Quenching of the Tb complex of the **150b** ligand (**152b**) with uridine (pH 7.4 aqueous MOPS buffer, excitation @ 328 nm, detection @ 545 nm).*

Base pairing is probably also occurring in this case with the result of an increase in the lifetime, but it has to compete with the quenching of the **Q** in the close proximity of the **D**, and direct quenching of the **D** by the added nucleoside. As Tb is relatively short-lived (approximately 0.5 ms), the diffusion-controlled base pairing, which is also dependent on the orientation of the

nucleosides, might not be able to compete with the quenching processes. The result is a decrease in the luminescence intensity.

5.9.2.2 Changes in the luminescent lifetime

The two terbium complexes behaved differently when their luminescent lifetimes were determined in the presence of their complementary bases. The lifetime of the complex **152a** increased when adenosine was added. The change in the τ levelled after the addition of approximately 50 equivalents of adenosine, and in total amounted to ~1 μs (*Figure 49*). The increase in the lifetime is due to the removal of the potent uridine quencher from the proximity of the donor because of the formation of the U-A pair.

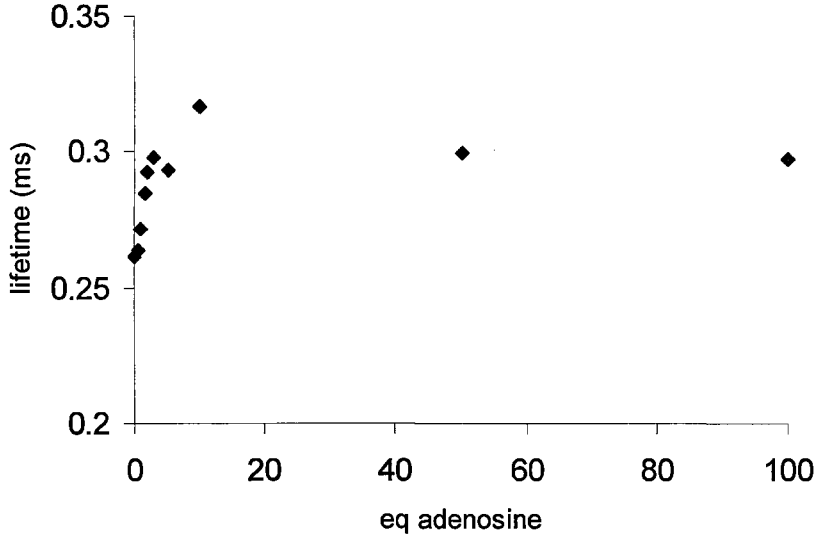

*Figure 49. Changes in the luminescent lifetime of the Tb complex **152a** upon the addition of adenosine (pH 7.4, exc @ 328 nm, det @ 615 nm).*

A decrease in the terbium τ of **152b** was seen in the presence of uridine (*Figure 50*). This is probably caused by direct quenching of the **D** by the added uridine.

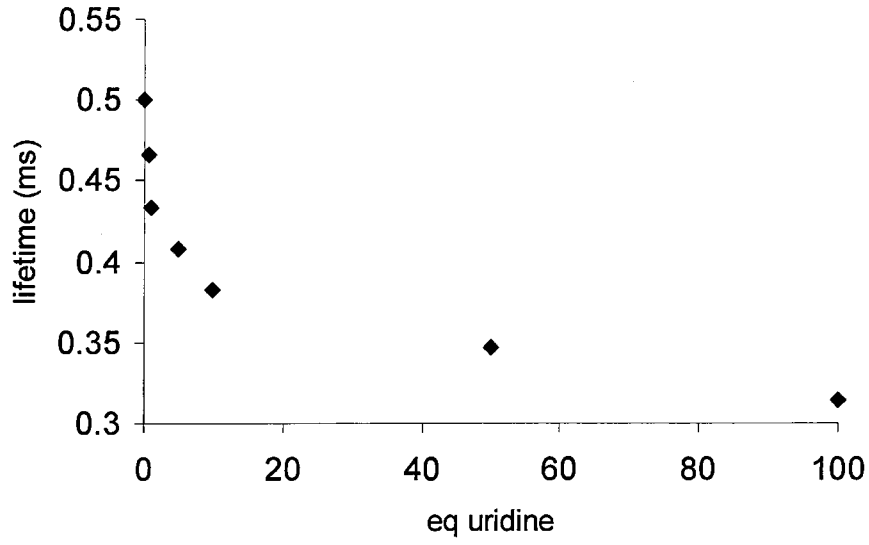

*Figure 50. Changes in the τ of the Tb in **152b** upon the addition of uridine (pH 7.4, exc @ 328 nm, det @ 615 nm).*

5.10 Lanthanide triads and DNA

5.10.1 Europium complexes

5.10.1.1 Changes in luminescence intensity

Addition of double stranded salmon testis DNA to pH 7.4 aqueous solutions of the europium complexes resulted in the decrease in luminescence intensities (*Figure 51*). This is probably due to intercalation of the coumarin 2 antenna with DNA. This is indicated by the decrease in the coumarin 2 excitation spectrum.

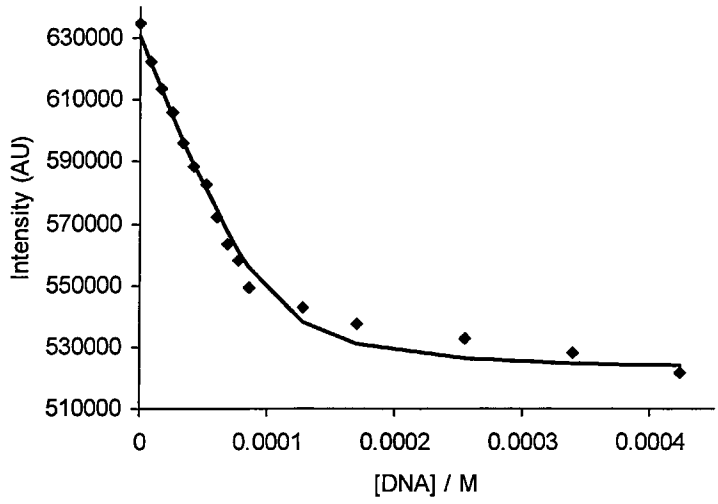

*Figure 51. Changes in the luminescence intensity of the Eu complex of the **150b** ligand upon the addition of DNA (pH 7.4, exc @ 328 nm, det @ 615 nm).*

5.10.1.2 Changes in luminescent lifetime

When determining the luminescent lifetimes of the europium complexes in the presence of DNA, no consistent data were obtained. It is probable that there are a number of competing reactions going on, including intercalation of the antenna, and binding of the central atom to the negatively charged phosphate backbone of the DNA. It is impossible for us to determine the individual effects of these processes, and their reaction rates. Intercalation of the antenna would decrease the luminescent lifetime, while base pairing of the quencher could act both ways. Replacement of the O-H oscillators of the bound water molecules with P-O oscillators increases the lifetimes, as P-O bonds cannot vibronically couple with Ln excited states.

5.10.2 Terbium complexes

5.10.2.1 Changes in luminescence intensity

The terbium complex **152a** behaves unpredictably. When DNA was added to the solution, both increase and decrease in the intensity has occurred, although not within the same measurement.

The intensity of the second terbium complex (**152b**) decreased considerably upon the addition of DNA (*Figure 52*), probably due to the intercalation of the coumarin 2 with the DNA strands.

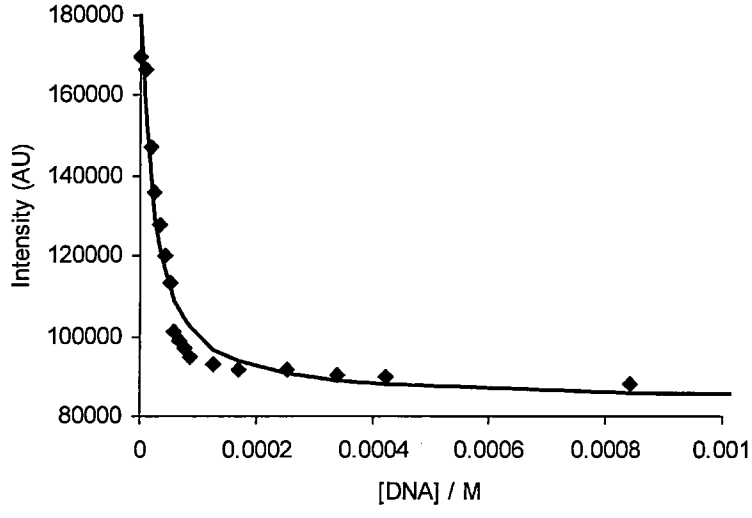

*Figure 52. Changes in the luminescence intensity of the Tb complex of the **150b** ligand upon the addition of DNA (pH 7.4, exc @ 328 nm, det @ 545 nm).*

5.10.2.2 Changes in luminescence lifetime

The luminescent lifetime of the terbium complex of ligand **150b** decreased in the presence of DNA, until a [complex] : [bp] = 1 :1 ratio (*Figure 53*) was reached.

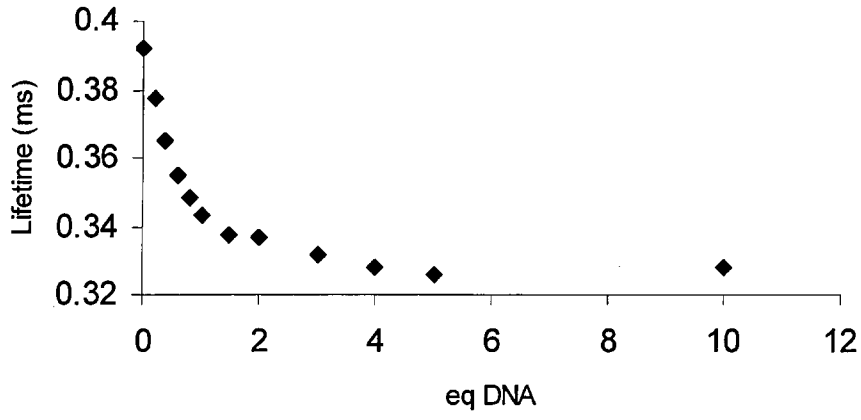

*Figure 53. Changes in τ of **152b** upon the addition of DNA (exc @ 328 nm, det @ 545 nm)*

When the ratio of the initial lifetime and the actual lifetime was plotted against the DNA base pair concentration, a Stern-Volmer-type plot was obtained, which behaved very similarly to the intensity-based plots. Fitting a curve to the linear section of the data provided a Stern-Volmer-type constant of $1.7 \cdot 10^3$, which is in good agreement with the $6.8 \cdot 10^3$ calculated previously.

The τ of the Tb complex of ligand **150a** increased in the presence of DNA. A tenfold excess of dsDNA raised the lifetime by 0.01 ms (*Figure 54*).

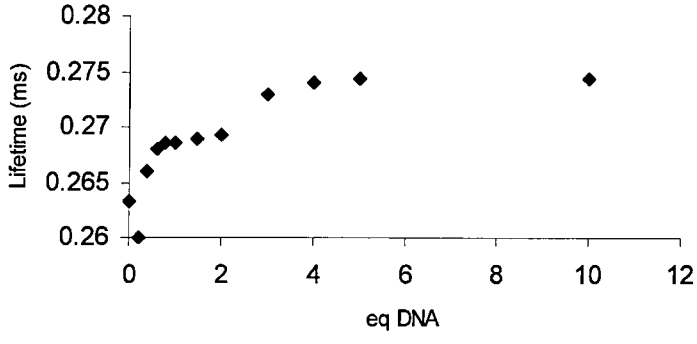

*Figure 54. Stern-Volmer-type plot of the quenching of **152a** with DNA (exc @ 328 nm, det @ 545 nm)*

5.11 Stern-Volmer constants for the quenching of the complexes

Stern-Volmer constants were calculated for the quenching of the lanthanide complexes with their complementary bases and dsDNA (*Figure 55a-b*).

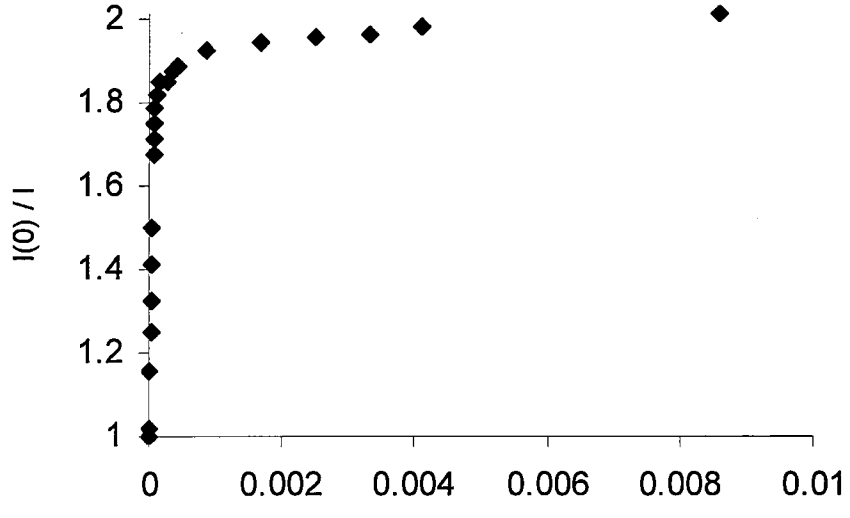

Figure 55a

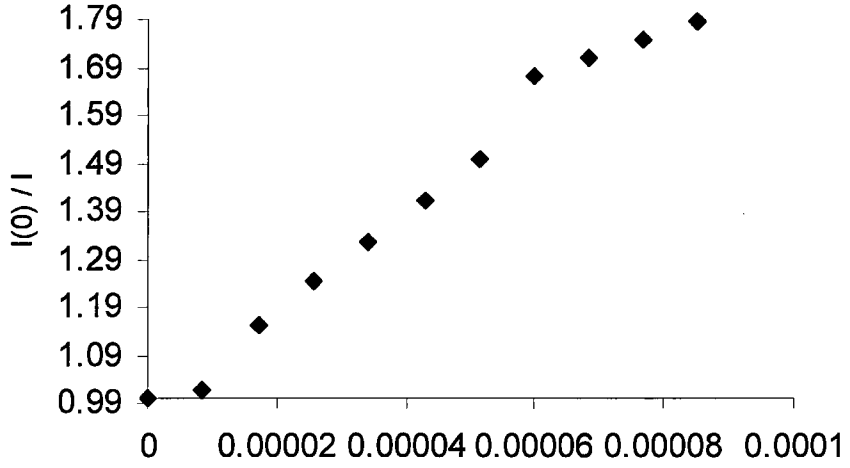

Figure 55b

Figure 55a and 55b. Stern-Volmer plot of the quenching of ***152a*** *with DNA. Fitting y = mx + b (b = 1.0, y = I_0 / I, x = [Q]) to the first part of the curve (55b) yields m = $1.0 \cdot 10^4$.*

The Stern-Volmer constants obtained by fitting linears to the data are summarized below (*Table 13*). The Stern-Volmer constants' values are in good correlation with the intensity changes observed.

	Eu(**150a**)	Tb(**150a**)	Eu(**150b**)	Tb(**150b**)
c.b.	*	$6.8 \cdot 10^3$	*	$8.4 \cdot 10^3$
DNA	*	$1.0 \cdot 10^4$	$1.8 \cdot 10^3$	$6.8 \cdot 10^3$

*Table 13. Stern-Volmer constants of the quenching of the lanthanide complexes by DNA and the complementary bases. *No consistent data were obtained and the K could not be calculated.*

5.12 Lanthanide ligands emitting in the near infrared region

Luminescent probes emitting in the near IR region have the advantage of interference-free detection of the target, as autofluorescence of the sample is usually insignificant at wavelengths longer than 500 nm. Tissue penetration of light increases with the wavelength, which means that near IR-emitting probes are better suited for *in vivo* imaging than those emitting in the UV-Vis region.

There are organic chromophores with suitable emission wavelengths available,[90] but they are usually insoluble in aqueous solutions, making them inappropriate for detection in biological samples. The lanthanide ions Nd and Yb have emission wavelengths > 850 nm, can be sensitized by fluorescein or rhodamine, and can be complexed by suitable ligands to yield water-soluble complexes.

5.12.1 Synthesis of the ligand with rhodamine B donor

Cyclen-based ligands for the sensitisation of near IR emitting lanthanides (Nd or Yb) were designed. The principle of the ligands was similar to that of the coumarin 2 bearing ones: a cyclen scaffold holding together an antenna – quencher pair and serving as a chelator for the metal. For the sensitisation of Yb and Nd antennae with energy levels closer to the lanthanides are necessary, typically fluorescein or rhodamine.

Rhodamine B was attached *via* an amide bond to 2-bromoethylamine. The reaction was carried out with 1.1 equivalent of EDCI coupling agent, 1 equivalent of 2-bromoethylamine hydrobromide neutralized by 1 equivalent of TEA. The product (**165**) was isolated after standard aqueous workup and silica column chromatography (*Scheme 22*).

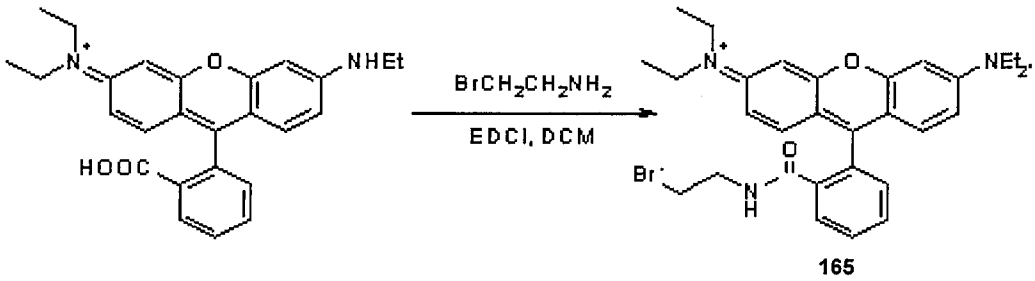

165

Scheme 22. Attachment of rhodamine B to bromoethylamine.

165 was used to alkylate cyclen in refluxing 100% ethanol under argon atmosphere in the presence of three equivalents of triethylamine base. The monoalkylated cyclen (**166**) was isolated after standard aqueous workup followed by chromatography on basic alumina.

166 was afterwards alkylated in chloroform with N-Boc-bromoethylamine with ten equivalents of triethylamine base. After silica column chromatography the bis-alkylated cyclen (**167**) was obtained in high purity in moderate (20%) yields (*Scheme 23*).

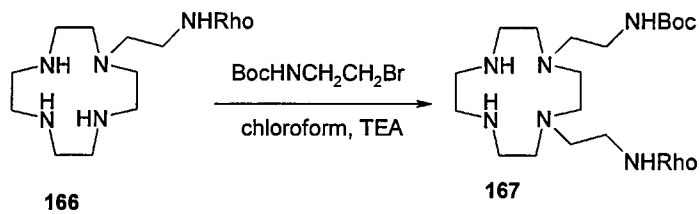

166 167

*Scheme 23. Alkylation of the N4 nitrogen of the rhodamine B-equipped monoalkylated cyclen (**166**) with N-Boc-bromoethylamine.*

Alkylation of the two remaining cyclen nitrogen atoms with ethyl bromoacetate proceeded smoothly in dry acetonitrile with potassium carbonate base and sodium iodide catalyst. After aqueous workup followed by silica column chromatography the tetrasubstituted cyclen (**168**) was isolated in good yields and high purity. Removal of the Boc protection was achieved by acidolysis in TFA / DCM to yield **170**. The 5'-carboxylic acid nucleosides (adenosine or

uridine) were attached to the primary amino group of **170** with EDCI coupling reagent. The final products (**171a-b**) were purified by silica column chromatography (*Scheme 24*).

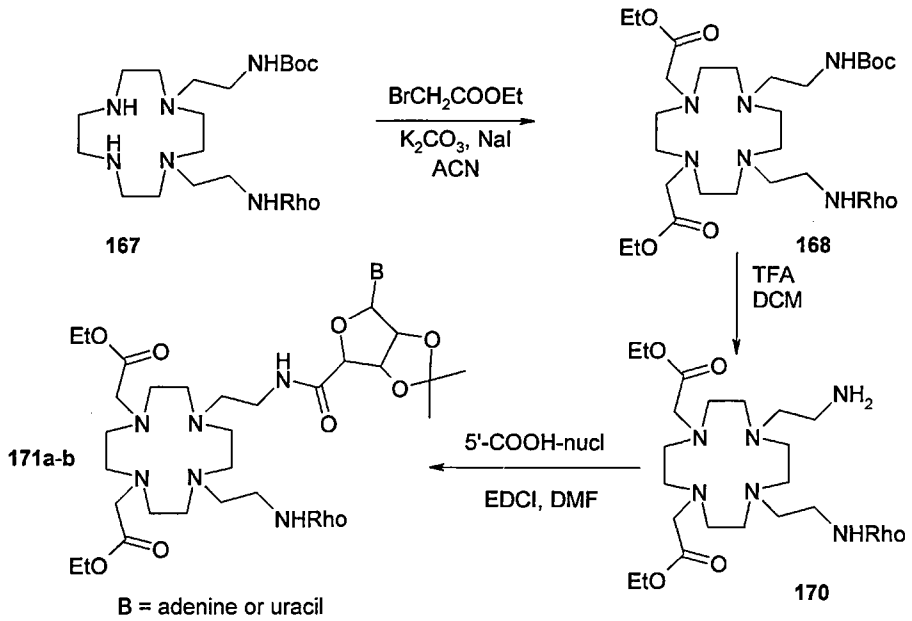

*Scheme 24. Attachment of the stabilizing ethylacetoxy arms and the nucleoside quenchers to the dialkylated cyclen **167** in the synthesis of the rhodamine antenna-bearing ligands **171a-b**.*

5.12.2 Synthesis of the ligand with coumarin 2 and rhodamine B donors

A cyclen-based ligand for near IR-emitter lanthanides was designed to signal DNA by the decrease in lanthanide luminescence intensity. The ligand was equipped with the fluorescent donor coumarin 2, that after excitation at ~330 nm could transfer its energy to rhodamine, situated in the *cis* position to coumarin 2. Rhodamine would act as an antenna for the lanthanide (Nd or Yb), so upon excitation of coumarin 2, emission from the lanthanide would be seen. When DNA is present, intercalation of the primary donor coumarin 2 would prevent lanthanide emission. If both donors intercalate, lanthanide luminescence would decrease irrespective of the excitation wavelength. If only coumarin 2 is quenched by the DNA, decrease in the luminescence intensity is expected upon

excitation of the complex at ~330 nm, while no changes are expected upon direct excitation of the rhodamine (440-500 nm).

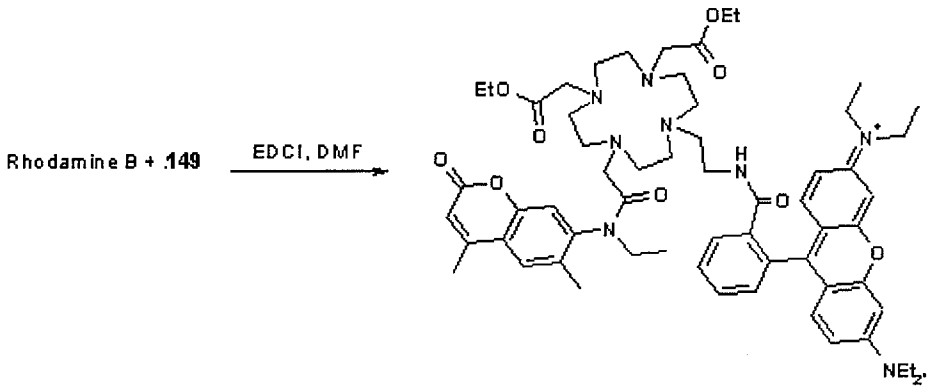

*Scheme 25. Coupling the secondary donor Rhodamine B to **149**.*

The ligand was prepared by attaching rhodamine B to the previously synthesised tetraalkylated cyclen-derivative (**149**). The carboxylic acid of rhodamine B was coupled to the primary amino group in the tetraalkylated cyclen (*Scheme 25*). The reaction was carried out in DCM with the help of 1.5 equivalents of EDCI. The rhodamine B was preactivated for 15 minutes, after which 1 equivalent of the cyclen derivative was added to the solution. The product was isolated after silica column chromatography in 65% yield.

5.12.3 Synthesis of the Nd and Yb complexes

Complexation of Nd and Yb with all three rhodamine-based ligands was carried out in refluxing HPLC-grade methanol. In 12 hours, under an inert atmosphere, the complexes formed in moderate yields (40-50%). Purification by trituration with cold diethyl ether followed by freeze-drying from water removed both remaining starting materials. Thin layer chromatography on both silica and alumina plates confirmed the purity of the samples.

The ^1H NMR-spectra of the complexes showed the most affected cyclen hydrogens shifted upfield and the aromatic protons shifted downfield. The free ligand spectrum was very complex due to the asymmetry of the ligand. This complexity was reduced significatly after complexation, as the CH_2 signals appeared unresolved. Similarly, the aromatic and sugar CH-signals lost their fine structure, and became broad singlets instead of multiplets.

The spectra showed the hydrolysis of the ethyl esters. This happened probably during the complexation reaction, the presence of the Lewis acid metal and the elevated temperature would both assist. The molecular ion of the complexes was seen only in one case on the mass spectra of the compounds, but the TLC in combination with the ^1H NMR, and the luminescence spectra prove the formation of the Nd and Yb complexes.

5.12.4 Photophysical properties of the near IR-emitting complexes

After complexation with neodymium and ytterbium the photophysical properties of the near IR-emitters were determined in HPLC-grade methanol. The ligands and the complexes absorbed strongly at 545 nm and 355 nm, because of the rhodamine. The exciplex ligand (**161**) had an additional absorption maximum at 320 nm, due to the coumarin 2 moiety.

The excitation and emission spectra of the exciplex ligand were taken in methanol. Excitation of the primary donor coumarin 2 at 328 nm resulted in a weak coumarin 2 emission at 440 nm, due to incomplete RET to the rhodamine, and a very intense emission at 580 nm from the rhodamine. Addition of dsDNA to the solution of the exciplex resulted in rapid decrease of the emission intensity when excitation was performed on the coumarin 2. Direct excitation of

the rhodamine was also possible, but the emission intensity remained unchanged. This was exactly the result expected, as this means that the rhodamine is not intercalating with the DNA, while the coumarin 2 is efficiently quenched by it (*Figure 56*).

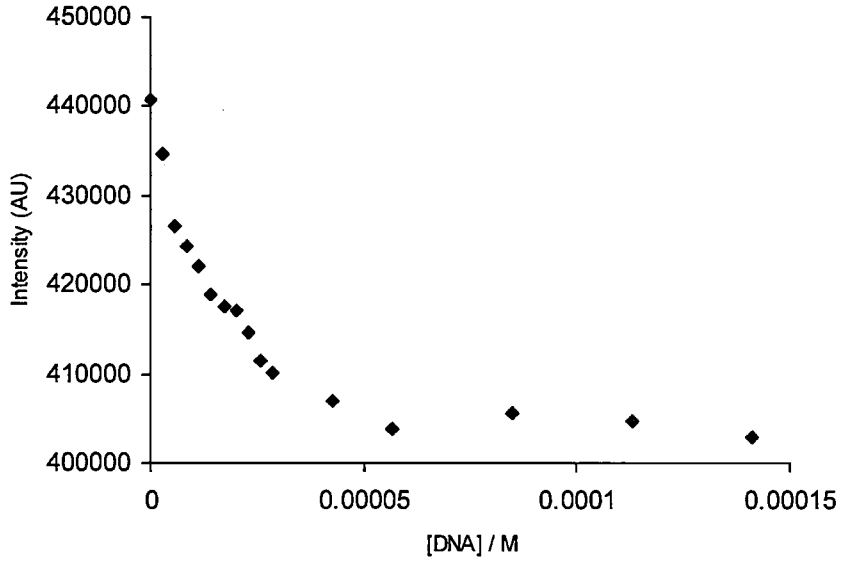

*Figure 56. Changes in the luminescence intensity of the exciplex ligand **161** upon addition of dsDNA. Excitation @328 nm (coumarin 2), emission @ 580 nm (rhodamine).*

It was not possible to fit a binding curve to the data points and calculate an association constant. The K is probably $>10^4$, and the interaction between the DNA and the ligand is very strong.

*5.12.4.1 Nd and Yb complexes of the exciplex **161***

The Nd and Yb complexes in methanol displayed the charateristic near IR emission. The **161**(Nd) complex had an emission line at 890 nm ($^4F_{3/2} \rightarrow {}^4I_{9/2}$)

and one at 1064 nm ($^4F_{3/2} \rightarrow {}^4I_{11/2}$). The ytterbium complex emitted at 980 nm ($^2F_{5/2} \rightarrow {}^2I_{7/2}$).

The emission intensity at 1065 nm in the Nd complex decreased significantly upon addition of one equivalent of DNA, when the emission was recorded 100 ns after excitation (*Figure 57*). The 890 nm emission band remained almost intact.

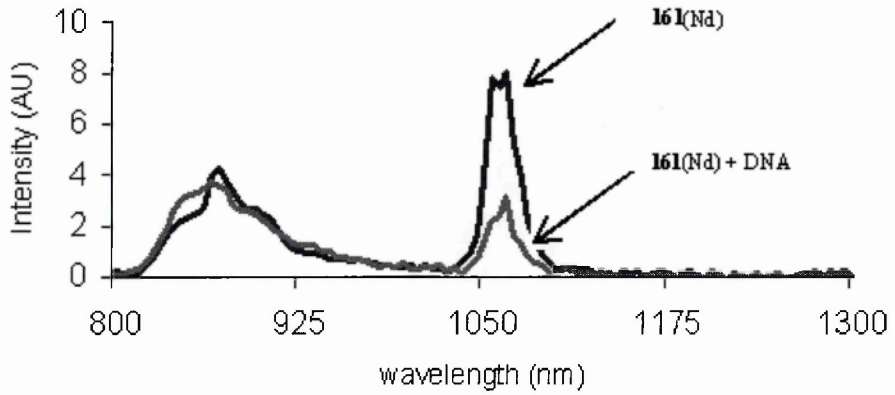

*Figure 57. Intensity changes of **161**(Nd) upon addition DNA. The broad emission band centred around 870 nm is partially caused by the rhodamine.*

Analysis of the time resolved spectrum at 890 nm revealed a minor decrease in the overall emission intensity (*Figure 58*). Unfortunately the 1065 emission band is overlapping with the beam of 1065 nm wavelength coming from the excitation, making it impossible to separate the two signals.

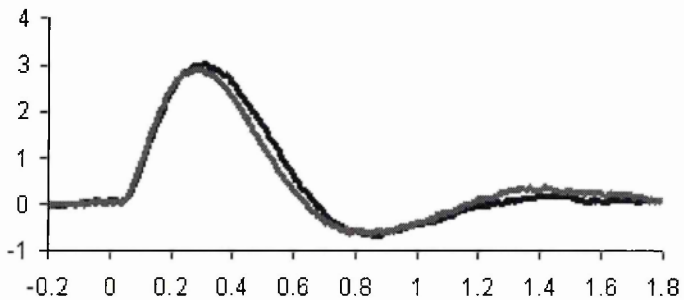

*Figure 58. Intensity changes of **161**(Nd) upon addition DNA. Emission detected at 890 nm between –200 ns and 1800 ns.*

5.12.4.2 *Emission of the Nd and Yb complexes of **171a** and **b***

The luminescence intensities of the Nd and Yb complexes of **171a** and **171b** were significantly lower than the Nd and Yb complexes of the exciplex (**161**). Although the intensity is strongly dependent on the experimental setup, and it is difficult to compare the two sets of compounds, the emission spectra suggest that the rhodamine is efficiently quenched by the adenosine, and to a lesser extent, by the uridine moieties (*Figure 59*).

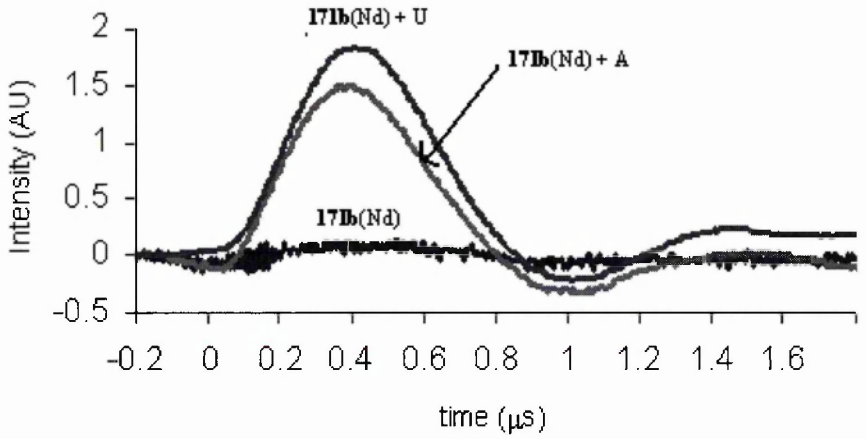

*Figure 59. Increase in the luminescence intensity of **171b**(Nd) at 890 nm (emission monitored for 1.8 μs).*

On the other hand comparision of the emission intensities of the complexes in the presence and in the absence of the **Q** complementary bases is possible. All else being equal, the emission intensity depends on the concentration of the solutions and the strength of the excitation beam. It is expected that addition of the complemetary bases in concentrated solutions is not going to affect the concentration significantly. The effect of the variations in the excitation intensity can be eliminated by removal of the pump signal from the recorded spectrum. This was carried out using data for one wavelength for each complex were processed. For the neodymium complexes this was the emission at 890 nm,

and for the ytterbium compounds the 980 nm. Theoretically it is possible to use the 1065 nm emission of the Nd, but it is very close to the third harmonics of the excitation wavelength (355 nm), which could make the results ambiguous.

The luminescence intensity of the Nd complex of ligand **171a** decreased upon addition of one equivalent of adenosine. Initially the complex **171b**(Nd) was non-luminescent. Addition of uridine complemetary base disrupted the quenching of the rhodamine by the adenosine because of base pairing between U and A. Thus the rhodamine could act as an antenna for the Nd, and emission from the metal was observed upon excitation of the rhodamine.

The luminescence intensity of the Yb complex of **171b** increased upon addition of the U complemetary base (*Figure 60*), while that of the **171a** decreased.

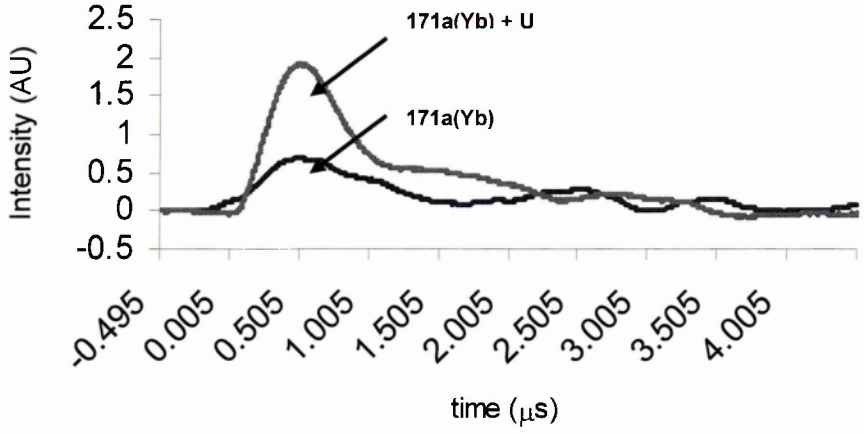

*Figure 60. Increase in the luminescence intensity of **171a**(Yb) at 890 nm (emission monitored for 1.8 μs).*

This seems to be contradictory to the results of the Nd complexes, where the rhodamine was quenched more efficiently by the adenosine. This contradiction can be explained if the differences in the luminescent lifetimes of the metals are taken into account. The τ for Nd(III) is typically shorter than 300 ns, it is

sometimes well below 200 ns.[91] Ytterbium compounds on the other hand can have lifetimes as long as several microseconds.[92] This means that diffusion-controlled quenching processes affect the Yb quantum yields more than the Nd quantum yields. So in a solution where the complementary base can both pair with the quencher and quench the antenna, both diffusion-controlled processes, these effects are going to be more pronounced in the case of the Yb complexes. It is likely that the adenosine, when part of the ligand, quenches the rhodamine, while uridine does it much less efficiently. This difference is more pronounced for Nd, where energy transfer from the rhodamine to the metal is fast, and the quenching by the uridine cannot compete with it. To Yb the energy transfer from the rhodamine is slower, and the uridine can quench the rhodamine excited state to some extent. Addition of the adenosine complementary base results in direct quenching of the rhodamine, which is seen for the Nd complex. Base pairing with the uridine **Q** is also likely, but is probably slower than the direct quenching, as the bases need to be in the appropriate orientation. Adenosine increases the Yb intensity by disrupting the quenching through base pairing with the U. Uridine is probably also quenching the rhodamine directly, but the overall effect is that of an increase in the emission intensity. This is supported by the observation that an even greater intensity increase is seen if, instead of adenosine, uridine is added to the solution of **171a**(Nd). Uridine can form base pairs with the uridine quencher of the ligand, and, as seen in *5.3.3* this interaction is of similar strength than the one forming the U-A Watson-Crick pair. Therefore the quencher is removed from the proximity of the rhodamine, which increases the emission intensity. In addition to this, the direct quenching of the dissolved uridine is less efficient

than that of the adenosine, which explains why adding uridine to the complex induces an even bigger intesity increase than adding adenosine.

It also explains why the complexes with adenosine quenchers behave in the opposite way. Adenosine is a very good quencher, and stops RET from the rhodamine to the metal. As uridine is not quenching the rhodamine very efficiently, the small diminishing effect of the direct quenching of the antenna by the complemtary base is overridden by the enhancement caused by the 'removal' of the adenosine from the proximity of the antenna. Uridine can pair with the adenosine, and disrupt the quenching of the rhodamine, as seen in the increase of the luminescent intensity of the **171b**(Nd) (*Figure 59*).

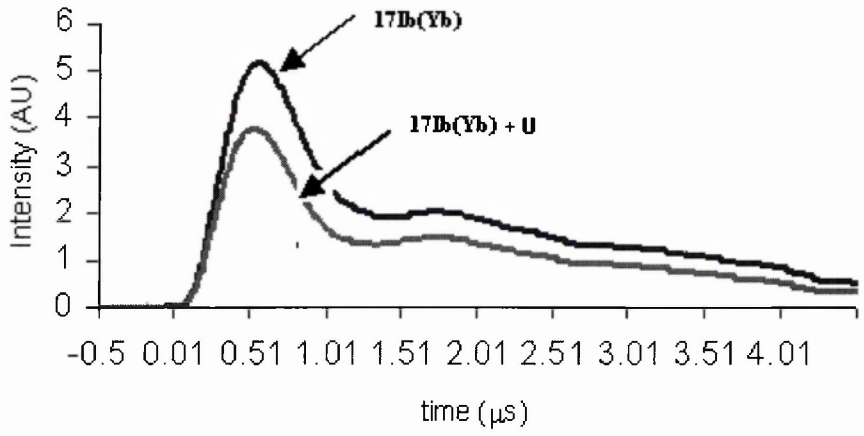

*Figure 61. Decrease of the luminescence intensity of the **171b**(Yb) complex upon addition of the uridine complementary base (methanol, excitation @ 355 nm, emission at 980 nm).*

In the case of the ytterbium complex the base pairing is probably not slowing the quenching down enough to induce an intensity increase, and the direct quenching is also able to compete with the energy transfer from the antenna to the metal. The result is that of a decrease in the emission intensity (*Figure 61*).

5.12.4.3 Luminescent lifetimes of the near IR-emitter complexes

The luminescent lifetimes of the Nd and Yb complex of the exciplex **161** and **171a** and **171b** were measured in methanol. The lifetimes of **161**(Nd) and **161**(Yb) were also determined in the presence of 1 equivalent of dsDNA. The τ of **171a**(Yb) and **171a**(Nd) were measured upon addition of 1 equivalent of adenosine, and that of **171b**(Yb) and **171b**(Nd) in the presence of 1 equivalent of uridine. The results are summarised in *Table 14.*

The results are in general in good agreement with the lumiescence emission data.

	161(Nd)	**161**(Yb)	**171a** (Nd)	**171a** (Yb)	**171b** (Nd)	**171b**(Yb)
τ(μs)	0.20	1.08	0.09	2.61	-[a]	2.23
τ(μs)*	0.54	0.73	-	-	-	-
τ(μs)**	-	-	0.47	0.89	0.23	1.17
τ(μs)***	-	-	0.81	-	0.16	-

*Table 14. Lumienescent lifetimes of the near IR-emitting lanthanide complexes in methanol. * 1 eq DNA added, ** 1 eq complementary base added, *** 1 eq own base added. [a] lifetime could not be calculated.*

The **161**(Yb) complex had an initial lifetime of over 1 microsecond, which decreased to 730 ns when DNA was added. This is expected if the coumarin 2 is intercalating with the DNA strands and this quenching can compete with the energy transfers from the coumarin 2 to the rhodamine and the from the rhodamine B to the Yb.

Complex **161**(Nd) had an initial lifetime of 201 ns. This value more than doubled when DNA was added to the solution. The result cannot be explained by

assuming that the coumarin 2 quenching by the DNA is much slower than the energy transfer steps. If this were the case, the lifetime would not change. The excitation spectrum of the free ligand has two maxima below 500 nm, one around 330 nm, the other at 355nm, which are overlapping. Excitation at 355 nm produces both **D1*** and **D2*** (excited rhodamine B). The energy levels of these two moieties lie sufficiently close to each other for energy transfer to take place both directions. It is likely that intercalation of the **D1** slows down the energy transfer from the rhodamine to the coumarin 2, and the **D2** → metal transfer does not have to compete with the **D2** → **D1** process anymore. The overall effect is that of an increased lifetime. The decrease in emission intensity is not in contradiction with this. It was not a huge effect and, as at 355 nm the rhodamine was mainly excited and not the coumarin 2, intercalation removes a species competing for the energy of the **D2**. The intensity decrease is due to a decrease in the 'total antenna area' of the coumarin 2 and rhodamine B.

The slowing down of the **D2** → **D1** transition probably determines tha lifetime of the Yb complex as well, but it is probably still not slow enough to make an efficient contribution to the τ. In this case, the removal of the excitable coumarin 2 donor from the energy accumulation is not compensated for by the slowing down of the **D2** → **D1** energy transfer, and τ therefore decreases. The other two ytterbium complexes have lifetimes well over 2 μs, indicating that there is an efficient procedure competing with metal sensitization in the **161** complexes. To decide unambiguously if it is RET from the rhodamine to the coumarin 2 that is causing the observed effects, selective excitation of the coumarin 2 should be performed at 328 nm, and selective excitation of the rhodamine B at 545 nm. If rhodamine B is excited at 545 nm, thermal repopulation of the coumarin 2

becomes impossible, and the energy transfer rate from the rhodamine to the metal can be determined.

The Nd and Yb complexes of the **171a** and **171b** ligands had luminescent lifetimes in accordance with those found in the literature, i.e., on the microsecond timescale for the Yb compounds, and on the nanosecond for the Nd compounds.[89] The measured lifetimes are somewhat shorter than most found in the literature for Yb and Nd complexes, suggesting that the quenchers are shortening the τ in all cases. Upon addition of the nucleotides to the solutions the changes in the lifetimes were of the same nature as the intensity changes. Adding adenosine or uridine to the strongly quenched **171a**(Nd) complex increased the lifetime because of the removal of the **Q** from the proximity of the rhodamine. The lifetimes of the ytterbium complexes were shortened by the direct quenching of the antenna by the added nucleoside. The magnitude of the lifetime shortening was in accordance with the quenching abilities of the nucleosides, as adding adenosine to **171a**(Yb) caused a larger drop in τ than adding uridine to **171b**(Yb).

5.13 NMR titrations

To establish where the interaction between the triads and their complementary bases occurs, the triads were titrated with their complementary bases, and the process was monitored by ^{1}H NMR. The bases could form pairs with the quenchers through hydrogen bonding, or it is also possible, that they interact directly with the donor. The latter is even more likely in the light of the fluorescence titrations, where instead of the expected increase of luminescence intensity, further quenching of the triads was observed. NMR is able to determine which of the two processes goes on. If base pairing occurs, the signal of the quencher base hydrogens is expected to shift. In the case of adenosine, the amino hydrogen signal could also change, either in intensity, or its chemical shift. If the complementary base interacts directly with the donor, the coumarin signals may alter, although the lack of such a change does not rule the direct quenching out.

The NMR titrations were carried out in deuterated DMSO, which was the only solvent to dissolve both the triads and the nucleotides in sufficiently high concentrations.

Fitting binding curves and calculating binding constants was not always possible. Where quantitative results were obtained the binding constants were approximately two orders of magnitude lower than calculated from the fluorescence data (*Table 15*).

	90a	90b	96b	150a	150b
K (d_6-DMSO)	-	$5.9 \cdot 10^2$	18	-	-

Table 15. Association constants calculated from the NMR-titrations in d_6-DMSO. Compounds were titrated with the complementary bases of the quenchers. 90a and 150a qith adenosine, 90b, 96b, and 150b with uridine.

Due to the diffences in the concentrations and the sensitivity of the two techniques, the data cannot be compared directly. Considering that the number of hydrgen bonds possible between the triad and the target is three at most, and that the binding was monitored in highly polar solvents at low concentrations, it is reasonable to accept the NMR titration results as the better approximations.

5.13.1 Organic triads

When the c120-c343-U (**90a**) organic triad was titrated with adenosine, neither the coumarin nor the uridine signals changed, apart from the shift caused by the changes in the solvent polarity.

Titration of the c120-c343-A (**90b**) triad with uridine shifted the aromatic and amide-NH signals downfield. While all coumarin signals, and the aromatic C-H protons of the quencher moved together by about 0.14 ppm, the NH_2 signal of the adenosine quencher was shifted by a further 0.10 ppm downfield. The quencher amine hydrogens moved from a starting position of 6.87 ppm to a final 7.11 ppm. Once one equivalent of the complementary base was added, changes were insignificant, suggesting a one to one binding between triad and target.

Similar results were obtained for the c151-c343-A (**96b**) triad, where the broad NH_2 signal moved from 6.23 ppm to 6.78 ppm. This titration was carried out in pure DMSO, which accounts for the difference in the position of the NH_2 signals. The large shift caused by the complementary base is probably due to better interaction between the uridine and the quencher in the aprotic DMSO.

5.13.2 Lanthanide ligands

The ^1H NMR spectrum of the cyclen-based ligand bearing coumarin 2 antenna and uridine quencher showed very interesting properties. The hydrogen signals for the OCH_3 groups of the uridine were expected to be singlets at approximately 1.35 ppm and 1.52 ppm. Similarly, the Me groups in the 4 and 7 positions of the coumarin are singlets around 2.33 and 2.50 ppm. One peak of each set is a singlet, but the OCH_3-signal at 1.36 ppm and the CH_3-peak at 2.33 ppm seem to be doublets, or two pairs of singlets of equal intensities. The latter is supported by the calculated coupling constants, 3.5 Hz and 2.7 Hz. One of the coumarin 2 aromatic hydrogens at 7.33 ppm, which is usually a siglet, becomes a pair of singlets with slightly different chemical shifts (7.32 and 7.34 ppm). These peaks cannot be due to some sort of through-space coupling of the groups to each other, and they cannot couple to any other hydrogens either, so it is more likely that two isomers of the ligand exist in solution.

During the titration, the two coumarin 2 aromatic hydrogen signals return to 7.33 ppm, and become one singlet again. The two aromatic methyl peaks at 2.33 and 2.34 ppm move closer to each other, and by the addition of three equivalents of adenosine they become one signal at 2.31 ppm. The OCH_3 peak

is more difficult to follow, as the 2'3'-isopropylideneadenosine, added during the titration, has two OCH_3 groups in very similar chemical environments.

One of the doublets of the uridine base C-H's, at 5.63 ppm is shifted to 5.73 ppm during the titration, suggesting the reduction of the electron density in its environment. The other signals corresponding to aromatic hydrogens remain at the same chemical shifts, which means that the interaction during the titration takes place between the quencher and its complementary base. What probably happens is that initially there are two isomers of the ligand in the solution. This might be because of the restricted movement of the quencher and the donor, caused by either some steric hindrance, or a stabilizing interaction between the aromatic rings of the two moieties. Addition of the complementary base means that the relative position of the **D** and the **Q** will be determined by the interaction of the **Q** and the adenosine. Either the **D** will be able to move freely, resulting in the simplification of the spectrum, or there will be one favoured conformation, which will have the same effect. Variable temperature NMR experiments could decide if there are two conformational isomers present. Increasing the temperature would increase the flexibility of the compound, and the two signals in the free ligand spectrum would collapse into one.

In the case of the ligand with the adenosine quencher, the OCH_3 peak at 1.59 ppm appeared as two singlets, similarly to the previous measurement. During the titration the two singlets became one singlet with an integration of three. As uridine has a much better solubility than adenosine, uridine could be added in the 2'3'-unprotected form, making it possible to follow the ligand OCH_3 peak. The broad singlet corresponding to the amino hydrogens of the adenosine were not detected, probably because the hydrogens have been exchanged in the

deuterated methanol, in which the sample was dissolved. There were some small changes visible in the spectrum, such as the broadening of the adenosine sugar hydrogen signals, and minor chemical shift changes in the aromatic region, but these could all be casued by the changes in solvent polarity.

6 CONCLUSIONS AND FUTURE WORK

A range of novel luminescent probes exploiting resonance energy transfer has been synthesised and characterised. The probes have a fluorescent donor and an acceptor, which can undergo RET, and a quencher, which regulates RET between the **D** and the **A**.

Three different types of compounds have been prepared: 'organic triads', bearing coumarin 343 **A**, lanthanide complexes equipped with europium and terbium lumophores, and near IR-emitting Nd and Yb complexes. In addition to these, model compounds with only the **D** and the **A** ('diads') have been synthesised to determine the unaffected photophysical properties of the **D-A** pair. A novel ligand for near IR-emitting Nd and Yb has been synthesised for the detection of DNA.

The three organic triads behaved in a way contrary to that expected, as their luminescence decreased in the presence of the target, instead of increasing. One of the triads, with c120 (**D**), c343 (**A**) and adenosine (**Q**) was successfully 'switched on' by the interaction with its target compound, the complementary base of the quencher. This indicates that careful tuning of the reaction rates of RET and quenching by altering the **D-A** and **D-Q** distances in the molecule, and varying the **D** and the **Q** to optimise the quenching can produce probes with enhanced emission wavelengths, zero, or significantly reduced emission in the absence of their targets, and increased emission upon target binding. The modular synthetic approach enables the simple and straightforward replacement of the functional units and the insertion of spacers.

Further possible synthetic targets could include the incorporation of novel quenchers both to optimise the quenching and to introduce recognition sites

with better discrimination. One such **Q** could be folic acid, as folic acid receptors are overexpressed on cancerous cells.[93] Other nucleosides, both natural and modified could be quenchers. Better water solubility could be achieved by the replacement of the ethyl acetylcarboxylate stabilizing arms with more hydrophilic moieties, for example sugars. Two such 'arms' have been synthesised (**122**, **123**). Their introduction into the ligands sould be analogous to the ethyl acetylcarboxylate introduction.

The lanthanide triads were rapidly quenched in pH 7.4 aqueous solutions by both the complementary bases and DNA, but in methanol an increase in the luminescence intensity of the Eu complex **150a** could be seen. As in the case of the organic triads, changes in the quencher could improve the photophysical properties of the probe.

Determination of the lifetimes of the probes both in the absence and in the presence of their target compounds suggested their ability to act as lifetime probes. Changes in the lifetimes of three of the organic probes (**90b**, **96a** and **96b**) were reproducible and significant. The changes caused by the nucleosides in the lifetimes of the Eu and Tb complexes enable the discrimination between adenosine and uridine in aqueous solutions. By determining the photophysical properties of the prepared compounds a qualitative overall picture was obtained of the rates of the energy transfer and quenching processes. This makes the design of better triads with optimised donor-quencher pairs possible.

The Yb and Nd complexes were incorporated into novel ligands, and the complexes behaved as near IR-emitting luminescent triads. The results obtained complete 'turning off' of one of the complexes (**171b**(Nd)) which was non-luminescent in the absence of its target. The compound became highly

luminescent when its substrate was added, making this complex the most successful of the synthesised triads in fulfilling the initial objectives of the project.

In addition of the luminescence results, a new, widely applicable synthetic strategy for the preparation of asymmetric, tetrasubstituted cyclen derivatives has been developed. This enables the convenient alteration of the functional units in the ligands, and the synthesis of a wide range of lanthanide-based luminescent probes.

7 LABELLING APTAMERS WITH RADIONUCLIDES

7.1 Introduction

7.1.1 Aptamers

Molecular recognition can be achieved with molecules of all sizes. In section ***2.3*** work carried out with relatively small molecules was described. Most of the probes presented there have been applied for the detection of the target species in model solutions containing a small number of components, while some of them were tested in non-aqueous media. A few of them have been used *in vitro* or *in vivo*. This is in large part due to their lack of discrimination between competing species, which is due to the flexibility of their recognition units. Much better specificity can be achieved using highly specified, naturally occurring probes. In biomedical research, target recognition by naturally occurring macromolecules and their *in vitro* modified versions is common. Antibodies, antibody fragments of various sizes and small proteins are all widely used for targeting.

Recently highly specific and selective molecular recognition has been achieved by DNA and RNA fragments. The methodology is based upon the selection of the better binding recognition units, their amplification, and determination of their structure. A library of oligonucleotides consisting of random DNA sequences is subjected to asymmetric PCR to obtain single-stranded DNA. In solution the DNA strands will each adopt a preferred 3D-geometry, as determined by their abilities to form intramolecular hydrogen bonds and other, weaker secondary bonds. This pool is brought into interaction with a target molecule on a solid support. Concentration of the binding sequences is

achieved by selective removal of the non-bound sequences, for example by washing, or with the application of a salt or pH gradient. If necessary, further selection and amplification steps can be performed. After 6-15 cycles the best fitting sequence or sequences are obtained, which can be determined by sequencing, and from then on produced in large quantities by solid-phase synthesis. This selection procedure is called SELEX, or 'systematic evolution of ligands by exponential enrichment' (*Figure A-1*).[94]

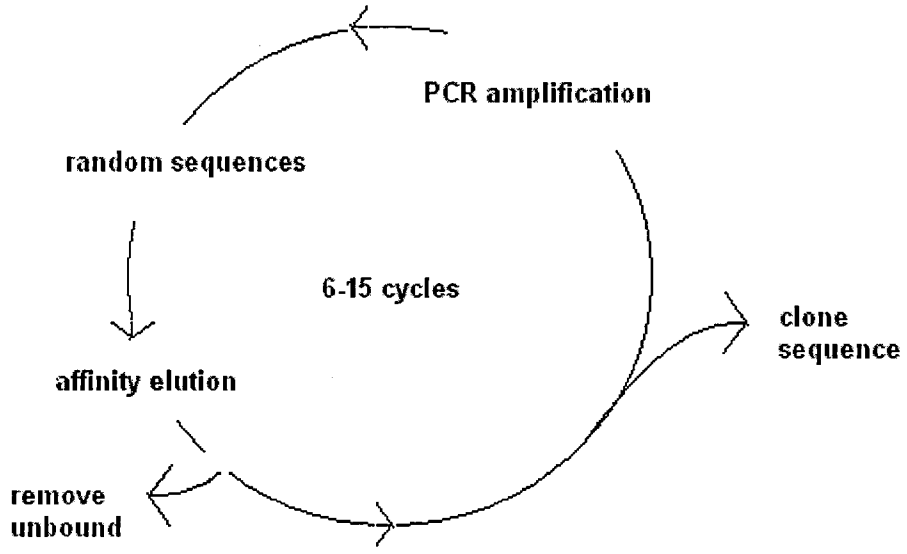

Figure A-1. The SELEX procedure.

The binding oligonucleotide obtained by this method is called an aptamer. The main advantages of aptamers over antibodies are that their synthesis can be automated once the sequence is known, chemical modifications can be carried out easily, and there is no need for *in vivo* experiments for their development. Compared to antibodies, which need several months to raise, aptamers can be developed in the space of a few weeks. It has also been possible to automate the aptamer acquisition.

Aptamers, being small oligonucleotides of 25-60 base pairs are quite unstable *in vivo*. Both for their increased stability and for the introduction of signalling and catalytic functions a number of chemical modifications can be carried out on the nucleotides (*Figure A-2*).[95]

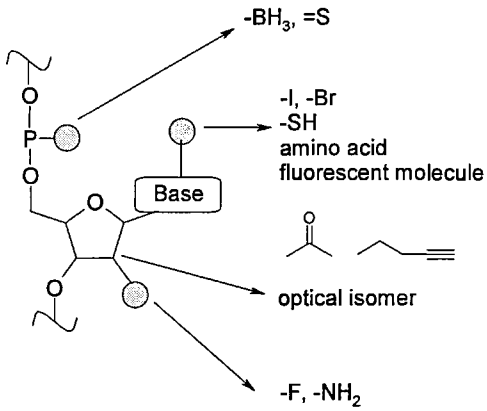

Figure A-2. Common modifications of nucleotides, introduced to enhance in vivo *stability, enable attachment of reporting moieties, or a catalytic function.*

Replacement of either the 3' or the 5' or both hydroxyl groups with fluoride or amino substituents increases nuclease resistance. Substitution of the oxo group in the phosphate backbone with sulfur, or the use of the non-natural optical isomer sugar has similar effects. Signalling or catalytic functions can be grafted onto the aptamer by the introduction of fluorescent labels instead of the bases. The modification of the natural bases with the introduction of bromine or iodine and thiol groups has been carried out to achieve photo-crosslinking and chemical crosslinking, respectively.

In a collaboration with Dr Sotiris Missailidis, aptamers raised against a tumour marker have been labelled with the fluorescent labels rhodamine and fluorescein. As a means of providing a standard, they have been labelled with the widely used radioactive metal technetium. Technetium-labelled aptamers could serve as efficient, easy-to-produce and relatively cheap *in vivo* imaging

tools, while their luminescent analogues could be used for *in vitro* detection of the targets.

7.1.2 Labelling of biomolecules

Molecules that are able to recognise biologically important targets have been labelled for various reasons. When having luminescent labels attached to them they are capable of visualising their target both *in vivo* and *in vitro*. It is possible to attach MRI-active compounds to molecules that are able to cross the blood-brain barrier to highlight anomalies in the brain, that are otherwise difficult to detect. γ-Emitting radionuclide carrying antibodies and tumour-specific peptides are applied for the visualisation of tumours (*Table A-1*). When the γ-emitter is replaced by a β- or α-emitter, or one emitting low energy electrons (Auger electrons), the labelled biomolecule can be used for the treatment of a number of illnesses, the most common being various forms of cancer.[96,97]

Nuclide	$T_{1/2}$	E_β (keV)	γ-ray (keV)	Source
^{64}Cu	12.8 h	570	511 (10%), 185 (24%)	Accelerator
^{67}Cu	2.6 d	570	184 (48%), 92 (23%)	Accelerator
^{99m}Tc	6.02 h	-	141 (89%)	^{99}Mo/^{99m}Tc generator
^{111}In	2.83 d	-	171 (88%), 247 (94%)	Cyclotron
^{131}I	8.0 d	810	364 (81%)	Reactor
^{67}Ga	3.3 d	-	93 (10%), 185 (24%), 296 (22%)	Generator
^{90}Y	2.7 d	2270	-	^{90}Sr parent decay[a]
^{186}Re	3.8 d	1070	137 (9%)	Reactor
^{188}Re	0.7 d	2110	155 (15%)	^{188}W/^{188}Re generator

Table A-1. Radionuclides used for therapeutic and imaging purposes, their half-lives and the energies of the β-particles and γ-radiation emitted. [a] ^{90}Sr is reactor-produced.

Radioactive labelling for both therapeutic and imaging purposes has as the advantage of high sensitivity and selectivity. Radioactive signals are easy to detect *in vivo*, as they are unique, and there is no interaction from the sample. It is also a well established method, with a wide range of radionuclides available with varying half-lives, LETs and particle energies. In many cases there are convenient methods for the production of the desired radioisotope in high isotopic purity. In most cases the radiolabelling of the biomolecule involves simple chemistry and the necessary ingredients for the therapeutic are available in a kit form requiring only the addition of the radionuclide.

The disadvantages associated with radiolabelling are the storage and disposal of the hot samples, generation of the compounds in acceptable radionuclidic purity and the radiation burden placed on the patient and the environment of the patient.

Radioactive labelling for imaging has been decreasing in importance, MRI contrast agents and fluorescent labelling taking over its place. These methods cannot match the sensitivity of radiolabelling, but are rapidly improving, and in the case of fluorescent labels, under special conditions, single-molecule detection has been achieved. Furthermore, the detection of emission from a fluorescent label can be achieved with relatively simple instrumentation, unlike the γ-cameras needed for radioimaging.

7.1.2.1 Radioactive labelling of MUC1

Human MUC1 mucin is a membrane-bound member of a glycoprotein family. It is expressed at the apical cell surface of normal glandular epithelium of several

organs, for example stomach, salivary gland, breast, bladder, pancreas and uterus. It is also expressed by hematopoietic cells.[98]

Normal mucin is a high-molecular weight (400 kDa) transmembrane glycoprotein, with a 69 amino acid-long cytoplasmic tail and a highly glycosylated extracellular domain. The extracellular domain consists of tandem repeats of 20 amino acids, of which five (19, 27, 34-36) can be glycosylated. Half of the residues are proline, threonine and serine.

In carcinomas MUC1 is expressed on the whole cell surface, reducing cell adhesion and helping metastases. In tumours the underglycolsylated version of the normal protein can be found (*Figure A-3*).

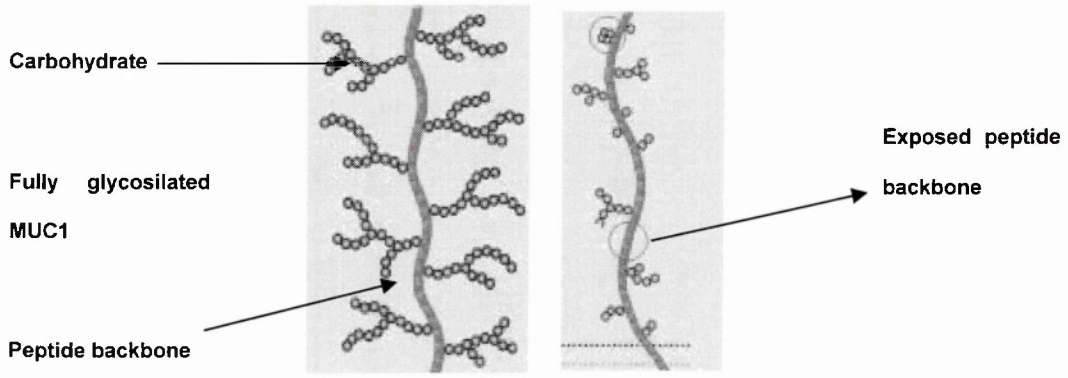

Figure A-3. Normal and tumour-associated MUC1.

Underglycosylation leaves the peptide backbone exposed, and this is a potential target for antibodies, peptides and aptamers. Most monoclonal antibodies react with the same epitope, the PDTRP sequence (*Figure A-4*).[99]

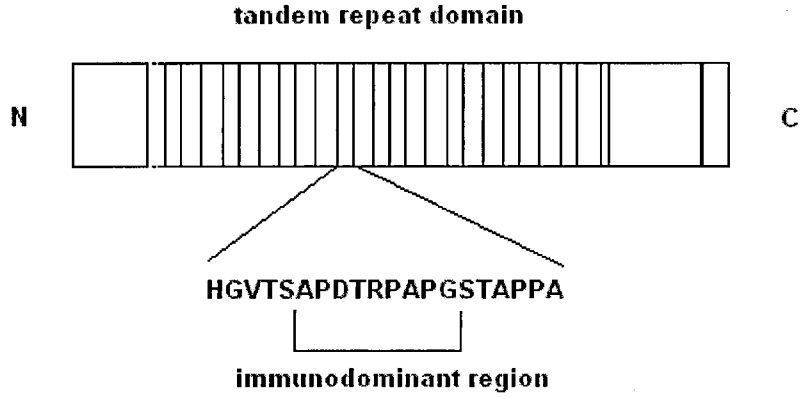

Figure A-4. The structure of the core MUC 1 protein.

Radiolabelling of anti-MUC1 antibodies has been performed with a number of radioactive nuclides, among them copper-64, technetium-99m and rhenium-188. As the incorporation of non-metal radionuclides usually requires either total synthesis or biochemical production of the radioactive sample, in most cases radioactive metal atoms are used for the labelling.

Direct attachment of the radiometals to the antibodies involves the reduction of the disulfide bonds by a suitable reducing agent, mercaptoethanol for example, and using the reduced thiols to co-ordinate the radionuclide. This method is applicable for the complexation of technetium, but has the disadvantage of reducing the stability of the antibody. The complexes thus derived are usually not very stable, therefore radioactive metals with longer half-lives cannot be incorporated this way. The co-ordination geometry and the oxidation state of the central atom cannot be determined, which leaves the characterisation of the therapeutics incomplete.

Radiolabelling with a bifunctional chelator is a widely applicable methodology resulting in stable and fully characterisable bioconjugates. The radiometal is complexed with a polydentate ligand, which can be coupled to the biomolecule

through a convenient reactive functional group. The functional groups can be carboxylic acids which can form amide bonds with the amino groups of lysine residues, and ester bonds with hydroxyl groups in serine and tyrosine. Thiols can be alkylated with maleimide selectively and isothiocyanates can form thiourea bonds with primary amines. The choice between the reactive groups depends on the labelling conditions, as all three have different optimal pH ranges for the reactions, which might be unsuitable for the given biomolecule.

The aptamers used in the studies have been 5'-amino modified to increase their stability against nucleases and to enable the attachment of the label. The introduction of amino groups makes the attachment of labels possible *via* amide bonds.

The chelate structure is determined by the chemical properties of the radiometal, its co-ordination number, oxidation state and hardness.

For imaging purposes the radionuclide of choice is the ^{99m}Tc, as it has a half-life of 6 hours, which makes simple preparations and efficient imaging of the tumours possible. The short half-life also enables the administration of millicurie doses of activity without the patient suffering significant radiation exposure. The photons emitted are monochromatic with 140 keV energy, which are easy to collimate to obtain images of excellent spatial resolution. Furthermore, technetium shares very similar chemical properties with rhenium, which is below technetium in the periodic table. It means that the chemistry of the therapeutic can be optimised using the non-radioactive rhenium. As an additional advantage, this chemistry can also be applied to two therapeutically important, β-emitting radioactive isotopes, ^{186}Re and ^{188}Re.

Technetium-99m is the decay product of the parent radionuclide, ^{99}Mo, and is available from ^{99}Mo-^{99m}Tc generators by elution with saline in the form of sodium pertechnetate. Molybdenum-99 molybdate is absorbed on alumina, where the decay of the ^{99}Mo yields ^{99m}Tc. Some of the ^{99}Mo decays directly to the decay product of ^{99m}Tc, the long-lived ^{99}Tc. Therefore the hot technetium sample is never carrier free. The specific activity of the sample can be very high, and is dependent on the age of the generator and the concentration of the sample.

7.1.2.2 Bifunctional ligands for the complexation of technetium and rhenium

There are a large number of bifunctional chelators in the literature for the complexation of technetium and rhenium. It is common to divide them into three parts: the functional group for the attachment to the biomolecule, the binding site for the metal complexation, and the spacer, which helps to minimise the interaction between the targeting molecule and the metal. The spacer might be completely missing, as, especially in the case of macromolecules, the properties of the biomolecule remain intact when a relatively small technetium complex is attached to them far away from the biologically active site.

Technetium has a rich redox chemistry and under a given set of conditions more than one oxidation state may be stable. The Mo-Tc generator provides technetium in the form of sodium pertechnetate, in which the technetium central atom is in the +7 oxidation state and its co-ordination sphere is saturated with four oxygen atoms. To enable complexation with a chelator the pertechnetate has to be reduced. This can be carried out with a variety of reducing agents, for example sodium borohydride, stannous chloride, water-soluble phosphines,

Sn(0), Ti(III), Cu(I), Fe(II), Zn(0). It is important for the reducing agent not to reduce the chelator. Stannous chloride is the most commonly used reagent because of its fast reduction kinetics, cheapness, availability and its reluctance to compete with the technetium for the binding site of the chelator. During the reduction of the pertechnetate with stannous chloride the initial reduction step yields Tc(VI), which can disproportionate, yielding the colloidal TcO_2. This not only reduces the labelling efficiency with respect to the radionuclide, but also makes the purification of the bioconjugate difficult. The oxidised tin can also precipitate out of solution, by the formation of the tin dioxide colloid. Therefore it is common practice to introduce a weak complexing agent, for example tricine,[#] which stabilises the metals and which the strongly binding chelator can replace as the ligand for the technetium.

The ligands can be categorised by the number of their donor atoms. Most of them have four donors, some have five, and there are examples of ligands with three donors (*Figure A-5*). Technetium, being a soft metal atom, can form stable complexes with the soft donors nitrogen and sulfur. It is not surprising to see that in most chelators there are 4-2 nitrogen atoms, the remaining being sulfurs or phorphorous. Although technetium can form stable complexes with open-chain ligands, the stability of the complexes can be further increased by closing the ligand structure into a ring.

[#] N-Tris-(hydroxymethyl)-methylglycine

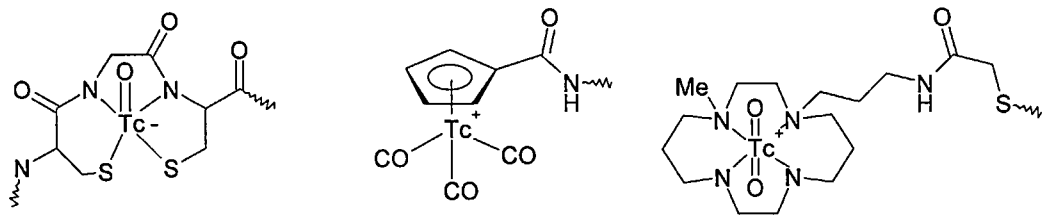

[TcO(Cys-Gly-Cys)] Tc(Cp-R)(CO)$_3$ [TcO$_2$(Cyclam)]

Figure A-5. Some commonly used technetium complexes.

The ligand designed for the labelling of the anti-MUC1 aptamers for labelling with technetium-99m is shown in *Figure A-6.*

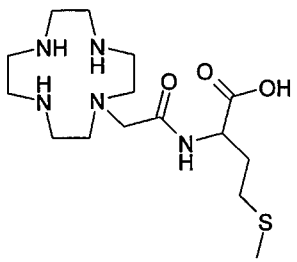

Figure A-6. The cyclen-based bifunctional chelator for the labelling of amino-modified aptamers with technetium. N^1-(methionylcarboxymethyl)-1,4,7,10-tetraazacyclohexadecane.

The technetium ion is co-ordinated by the four nitrogen atoms of the cyclen. The stability of the complex is increased by the introduction of a methionine arm, that can donate a sulfur atom for binding the technetium. The methionine is attached to the cyclen *via* an acetylcarboxylate linker, derived from chloroacetic acid.

Attachment of the aptamer is possible through amide bond formation with the carboxylic acid moiety of the methionine. Although the ligand contains secondary amino groups, it is unlikely that these would compete with the primary amino group of in the modified aptamer.

7.2 Experimental

Sodium perrhenate was supplied by Aldrich. All other chemicals were purchased from Acros and used without further purification. Sodium iodide and potassium carbonate were dried at 90 °C for 24 hours prior to use. TEA was distilled from calcium hydride under argon and stored under argon over molecular sieves. All other solvents were obtained from Fischer and used as purchased.

Tri-Boc-cyclen and methionine ethyl ester were synthesised according to literature procedures.[78, 98]

Thin Layer Chromatography was done on Merck fluorescent silica or on Fluka fluorescent alumina plates with iodine, $KMnO_4$ or UV visualisation. ^1H NMR and ^{13}C NMR data were obtained using a 300 MHz JEOL instrument. LC-MS was performed on a VG Quattro 2 equipment coupled to a Waters HPLC system. UV spectra were measured on a Uvikon XL (Bio-Tek Instruments) spectrometer.

Radioactive sodium pertechnetate solution in saline was obtained from a Molybdenum-technetium generator, typical activity values being 2000-6000 MBq in 1 to 2 mL. Modified aptamers were purchased from Aldrich. The labelled aptamers were purified by size-exclusion chromatography on PD-10 SEC columns (Amersham Biosciences). Three week-old nude female mice with mcf-7 xenografts in the left flank were supplied by the Department of Academic Medical Physics, University of Nottingham.

7.2.1 Ligand synthesis for aptamer labelling

7.2.1.1 DL-Methionine-ethyl ester chloroamide

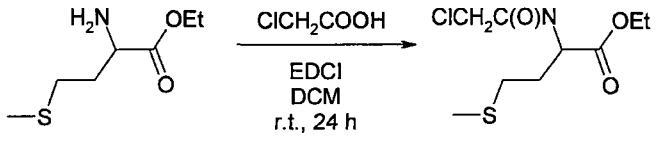

176 **177**

DL-Methionine ethyl ester (**176**) (0.18 g, 1 mmol) was dissolved in DCM (10 mL), chloroacetic acid (0.18 g, 2 mmol) and EDCI (0.38 g, 2 mmol) were added, and the solution was stirred at room temperature for 24 hours. DCM (30 mL) and water (40 mL) were added, the phases were separated, and the aqueous phase was extracted with DCM (2·25 mL). The combined organic phases were washed with water (30 mL), dilute acid (30 mL, 1 M HCl), dilute base (30 mL, 1 M NaOH), dried over $MgSO_4$, filtered, and evaporated to dryness to yield **177** in >95% yield as a colourless solid. ^1H NMR ($CDCl_3$, δ): 1.16-1.26 (t, 3 H, CH_3), 1.92-2.20 (m, 2 H, CH_2), 2.02 (s, 3 H, S-CH_3), 2.40-2.49 (t, 2 H, CH_2), 2.78 (s, 1 H, NH), 4.02 (s, 2 H, $ClCH_2$), 4.60-4.67 (m, 1 H, CH); ^{13}C NMR: 14.09 (CH_3), 15.44 (CH_3), 29.81 (CH_2), 31.40 (CH_2), 42.41 (CH_2), 51.89 (CH), 61.87 ($ClCH_2$), 165.89 (CO), 171.18 (CO).

*7.2.1.2 Alkylation of tri-Boc-cyclen with **177***

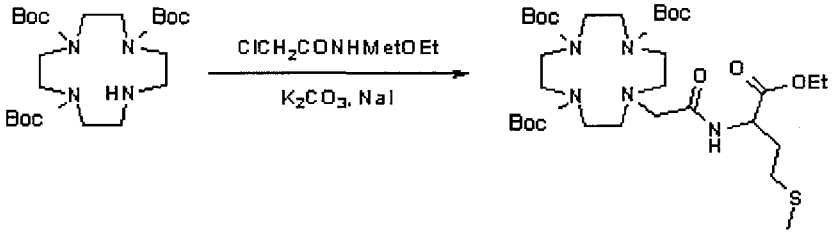

178 **179**

Tri-Boc-cyclen (**178**) (0.23 g, 0.5 mmol) was dissolved in DMF (8 mL), K_2CO_3 (2.00 g), NaI (1.00 g) and DL-methionine ethyl ester chloroamide (**177**) (0.26 g, 1 mmol) were added and the mixture was stirred at 80 °C under argon for 24 hours. The DMF was removed *in vacuo*, the residue was suspended in DCM (50 mL), water was added (50 mL), the phases were separated, and the aqueous phase was extracted with DCM (3·30 mL). The combined organic phases were washed with water (2·30 mL), dried over $MgSO_4$, filtered, and concentrated to ~2 mL. The solution was applied onto a silica column and chromatographed with EtOAc / hexane (1:1). Evaporation of the solvents gave **179** in 35% yield (0.12 g) as a colourless solid. ^1H NMR ($CDCl_3$, δ): 1.17-1.25 (m, 3 H, CH_3), 1.38 (s, 18 H, Boc), 1.40 (s, 9 H, Boc), 2.03 (s, 3 H, SCH_3), 2.44-2.53 (m, 1 H, CH_2-1), 2.53-3.55 (m, 19 H, CH_2+CH_2-2), 4.04-4.15 (m, 1 H, CH).

*7.2.1.3 Removal of the ethyl ester protection from **179***

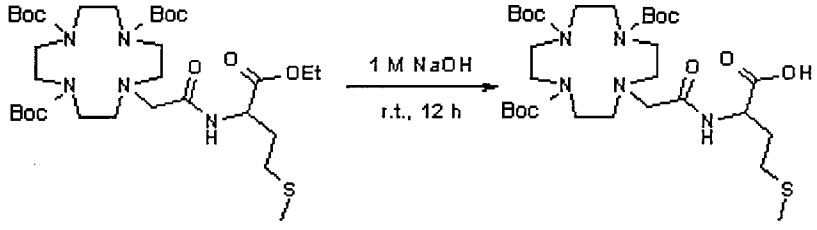

179 **180**

179 (0.27 g, 0.4 mmol) was dissolved in DCM (10 mL), NaOH (1 M, 10 mL) was added, and the solution was stirred vigorously at room temperature overnight. The pH was adjusted to 2 with 1:1 HCl, dichloromethane (30 mL) was added to the mixture, the phases were separated, and the water phase was extracted with DCM (2·25 mL). The combined organic phases were washed with water (2·30 mL), dried over $MgSO_4$, filtered, and evaporated to dryness to give **180** as

a white solid. Yield: >95% (0.26 g), ^{1}H NMR ($CDCl_3$, δ): 1.40 (s, 18 H, Boc), 1.43 (s, 9 H, Boc), 1.98 (s, 3 H, S-CH_3), 2.46-2.54 (m, 2 H, CH_2), 2.75-3.45 (m, 18 H, CH_2), 4.47-4.54 (m, 1 H, CH); ^{13}C NMR: 15.32 (SCH_3), 28.35 (CH_3-Boc), 28.60 (CH_3-Boc), 30.18 (CH_2), 47.09 (CH_2), 48.71 (CH_2), 50.24 (CH_2), 50.43 (CH_2), 51.95 (CH_2), 53.38 (CH_2), 79.85 (C_q), 81.02 (C_q), 156.26 (CO), 156.36 (CO), 170.57 (CO).

7.2.1.4 Removal of the Boc protecting groups from ***180***

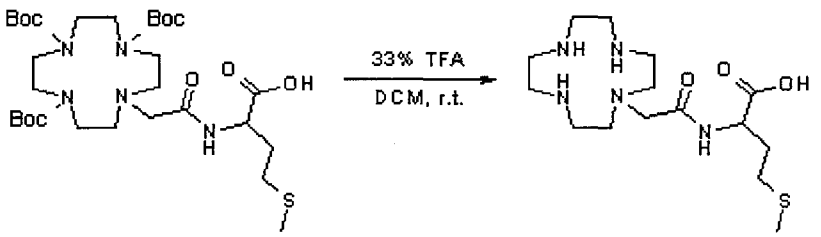

180 **181**

180 (0.26 g, 0.4 mmol) was dissolved in dichloromethane (10 mL), trifluoroacetic acid (5 mL) was added and the solution was stirred at room temperature for 30 min. The volatile components were evaporated and the sample was dried for 24 hours at high vacuum. Recrystallisation from ethanol / conc. HCl gave **181** in 50% yield the HCl salt as an off-white solid. MS: 381 $[M+NH_4]^+$, 519 unassigned; ^{1}H NMR (CD_3OD, δ): 1.77-2.23 (m, 5 H, CH_2 + SCH_3), 2.08 (s, 3 H, SCH_3), 2.45-3.76 (m, 21 H, CH_2 + CH); ^{13}C NMR: 14.02 (CH_3), 14.83 (CH_2), 24.85 (CH_2), 30.17 (CH_2), 52.65 (CH_2), 55.73 (CH_3), 128.94 (CO).

*7.2.1.5 Alkylation of cyclen with **177***

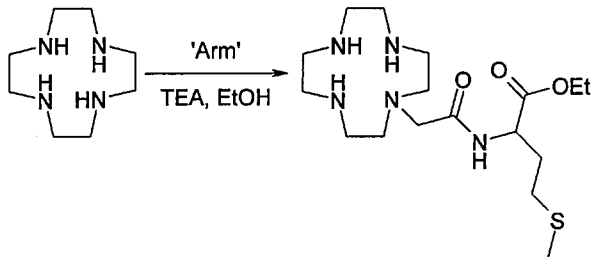

137 **182**

Cyclen (**137**) (4.71 g, 27.4 mmol, 1.5 eq) was dissolved in 100% ethanol (25 mL), TEA (0.70 mL, 5.54 g, 54.9 mmol, 7 3 eq) was added, and DL-methionine ethyl ester choloracetate (**177**) (4.64 g, 18.3 mmol). The solution was refluxed under argon atmosphere for 24 hours. The ethanol and the triethylamine were removed at reduced pressure, the residue redissolved in a mixture of DCM and water (mL each), the phases were separated, and the aqueous phase was extracted with DCM (2·30 mL). The combined organic phases were washed with water (40 mL), dried over $MgSO_4$, filtered, and concentrated to ~5 mL. The desired compound was isolated after purification of the crude sample by means of alumina column chromatography (pH 9.5, elution with DCM / MeOH (0.2-4%)). After evaporation of the solvents the product (**182**) was obtained in 13.5% yield (0.96 g) as a colourless solid. ^{1}H NMR ($CDCl_3$, δ): 1.21 (t, 3 H, CH_3, J = 7.2 Hz), 1.87-2.15 (m, 2 H, CH_2), 2.04 (s, 3 H, SCH_3), 2.45-3.01 (m, 18 H, CH_2), 3.15 (dd, 2 H, CH_2, J_1 = 17.4 Hz, J_2 = 12.5 Hz), 4.11 (q, 2 H, CH_2, J = 7.2 Hz), 4.57-5.65 (m, 1 H, CH), 8.76 (d, 1 H, NH, J = 8.4 Hz); ^{13}C NMR: 14.07 (CH_3), 15.40 (SCH_3), 30.37 (CH_2), 31.55 (CH_2), 45.84 (CH_2), 46.23 (CH_2), 47.19 (CH_2), 51.23 (CH_2), 53.43 (CH_2), 58.99 (CH_2), 61.32 (CH), 172.37 (CO).

*7.2.1.6 Removal of the ethyl ester protection from **182***

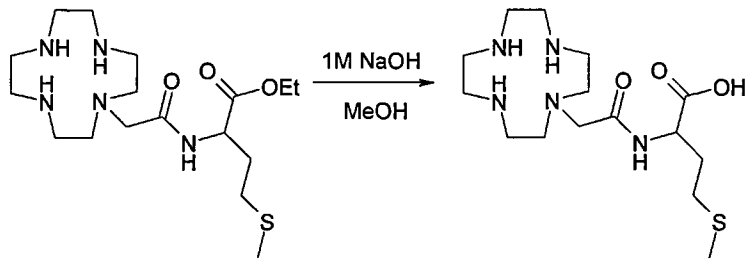

182 **181**

182 was dissolved in methanol (10 mL), 2 M NaOH (10 mL) was added, and the solution was stirred at room temperature overnight. The pH of the solution was adjusted to 7.0 with dilute HCl (2 M), and the solvents were evaporated at reduced pressure. The residue was dissolved in a mixture of DCM and 10% methanol, dried over $MgSO_4$, filtered, and evaporated to dryness to give the ligand as an off-white solid in 75% yield. Characterisation data same as reported before for **181**. MS: 361 $[M+H]^+$.

7.2.2 Complexation with Tc and Re and bioconjugation

*7.2.2.1 Synthesis of the technetium complex of **181***

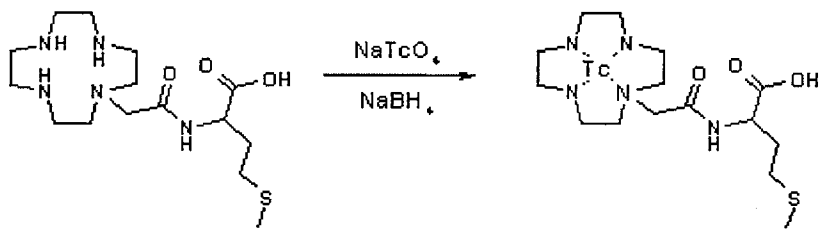

181 **183**

Metastable sodium pertechnetate in saline (0.2 mL) was reduced for ten minutes with sodium borohydride (4 mg, 0.1 mmol). **181** (36 mg, 0.1 mmol) in HPLC-grade methanol (2 mL) was added, and the solution was heated to reflux. The reaction continued overnight. The solution was allowed to cool back to

room temperature and the sample was filtered through a plug of cotton wool into diethyl ether (5 mL). The white precipitate was concentrated by centrifugation. The ether was poured off the sample, the solid residue was dissolved in distilled water, filtered, and freeze-dried to give **183** in 14% yield as an off-white solid. MS: 361 [M(**181**)+H]$^+$;

*7.2.2.2 Synthesis of the rhenium complex of **181***

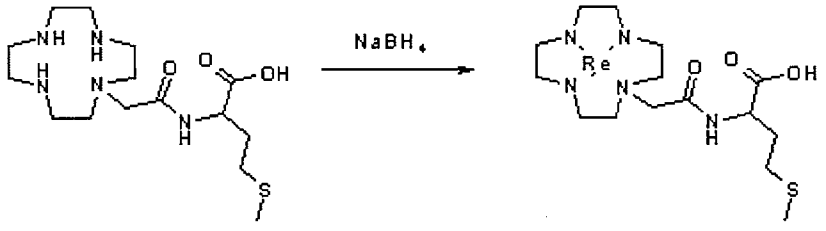

181 **184**

Sodium perrhenate (25 mg, 0.1 mmol) was suspended in HPLC-grade methanol (2 mL), and sodium borohydride (4 mg, 0.1 mmol) was added to the suspension. The reaction was allowed to proceed at room temperature for ten minutes, after which **181** (36 mg, 0.1 mmol) was added, and the solution was heated to reflux. The reaction continued overnight. The solution was allowed to cool back to room temperature and the sample was filtered through a plug of cotton wool into diethyl ether (5 mL). The white precipitate was concentrated by centrifugation. The ether was poured off the sample, the solid residue was dissolved in distilled water, filtered, and freeze-dried to give **184** in 25% yield as an off-white solid. MS: 361 [M(**181**)+H]$^+$.

*7.2.2.3 Attachment of **183** to the modified aptamer*

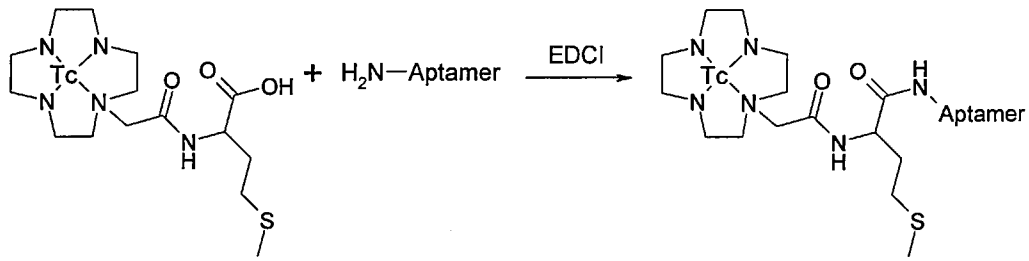

183 **185**

Sodium pertechnetate in saline (1 mL, varying activity) was incubated with sodium borohydryde (4 mg, 0.11 mmol) at room temperature for 10 minutes. **181** (36 mg, 0.1 mmol) was added, and the solution was heated to approximately 60 °C, and was kept at this temperature for 30 minutes. The solution was allowed to cool back to room temperature and was used without further purification for the labelling of the amino-modified aptamers.

Aptamer (25-mer, 5'-amino-3'-fluoropirimidine-modified, 11 mg) and EDCI (19 mg, 0.1 mmol) were added to the solution of the technetium complex, and the reaction was allowed to proceed for 45 minutes at room temperature. The reaction volume was adjusted to 3 mL with sterile distilled water, and the sample was applied onto a PD-10 size exclusion chromatographic column. Elution with sterile distilled water yielded the labelled aptamer in the second, third and fourth fractions. The presence of the aptamers was detected with UV-spectrometry, and the activity of the samples was measured, confirming the presence of the technetium in the bioconjugates. The complexed but unconjugated technetium eluted in the following fractions (fractions 5 to 8).

Fraction four, containing **185** was used for the animal studies without further purification.

7.3 Results and discussion

7.3.1 Ligand synthesis

7.3.1.1 Ligand synthesis starting with protected cyclen derivatives

For the selective and unambigous labelling of aptamers with chelators it is necessary for the chelators to be monofunctional. More than one reactive group in the molecule could result in bioconjugates having other than 1:1 chelator:aptamer ratio, giving rise to a mixture of products. Therefore only one nitrogen atom of the cyclen should be functionalised with a carboxylic acid.

Bioconjugation between the ligand and the aptamer is carried out in aqueous solutions, and in the case of the short-lived isotopes techetium-99m and rhenium-188, under a short period of time (typically 45-60 minutes). It is expected that under these conditions the secondary nitrogens of the cyclen react more slowly than the primary amine in the 3'-modified aptamer.

The triprotected cyclen derivative (**113**) already prepared for the lanthanide syntheses was alkylated with chloroacetic acid in the presence of potassium carbonate and sodium iodide. The product was isolated in moderate yields and was reacted with methionine ethyl ester and EDCI to form an amide bond between the amino group of the methionine and the carboxylic acid function of the cyclen derivative. Removal of the ^{t}Butyl-oxycarbonyl group was followed by alkalyne hydrolysis of the oxalamide protection with 10 M aqueous sodium hydroxide at room temperature. The final step also resulted in the decomposion of the product and and alternative protection strategy was necessary (*Scheme A-1*).

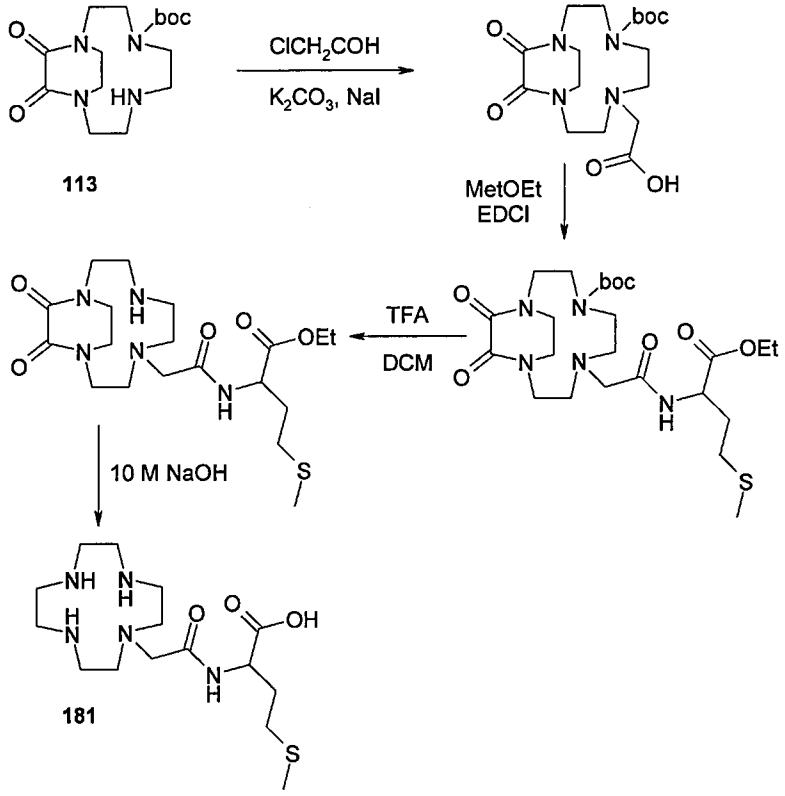

*Scheme A-1. Synthesis of the bifunctional chelator **181** from protected cyclen **113**.*

As the orthogonal oxalamide and ^{t}butyloxycarbonyl protecting groups are not needed in this reaction sequence, they can be replaced by three identical protecting groups. Unlike the oxalamide, this group can be non-electron withdrawing. This is essential for the efficient alkylation of the fourth nitrogen atom. The introduction of three Boc protecting groups onto the cyclen was carried out according to a literature procedure.[100] The fourth nitrogen atom was alkylated with methionine ethyl ester chloroamide (**177**) in DMF solvent with potassium carbonate base and sodium iodide catalyst. The desired product **179** was obtained in high purity and moderate yields after conventional workup followed by silica column chromatography. The ethyl ester protection was removed by hydrolysis in 1 M sodium hydroxide solution. After isolation of the free acid, the Boc protecting groups of **180** were cleaved by 33% TFA in DCM.

Evaporation of the solvents, followed by recrystallisation from hot ethanol / conc. HCl afforded the final ligand (**181**) as an off-white solid (*Scheme A-2*).

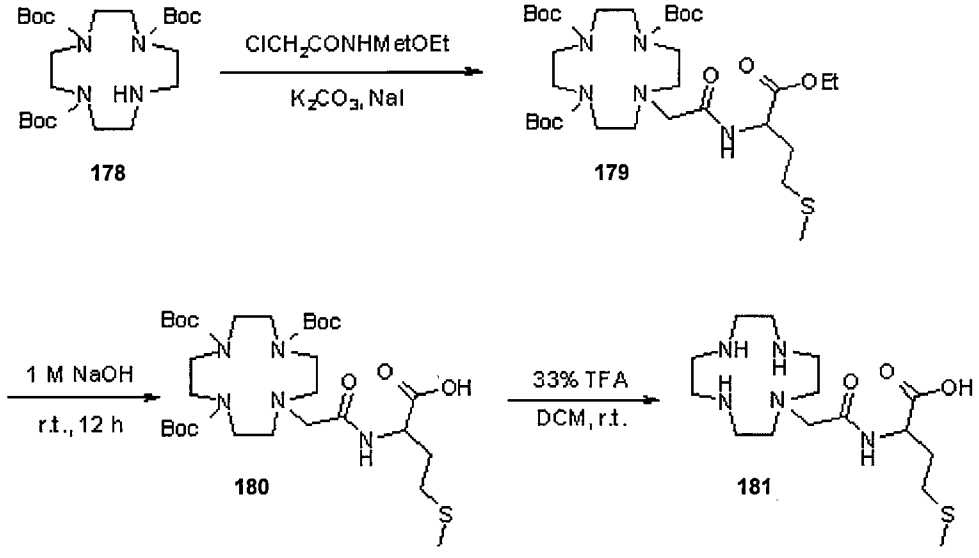

*Scheme A-2. Synthesis of **181** form tri-Boc cyclen (**178**).*

*7.3.2 Synthesis of **181** from unprotected cyclen*

During the synthesis of the lanthanide-binding ligands (**150a-b**, **161**, **171a-b**) it was found that it is possible to achieve monosubstitution of cyclen in absolute ethanol with triethylamine base with a number of alkylating agents. The reaction gives rise to a small amount of side-products, but these can be easily removed. The gain in yields and required time far outweighs the losses caused by overalkylation.

Cyclen was reacted in refluxing hot ethanol in the presence of triethylamine under inert atmosphere with methionine ethyl ester chloroacetate (**177**). The monoalkylated derivative was isolated in good yields and high purity after conventional aqueous workup followed by chromatography on basic alumina.

The ethyl ester was hydrolysed with 1 M sodium hydroxyde to yield the final product in good yields (*Scheme A-3*).

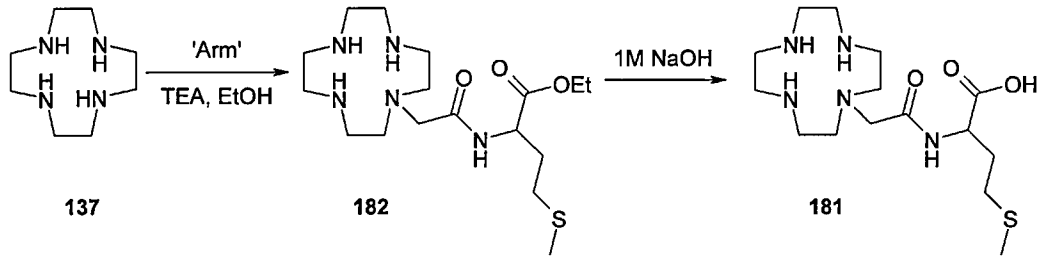

*Scheme A-3. Two-step synthesis of **181** from cyclen (**137**).*

*7.3.3 Complexation of **181** with technetium and rhenium*

The ligand-rhenium complex (**184**) was prepared as a model molecule for the radioactive ligand-technetium complex. Rhenium is below technetium in the periodic table, and their chemical properties are very similar. Sodium perrhenate is readily available in large quantities as a solid. Furthermore, rhenium has two β-emitting isotopes (^{186}Re and ^{188}Re), that have found application in radiotherapy. It is common practice to use the technetium complex for imaging tumours, and the rhenium analogues for therapy.

Sodium perrhenate was suspended in HPLC-grade methanol, and 1 equivalent of sodium borohydride was added. The reduction was allowed to proceed for 15 minutes, after which the ligand was added in 10% excess to the solution. The mixture was refluxed under inert atmosphere overnight. The product was isolated by pouring the solution into diethyl ether, and collecting the solid precipitate by centrifugation. The complex was formed in moderate yields. TLC showed that no free ligand residues were remaining in the sample.

The oxidation state of the metal cannot be decided, and the overall charge of the complex depends on the redox state of the metal and the pH of the medium. The complexation reaction with metastable technetium was carried out under similar conditions, using a mixture of saline and methanol for the reaction, as

technetium pertechnetate was supplied as a saline solution. Both complexes were stable in solution for up to 24 hours at room temperature, as confirmed by TLC (*Scheme A-4*).

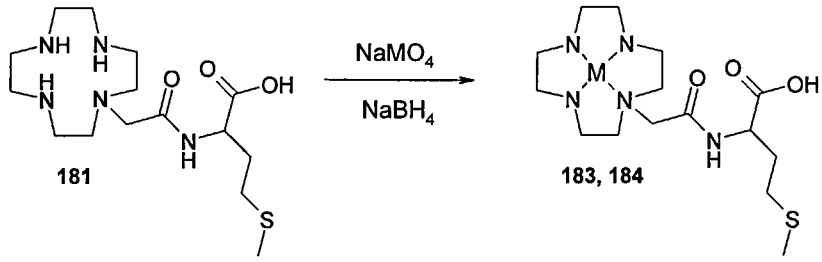

*Scheme A-4. Reduction and complexation of technetium and rhenium with **181**. M = Tc (**183**) or Re (**184**). The overall charge of the complex depends on the exact experimental conditions.*

7.3.4 Synthesis of the radiometal-labelled aptamers

The radioactive technetium complex was prepared by the reduction of a aqueous solution of sodium pertechnetate by sodium borohydryde, and heating the solution to 60 °C for 45 minutes. The complex was coupled to the aptamer without isolation. Test reactions with non-radioactive samples were carried out to couple the complex to 3', 5', or both-end amino-modified. Initially these modifications served to stabilise the molecule against nucleases, but they also provide a convenient attachment site for the label.

The conjugation to 3'-modified aptamer was carried out at room temperature with the water-soluble EDCI coupling reagent. After one hour the labelled aptamer was isolated by size-exclusion column chromatography. Characterisation of the product (**185**) was possible by UV-spectroscopy and by measuring the labelling efficiency with a scintillation counter. In an analogous reaction technetium was complexed with the commercially available MAG3 ligand, and this complex was attached to the aptamer to compare the new compound to an established label. All bioconjugates were stable and there was

no leakage of the metal seen. The excess radioactive salt could be efficiently separated from the labelled aptamer. Fractions 1-4 contained the labelled aptamer, while in fractions 5 and 6 the salt was eluted (*Table A-2*).

Fraction (1 mL each)	Apt-MAG3(Tc) (MBq)	Apt-**999**(Tc) (MBq)
0	0.013	0.013
1	0.286	0.199
2	18.35	10.45
3	15.67	9.99
4	12.34	15.81
5	8.564	19.68
6	5.653	12.10
column	856	1054

Table A-2. Activity of the fractions after the purification of the labelled aptamers.

Due to the low concentration of the aptamer, the labelling efficiency was poor for both complexes, although it was marginally higher for the cyclen-based ligand. Despite the low labelling efficiencies there was enough labelled aptamer available in each experiment to inject three mice with approximately 5 MBq activity in 0.1-0.2 mL.

After injection the mice were monitored with a γ-camera for 10 minutes to follow the takeup of the radioactivity. It was found that the labelled aptamer was immediately metabolised in the liver and excreted through the kidneys and the bladder, without any tumour uptake (*Figure A-6*).

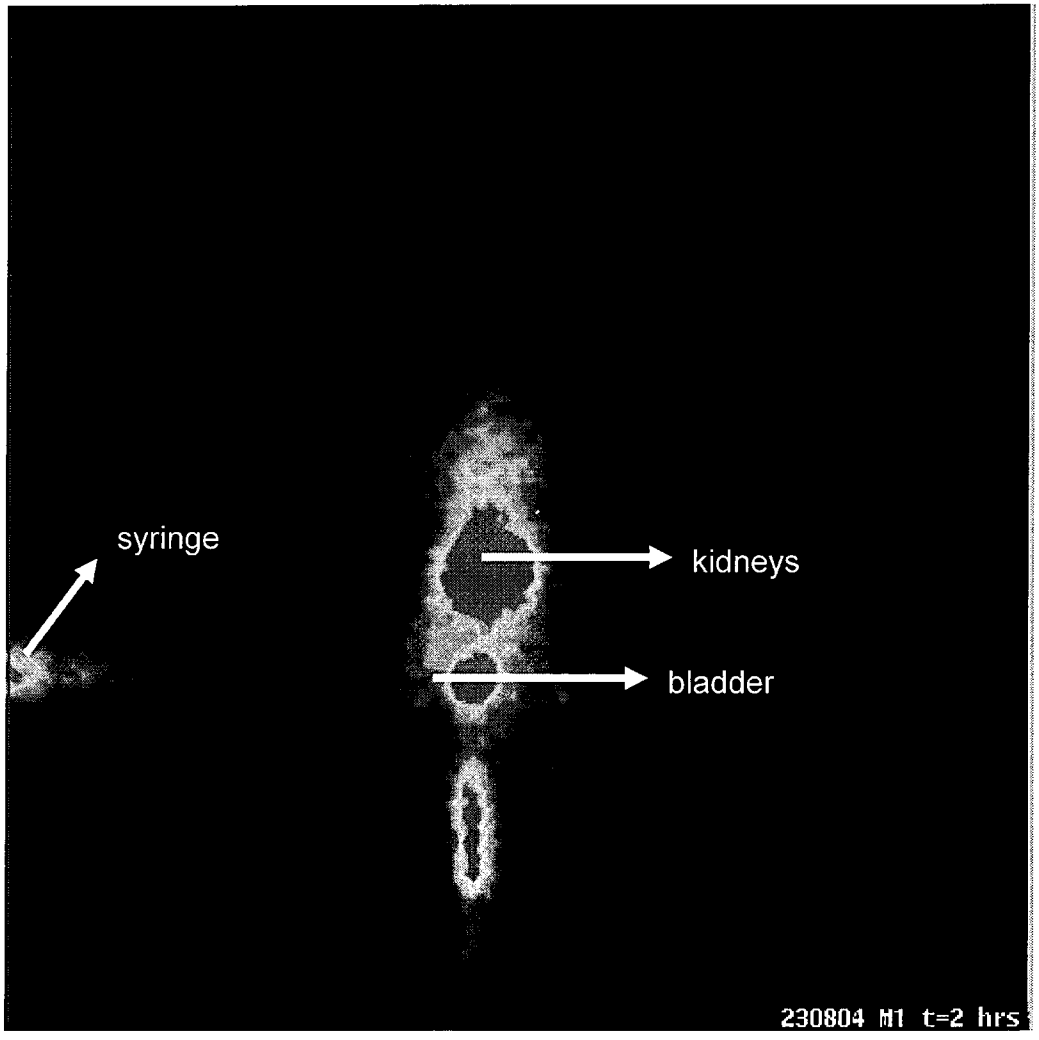

*Figure A-6. γ-Camera images of a mouse injected with the aptamer-**181**-Tc conjugate. The radioactivity is accumulated in the liver, the kidneys and later the bladder. The tumour is not visible, but is located next to the syringe. The tail is radioactive as it was the injection site.*

After 30 minutes almost all the radioactivity was accumulated in the bladder. This was caused by the small size of the aptamer, as it is approximately ¼ of the size considered ideal for tumour targeting. Data collection was continued for 5 hours, after which the mice were sacrificed, the tumours removed and analysed. No radioactivity was detected in the tumour slices.

In further experiments conducted by C. S. M. Ferreira and S. Missailidis a DOTA-Tc-complex was equipped with four identical aptamer arms, giving rise to

a fourfold increase in the molecular weight. Efficient tumour uptake occurred under identical conditions, as demonstrated by the images of the tumour slices (*Figure A-7*).

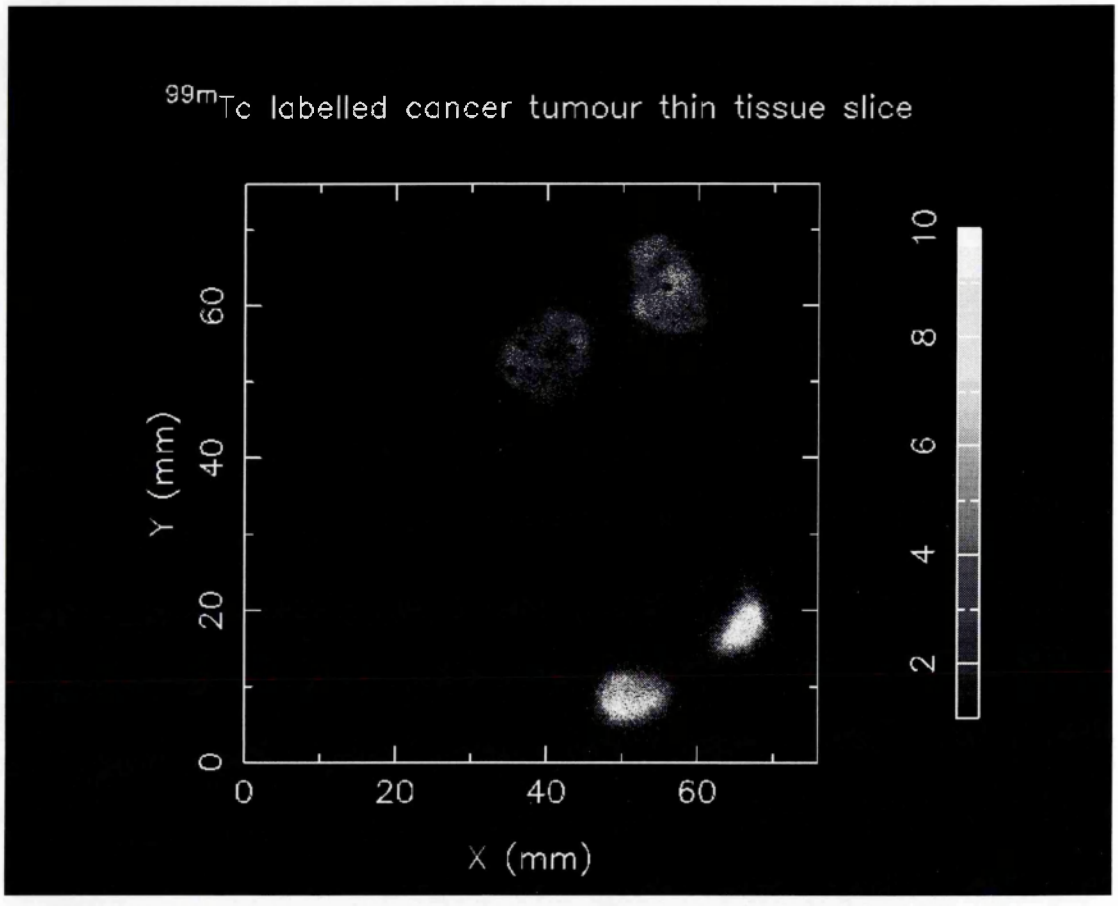

Figure A-7. Images of tumour slices. Mice were injected with multiaptamer-DOTA Tc complex.

7.4 Conclusions

A novel, cyclen-based ligand (**181**) for the complexation of technetium and rhenium was designed and synthesised. The ligand contains an attachment site for biomolecules with amino groups available. It forms stable complexes with both metals within 30-60 minutes, and can be coupled to amino-modified aptamers in good yields.

The tumour uptake of radiolabelled aptamers with **181** and MAG3 chelators was determined by injecting them into 3 week-old nude female mice with mcf-7 xenografts in the left flank, and monitoring the distribution of the radioactivity. No tumour uptake was observed for either the **181**-labelled or the MAG3-labelled aptamers. In consecutive studies, when four aptamers, held together by a tetravalent DOTA(Tc) scaffold were injected, good accumulation of the bioconjugates in the tumour was seen.

The quality of the imaging could be further improved by the usage of double-modified tetravalent aptamers, to which **181**(Tc) complexes could be attached. This method could also be therapeutically useful if technetium is replaced by the β-emitting ^{188}Re. A multivalent aptamer with potentially five metal-binding sites could deliver a large dose of radiation specifically to the tumour.

8 REFERENCES

[1] E. Fisher, Ber. Dtsch. Chem. Ges. **1894,** 27, 2985-2987

[2] D. E. Koshland Jr, *Proc. Natl. Acad. Sci.* **1958,** *44,* 98-107

[3] D. J. Cram, I. B. Dicker, M. Lauer, C. B. Knobler, K. N. Trueblood, *J. Am. Chem. Soc.* **1984,** *106,* 7150-7168

[4] *Biochemistry,* L. D. Stryer, Freeman, New York, 3rd edn., **1988**

[5] *Essential immunology,* I. M. Roitt, 9th ed. Blackwell Science Ltd., Oxford, **1997**

[6] M. Mammen, S-K. Choi, and G. M. Whitesides, *Angew. Chem. Int. Ed.* **1998,** *37,* 2754-2794

[7] K. Tanaka, T. Miura, N. Umezawa, Y. Urano, K. Kikuchi, T. Higuchi, and T. Nagano, *J. Am. Chem. Soc.*, **2001**, *123*, 2530-2536

[8] *Molecular Fluorescence,* B. Valeur, WILEY-VCH Verlag GmbH, Weinheim, **2002**

[9] S. T. Mullins, P. G. Sammes, R. M. West, and G. Yahioglu, *J. Chem. Soc. Perkin Trans. 1,* **1995,** 75-81

[10] *Principles of fluorescence spectroscopy,* J. R. Lakowicz, Plenum Press, New York, **1983**

[11] T. Forster, *Naturwissenschaften,* **1946,** *33,* 166-175

[12] T. Forster, *Ann. Phys.,* **1948,** *2,* 55-73

[13] D. L. Dexter, *J. Chem. Phys.,* **1953,** *21,* 836-850

[14] S. Weiss, *Science,* **1999,** *283,* 1676-1683

[15] S. Tyagi and F. R. Kramer, *Nature Biotechnol.,* **1996,** *14,* 303-308

[16] D. L. Sokol, X. Zhang, P. Lu, and A. M. Gewirtz, *Proc. Natl. Acad. Sci. USA,* **1998,** *95,* 11538-11543

[17] S. Tyagi, S. A. E. Marras, and F. R. Kramer, *Nature Biotechnol.,* **2000,** *18,* 1191-1196

[18] *Concepts of Inorganic Photochemistry,* Eds.: A. W. Adamson and P. D. Fleischauer, John Wiley and Sons, New York, **1975**

[19] J. I. Bruce, M. P. Lowe, and D. Parker in *The Chemistry of Contrast Agents in Medical Resonance Imaging,* Eds.: A. E. Merbach and E. Toth, John Wiley & Sons, Ltd., New York, **2001**

[20] A. Beeby, I. M. Clarkson, R. S. Dickins, S. Faulkner, D. Parker, L. Royle, A. S. de Souza, J A. G. Williams, and M. Woods, *J. Chem. Soc., Perkin Trans 2,* **1999,** 493-503

[21] Y. J. Marcus, *J. Chem. Soc. Faraday Trans.* **1991,** *87,* 2995

[22] S. C. Brudette, G. K. Walkup, B. Spingler, R. Y. Tsien, and S. J. Lippard, *J. Am. Chem. Soc.* **2001,** *123,* 7831-7841

[23] G. K. Walkup, S. C. Burdette, S. J. Lippard, *J. Am. Chem. Soc.* **2000,** *122,* 5644-5645

[24] T. Hirano, K. Kikuchi, Y. Urano, T. Higuchi, and T. Nagano, *Angew. Chem. Int. Ed.* **2000,** *39,* 1052-1054

[25] J. Yoon, N. E. Ohler, D. H. Vance, W. D. Aumiller, and A. W. Czarnik, *Tetrahedron Lett.* **1997,** *38,* 3845-3848

[26] Y. Shen and B. P. Sullivan, *Inorg. Chem.* **1995,** *34,* 6235-6236

[27] D. W. Jung, C. J. Chapman, K. Baysal, D. R. Pfeiffer, and G. P. Brierley, *Archives of Biochem. and Biophys.* **1996,** *332,* 19-29

[28] Y. Nakahara, Y. Matsumi, W. Zhang, T. Kida, Y. Nakatsuji, and I. Ikeda, *Organic Lett,* **2002**, *4*, 2641-2644

[29] G. Grynkiewicz, M. Poenie, and R. Y. Tsien, *J. Biol. Chem.* **1985,** *260,* 3440-3450

[30] C. Blackburn, M. Bai, K. A. LeCompte, and M. E. Langmuir, *Tetrahedron Lett.* **1994,** *35,* 7915-7918

[31] G. A. Smith, P. G. Morris, T. R. Hesketh, and J. C. Metcalfe, *Biochim. Biophys. Acta,* **1986,** *889,* 82-83

[32] G. A. Smith, T. R. Hesketh, and J. S. Metcalfe, *Biochem. J.* **1988,** *250,* 227-232

[33] A. Minta and R. Y. Tsien, *J. Biol. Chem.* **1989,** *264,* 19449-19457

[34] A. T. Harootunian, J. P. Y. Kao, B. K. Eckert, and R. Y. Tsien, *J. Biol. Chem.* **1989,** *264,* 19458-19467

[35] R. Crossley, Z. Goolamali, J. J. Gosper, and P. G. Sammes, *J. Chem. Soc. Perkin Trans. 2,* **1994,** 513-520

[36] R. Crossley, Z. Goolamali, and P. G. Sammes, *J. Chem. Soc. Perkin Trans. 2,* **1994,** 1615-1623

[37] F. Arnaud-Neu, Z. Asfari, B. Souley and J. Vicens, *New J. Chem.,* **1996,** *20,* 453-463

[38] A. P. de Silva, H. Q. N. Gunaratne, T. Gunnlaugsson, A. J. M. Huxley, C. P. McCoy, J. T. Rademacher, and T. E. Rice, *Chem. Rev.* **1997,** *97,* 1515-1566

[39] M-Y Chae, X. M. Cherian, and A. W. Czarnik, *J. Org. Chem.* **1993,** *58,* 5797-5801

[40] J. Bourson, J. Pouget, and B. Valeur, *J. Phys. Chem.* **1993,** *97,* 4552-4557

[41] A. P. de Silva, H. Q. N. Gunaratne, P. L. M. Lynch, A. J. Patty, and G. L. Spence, *J. Chem. Soc. Perkin Trans. 2,* **1993,** 1611-1616

[42] P. D. Beer, *Chem. Commun.* **1996,** 689-696

[43] M. Shionoya, H. Furuta, V. Lynch, A. Harriman, and J. L. Sessler, *J. Am. Chem. Soc.* **1992,** *114,* 5714-5722

[44] S. K. Kim and J. Yoon, *Chem. Commun,* **2002,** 770-771

[45] G. de Santis, L. Fabbrizzi, M. Licchelli, A. Poggi, and A. Taglietti, *Angew. Chem. Int. Ed. Engl.* **1996,** *35,* 202-204

[46] M. E. Huston, E. U. Akkaya, and A. W. Czarnik, *J. Am. Chem. Soc.* **1989,** *111,* 8735-8737

[47] D. H. Vance and A. W. Czarnik, *J. Am. Chem. Soc.* **1994,** *116,* 9397-9398

[48] T. Gunnlaugsson, A. P. Davis, J. E. O'Brien, and M. Glynn, *Org. Lett.* **2002,** *4,* 2449-2452

[49] T. Gunnlaugsson, A. P. Davis, and M. Glynn, *Chem. Commun.* **2001,** 2556-2557

[50] M. W. Hosseini, A. J. Blacker, and J-M. Lehn, *J. Am. Chem. Soc.* **1990,** *112,* 3896-3904

[51] S. T. Mullins, P. G. Sammes, R. M. West, and G. Yahioglu, *J. Chem. Soc. Perkin Trans. 1,* **1995,** 75-81

[52] G. Bobba, J. C. Frias, and D. Parker, *Chem. Comm.* **2002,** 890-891

[53] A. Beeby, R. S. Dickins, S. FitzGerald, L. J. Govanlock, C. L. Maupin, D. Parker, J. P. Riehl, G. Siligardi, and J. A. G. Williams, *Chem. Commun,* **2000,** 1183-1184

[54] I. M. Clarkson, A. Beeby, J. I. Bruce, L. J. Govenlock, M. P. Lowe, C. E. Mathieu, D. Parker, and K. Senanayake, *New J. Chem.* **2000,** *24,* 377-386

[55] D. Parker, K. Senanayake, and J. A. G.Williams, *Chem. Commun.* **1997,** 1777-1778

[56] J. I. Bruce, R. S. Dickins, L. J. Govenlock, T. Gunnlaugsson, S. Lopinski, M. P. Lowe, D. Parker, R. D. Peacock, J. J. B. Berry, S. Aime, and M. Botta, *J. Am. Chem. Soc.* **2000,** *122,* 9674-9684

[57] P. D. Beer, *Chem. Commun.* **1996,** 689-696

[58] P. D. Beer, Z. Chen, A. J. Goulden, A. Grieve, D. Hesek, F. Szemes, and T. Wear, *J. Chem. Soc., Chem. Commun.* **1994,** 1269

[59] F. Szemes, D. Hesek, Z. Che, S. W. Dent, M. G. B. Drew, A. J. Goulden, A. R. Graydon, A. Grieve, R. J. Mortimer, T. Wear, J. S. Weightman, and P. D. Beer, *Inorg. Chem.* **1996,** *35,* 5868-5879

[60] P. D. Beer and F. Szemes, *J. Chem. Soc, Chem. Commun,* **1995,** 2245

[61] L. J. Charbonniere, R. Ziessel, M. Montalti, L. Prodi, N. Zaccheroni, C. Boehme, and G. Wipff, *J. Am. Chem. Soc.* **2002,** *124,* 7779-7788

[62] J. Yoon, A. W. Czarnik, *J. Am. Chem. Soc.* **1992,** *114,* 5874

[63] M. Takeuchi, T. Mizuno, H. Shinmori, M. Nakashima, and S. Shinkai, *Tetrahedron,* **1996,** *52,* 1195-1204

[64] M. Yamamoto, M. Takeuchi, and S. Shinkai, *Tetrahedron,* **1998,** *54,* 3125-3140

[65] M. Takeuchi, S. Yoda, T. Imada, and S. Shinkai, *Tetrahedron,* **1997,** *53,* 8335-8348

[66] C. R. Cooper and T. D. James, *Chem. Commun.* **1997,** 1419-1420

[67] A. P. de Silva, H. Q. Gunaratne, C. McVeigh, G. E. M. Maguire, P. R. S. Maxwell, and E. O'Hanlon, *Chem. Commun,* **1996,** 2191-2192

[68] K. Motesharei and D. C. Myles, *J. Am. Chem. Soc.* **1994,** *116,* 7413-7414

[69] A. P. de Silva, H. Q. Gunaratne, and T. Gunnlaugsson, *Tetrahedron Lett.* **1998,** *39,* 5077-5080

[70] J. V. Ros-Lis, B. Garcia, D. Jimenez, R. Martinez-Manez, F. Sancenon, J. Soto, F. Gonzalvo, and M. C. Valldecabres, *J. Am. Chem. Soc.*, **2004**, *126*, 4064-4065

[71] R. M. Palmer, A. G. Ferrige, and S. Moncada, *Nature,* **1987**, *327,* 524-526

[72] Y. Gabe, Y. Urano, K. Kikuchi, H. Kojima, and T. Nagano, *J. Am. Chem. Soc.*, **2004**, *126,* 3357-3367

[73] K. Tanaka, T. Miura, N. Umezawa, Y. Urano, K. Kikuchi, T. Higuchi, and T. Nagano, *J. Am. Chem. Soc.*, **2001**, *123*, 2530-2536

[74] S. Blair, R. Kataky, and D. Parker, *New J. Chem.* **2002,** *26,* 530-535

[75] A.P. de Silva and N. D. McClenaghan, *Chem. Eur. J.,* **2004,** *10,* 574

[76] A. P. de Silva, H. Q. N. Gunaratne, and C. P. McCoy, *Nature,* **1993,** *364,* 42

[77] *Molecular Switches,* ed: B. L. Feringa, WILEY-VCH, Weinheim, **2001**

[78] C. A. M. Seide, A. Schulz, M. H. M. Sauer, *J. Phys. Chem.* **1996,** *100,* 5541-5553

[79] F. Bellouard , F. Chuburu , N. Kervarec , L. Toupet , S. Triki , Y. Le Mest, and H. Handel, *J. Chem. Soc., Perkin Trans. 1*, **1999,** *23*, 3499 - 3505

[80] J. B. Epp and T. S. Widlanski, *J. Org. Chem.,* **1999,** *64(1),* 293-295

[81] *The practice of peptide synthesis,* M. Bodanszky and A. Bodanszky, **1984,** Spinger-Verlag, Berlin; New York

[82] S. R. Trenor, A. R. Shultz, B. J. Love, and T. E. Long, *Chem. Rev.,* **2004,** *104,* 3059-3077

[83] S. L. Gilat, A. Adronov, and J. M. J. Frechet, *Angew. Chem. Int. Ed.,* **1999,** *38,* 1422-1427

[84] *March's Advanced Organic Chemistry,* 5th ed., M. B. Smith and J. March, John Wiley and sons, Inc., New York, **2001**

[85] B. Falkiewicz, A. S. Kolodziejczyk, B. Liberek, and K. Wisniewski, *Tetrahedron,* **2001,** *57,* 7909-7917

[86] T. L. Arbeola, F. L. Arbeola, M. J. Tapia, I. Lopez. I. L. Arbeola, *J. Phys. Chem.,* **1993,** *97,* 4704-4707

[87] s. Nad and H. Pal, *J. Phys. Chem.,* **2001,** *105,* 1097-1106

[88] A. Dunger, H.-H. Limbach, and K. Weisz, *J. Am. Chem. Soc.,* **2000,** *122,* 10109-10114

[89] Li, C.; Wong, W.-T., *J. Org. Chem.,* **2003**, *68*, 2956-2959

[90] J. M. Serin, D. W. Brousmiche, and J. M. J. Frechet, *J. Am. Chem. Soc.,* **2002,** *124,* 11848-11849

[91] G. A. Hebbink, L. Grave, L. A. Woldering, D. N. Reinhoudt, and F. C. J. M. van Veggel, *J. Phys. Chem. A*, **2003,** *107,* 2483-2491

[92] S. Faulkner and S. J. A. Pope, *J. Am. Chem. Soc.,* **2003,** *125,* 10526-10527

[93] S. Wang, J. Luo, D. A. Lantrip, D. J. Waters, C. J. Mathias, M. A. Green, P. L. Fuchs, and P. S. Low, *Bioconjugate Chem.,* **1997,** *8,* 673-679

[94] C. Tuerk, L. Gold, *Science,* **1990,** *249,* 505-510

[95] Y. Ito and E. Fukusaki, *J. Mol. Catal. B,* **2004**, *28,* 155-166

[96] S. Liu and D. S. Edwards, *Chem. Rev.*, **1999**, *99,* 2235-2268

[97] W. A. Volkert and T. J. Hoffman, *Chem. Rev.,* **1999,** *99,* 2269-2292

[98] S. von Mendorff-Pouilly, F. G. M. Snijdewint, A. A. Verstraeten, R. H. M. Verheijen, and P. Kenemans, *Int. J. Biol. Markers*, **2000,** *15,* 343-356

[99] A. Moore, Z. Medarova, A. Potthast, and G. Dai, *Cancer Res.,* **2004,** *64,* 1821-1827

[100] E. Kimura, S. Aoki, T. Koike, and M. Shiro, *J. Am. Chem. Soc.* **1997,** *119,* 3068-3076

STRUCTURES OF PRODUCTS

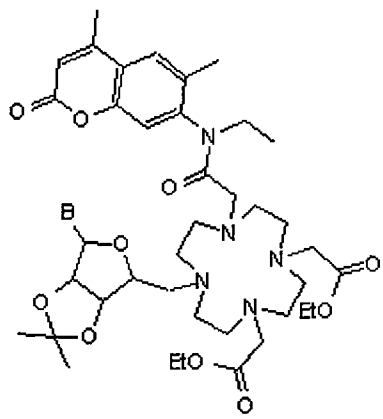

B = U **150a**
B = A **150b**

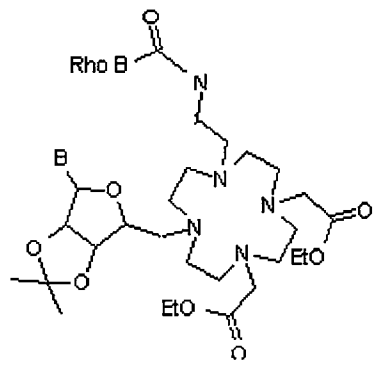

B = U **170a**
B = A **170b**

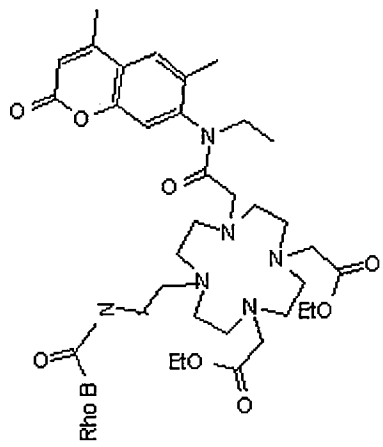

161

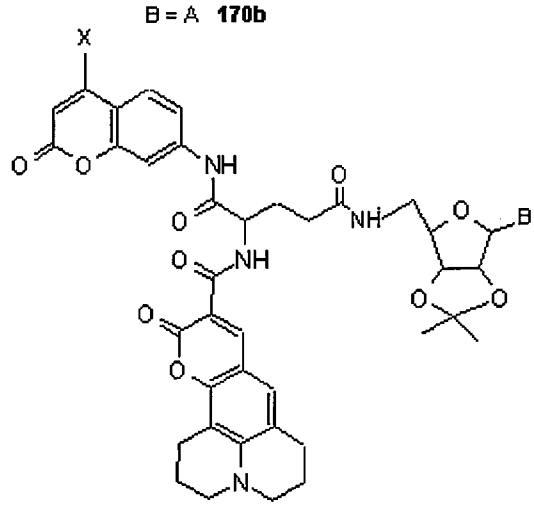

X = H, B = U **90a**
X = H, B = A **90b**
X = CF_3 , B = U **96a**
X = CF_3 , B = A **96b**